

**CORRELATION TRANSFER THEORY: APPLICATION OF  
RADIATIVE TRANSFER SOLUTION METHODS TO  
PHOTON CORRELATION IN FLUID/PARTICLE  
SUSPENSIONS**

By

**NAFAA M. REGUIGUI**

Bachelor of Science  
Oklahoma State University  
Stillwater, Oklahoma  
1987

Master of Science  
Oklahoma State University  
Stillwater, Oklahoma  
1990

Submitted to the Faculty of the  
Graduate College of the  
Oklahoma State University  
in partial fulfillment of  
the requirements for  
the Degree of  
DOCTOR OF PHILOSOPHY  
December, 1994

CORRELATION TRANSFER THEORY: APPLICATION OF  
RADIATIVE TRANSFER SOLUTION METHODS TO  
PHOTON CORRELATION IN FLUID/PARTICLE  
SUSPENSIONS

Thesis Approved:

*Ronald L. Daugherty*  
\_\_\_\_\_  
Thesis Adviser

*A. J. Yghajian*  
\_\_\_\_\_  
\_\_\_\_\_

*Ben Q. Adair*  
\_\_\_\_\_  
\_\_\_\_\_

*Thomas C. Collins*  
\_\_\_\_\_  
Dean of the Graduate College

## PREFACE

In this study, the derivation of the correlation transfer equation (CTE) governing the temporal field correlation function for multiple scattering of light through suspensions of diffusing particles is presented. It was shown here that there exists a formal similarity between the CTE and the radiative transfer equation (RTE). Several radiative transfer solution techniques (approximate and exact) were applied to obtain solutions for the field correlation function in isotropic and anisotropic one-dimensional media subjected to either natural or polarized radiation.

I am deeply grateful to my major advisor, Dr. Ronald L. Dougherty for the continuous guidance, support and encouragement he has given me throughout my graduate work.

I am also indebted for comments and advice on various topics related to this work to Dr. Bruce J. Ackerson. I also wish to thank Dr. Afshin J. Ghajar and Dr. Frank W. Chambers for the trust they gave me and for their gracious help.

My warm thanks go to Farhad Dorri-Nowkooorani, Ulf Nobbmann, Cho-Chun Liu, and Y. Tian for their invaluable contributions and assistance. Special thanks go to all the

faculty and staff of the Mechanical and Aerospace Engineering department.

Finally, and most important, I must thank my father Mohammed and my mother Meriam, whose loving encouragement and support enabled me to bring this project to completion.

## TABLE OF CONTENTS

Chapter	page
I. INTRODUCTION .....	1
II. LITERATURE REVIEW .....	5
II.1. General Introduction .....	5
II.2. Radiative Transfer Solution Methods .....	7
II.3. Dynamic Light Scattering .....	9
II.4. Multiple Scattering .....	11
II.5. Applications .....	13
III. FROM SINGLE TO MULTIPLE SCATTERING .....	16
III.1. Single Scattering Photon Correlation Theory .....	16
III.2. Multiple Scattering Theory.....	20
III.2.a. Foldy-Twersky Integral Equation for the Average Field .....	21
III.2.b. Integral Equation for the Field Spatial Correlation Function ...	26
IV. DEVELOPMENT OF THE FIELD CORRELATION TRANSFER EQUATION .....	32
IV.1. The Mutual Coherence Function for Diffusing Particles .....	33
IV.2. The Correlation Transfer Equation for Diffusing Particles .....	36
V. APPROXIMATE SOLUTION METHODS .....	44
V.1. Isotropic Scattering From Plane Parallel Media .....	44
V.1.a. Preaveraging .....	48
V.1.a.i. Exact Numerical Solution ...	53
V.1.a.ii. Exponential Kernel Approximation .....	55
V.1.b. Legendre Expansion of $g^1$ .....	63
V.2. Anisotropic Scattering .....	66
V.2.a. Legendre Expansion .....	67
V.2.b. Diffusion Approximation .....	70

Chapter	page
V.2.b.i. Plane Wave Incident Normal To Slab Containing Isotropic Pure Scatterers .....	76
VI. POLARIZED LIGHT AND THE EQUATION OF CORRELATION TRANSFER .....	83
VI.1. Fundamentals of Polarized Light .....	84
VI.2. Spherical Harmonics Expansion .....	88
VI.2.a. Diffuse Intensity Vector .....	90
VI.2.b. The Basic Scattering Constants .	91
VI.2.c. Azimuthally Symmetric Radiation	93
VI.2.d. The $P_1$ Approximation With Rayleigh Scattering .....	96
VII. RESULTS AND DISCUSSION .....	108
VII.1. Comparison With Diffuse Wave Spectroscopy	110
VII.2. Results With the Legendre Expansion of $g^1$	114
VII.2.a. Effect of Optical Thickness ...	118
VII.2.b. Comparison of the CTE to the Very Thin Limit Results .....	119
VII.3. Preaveraging and Off-angle Detection ....	120
VII.4. Comparison With Experimental Data; Index of Refraction and Anisotropy Effects ....	121
VII.5. Polarization Effects .....	122
VII.6. Extensions .....	126
VIII. CONCLUSIONS AND RECOMMENDATIONS .....	177
VIII 1. Conclusions .....	177
VIII.2. Recommendations .....	182
REFERENCES .....	185
APPENDIX A. MODIFIED BESSEL FUNCTIONS .....	197
APPENDIX B. EXPANSION OF THE PHASE MATRIX ELEMENTS ....	200
APPENDIX C. SPHERICAL AND GENERALIZED SPHERICAL HARMONIC FUNCTIONS .....	202
C.I. Legendre and Associated Legendre Functions .....	202
C.II. Generalized Spherical Functions .....	203
APPENDIX D. RECURSIVE RELATIONS FOR THE MATRICES	

Chapter	page
$\Pi_1^m(\mu)$ AND $P_1(\mu)$ .....	207
D.I. The $\Pi_1^m(\mu)$ Matrices .....	207
D.II. The $P_1^m(\mu)$ Matrices .....	210
APPENDIX E. FORWARD SCATTERING APPROXIMATION .....	212
APPENDIX F. SPHERICAL HARMONIC SOLUTIONS TO CTE .....	214
F.I. Non-Polarized Radiation .....	214
F.I.a. Two-Moment Expansion of $G^m$ .....	216
F.I.b. Gaussian Phase Function .....	218
F.II. Polarized Radiation with Rayleigh Scattering .....	219
F.II.a. Two-Moment Expansion .....	223
APPENDIX G. SPHERICAL HARMONICS .....	226
G.I. Definitions .....	226
G.II. Spherical Harmonics and the Transformation Matrix .....	229

## LIST OF FIGURES

Figure	Page
1. The Scattering Geometry .....	128
2. Scattering From a Moving Particle.....	129
3. Rotation of the l and r Axes.....	130
4. Transformation Between the Plane of Scattering and the Meridian Planes.....	131
5. Comparison Between DWS and EKA for the Transmitted Correlation Function For Different Optical Thicknesses.....	132
6. Single Scattering Field Correlation Function as a Function of the Scattering Angle and the Delay Time.....	133
7. Comparison of DWS, Preaveraged CTE, 1TL, 2TL, and 3TL for the Back-Scattered Correlation Function From A Semi-Infinite Medium.....	134
8. Comparison of DWS and 3TL For The Back-Scattered Correlation Function From A Semi-Infinite Medium.....	135
9. Comparison of 3TL and DWS For The Back-Scattered Correlation Function For Different Optical Thicknesses And Deposition Lengths.....	136
10. Comparison of 3TL and DWS For The Transmitted Correlation Function For Different Optical Thicknesses And Deposition Lengths.....	137
11. Comparison of 3TL, DCT and DWS For The Transmitted Correlation Function From A Medium With An Optical Thickness of L=10 (The Asymmetry Factor, f, for DCT Is Taken As Zero) .....	138
12. Comparison of 3TL, DCT and DWS For The Transmitted Correlation Function From A Medium With An Optical Thickness of L=10 (The Asymmetry Factor, f, for DCT Is Taken As Zero) .....	139



Figure	Page
13. Percent Relative Error Between $g^1$ And Its 3TL Approximation.....	140
14. Percent Relative Error Between $g^1$ And Its 8TL Approximation.....	141
15. Comparison of the Back-Scattered Correlation Function From A Semi-Infinite Medium for The Preaveraged CTE, 1TL, 2TL, and 3TL.....	142
16. Comparison of 3TL and EKA For The Back-Scattered Correlation Function For Different Optical Thicknesses.....	143
17. Comparison of 3TL and EKA For The Transmitted Correlation Function For Different Optical Thicknesses.....	144
18. Comparison of 3TL and EKA For The Transmitted Correlation Function For Different High Optical Thicknesses.....	145
19. Comparison of The Preaveraged CTE, The 1TL, The 2TL, and The 3TL For The Back-Scattered Correlation Function From A Medium With An Optical Thickness $L=25$ .....	146
20. Comparison of The Preaveraged CTE, The 1TL, The 2TL, and The 3TL For The Transmitted Correlation Function From A Medium With An Optical Thickness $L=25$ .....	147
21a. Comparison of The 3TL and The 8TL For The Transmitted Correlation Function For Different Optical Thicknesses Showing Several Orders of Magnitude of The Decay of The Correlation Function.....	148
21b. Comparison of The 3TL and The 8TL For The Transmitted Correlation Function For Different Optical Thicknesses Showing Few Orders of Magnitude of The Decay of The Correlation Function.....	149
22. Comparison of The 3TL and The 8TL For The Back-Scattered Correlation Function For Different Optical Thicknesses ( $\mu=1$ ).....	150
23. Effect of The Optical Thickness and The Delay Time on The Decay Rate of The Transmitted 3TL Correlation Function Plotted on A Base 10 Log Scale.....	151

Figure	Page
24. Effect of The Optical Thickness and The Delay Time on The Decay Rate of The Back-Scattered 3TL Correlation Function Plotted on A Base 10 Log Scale .....	152
25a. Effect of The Optical Thickness on The Decay Rate of The Back-Scattered 3TL Correlation Function Plotted Versus A Linear Non-Dimensional Delay Time.....	153
25b. Effect of The Optical Thickness on The Decay Rate of The Back-Scattered 3TL Correlation Function Plotted Versus The Square Root of The Non-Dimensional Delay Time.....	154
26a. Effect of Low Optical Thickness on The Decay Rate of The Transmitted 3TL Correlation Function Plotted Versus The Square Root of The Non-Dimensional Delay Time.....	155
26b. Effect of High Optical Thickness on The Decay Rate of The Transmitted 3TL Correlation Function Plotted Versus The Square Root of The Non-Dimensional Delay Time.....	156
27. Comparison of The 3TL With The Analytic Form of $g^1$ For The Back-Scattered Correlation Function For Different Very Low Optical Thicknesses....	157
28. Comparison of The 8TL With The Analytic Form of $g^1$ For The Transmitted Correlation Function at Different Exit Angles From A Medium With an Optical Thickness $L= 0.001$ and Plotted on A Base 10 Log Scale.....	158
29. Comparison of The 8TL With The Analytic Form of $g^1$ For The Back-Scattered Correlation Function at Different Exit Angles From A Medium With an Optical Thickness $L= 0.001$ and Plotted on A Base 10 Log Scale.....	159
30. Comparison of The 3TL With The Analytic Form of $g^1$ For The Back-Scattered Correlation Function at $\mu=0.985$ (10 Deg.) For Different Low Optical Thicknesses and Plotted on A Base 10 Log Scale .....	160
31. Effect of Different Detection Angles On The Back-Scattered Correlation Function From A Medium With An Optical Thickness $L=10$ . The Results Were Obtained From The Isotropic Preaveraged CTE.....	161

32. Comparison Between Theory And Experimental Data For The Back-Scattered Correlation Function From Media With Different Optical Thicknesses Containing  $0.3\mu\text{m}$  Polystyrene Particles. The Preaveraged Isotropic CTE With No Index of Refraction Change At The Boundaries Is Used... 162
33. Comparison Between Theory And Experimental Data For The Back-Scattered Correlation Function From Media With Different Optical Thicknesses Containing  $0.3\mu\text{m}$  Polystyrene Particles. The Preaveraged CTE Using The Forward Approximation (With  $f=0.727$ ) And An Index of Refraction Change ( $n=1.33$ ) At The Top Boundary Are Used.. 163
34. Comparison Between Theory And Experimental Data For The Transmitted Correlation Function From Media With Different Optical Thicknesses Containing  $0.3\mu\text{m}$  Polystyrene Particles. The Preaveraged Isotropic CTE With No Index of Refraction Change At The Boundaries Is Used... 164
35. Comparison Between Theory And Experimental Data For The Transmitted Correlation Function From Media With Different Optical Thicknesses Containing  $0.3\mu\text{m}$  Polystyrene Particles. The Preaveraged CTE Using The Forward Approximation (With  $f=0.727$ ) And An Index of Refraction Change ( $n=1.33$ ) At The Top Boundary Are Used.. 165
36. Comparison Between Theory And Experimental Data For The Back-Scattered Correlation Function From A Semi-Infinite Medium Containing  $0.3\mu\text{m}$  Polystyrene Particles. The 3TL And DWS With Different Deposition Length Values Are Used... 166
37. Comparison Between Theory And Experimental Data For The Transmitted Correlation Function At Different Exit Angles From A Medium With An Optical Thicknesses  $L= 10$ , Containing  $0.3\mu\text{m}$  Polystyrene Particles. The Preaveraged CTE Using The Forward Approximation (With  $f=0.727$ ) And An Index of Refraction Change ( $n=1.33$ ) At The Top Boundary Are Used..... 167
38. Comparison of The Scalar CTE, Using The 3TL, The  $P_1$  and The  $P_0$  Approximations, With The Polarized CTE, With Rayleigh Scattering Using The  $P_1$  Approximation With Unpolarized Boundary Condition, For The Back-Scattered Correlation Function From A Medium With An Optical Thickness  $L=20$ ..... 168

Figure	Page
39. Comparison of The Scalar CTE, Using The 3TL And The $P_1$ Approximation, With The Polarized CTE, With Rayleigh Scattering Using The $P_1$ Approximation With Unpolarized Boundary Condition, For The Transmitted Correlation Function From A Medium With An Optical Thickness $L=20$ .....	169
40a. Comparison of The Scalar CTE, Using The 3TL, The $P_1$ and The $P_0$ Approximations, With The Polarized CTE, With Rayleigh Scattering Using The $P_1$ Approximation With Unpolarized Boundary Condition, For The Back-Scattered Correlation Function From A Medium With An Optical Thickness $L=5$ ; Showing The Long Time Behavior.	170
40b. Comparison of The Scalar CTE, Using The 3TL, The $P_1$ and The $P_0$ Approximations, With The Polarized CTE, With Rayleigh Scattering Using The $P_1$ Approximation With Unpolarized Boundary Condition, For The Back-Scattered Correlation Function From A Medium With An Optical Thickness $L=5$ ; Showing The Short Time Behavior	171
41a. Comparison of The Scalar CTE, Using The 3TL, And The $P_1$ Approximation (For Isotropic And Rayleigh Scattering) With The Polarized CTE, With Rayleigh Scattering Using The $P_1$ Approximation With Unpolarized Boundary Condition, For The Transmitted Correlation Function From A Medium With An Optical Thickness $L=5$ ; Showing The Long Time Behavior.....	172
41b. Comparison of The Scalar CTE, Using The 3TL, And The $P_1$ Approximation (For Isotropic And Rayleigh Scattering) With The Polarized CTE, With Rayleigh Scattering Using The $P_1$ Approximation With Unpolarized Boundary Condition, For The Transmitted Correlation Function From A Medium With An Optical Thickness $L=5$ ; Showing The Short Time Behavior.....	173
42. Comparison of The Scalar CTE, Using The 3TL And The Modified $P_1$ Approximation, With The Polarized CTE, With Rayleigh Scattering Using The $P_1$ Approximation With Unpolarized Boundary Condition, For The Back-Scattered Correlation Function From A Medium With An Optical Thickness $L=1$ .....	174

43. Comparison of The Scalar CTE, Using The 3TL, The  $P_1$  And The Modified  $P_1$  Approximations, With The Polarized CTE, With Rayleigh Scattering Using The  $P_1$  Approximation With Unpolarized Boundary Condition, For Transmitted Correlation Function From A Medium With An Optical Thickness  $L=1$ ..... 175
44. Effect of Movement Constraints On Diffusing Particles (Stiffness, As In Gels) On The Back-Scattered Correlation Function From A Semi-Infinite Medium Using The 3TL..... 176

## NOMENCLATURE

A	constant, Eq. (96)
$A_i$	delay-time dependent coefficient matrix (Eq. (213))
$\mathbb{A}$	matrix defined by Eq. (186)
$a_i$	coefficients in the phase matrix, Eqs. (B1)-(B4)
$b_i$	coefficient of the phase matrix, $i=1,2$ , Eqs. (B5)-(B6)
$a_{ij}^{01}$	element (i,j) of the matrix given by $A_0 A_1$
$a_{ij}^{-1}$	element (i,j) of the matrix given by $A^{-1}$
a, b	coefficients in the exponential kernel approximation
B	fundamental source function, Eq. (75)
$\mathbb{B}_i$	Greek constants matrix, defined by Eq. (189)
C	intensity correlation function
$C_i$	constant coefficient of the vector C, $i=1,2,3,4$
$C_a$	absorption cross section ( $m^2$ )
$C_d$	differential scattering cross section ( $m^2/sr$ )
$C_s$	scattering cross section ( $m^2$ )
$C_t$	total cross section, $C_a + C_s$ ( $m^2$ )
$\mathbb{C}$	matrix defined by Eq. (185a)
c	speed of light in the medium (m/sec)
$\mathbb{D}_1$	= diag{1,0,0,0}
$\mathbb{D}_2$	= diag{1,1,-1,-1}
$\mathbb{D}_3$	= diag{1,0}
D	constant, Eq. (153)
$D_0$	diffusion constant of single particles in the medium ( $m^2/s$ )
d	typical dimension of a particle; diameter for a sphere (m)
$d_1$	constant defined by Eq. (222)
$d_2$	constant defined by Eq. (223)
E	scalar electric field (N/C)
$E^a =$	$E(r_a, t_a)$ , scalar electric field at a location $r_a$ and time $t_a$ (N/C)

$\mathbb{E}^s = E(\mathbf{r}_s, t_s)$ , effective field incident upon the scatterer 's' after being scattered from all other particles (not including the incident field) (N/C)  
 $E_{\text{inc}}^a = E_{\text{inc}}(\mathbf{r}_a, t_a)$ , incident wave at  $\mathbf{r}_a$  and time  $t_a$  (N/C)  
 $E_n$  exponential integral,  $n=1,2,\dots$ , Eq. (73)  
 $\mathbb{F}$  attenuated flux vector, defined Eq. (192)  
 $\mathbf{F}$  flux vector =  $[F_I, F_Q, F_U, F_V]^T$   
 $F$  flux vector magnitude  
 $F_0^{1,r}$  constant defined by Eq. (229b)  
 $f$  asymmetry factor  
 $\mathbf{f}$  electric field scattering function  
 $f = |\mathbf{f}|$   
 $\mathbb{G}$  expansion coefficient matrix, Eq. (212)  
 $G^m$  unnormalized multiple scattering field correlation function  
 $\mathbf{G}^m$  unnormalized multiple scattering field correlation vector  
 $g^m$  normalized multiple scattering field correlation function  
 $g^1$  normalized single scattering field correlation function  
 $\mathbb{H}$  matrix defined by Eq. (234)  
 $H$  t-dependent phase function normalized to 1  
 $H_0^{1,r}$  constant defined by Eq. (229a)  
 $h = 2I^1(\tau)/3$   
 $h_i^\pm$  defined in Eqs. (100)-(107),  $i=1,2,3,4$   
 $I$  specific intensity of radiation ( $\text{Wm}^{-2}\text{sr}^{-1}\text{Hz}^{-1}$ )  
 $\mathcal{I}$  intensity of a polarized beam,  $= I_1 + I_r$  ( $\text{Wm}^{-2}\text{sr}^{-1}\text{Hz}^{-1}$ )  
 $I_1$  parallel component of polarized intensity ( $\text{Wm}^{-2}\text{sr}^{-1}\text{Hz}^{-1}$ )  
 $I_r$  perpendicular component of polarized intensity ( $\text{Wm}^{-2}\text{Hz}^{-1}/\text{sr}$ )  
 $I_0$  magnitude of the incident radiation ( $\text{Wm}^{-2}\text{sr}^{-1}\text{Hz}^{-1}$ )  
 $I_{i+\frac{1}{2}}$  modified Bessel function  
 $I_{\text{inc}}$  incident radiation ( $\text{Wm}^{-2}\text{sr}^{-1}\text{Hz}^{-1}$ )  
 $i = \sqrt{-1}$

$J_i$	matrix coefficient defined by Eq. (D21)
$J$	number of Legendre terms in a specific expansion
$K_i$	matrix coefficient defined by Eq. (D20)
$K$	the medium's effective wave number ( $m^{-1}$ ), $=  K $
$\mathbf{K}$	the medium's effective wave vector ( $m^{-1}$ )
$k$	the medium's wave number ( $m^{-1}$ ), $=  \mathbf{k} $
$\mathbf{k}$	the medium's wave vector
$k_0$	wave number outside the medium ( $m^{-1}$ )
$k_B$	Boltzmann's constant, $= 1.3806 \times 10^{-23}$ J/K
$L$	optical thickness of the medium
$L_k$	physical thickness of the medium (m)
$l$	mean free path (m)
$l^*$	transport mean free path (m)
$l^{\dagger}$	delay-time dependent mean free path (m), Eq. (147)
$M(\varphi)$	linear transformation matrix, defined by Eq. (180)
$N$	number of particles in the scattering volume
$n$	index of refraction
$\hat{n}$	unit vector normal to the surface of the medium
$O$	origin of the coordinate system (see Fig. 4)
$P_i$	$= \text{diag} \{P_i(\mu), R_i(\mu)\}$
$P$	phase function (or form factor), normalized to 1
$\mathbf{P}$	phase matrix for the vector (polarized) CTE
$P_i$	Legendre polynomials of order $i$
$P_i^m$	associated Legendre function of order $i$
$p_1$	cosine average of the correlated phase function, Eq. (141)
$Q$	second Stokes parameter, $= I_1 - I_r$
$Q_0$	defined by Eq. (154)
$Q_1$	defined by Eq. (148)
$Q_1$	$= Q_1 \cdot \hat{\Omega}_z$ , defined by Eq. (156)
$Q_c$	source term, defined by Eq. (132)
$q$	$=  \mathbf{q} $
$\mathbf{q}$	wave vector representing momentum transfer
$R$	scattering matrix defined by Eq. (181)
$R$	$=  \mathbf{r} - \mathbf{r}_s $ (m)
$R_i^m$	related to the associated Legendre function of order $i$



$\bar{r}$  average between two observation vectors,  $=(\mathbf{r}_a + \mathbf{r}_b)/2$  (m)  
 $\mathbf{r}_a$  position vector between scatterers (m)  
 $\mathbf{r}_d$  difference between the coordinates of observation points; a position vector in the scattering medium,  $= (\mathbf{r}_a - \mathbf{r}_b)$  (m)  
 $\mathbf{r}_s$  average vector between two locations of a single scatterer,  $= (\mathbf{r}_{s'} + \mathbf{r}_{s''})/2$  (m)  
 $\mathbf{r}_{sd}$  difference vector between two locations of a single scatterer,  $= (\mathbf{r}_{s'} - \mathbf{r}_{s''})$  (m)  
 $S$  source function of the CTE  
 $\mathcal{S}$  matrix defined by Eq. (185b)  
 $T$  temperature (K)  
 $T_1$  reference point (see Fig. 4)  
 $T_2$  reference point (see Fig. 4)  
 $T_1^m$  related to the associated Legendre polynomials  
 $t$  real time (s)  
 $\tau$   $= 2\tau/\tau_0$ , nondimensional delay-time (correlation time)  
 $U(\mathbf{r})$  total energy density at  $\mathbf{r}$  ( $\text{Wm}^{-1}\text{sr}^{-1}\text{Hz}^{-1}$ )  
 $\mathcal{U}$  operator defined in Eq. (38)  
 $\mathcal{U}$  third Stokes parameter, defined in Eq. (176)  
 $u_s^a$  operator that represents the scattering characteristics of the particle located at  $\mathbf{r}_s$  as observed at  $\mathbf{r}_a$ ,  $\equiv u(\mathbf{r}_a - \mathbf{r}_s)$   
 $V$  the scattering volume ( $\text{m}^3$ )  
 $\mathbf{V}$  velocity of the particles in the medium (m/s)  
 $\mathcal{W}$  operator defined in Eq. (40)  
 $\mathbf{V}_f$  velocity fluctuation of the particles (m/s)  
 $\mathcal{V}$  fourth Stokes parameter, defined by Eq. (177)  
 $v_s^a$  operator that represents the scattering process from scatterer 's' to a location 'a' going through various scatterers,  $\equiv v(\mathbf{r}_a - \mathbf{r}_s)$   
 $w$  single particle probability density function  
 $Y_1^m$  matrix coefficient defined by Eqs. (D6) and (D11)  
 $W_i$  matrix coefficient defined by Eq. (D12)  
 $\mathbf{W}$  ( $= W_{ij}$ ) defined by Eqs. (233)  
 $X_1^m$  matrix coefficient defined by Eq. (D5) and (D10)

$x_i$  coefficient in the Legendre expansion  
 $y_i$  coefficient in the Legendre expansion with Rayleigh law  
 $Z$  defined by Eq. (209b)  
 $Z$  reference point (see Fig. 4)  
 $z$  optical depth in plane-parallel media  
 $z_k$  physical depth in plane-parallel media (m)  
 $z_0$  deposition length in DWS theory (m)

#### Greek

$\alpha_i$  defined by Eq. (194f)  
 $\beta$  arctangent of the ratio of the axes of the ellipse of polarization  
 $\beta_i$  defined by Eq. (194a)  
 $\Gamma$  mutual coherence function  
 $\gamma_i$  defined by Eq. (194c)  
 $\Delta$  defined by Eq. (175)  
 $\delta$  Dirac delta function  
 $\delta_i$  defined by Eq. (194b)  
 $\epsilon_i$  defined by Eq. (194d)  
 $\zeta_i$  defined by Eq. (194e)  
 $\eta$  viscosity of the solvent (N-s/m<sup>2</sup>)  
 $\Theta$  angle between incident and scattered intensity (rad)  
 $\theta$  polar angle with respect to the z axis (rad)  
 $\kappa$  proportionality constant, Eq. (2)  
 $\Lambda$  defined by Eq. (226)  
 $\lambda$  wavelength of the wave in the medium (m)  
 $\lambda_0$  wavelength of the incident wave (m)  
 $\mu$  cosine of the polar angle, =  $\cos(\theta)$   
 $\mu_s$  cosine of the scattering angle, =  $\cos(\Theta)$   
 $\mu_0$  cosine of the polar angle of incident radiation,  
 =  $\cos(\theta_0)$   
 $\nu$  constant defined in Eq. (92)  
 $\Pi$  matrix defined by Eq. (188)  
 $\rho(\mathbf{r})$  number density, number of scatterers per unit volume  
 around  $\mathbf{r}$  (m<sup>-3</sup>)  
 $\rho_L$  Lambert reflection coefficient

$\psi$  constant defined by eq. (91)  
 $\Sigma$  stiffness coefficient for a gel  
 $\sigma_a$  absorption coefficient,  $= \rho C_a$  ( $m^{-1}$ )  
 $\sigma_t$  extinction coefficient  
 $= \sigma_a + \sigma_s$  for time invariant particles  
 $= \sigma_s(2-a_0(t))$  for moving particles in the preaveraged CTE  
 $\sigma_s$  scattering coefficient,  $= \rho C_s$  ( $m^{-1}$ )  
 $\sigma_t$  extinction coefficient,  $= \sigma_a + \sigma_s$  ( $m^{-1}$ )  
 $\tau$  correlation delay time (s)  
 $\tau_0$  correlation delay time constant,  $1/D_0 k_0^2$  (s)  
 $\Phi$  product of the phase function and  $g^1$ , Eq. (116)  
 $\phi$  azimuthal angle (rad)  
 $\chi$  angle between the principle axis of the polarization ellipse and the direction  $l$  (parallel to the scattering plane)  
 $\omega$  albedo of single scattering  
 $\omega_e$  delay-time-dependent effective albedo for a general phase function  
 $\omega_L$  delay-time-dependent effective albedo resulting from the Legendre expansion approximation  
 $\omega_p$  delay-time-dependent effective albedo resulting from the preaveraging approximation  
 $\omega_R$  delay-time-dependent effective albedo resulting from the Rayleigh phase function  
 $\omega_d$  delay-time-dependent effective albedo resulting from the diffusion approximation  
 $\hat{\Omega}$  unit vector in the scattered direction of the wave  
 $\hat{\Omega}'$  unit vector in the incident direction of the wave  
 $d\Omega$  differential solid angle around the direction  $\hat{\Omega}$  (sr)

#### Subscripts

a (or b) at the location  $r_a$  (or  $r_b$ ), a point in the medium between scatterers  
c collimated  
d diffuse term

i incoherent  
 inc incident  
 l polarization parallel to the scattering plane  
 p related to (or a result of) the preaveraged solution  
 r polarization perpendicular to the scattering plane  
 r real part of a complex number  
 t (or p) at the location  $r_t$  (or  $r_p$ ) of a point scatterer  
 in the medium  
 // polarization parallel to the scattering plane  
 ⊥ polarization perpendicular to the scattering plane

#### Superscripts

l for single scattering  
 m for multiple scattering  
 \* complex conjugate  
 ± either in the positive ( $\hat{n} \cdot \hat{\Omega} > 0$ ) or negative ( $\hat{n} \cdot \hat{\Omega} < 0$ )  
 direction

#### Symbols

$\Upsilon(\Theta) = k_0 d \sin(\Theta/2)$   
 $\varphi_{1,2}$  angle between the meridian plane  $OT_{1,2}Z$  and the  
 plane of scattering  $OT_1T_2$  (see Fig. 4)  
 $\nabla$  gradient operator  
 $\nabla^2$  Laplace operator  
 $\kappa$  defined in Eq. (219)  
 $\partial$  partial derivative  
 $\Psi$  defined in Eq. (220)  
 $\Phi$  defined in Eq. (225)  
 $\langle \rangle$  ensemble average  
 $\hat{\phantom{x}}$  unit vector  
 $\sim$  Fourier transformed  
 $-$  matrix quantity  
**Bold** vector quantity

#### Abbreviation

1TL one-term Legendre expansion of  $g^1$

2TL two-term Legendre expansion of  $g^1$   
3TL three-term Legendre expansion of  $g^1$   
CT(E) correlation transfer (equation)  
DCT diffusion approximation to CTE  
DLS dynamic light scattering  
DWS diffusive wave spectroscopy  
EKA exponential kernel approximation  
EM electromagnetic  
MCF mutual coherence function  
MS multiple scattering  
PCS photon correlation spectroscopy  
RT(E) radiative transfer (equation)  
SS single scattering

## I. INTRODUCTION

The motion of particles in fluid/particle suspensions give rise to temporal fluctuations in the intensity of multiply scattered light. The measurements of the temporal autocorrelation functions of these fluctuations contain very useful information about the dynamics of the scatterers in the medium. From the measured correlation functions, one can in principle, determine fluid/particle properties such as particle diameter, fluid viscosity and diffusion constants. These properties are very important in various fields that include engineering, physics, and bio-chemistry.

The problem however has always been the lack of a comprehensive theory that would be able to interpret and predict data obtained by various photon correlation measurements, usually referred to as Dynamic Light Scattering (DLS) techniques. The few existing theories today, namely, the single scattering and the diffusion approximations, treat only the extreme ends of the scattering orders that may exist in any fluid/particle suspension subjected to a source of radiation. On the lower end of scattering, the single scattering approximation requires the suspensions to be very dilute (optically thin) which is usually not possible for most industrial in-situ applications. On the upper (or higher) end of scattering,

the diffusion approximation is only valid for very dense (optically thick) suspensions. Thus, results for arbitrary orders of scattering could not be predicted and modeled by either of the two theories mentioned above.

In this work, a new correlation equation for the electric field temporal correlation function, termed the Correlation Transfer Equation (CTE), is developed from the multiple scattering theory for wave propagation. The derivation assumes ballistic transfer of light, in accordance with radiation transfer, and thus, results in an integral equation similar to the Radiative Transfer Equation (RTE) but with a delay-time dependent phase function.

Because of the general nature of the CTE, arbitrary orders of multiple scattering and polarization effects can be theoretically treated. Also, because of the similarities that exist between both the CTE and the RTE, radiative transfer solution methods, that are widely available, can be used to obtain results for the temporal field correlation function of light multiply-scattered from fluid/particle suspensions of arbitrary concentrations (optical thickness). The particles are assumed to be monodisperse, non-interacting and diffusing in accordance with Brownian motion.

All solution methods presented here are for plane parallel media with azimuthal symmetry subject to collimated incident radiation at one boundary. An explicit closed form solution is presented using the exponential kernel

approximation technique applied to a preaveraged CTE with isotropic scattering. Also the diffusion approximation is employed to derive a closed form solution to the CTE for optically thick media. And to investigate polarization effects for Rayleigh scattering particles, the  $P_1$  approximation is used to obtain a closed form solution for the two-component field correlation vector field in media with axial symmetry.

Exact numerical solution techniques based on a Legendre series expansion of the delay-time dependent phase function are also presented for both isotropic and anisotropic media. And Chandrasekhar's X- and Y-functions are employed to obtain exact solutions for the preaveraged isotropic CTE.

Effects of optical thickness, off-angle scattering, index of refraction, anisotropy, and polarization are investigated. Solutions that demonstrate these various effects on the transmitted and back-scattered field correlation functions are presented in graphical form. Comparisons of the different solution methods described here are also presented. In addition, CT is successfully compared to Diffusive Wave Spectroscopy in the thick limit, and to the single scattering field correlation function in the very thin limit. And finally, a particular application of CT to gel suspensions is presented to demonstrate that CT can, in principle, be extended to more general fluid/particle suspensions (other than diffusing particles).

A general review of the literature related to radiative



transfer, dynamic light scattering (DLS), and multiple scattering (MS) theory is presented in Chapter II. The fundamental theories of single and multiple scattering as they relate to this work are reviewed in Chapter III. These theories are used in Chapter IV to derive the correlation transfer equation for freely diffusing particles. Several solution methods for CTE are presented in Chapter V for the scalar CTE and in Chapter VI for the vector (polarized) CTE. Finally, Chapter VII contains results and discussion.

## CHAPTER II

### LITERATURE REVIEW

#### II.1. General Introduction

The theory of light scattering and its application extend over an enormous number of scientific and engineering fields. Any comprehensive review of the related literature requires a significant amount of time and energy and would constitute a separate area of research by itself. In this section, much attention will be given to review theoretical work concerning light scattering and the interaction of electromagnetic (EM) radiation with matter. Applications and techniques of light scattering measurements will be briefly reviewed as they do not constitute the main focus of this study.

In general, there are two classes of problems in the theory of wave-matter interactions; the direct problem and the inverse problem [Bohren and Huffman, 1983]. The direct problem consists of finding the characteristics of the waves propagating in the medium given that the incident wave and size, shape, and composition of the scatterers in the medium are known. In this case, radiative transport (RT) theory and the more rigorous multiple scattering (MS) theory provide the solution to the intensity of radiation or

electric wave fields after interacting with the medium.

Among the numerous works on the general theory of radiative transfer, I found the following books most useful: the treatise of Chandrasekhar (1960) dealing with RT in plane-parallel media, the book by Siegel and Howell (1981) on thermal radiation and heat transfer, the work of Pomraning (1973) on radiation hydrodynamics, and the radiative transfer book by Ozisik (1973). Other books that were devoted entirely to the treatment of scattering characteristics of particles of known sizes and shapes include those of Bohren and Huffman (1983), van de Hulst (1980a and 1980b), and Kerker (1969).

In general, the characteristics of the medium and the particles within it are not known *a priori*, and the focus of the investigator must then shift towards the inverse problem. Here, one tries to describe the characteristics (optical and physical) of the medium and the scattering centers in it from analyzing the scattered light.

Optical properties, such as scattering efficiency and phase function, are usually determined through radiative transfer scattering techniques. In this context, RT is concerned with the measurement of the static or mean intensity, from which, the optical thickness, absorbing and scattering coefficients, phase function, and/or index of refraction for a certain situation can be determined [Charalampopoulos and Chang, 1988, Lazaro and Lasheras, 1992, Fante, 1974, Ishimaru and Kuga, 1983].

On the other hand, physical transport properties, such as diffusion coefficient and viscosity, require dynamic light scattering (DLS) techniques, where the correlation functions, spectra, and other statistical moments of the scattered electric fields are measured [Berne and Pecora, 1976]. Combined techniques, DLS and RT extinction methods, are often used for *in situ* measurements of fluid particle suspensions [Charalampopoulos and Chang, 1988].

The relation between the direct approach and the inverse approach has been established for a few first moments of the electric field such as the mean bilinear field quantities and the intensity of radiation [Barabanenkov et al., 1971, Ishimaru, 1978b]. This relationship will be exploited in this study to combine RT and MS formalism and methods of solution with DLS requirements to derive the CTE which will allow the interpretation of data from samples of arbitrary multiple scattering orders.

Next, I will review the RT methods of solution that will be used in this study to obtain results for the CTE followed by a brief review of theoretical and experimental work being done in DLS. Literature dealing with MS will be reviewed last.

## II.2. Radiative Transfer Solution Methods

Most of the RT solution methods available deal primarily with the direct problem. Correlation transfer

theory, however, makes it relatively simple to use more elaborate RT solution methods to interpret experimental data. Some of the methods that will be used here to solve the CTE include the closed form exponential kernel approximation for semi-infinite [Armaly and Lam, 1974] and finite [Armaly and Lam, 1977] plane-parallel media. The diffusion approximation is also widely used in the radiative transfer and dynamic light scattering fields. The method has been reported by several authors including Pomraning (1973), Ishimaru (1978a), and Ozisik (1973).

Exact one-dimensional solutions for preaveraged isotropic scattering will be based on the H-function and the X- and Y-functions for the semi-infinite and the finite cases, respectively [Chandrasekhar, 1960]. Index of refraction effects for isotropic media will be handled based on Jiang's work for one dimensional media [Jiang, 1990], and on Reguigui's work for multi-layered media [Reguigui, 1990, Reguigui and Dougherty, 1992].

For anisotropic scattering, the solution to the RTE becomes much more complicated and far more elusive. In certain situations however, the anisotropic problem can be transformed into an isotropic problem by assuming a phase function that is peaked in the forward direction and superimposed on an otherwise, isotropic phase function. This is the basis for the forward scattering approximation [van de Hulst, 1980b]. In general however, this approximation fails to describe the true nature of

scattering, and an expansion of the phase function in a series of Legendre polynomials becomes the most attractive alternative [Chandrasekhar, 1960, Chu et al., 1963, Jendoubi et al., 1992, Sekera, 1963, Crosbie and Dougherty, 1980, 1983, and 1985].

When polarization effects can not be neglected, a vector solution to the CTE needs to be obtained. Chandrasekhar (1960) gave the exact solution for the parallel and perpendicular components of polarized radiation emerging from an axisymmetric plane medium. A more extensive list of polarization related literature will be included in the chapter dealing with polarization.

### II.3. Dynamic Light Scattering

Much of the theoretical work that has been done to interpret the results from DLS experiments has been limited to single scattering (the Born approximation) [Pussey and Tough, 1985, Weiner, 1984, Berne and Pecora, 1976, and Chu, 1974], and the full potential of DLS has not been fully explored due to analytical complexities. A few more elaborate routines such as the CONTIN Laplace inversion routine, MARLIN (a discrete exponential fitting program) and EXSAMP (a rapid, smoothed algorithm for Laplace inversion of the first order autocorrelation function) have been used to analyze correlation functions for complex particle size distributions [O'Hern et al., 1993, Russo et al., 1988, Provder, 1987]. Thus, optically thick samples had to be

diluted for testing which can be costly or difficult to do in some situations, or it may even change the character of the suspension.

Recently, the study of the time-dependence of intensity fluctuations in the highly multiple scattering limit, termed diffusive wave spectroscopy (DWS), has been examined both theoretically [Zhu et al., 1991, Pine et al., 1990, Wolf and Maret, 1990, MacKintosh and John, 1989, Stephen, 1988] and experimentally [Pine et al., 1990, 1988, Maret and Wolf, 1987] with success. Assuming that the propagation of light in the medium is diffusive, Stephen (1988) studied the effect of time-dependent fluctuations of the medium on the spectral intensity and the intensity fluctuations of light scattered from it. The spectral intensity in coherent back-scattering was also discussed. He observed that the relaxation time depends on the multiple-scattering paths. Thus, the scattered intensity exhibits a broad range of relaxation times, and it will not depend in an important way on the scattering angle due to multiple scattering.

From the requirements of DWS theory, it appears that DWS may not be interpreted in the intermediate scattering regime, and it remains applicable only to optically thick media (optical thickness  $> 10$ ) [Yoo et al., 1990]. Also, in the case of highly anisotropic scatterers, the diffusion model does not suffice to describe a photon's ballistic path [Middleton and Fisher, 1991], although it does attempt to correct for this by using the transport mean free path  $l^*$

[Pine *et al.*, 1990]. In addition, DWS does not take into consideration the wave number renormalization due to multiple scattering as discussed by early researchers (reviewed in the following section).

#### II.4. Multiple Scattering

Although a variety of solution techniques for the RT equation exists in the literature [Chandrasekhar, 1960, Ishimaru, 1978a], the RT approach using intensity fails to fully describe the problem of wave propagation in continuous media and media containing particles [Furustu, 1975, Wolf, 1976]. A more rigorous approach, that has been termed multiple scattering (MS) theory or analytical theory for the electric field, has been used to fully describe the wave propagation problem [Foldy, 1945, Lax, 1951, Twersky, 1964, 1962, Barabanenkov *et al.*, 1971, Furustu, 1975, Ishimaru, 1978b] where, in principle, all multiple scattering, diffraction, and interference effects can be included. However, an explicit solution still requires neglecting some of these effects [Barabanenkov, 1969]. For example, Barabanenkov *et al.* (1971) list the method of small perturbations, the method of smooth perturbations, and the parabolic equation method as examples of such approximations.

The analytical theory is based on fundamental differential equations governing field quantities and some statistical considerations. One of the earliest papers on



the subject of MS of waves was that of Foldy (1945) who solved a problem for point isotropic scatterers distributed in an uncorrelated way. However, Foldy's simplifications concerning conditional and unconditional averages still remained questionable [Barabanenkov, 1969, Twersky, 1964]. Twersky (1964) gave a more systematic description of the physical processes involved in MS, and derived integral equations for the coherent field and the mutual coherence function that are similar to those given by Foldy (1945). Subsequent papers have concentrated on deriving a generalized transport equation for the spectral density of the wave field, of which, RTE is a special case, from more rigorous arguments using the MS theory [Barabanenkov, 1969, Barabanenkov et al., 1971, Furustu, 1975, Ishimaru, 1978b]. Most of the work on field correlations that is fundamental to the MS theory dealt mainly with the diffusion approximation [Stephen, 1988] or was carried on experimentally [Pine et al., 1990, 1988, Maret and Wolf, 1987].

Work on the concept of spectral density of random wave fields, was pioneered by Barabanenkov (1969) who derived equations for the spectral field densities that satisfy a generalized transport equation. Equations for the spectral densities within and outside a plane scattering medium in the approximation of weak non-locality were also presented. Conditions were investigated under which the spectral densities as functions of the wave vector modulus lead to

the equations that could be reduced to the phenomenological transport equation (RTE). It was shown that the transport equation describes only a part of the spectrum of a random field, which had been termed the Fraunhofer part.

In the Fraunhofer limit, the effects of the spatial dispersion of the waves, spatial variation in the spectral density over an effective length scale characteristic of the spatial inhomogeneity of the medium, and diffraction effects are neglected [Barabanenkov, 1969].

### II.5. Applications

The methods of DLS and RT extinction measurements find a wide range of applications that encompass physics, chemistry, biology [Berne and Pecora, 1976], and of course, engineering [O'Hern et al., 1993, Lazaro and Lasheras, 1992, Charalampopoulos and Chang, 1988, Russo, 1988, Flower, 1983, Fisher and Krause, 1967].

From the important applications of light attenuation methods and DLS in engineering, characterization of soot particles in combustion systems take the front seat. Flower (1983) used light extinction measurements to study soot formation in premixed flames. Charalampopoulos and Chang (1988) used combined DLS and classical scattering extinction measurements to determine several optical properties of soot particles in propane/oxygen flames.

Light attenuation methods have also been used to study the mixing of two fluids [Becker et al., 1983] and a

turbulent mixing region containing a fine suspension of particles [Fisher and Krause, 1967, Lazaro and Lasheras, 1992]. In addition, photon correlation spectroscopy (PCS) was used to study the thermal stability of aviation fuels and the formation and growth of particles formed during the thermal degradation of the fuel [O'Hern et al., 1993].

An overview of the rigorous derivation of the CTE is the main subject of this work. Previously, a heuristic derivation of the CTE was presented by Ackerson *et al.* (1992) through appropriate modifications of the RTE. The rigorous derivation that will be presented here follows similar arguments used by Twersky (1964) in deriving his spatial field correlation equation for stationary particles, and by Ishimaru (1978b) in deriving the mutual coherence function (MCF) for particles moving with a constant velocity. It will be shown that the field correlation equation derived here is related to the intensity correlation function that is usually obtained in laboratory measurements.

In addition, several radiative transfer solution techniques (approximate and exact) are applied to CTE and then solved to obtain solutions for the field correlation function in isotropic and anisotropic one-dimensional media. These techniques are compared to each other. Also, a comparison of the CTE behavior in both the single scattering regime and the diffusion limit to the available theories in both of these limits is presented. The effects of the

optical thickness, scattering angle, and index of refraction on the correlation function have been investigated and will be briefly discussed in this work.

Finally, a preliminary investigation of polarized radiation and a method of solution is presented. Explicitly, the  $P_1$  approximation to the two-component correlation vector in plane symmetry is presented in closed form solution. Numerical solutions are presented in graphical form.

## CHAPTER III.

### FROM SINGLE TO MULTIPLE SCATTERING

#### III.1. Single Scattering Photon Correlation Theory

Among the most popular DLS techniques available for measurement of sub-micron diameter particles suspended in a liquid is photon correlation spectroscopy (PCS). The capability of PCS for accurate sizing of small particles is particularly important in the single scattering regime (dilute samples) since the theory for data interpretation is well developed. In this section, a brief review of the single scattering theory for an optically dilute suspension of independent, non-interacting, diffusing particles is presented.

The fluid/particle suspension is usually illuminated by a light beam consisting of plane EM waves having a wave vector  $k_0\hat{\Omega}'$  where  $k_0=2\pi n/\lambda_0$  is the wave number and  $\hat{\Omega}'$  is a unit vector in the incident direction of the beam as shown in Fig. 1. All the figures in this work are grouped together in a section that follows Chapter VII.  $n$  is the index of refraction of the solvent and  $\lambda_0$  is the wavelength of the incident beam outside the medium. The intensity is usually detected at a large distance from the scattering volume (in the far field) so that the scattered wave is

approximated by a plane wave with the same wave number  $k_0$  and travelling in a direction given by the unit vector  $\hat{\Omega}$  [Berne and Pecora, 1976]. Here it is assumed that the scattering is quasi-elastic so that frequency does not change upon scattering. The momentum transfer resulting from this scattering event is proportional to  $\mathbf{k} = k_0(\hat{\Omega} - \hat{\Omega}')$  where the magnitude of the scattering vector  $\mathbf{k}$  is given by

$$|\mathbf{k}| \equiv k = \frac{4\pi}{\lambda_0} n \sin\left(\frac{\Theta}{2}\right) = 2k_0 \sin\left(\frac{\Theta}{2}\right) \quad (1)$$

where  $\Theta$  is the scattering angle given by  $\cos(\Theta) = \hat{\Omega} \cdot \hat{\Omega}'$ .

In static measurements, the average scattered intensity in a given direction  $\hat{\Omega}$  at a location  $\mathbf{r}$ ,  $\langle I(\mathbf{r}, \hat{\Omega}, t) \rangle$ , is obtained by performing an ensemble average of the instantaneous intensity  $I(\mathbf{r}, \hat{\Omega}, t)$ . The scattered intensity is fluctuating in time ( $t$ ) due to the particles' movement in the sample. The ensemble average may be replaced by a time average for ergodic (stationary) processes [Berne and Pecora, 1976]. This average intensity is proportional to the product of the scattered electric field and its complex conjugate:

$$\langle I(\mathbf{r}, \hat{\Omega}, t) \rangle = \kappa \langle E(\mathbf{r}, \mathbf{k}, t) E^*(\mathbf{r}, \mathbf{k}, t) \rangle \quad (2)$$

where  $\mathbf{k}$  is the wave vector representing the momentum transfer after a scattering event. The proportionality constant  $\kappa$  depends on the detection area and other physical

characteristics of the detection system.

For time-independent illumination, the time dependence of the intensity (fluctuations) is due to the movement of the particles in the medium. A field correlation function ( $G^m$ ) is used to correlate the time history of the electric field to the time history of the same field shifted by a delay time  $\tau$ . Thus,

$$G^m(\mathbf{r}, \mathbf{k}, t, \tau) \equiv \langle E(\mathbf{r}, \mathbf{k}, t) E^*(\mathbf{r}, \mathbf{k}, t+\tau) \rangle \quad (3)$$

The superscript  $m$  (in Eq. (3)) is used to indicate multiple scattering. For uniform illumination and for single scattering, the correlation function becomes independent of location, and  $G^m$  will be designated by  $G^1$ . The normalized  $G^1$  with respect to its initial value at  $\tau=0$  will be designated by  $g^1$ . Note that for stationary systems,  $G^m$  does not depend on time  $t$ , rather, it is a function only of the delay time  $\tau$  and the spatial ( $\mathbf{r}$ ) and angular ( $\mathbf{k}$ ) variable.

For monodisperse, diffusing, and independent particles, the exact single scattering field correlation function is given by [Wiener, 1984]

$$g^1(\mathbf{k}, \tau) = \exp(-D_0 k^2 \tau) = \exp\left(-2\frac{\tau}{\tau_0}(1-\cos\theta)\right) \quad (4a)$$

$$= \exp(-\tau(1-\mu_s)) \quad (4b)$$

where Eq. (1) has been used,  $\tau_0$  is a characteristic time

scale defined by  $\tau_0 = 1/D_0 k_0^2$ ,  $D_0$  is the single particle diffusion coefficient and  $\mu_s = \cos\theta$ . Note that  $g^1$  depends explicitly on  $t = 2\frac{\tau}{\tau_0}$ . This notation will be used throughout the remainder of this work.

For spherical particles,  $D_0$  is given by the following Stokes-Einstein relation [Berne and Pecora, 1976]

$$D_0 = k_B T / (3\pi\eta d) \quad (5)$$

with  $k_B$  being the Boltzmann constant,  $T$  and  $\eta$  are the temperature and the viscosity of the solvent, respectively, and  $d$  is the particle's diameter.

Usually, the intensity correlation function,  $C^m(\mathbf{r}, \mathbf{k}, t, \tau) \equiv \langle I(\mathbf{r}, \hat{\Omega}, t) I(\mathbf{r}, \hat{\Omega}, t + \tau) \rangle$ , is the quantity that is obtained in actual laboratory setups, rather than  $G^m$ . These two quantities are related by the Siegert relation [Weiner, 1984]

$$G^m(\mathbf{r}, \mathbf{k}, \tau) = [C^m(\mathbf{r}, \mathbf{k}, \tau) / C^m(\mathbf{r}, \mathbf{k}, 0) - 1]^{0.5} \quad (6)$$

For single scattering ( $m=1$ ), it is assumed that the wave encounters only one single particle, and thus,  $C$  is not a function of position. Note that the  $t$ -dependence (real time) is also dropped from Eq. (6) when assuming stationary systems. It is apparent from Eqs. (1)-(6) how one or more parameters (i.e.,  $D_0$ ,  $d$ , and  $\eta$ ) can be determined from the measurement of  $g^1$  in dilute samples.



Unfortunately, in many practical applications, the suspensions are too concentrated for the single scattering approximation to remain valid. When multiple scattering is present, the scattered field at the detector is a sum of electric fields, each representing one of the possible multiple scattering paths through the scattering volume. A careful handling of these multiple scattering events becomes necessary. The physical interpretation of the multiple scattering of waves will be discussed in the following section followed by the derivation of the correlation transfer equation.

### III.2. Multiple Scattering Theory

In this section, the fundamental equations and formulations for the multiple scattering theory will be presented. Only concepts that will be directly used in Chapter IV to derive the CTE are covered here.

The RTE was derived from an energy conservation point of view. This approach results in equations that govern the intensity of radiation and the flux that give results accurate to the degree desired in most engineering situations where the intensity of radiation and/or the flux are the primary quantities of interest. However, when wave propagation is the problem of interest, this approach cannot account for the effects that take place, namely, wave interference, diffraction and dispersion. A more rigorous approach, termed multiple scattering or analytical theory,

has been used to fully describe the wave propagation problem.

In multiple scattering theory, researchers start with fundamental differential equations governing field quantities and then introduce statistical considerations to characterize the moments of the wave field. In the following section, a brief review of the derivation contained in Twersky's theory leading to the average field and the field spatial correlation will be presented. Then, it will be shown that the RTE can be derived from the multiple scattering results. This later exercise will in effect serve as a springboard later on to derive the CTE equation based on analogous arguments.

III.2.a. Foldy-Twersky Integral Equation for the Average Field: Consider a random distribution of  $N$  particles located at  $r_1, r_2, \dots, r_N$  in a scattering volume  $V$ , and consider a scalar field  $E(r_a)$ , ( $\equiv E^a$ ), that may be a rectangular component of the electric or magnetic field, at the location  $r_a$ , a point in space between the scatterers. For the remainder of this work, it will be assumed that the medium is isothermal, homogeneous, and in equilibrium. At this first stage, it will be also assumed that the field is independent of time and that it satisfies the usual wave equation [Ishimaru, 1978b]

$$(\nabla^2 + k^2)E(r_a) = 0 \quad (7)$$

where  $k$  is the wave number of the medium excluding the particles.

Theoretically, the instantaneous scattered electric field observed at  $r_a$  may be represented as a summation of the singly scattered fields from each of the particles in the scattering volume plus the incident wave at  $r_a$  ( $E_{inc}(r_a)$ ) in the absence of any particles

$$E(r_a) = E_{inc}(r_a) + \sum_{s=1}^N u_s^a E(r_s) \quad (8)$$

$u_s^a E(r_s)$  is the wave at  $r_a$  scattered from the scatterer 's' located at  $r_s$  where  $u_s^a \equiv u(r_a - r_s)$  is an operator (operating on  $E(r_s)$ ) that represents the scattering characteristics of the particle located at  $r_s$  when the field  $E(r_s)$  is incident upon it as observed at  $r_a$ . It should be noted however, according to Ishimaru (1978b) and Twersky (1962), that it is impossible to obtain the explicit exact representation of this operator, and it will be necessary to resort to approximate representations.  $E(r_s)$  is the effective field incident upon the scatterer 's', and it consists of the incident wave  $E_{inc}(r_s)$  and the waves scattered from all of the other particles except the one at  $r_s$ . Thus,  $E(r_s)$  can be represented by a summation similar to Eq. (8)

$$E(r_s) = E_{inc}(r_s) + \sum_{\substack{t=1 \\ t \neq s}}^N u_t^s E(r_t) \quad (9)$$

where  $u_t^s E(r_t)$  is the wave scattered from all particles except the one at  $r_s$ . Substituting Eq. (9) into Eq. (8) to eliminate  $E(r_s)$  and repeating the process to eliminate  $E(r_t)$  and so on, we find,

$$\begin{aligned}
 E(r_a) = & E_{\text{inc}}(r_a) + \sum_{s=1}^N u_s^a \left( E_{\text{inc}}(r_s) + \sum_{\substack{t=1 \\ t \neq s}}^N u_t^s E(r_t) \right) = E_{\text{inc}}(r_a) \\
 & + \sum_{s=1}^N u_s^a E_{\text{inc}}(r_s) + \sum_{s=1}^N \sum_{\substack{t=1 \\ t \neq s}}^N u_s^a u_t^s E_{\text{inc}}(r_t) \\
 & + \sum_{s=1}^N \sum_{\substack{t=1 \\ t \neq s}}^N \sum_{\substack{p=1 \\ p \neq t}}^N u_s^a u_t^s u_p^t E_{\text{inc}}(r_p) + \dots \quad (10)
 \end{aligned}$$

Note that the first term on the right hand side of Eq. (10) is the incident wave at  $r_a$ , the second term represents all of the single scattering, the third term represents all of the double scattering and so on. These different multiple scattering chains consist mainly of two groups: one group that represents all of the multiple scattering chains that go through a particular particle no more than once, and a second group that represents the remaining chains of multiple scattering: namely, those chains that contains paths that go through a scatterer more than once. In Twersky's theory, the second group of chains, that result mainly from back scattering, was neglected. With this

approximation in mind, Eq. (10) becomes

$$\begin{aligned}
 E(\mathbf{r}_a) = & E_{\text{inc}}(\mathbf{r}_a) + \sum_{s=1}^N u_s^a E_{\text{inc}}(\mathbf{r}_s) + \sum_{s=1}^N \sum_{\substack{t=1 \\ t \neq s}}^N u_s^a u_t^s E_{\text{inc}}(\mathbf{r}_t) \\
 & + \sum_{s=1}^N \sum_{\substack{t=1 \\ t \neq s}}^N \sum_{\substack{p=1 \\ p \neq t \\ p \neq s}}^N u_s^a u_t^s u_p^t E_{\text{inc}}(\mathbf{r}_p) + \dots
 \end{aligned} \tag{11}$$

where the scatterer 's' is now removed from the third summation, and so on. Ishimaru (1978b) has shown that the relative difference between the exact equation, Eq. (10), and its approximation, Eq. (11), varies as a function of  $(3N-5)/(N-1)^2$ . Therefore, as  $N$  becomes large, it becomes obvious that the Twersky process approaches the exact process.

The expanded representation of the field, given by Eq. (11), is useful in understanding the nature of the scattering process, but it is not easy to solve. Foldy (1945) and Twersky (1964) developed the following integral equation for the average field, also called the coherent field

$$\langle E(\mathbf{r}_a) \rangle = E_{\text{inc}}(\mathbf{r}_a) + \int u_s^a \langle E(\mathbf{r}_s) \rangle \rho(\mathbf{r}_s) d\mathbf{r}_s \tag{12}$$

where  $\rho(\mathbf{r}_s)$  is the number density of point scatterers and  $d\mathbf{r}_s$  represents a differential volume. The incident wave at  $\mathbf{r}_a$  has not suffered any scattering and therefore is

invariant under ensemble averaging. One can arrive at Eq. (12) by first noting the ensemble average definitions for non-interacting (independent) particles, all represented by the same statistical characteristics:

$$\begin{aligned} \langle E(\mathbf{r}; \mathbf{r}_1, \dots, \mathbf{r}_N) \rangle &= \int \dots \int E(\mathbf{r}; \mathbf{r}_1, \dots, \mathbf{r}_N) w(\mathbf{r}_s) \dots w(\mathbf{r}_N) d\mathbf{r}_1 \dots d\mathbf{r}_N \\ &= \int \langle E(\mathbf{r}; \mathbf{r}_1, \dots, \mathbf{r}_N) \rangle_s w(\mathbf{r}_s) d\mathbf{r}_s \end{aligned} \quad (13)$$

where  $E$  is a random function of the scattering locations  $\mathbf{r}_1 \dots \mathbf{r}_N$ , measured at location  $\mathbf{r}$  and the integration is done with respect to the variables to the right of the semicolon. The dependence of  $E$  on the scattering locations will not be shown explicitly and  $\langle E(\mathbf{r}) \rangle$  will denote  $\langle E(\mathbf{r}; \mathbf{r}_1 \dots \mathbf{r}_N) \rangle$ . The brackets with the subscript  $s$  ( $\langle \rangle_s$ ) indicate an ensemble average with respect to all locations of scatterers except the one at location  $\mathbf{r}_s$ , and  $w(\mathbf{r}_s) d\mathbf{r}_s$ , represents the probability of finding the scatterer 's' within the differential volume  $d\mathbf{r}_s$ , where  $w(\mathbf{r}_s)$  is the probability density function. If  $E$  depends on the location of only one scatterer, then Eq. (13) can be rewritten as

$$\langle E(\mathbf{r}; \mathbf{r}_s) \rangle = \int E(\mathbf{r}; \mathbf{r}_s) w(\mathbf{r}_s) d\mathbf{r}_s \quad (14a)$$

and if  $E$  depends on the location of two scatterers, then Eq. (13) can be written as

$$\langle E(\mathbf{r}; \mathbf{r}_s, \mathbf{r}_t) \rangle = \iint E(\mathbf{r}; \mathbf{r}_s, \mathbf{r}_t) w(\mathbf{r}_s) w(\mathbf{r}_t) d\mathbf{r}_s d\mathbf{r}_t \quad (14a)$$

and so on. Applying this ensemble averaging to Eq. (11), we get, in the limit  $N \rightarrow \infty$ , an iterated version of Eq. (12) [Ishimaru, 1978b], i.e.,

$$\begin{aligned} \langle E(\mathbf{r}_a) \rangle = & \\ & E_{\text{inc}}^a + \int u_s^a E_{\text{inc}}^s \rho(\mathbf{r}_s) d\mathbf{r}_s + \iint u_s^a u_t^s E_{\text{inc}}^t \rho(\mathbf{r}_s) \rho(\mathbf{r}_t) d\mathbf{r}_s d\mathbf{r}_t \\ & + \iiint u_s^a u_t^s u_m^t E_{\text{inc}}^m \rho(\mathbf{r}_s) \rho(\mathbf{r}_t) \rho(\mathbf{r}_m) d\mathbf{r}_s d\mathbf{r}_t d\mathbf{r}_m + \dots \end{aligned} \quad (15)$$

where, for suspended particles, the number density of a point scatterer is given by

$$Nw(\mathbf{r}_s) = \rho(\mathbf{r}_s) \quad (16)$$

and where the average field acting on the scatterer 's' has been approximated by the average field that would exist at the scatterer's location if the scatterer did not exist [Foldy, 1945], i.e.,  $\langle E(\mathbf{r}_s) \rangle_s \cong \langle E(\mathbf{r}_s) \rangle$ .

III.2.b. Integral Equation for the Field Spatial Correlation Function: Using a similar development as in the previous section, Twersky (1964) derived an integral equation for the spatial correlation function, (sometimes referred to as the Mutual Coherence Function, MCF), that has the following form:

$$\begin{aligned} \Gamma(\mathbf{r}_a, \mathbf{r}_b) &\equiv \langle E(\mathbf{r}_a) E^*(\mathbf{r}_b) \rangle \\ &= \langle E(\mathbf{r}_a) \rangle \langle E^*(\mathbf{r}_b) \rangle + \int v_s^a v_s^{b*} \langle |E(\mathbf{r}_s)|^2 \rangle \rho(\mathbf{r}_s) d\mathbf{r}_s \end{aligned} \quad (17)$$

where  $v_s^a$  represents the multiple scattering processes from 's' to 'a' and satisfies the following integral equation

$$v_s^a = u_s^a + \int u_t^a v_s^t \rho(r_t) dr_t \quad (18)$$

The first term on the right side of Eq. (17) represents the product of the coherent field at 'a' and the complex conjugate of the coherent field at 'b'. Equation (17) can be iterated to arrive at a form for the spatial correlation function similar to Eq. (15), which shows that the Twersky integral equation can be generated by the average of the product of  $E(r_a)$  and  $E^*(r_b)$  as given by the basic chains of scattering processes in Eq. (11). The integral equations (12) and (17) are consistent with the first order smoothing approximation to the more rigorous Dyson and Bethe-Salpeter equations, respectively [Barabanenkov et al., 1971, Twersky, 1964, Frish, 1968].

It is often more convenient to use the "center of gravity" of the observation points  $r = (r_a + r_b)/2$  and the difference between the coordinates of the observation points  $r_d = (r_a - r_b)$  as new coordinates [Stephen, 1988]. Then the MCF becomes

$$\Gamma(r, r_d) = \langle E(r + \frac{1}{2}r_d) E^*(r - \frac{1}{2}r_d) \rangle \quad (19)$$

The MCF,  $\Gamma(r, r_d)$ , can be decomposed into its Fourier components as [Stephen, 1988]



$$\Gamma(\mathbf{r}, \mathbf{r}_d) = \int \tilde{\Gamma}(\mathbf{r}, \mathbf{q}) \exp(i\mathbf{q} \cdot \mathbf{r}_d) d^3\mathbf{q} \quad (20)$$

where  $\mathbf{q}$  is a wave vector that represents the momentum transfer,  $i=\sqrt{-1}$ , and  $\tilde{\Gamma}(\mathbf{r}, \mathbf{q})$  is the spectral density of the field [Stephen, 1988]. Equation (20) is analogous to the electric field Fourier decomposition [Wolf, 1976] given by

$$\mathbf{E}(\mathbf{r}) = \int \tilde{\mathbf{E}}(\mathbf{q}) \exp(i\mathbf{q} \cdot \mathbf{r}) d^3\mathbf{q} \quad (21)$$

Note that for monochromatic waves traveling in a medium with a wave number  $k$ , only those Fourier components for which  $q^2 = k^2$  contribute to  $\mathbf{E}(\mathbf{r})$  in Eq. (21). Therefore,  $\mathbf{E}(\mathbf{r})$  can be represented by an angular spectrum of plane waves [Wolf 1976], all of the same wave number  $|\mathbf{q}|=k$ , propagating in a distribution of directions, each specified by  $\hat{\Omega}$ .

The spectral density function for time-invariant particles (not moving in the suspension),  $\tilde{\Gamma}(\mathbf{r}, \mathbf{q})$ , has also been shown [Barabanenkov, 1969] to be concentrated on the energy surface with a wave number equal to that of the free medium,  $q^2 = k^2$ . Therefore,  $\tilde{\Gamma}(\mathbf{r}, \mathbf{q})$  is related to the time-independent intensity  $I(\mathbf{r}, \hat{\Omega})$  by

$$\tilde{\Gamma}(\mathbf{r}, \mathbf{q}) \cong \delta(q-k) I(\mathbf{r}, \hat{\Omega}) / k^2 \quad (22)$$

where  $q$  ( $= |\mathbf{q}|$ ) is the modulus of the wave vector  $\mathbf{q}$  and  $\hat{\Omega}$  is the direction of propagation of the intensity. Equation (22) is valid when the medium is nearly homogeneous so that

$\Gamma(r_a, r_b)$  is weakly dependent on the vector difference ( $r_d$ ) between  $r_a$  and  $r_b$  and  $\Gamma$  is a slowly varying function of  $r$ .  $\tilde{\Gamma}(r, \mathbf{q})$  has the meaning of the energy density of the scattered field at  $r$  with a wave vector  $\mathbf{q}$ . Therefore, the total scattered energy density,  $U(r)$ , is proportional to the sum over all  $\mathbf{q}$  at  $r$ , i.e., to  $\Gamma(r, r_d=0)$ , and from Eq. (20) we find

$$U(r) \propto \Gamma(r) = \int \tilde{\Gamma}(r, \mathbf{q}) d^3\mathbf{q} \quad (23a)$$

where the proportionality constant is the inverse of the speed of light ( $c$ ). It is also known that the total energy density is related to the specific intensity by the following equation

$$U(r) = \int I(r, \hat{\Omega}) d\Omega \quad (23b)$$

Comparing Eq. (23a) with Eq. (23b) and noting that

$$d^3\mathbf{q} = q^2 dq d\Omega \quad (24)$$

where  $\mathbf{q} = q\hat{\Omega}$  and  $d\Omega$  is a differential solid angle around the direction of unit vector  $\hat{\Omega}$ , we see that  $\tilde{\Gamma}(r, \mathbf{q})$  must be given by Eq. (22).  $\tilde{\Gamma}(r, \mathbf{q})$  is the quantity that is usually obtained in the laboratory rather than  $\Gamma(r, r_d)$ .

Substituting Eq. (22) into Eq. (20), we get

$$\Gamma(\mathbf{r}, \mathbf{r}_d) = \int I(\mathbf{r}, \hat{\Omega}) \exp(ik\hat{\Omega} \cdot \mathbf{r}_d) d\Omega \quad (25)$$

Equation (25) represents the fundamental link between the multiple scattering theory and transport theory. It is important to note the major assumptions employed in order to arrive at Eq. (25) [Barabanenkov, 1969, Barabanenkov et al. 1971], mainly that of neglecting the spatial variation of the spectral field density over a typical length scale of the medium. It can be shown [Ishimaru, 1978b] that by substituting Eq. (25) into Eq. (17) and by using the far field approximation for  $v_s^a$ , one can derive the Radiative Transport (RT) equation from Eq. (17). A similar derivation will be shown later explicitly for the temporal field correlation. The resulting integral form of the RT equation is given by [Ishimaru, 1978b]

$$I(\mathbf{r}, \hat{\Omega}) = I_{\text{inc}}(\mathbf{r}, \hat{\Omega}) + \frac{1}{4\pi} \int \int I(\mathbf{r}', \hat{\Omega}') P(\hat{\Omega}, \hat{\Omega}') \exp(-\sigma_t |\mathbf{r} - \mathbf{r}'|) d\Omega' d\mathbf{r}' \quad (26)$$

where  $\sigma_t$  is the extinction coefficient, and  $P$  is the phase function which is normalized according to

$$\frac{1}{4\pi} \int_{4\pi} P(\hat{\Omega}, \hat{\Omega}') d\Omega = \frac{C_s}{C_t} = \frac{\sigma_s}{\sigma_t} \equiv \omega \quad (27)$$

where  $\omega$  is the albedo for single scattering, and  $C_s$  and  $C_t$  are the scattering and extinction cross sections, respectively, and  $\sigma_s$  and  $\sigma_t$  are the scattering and total (or

extinction) coefficients, respectively.

Note that  $\tilde{\Gamma}(r, q)$  depends both on the direction and on the modulus of the wave vector  $q$ , whereas the specific intensity ( $I(r, \hat{\Omega})$ ) depends only on a fixed modulus  $|q|$  that is equal to  $k$  and on an arbitrary ray direction  $\hat{\Omega} = k/k$ .

In the preceding sections, it was assumed that the particles are not moving (stationary), and as a consequence, the wave field was independent of time. However, in most fluid/particle suspensions, the particles are in continuous motion due mainly to thermal fluctuations. When this is the case, the scattered wave field will be a fluctuating function of time due to the continuous phase (and/or magnitude) change resulting from the particle movements. These fluctuations can be analyzed by studying the temporal field correlations. The derivation of such functions are similar, in principle, to the derivation presented here for stationary particles, with the redefinition of the averaging process and the probability density of the moving particles.

This topic will be the subject of the next chapter, where the temporal field correlation transfer equation, CTE, for diffusing particles will be derived.

## CHAPTER IV.

### DEVELOPMENT OF THE FIELD CORRELATION TRANSFER EQUATION

In Chapter III, several theories and governing equations for wave propagation in continuous media were presented. Although the arguments leading to the final equations and/or the form of these equations may be different depending on the methods and the assumptions used, and on the quantities of interest, all of them deal with the same underlying fundamental problem. It was indicated in section III.2 that the RTE can be derived from the multiple scattering theory. Similar and explicit derivations will be presented next that will lead to the temporal field correlation function ( $G^m$ ) characterizing the light that is being multiply-scattered from a medium with moving particles imbedded in it. In particular,  $G^m$  will be derived explicitly for the case of freely diffusing non-interacting particles. Other constraints on the particles in the medium, such as dependent scattering and gelling of the suspensions, will be dealt with briefly at the end of this chapter. Also, it will be assumed throughout the next section that the fields are scalars and polarization will be neglected. The polarization effects on the waves and on the field correlation function will be considered in Chapter VI.

#### IV.1. The Mutual Coherence Function For Diffusing Particles

The Mutual Coherence Function (MCF) for stationary particles is given by Eq. (17). When the particles are moving, this equation becomes correlated in time, and therefore, it needs to be modified accordingly.

Consider a single moving particle 's' with a certain velocity  $V$ , and which is located at  $r_{s''}$  at time  $t_{s''}$  and at  $r_s$ , at a later time  $t_s$ , (see Fig. 2). The scattering volume is assumed to be stationary, isothermal, and homogeneous. The scattered field from this (and other scatterers) will now be dependent on time. Let  $E(r_a, t_a)$  be the wave field at a location  $r_a$  and time  $t_a$  within the scattering volume  $V$  between the scatterers, and let  $E(r_b, t_b)$  be the field at another location  $r_b$  between scatterers at a time  $t_b$ . Let's assume at this stage that there is no correlation between moving particles in the scattering volume, and that averaging is done for a single identified particle, then Eq. (17) for the MCF can be generalized as

$$\Gamma(r_a, r_b, t_a, t_b) \equiv \langle E(r_a, t_a) E^*(r_b, t_b) \rangle = \langle E(r_a, t_a) \rangle \langle E^*(r_b, t_b) \rangle \\ + \iint V_s^a V_{s''}^{b*} \langle E(r_s, t_s) E^*(r_{s''}, t_{s''}) \rangle \rho(r_s, t_s | r_{s''}, t_{s''}) dr_s, dr_{s''} \quad (28)$$

where

$$\rho(r_s, t_s | r_{s''}, t_{s''}) = NW(r_s, t_s | r_{s''}, t_{s''}) \quad (29)$$

with  $\rho(r_s, t_s | r_{s''}, t_{s''})$  being the single particle density, and  $w$  now represents a conditional probability (as compared to Eq. (16)), i.e., given one particle at location  $r_{s''}$  and at time  $t_{s''}$ ,  $w$  is the probability of finding it at  $r_s$  at the later time  $t_s$ .

Ishimaru (1978b) presented an integral equation for the time dependent MCF similar to Eq. (28) when the particles were not correlated, but were allowed to move independently with a constant velocity  $V$  during the time  $\tau = t_s - t_{s''}$ . Therefore, the average number density of a single particle at both times and locations as the particle moves has been represented by a delta function, and Eq. (29) becomes

$$Nw(r_s, t_s | r_{s''}, t_{s''}) = \rho(r_s, t_s) \delta[(r_s - r_{s''}) - V\tau] \quad (30)$$

where  $\rho(r_s, t_s)$  represents a single particle number density associated with the field at the location  $r_s = (r_s + r_{s''})/2$  and time  $t_s = (t_s + t_{s''})/2$ . Instead of the term  $\langle E(r_s, t_s) E^*(r_{s''}, t_{s''}) \rangle$ , appearing under the integral in Eq. (28), Ishimaru (1978b) used the average square field at the average location and time,  $\langle |E(r_s, t_s)|^2 \rangle$ , and he showed that the resulting equation has an approximation of the same form as the radiative equation of transfer. It will be shown in this section that the CTE can be obtained by modifying Eq. (28) using similar approximations given by Ishimaru for moving particles.

Assuming that the particles are undergoing Brownian

motion with no correlation among them, we can represent the average number density for a single particle using the probability density for Brownian motion [Kac, 1957] as follows

$$Nw(\mathbf{r}_s, t_s, |\mathbf{r}_{s''}, t_{s''}) = \rho(\mathbf{r}_{s''}, t_{s''}) \frac{\exp(-|\mathbf{r}_{sd}|^2/4D_0\tau)}{(4\pi D_0\tau)^{3/2}} \quad (31)$$

where  $D_0$  is the diffusion coefficient of the particles in the medium,  $\tau = t_s - t_{s''}$ , and  $\mathbf{r}_{sd} = \mathbf{r}_s - \mathbf{r}_{s''}$ . Substituting Eq. (31) for  $w$  into Eq. (29) and then substituting the result back into Eq. (28), we get the following equation for the MCF for diffusing particles

$$\begin{aligned} \Gamma(\mathbf{r}, \mathbf{r}_d, t, t_d) &= \langle E(\mathbf{r} + \frac{1}{2}\mathbf{r}_d, t_a) \rangle \langle E^*(\mathbf{r} - \frac{1}{2}\mathbf{r}_d, t_b) \rangle \\ &+ \iint v_s^a, v_{s''}^{b*} \Gamma(\mathbf{r}_s, \mathbf{r}_{sd}, t_s, \tau) \rho(\mathbf{r}_{s''}, t_{s''}) \frac{\exp(-|\mathbf{r}_{sd}|^2/4D_0\tau)}{(4\pi D_0\tau)^{3/2}} d\mathbf{r}_s d\mathbf{r}_{sd} \quad (32) \end{aligned}$$

where the relative coordinates  $\mathbf{r}$  and  $\mathbf{r}_d$  were used instead of  $\mathbf{r}_a$  and  $\mathbf{r}_b$ , and  $\mathbf{r}_s (= (\mathbf{r}_s + \mathbf{r}_{s''})/2)$  were used instead of  $\mathbf{r}_s$ , and  $\mathbf{r}_{s''}$ .  $\Gamma(\mathbf{r}_s, \mathbf{r}_{sd}, t_s, \tau) = \langle E(\mathbf{r}_s + \frac{1}{2}\mathbf{r}_{sd}, t_s) \rangle \langle E^*(\mathbf{r}_s - \frac{1}{2}\mathbf{r}_{sd}, t_{s''}) \rangle$ ,  $t_d$  is the time difference at the observation locations, i.e.,  $t_d = t_a - t_b$ , and  $t$  is the average time at the observation locations, i.e.,  $t = (t_a + t_b)/2$ . Equation (32) is a general integral equation for the space and time field coherence function for diffusing particles and  $v_s^a$ , given by Eq. (18), is yet to be defined.



## IV.2 The Correlation Transfer Equation For Diffusing Particles

In the remainder of this chapter, it will be assumed that the field fluctuations are statistically stationary which is a good assumption in most practical situations [Ishimaru, 1978b]. Therefore, the MCF,  $\tilde{\Gamma}(\mathbf{r}, \mathbf{q}, t, t_d)$ , does not depend on  $t$ .

By analogy to Eq. (20), we can define a spectral density function,  $\tilde{\Gamma}(\mathbf{r}, \mathbf{q}, t_d)$ , by a Fourier decomposition of the MCF [Stephen, 1988]

$$\Gamma(\mathbf{r}, \mathbf{r}_d, t_d) = \int \tilde{\Gamma}(\mathbf{r}, \mathbf{q}, t_d) \exp(i\mathbf{q} \cdot \mathbf{r}_d) d^3\mathbf{q} \quad (33)$$

A similar equation can also be written for the product of the average field [Barabanenkov, 1969]

$$\begin{aligned} \langle E(\mathbf{r} + \frac{1}{2}\mathbf{r}_d, t_a) \rangle \langle E^*(\mathbf{r} - \frac{1}{2}\mathbf{r}_d, t_b) \rangle \\ \equiv \Gamma_{\text{inc}}(\mathbf{r}, \mathbf{r}_d, t_d) = \int \tilde{\Gamma}_{\text{inc}}(\mathbf{r}, \mathbf{q}, t_d) \exp(i\mathbf{q} \cdot \mathbf{r}_d) d^3\mathbf{q} \end{aligned} \quad (34)$$

where  $\tilde{\Gamma}_{\text{inc}}$  is the spectral field density corresponding to the average of the incident field. It can be shown that  $\tilde{\Gamma}(\mathbf{r}, \mathbf{q}, t_d)$  is related to the field correlation function  $G^m$  defined by

$$G^m(\mathbf{r}, K\hat{\Omega}, t_d) = \langle E(\mathbf{r}, K\hat{\Omega}, 0) E^*(\mathbf{r}, K\hat{\Omega}, t_d) \rangle \quad (35)$$

through an equation similar to Eq. (22), i.e.,

$$\tilde{\Gamma}(\mathbf{r}, \mathbf{q}, t_d) \cong \delta(\mathbf{q}-\mathbf{K})G^m(\mathbf{r}, K\hat{\Omega}_q, t_d)/K^2 \quad (36)$$

where  $\hat{\Omega}_q$  is the direction of propagation of the intensity and  $G^m$  is also independent of  $t$ . Using Eq. (36) in Eq. (33) and introducing spherical polar coordinates in  $\mathbf{q}$  space, i.e.,  $\mathbf{q} = q\hat{\Omega}_q$  and  $d^3q = q^2 dq d\Omega_q$ , we can write

$$\Gamma(\mathbf{r}, \mathbf{r}_d, t_d) = \int G^m(\mathbf{r}, K\hat{\Omega}_q, t_d) \exp(iK\hat{\Omega}_q \cdot \mathbf{r}_d) d\Omega_q \quad (37)$$

where the integration extends over the whole solid angle ( $4\pi$ ). Similar equations can be written for  $\Gamma(\mathbf{r}_s, \mathbf{r}_{sd}, \tau)$  and  $\tilde{\Gamma}_0(\mathbf{r}, \mathbf{r}_d, t_d)$ .

At this point, we need to turn our attention to the explicit form of the operators  $u_s^a$  and  $v_s^a$ . In Eq. (8), the wave field at  $r_a$  was symbolically represented by  $u_s^a E(\mathbf{r}_s)$ , where  $u_s^a$  is a general operator that represents the single scattering characteristics of a particle located at  $r_s$  as observed at  $r_a$ . The scattered wave (in the far field) in a direction  $\hat{\Omega}$  from a particle that is subjected to a plane wave with a unit amplitude and that is incident in the direction specified by the unit vector  $\hat{\Omega}'$  is given by [Ishimaru, 1978a, Twersky, 1962]

$$E(\mathbf{r}_s) = f(\hat{\Omega}', \hat{\Omega}) \exp(ikr_{as})/r_{as} \equiv U(r_{as}, \hat{\Omega}, \hat{\Omega}') \quad (38)$$

where  $f$  is the scattering function,  $\hat{\Omega}'$  is the incident direction to  $r_s$ , and  $r_{as}$  is the distance between the

observation point  $r_a$  and the scatterer location  $r_s$  ( $=|r_a-r_s|$ ). It should be noted here, that Eq. (38) is only valid when the distance between  $r_s$  and  $r_a$  is large enough so that the scattered wave at  $r_s$  becomes a plane wave by the time it reaches  $r_a$  (i.e.,  $r_{as} \gg d^2/\lambda$ , where  $d$  is a typical dimension of the particle, such as its diameter for a sphere, and  $\lambda$  is the wavelength in the medium). In general, however,  $E(r_s)$  is constructed of a spectrum of plane waves as given by Eq. (21), where each component is a result of Eq. (38). Therefore, combining Eq. (38) with Eq. (21), we see that  $u_s^a E(r_s)$  must be given by

$$u_s^a E(r_s) = \int U(r_{as}, \hat{\Omega}, \hat{\Omega}') \tilde{E}(q\hat{\Omega}) \exp(iq\hat{\Omega} \cdot r_s) d^3q \quad (39)$$

In the far field limit,  $v_s^a$  can also be represented by a similar expression to that of  $u_s^a$ , given by Eqs. (38) and (39). Assuming  $\rho$  is constant, the multiply scattered wave from  $r_s$  is given by [Twersky, 1962, 1964, Ishimaru, 1978b]

$$E(r_s) = f(\hat{\Omega}', \hat{\Omega}) \exp(iKr_{as})/r_{as} \equiv W(r_{as}, \hat{\Omega}, \hat{\Omega}') \quad (40)$$

where  $\hat{\Omega}'$  is the incident direction to  $r_s$ , and  $r_{as}$  is the distance between the observation point  $r_a$  and the scatterer location  $r_s$ , ( $=|r_a-r_s|$ ). It should be noted here that in Eq. (40), the wave originating at  $r_s$  arrives at  $r_a$  after being multiply scattered from other particles in the medium. This multiple scattering process is apparent in the

effective wave number ( $K$ ) appearing in Eq. (40) as opposed to the medium's wave number  $k$ , appearing in Eq. (38). In general,  $K$  is a complex number and can be approximated by [Foldy, 1945]

$$K^2 = k^2 + 4\pi\rho f(\hat{\Omega}, \hat{\Omega}) \quad (41)$$

for  $\rho$  independent of position.  $K$  represents an effective wave number, since  $v_s^a$  represents the wave propagation from 's' to 'a' through multiple scattering, whereas,  $u_s^a$  represents the single-scattered wave from 's' to 'a' propagating through the free medium. An effective wave traveling in a multiple scattering medium will satisfy the same wave equation, Eq. (7), that describes wave propagation in free (from scattering) media with an effective wave number given by Eq. (41) [Foldy, 1945]. Similar to the method for obtaining Eq. (39), and using Eqs. (40) and (20), we can write an equation for the operator  $v_s^a, v_s^{b*}$  appearing in Eq. (32) as follows

$$v_s^a, v_s^{b*} \Gamma(r_s, r_{sd}, \tau) = \int \mathbb{W}(r_{as}, \hat{\Omega}_a, \hat{\Omega}') \mathbb{W}(r_{bs}, \hat{\Omega}_b, \hat{\Omega}') \Gamma(r_s, q\hat{\Omega}', \tau) \exp(iq\hat{\Omega}' \cdot r_s) d^3q \quad (42)$$

where it was assumed that  $\hat{\Omega} \cong (\hat{\Omega}_a + \hat{\Omega}_b)/2$ . This approximation is possible because the particles are moving with a velocity negligible as compared to the speed of propagation of the wave. This also results in the approximation that  $t_d$  is on

the order of the correlation time  $\tau$ .

Using Eq. (40), we can write an equation for the product  $V_s^a, V_{s''}^{b*}$  appearing in Eq. (42) as follows

$$V_s^a, V_{s''}^{b*} \equiv V(r_{as}, \hat{\Omega}_a, \hat{\Omega}') V(r_{bs''}, \hat{\Omega}_b, \hat{\Omega}') =$$

$$f(\hat{\Omega}', \hat{\Omega}_a) f^*(\hat{\Omega}', \hat{\Omega}_b) \exp(iKr_{as}, -iKr_{bs''}) / (r_{as},) (r_{bs''}) \quad (43)$$

Equation (43) can further be simplified by noting that  $\hat{\Omega}_a \cong \hat{\Omega}$  and  $\hat{\Omega}_b \cong \hat{\Omega}$ , and similarly,  $\hat{\Omega}'_s \cong \hat{\Omega}'$  and  $\hat{\Omega}'_{s''} \cong \hat{\Omega}'$  where  $\hat{\Omega}' = (\hat{\Omega}'_s + \hat{\Omega}'_{s''})/2$ , based on the previous approximations. These approximations are valid as long as the ratio of the particle velocity to that of the speed of propagation of the wave is negligible, and  $r_{as} \gg d^2/\lambda$ , which is valid in most non-relativistic applications. Using these approximations, and noting that

$$t_d \cong \tau$$

it can be shown that [Ishimaru, 1978b]

$$K|\mathbf{r}_a - \mathbf{r}_{s'}| \cong K|\mathbf{r} - \mathbf{r}_s| + (\mathbf{r}_d - \mathbf{r}_{sd}) \cdot \hat{\Omega} \quad (44a)$$

$$K|\mathbf{r}_b - \mathbf{r}_{s''}| \cong K|\mathbf{r} - \mathbf{r}_s| - (\mathbf{r}_d - \mathbf{r}_{sd}) \cdot \hat{\Omega} \quad (44b)$$

and

$$|\mathbf{r}_a - \mathbf{r}_s|^{-1} |\mathbf{r}_b - \mathbf{r}_s|^{-1} \cong |\mathbf{r} - \mathbf{r}_s|^{-2} \quad (45)$$

When the approximations given by Eqs. (44) and (45) are put back into Eq. (43), we get

$$V_s^a, V_s^{b*} \cong \frac{C_t}{4\pi} P(\hat{\Omega}, \hat{\Omega}') \exp(iK_r \hat{\Omega} \cdot \mathbf{r}_d) \exp(-iK_r \hat{\Omega} \cdot \mathbf{r}_{sd}) \exp(-\sigma_t R) / R^2 \quad (46)$$

where the phase function  $P(\hat{\Omega}, \hat{\Omega}')$  is related to  $f$  via [Ishimaru, 1978a]

$$|f(\hat{\Omega}, \hat{\Omega}')|^2 = \frac{C_t}{4\pi} P(\hat{\Omega}, \hat{\Omega}') \quad (47)$$

and where  $\sigma_t = \rho C_t = i^{-1}(K - K^*)$  is the extinction coefficient (the second equality is the optical theorem), with the assumption that  $\rho$  is constant,  $K_r = (K + K^*)/2$ , and  $R = |\mathbf{r} - \mathbf{r}_s|$ . We need to point out here that Eq. (42) is an operator and that  $v_s^a, v_s^{b*} \Gamma(\mathbf{r}_s, \mathbf{r}_{sd}, \tau)$  under the integral in Eq. (32) is not a product of  $v_s^a, v_s^{b*}$  and  $\Gamma(\mathbf{r}_s, \mathbf{r}_{sd}, \tau)$ , but  $v_s^a, v_s^{b*}$  should represent the scattered field in the direction  $\hat{\Omega}$  as given by Eq. (42) when a spectrum of power  $\Gamma(\mathbf{r}_s, \hat{\Omega}', \tau)$  is pointed in the direction  $\hat{\Omega}'$ . Thus,  $v_s^a, v_s^{b*} \Gamma(\mathbf{r}_s, \mathbf{r}_{sd}, \tau)$  should represent the contribution from all incident directions  $\hat{\Omega}'$ ; i.e., each component  $G^m(\mathbf{r}, K\hat{\Omega}'_q, \tau)$  in Eq. (37) should produce scattering according to Eq. (46). Therefore, substituting Eq. (46) into Eq. (42) and making use of Eq. (36), where  $\hat{\Omega}_q = \hat{\Omega}'$  we

find

$$v_s^a v_s^{b*} \Gamma(\mathbf{r}_s, \mathbf{r}_{sd}, \tau) = \frac{C_t}{4\pi} \int P(\hat{\Omega}, \hat{\Omega}') G^m(\mathbf{r}, K\hat{\Omega}', \tau) \\ \times \exp(iK_r \hat{\Omega} \cdot \mathbf{r}_d) \exp[-iK_r (\hat{\Omega} - \hat{\Omega}') \cdot \mathbf{r}_{sd}] \exp(-\sigma_t R) d\hat{\Omega}' \quad (48)$$

Substituting Eqs. (37) and (48) into Eq. (32) we obtain

$$\int G^m(\mathbf{r}, K\hat{\Omega}, \tau) \exp(iK\hat{\Omega} \cdot \mathbf{r}_d) d\Omega = \\ \int G_{inc}^m(\mathbf{r}, K\hat{\Omega}, \tau) \exp(iK\hat{\Omega} \cdot \mathbf{r}_d) d\Omega + \frac{C_t}{4\pi} \iiint P(\hat{\Omega}, \hat{\Omega}') G(\mathbf{r}_s, K', \tau) \\ \times \exp(iK_r \cdot \mathbf{r}_d) \exp[-iK_r (\hat{\Omega} - \hat{\Omega}') \cdot \mathbf{r}_{sd}] \exp(-\sigma_t R) dr_s dr_{sd} d\Omega' \quad (49)$$

It should be clear that in Eq. (37)  $\hat{\Omega}_q$  is equal to  $\hat{\Omega}$  for the scattered ray and to  $\hat{\Omega}'$  for the incident ray. Finally, replacing  $dr_s$  by  $|\mathbf{r} - \mathbf{r}_s|^2 dR d\Omega$  in Eq. (49) and then removing the integrals over the solid angle  $\hat{\Omega}$  from both sides of the equation, we obtain our Correlation Transfer Equation

$$G^m(\mathbf{r}, K_r \hat{\Omega}, \tau) = G_{inc}^m(\mathbf{r}, K_r \hat{\Omega}, \tau) \\ + \frac{C_t}{4\pi} \int_{r_0}^r \int_{4\pi} P(\hat{\Omega}, \hat{\Omega}') G^m(R, K_r \hat{\Omega}', \tau) g^1[K_r (\hat{\Omega} - \hat{\Omega}'), \tau] \exp(-\sigma_t R) dR d\Omega' \quad (50)$$

where  $r_0$  is a coordinate on the boundary, and where  $g^1(\mathbf{q}, \tau)$  is the single scattering field correlation function defined as

$$g^1(\mathbf{q}, \tau) = \int \exp(-i\mathbf{q} \cdot \mathbf{r}_{sd}) \frac{\exp(-|\mathbf{r}_{sd}|^2/4D_0\tau)}{(4\pi D_0\tau)^{3/2}} d\mathbf{r}_{sd} = e^{-D_0\mathbf{q}^2\tau} \quad (51)$$

Equation (51) could have a more general form if a more general distribution function were used in Eq. (31).

Equation (50) is an integral equation for the field correlation function that is of the same form as the intensity of the radiation transfer equation, Eq. (26). The phase function is now modified by the single scattering correlation function ( $g^1$ ). Note that  $G^m$  as given by Eq. (50), reduces to the specific intensity,  $I(\mathbf{r}, \hat{\Omega})$  for zero delay time, given by Eq. (26), as expected.

Because of the formal similarity between CTE (Eq. (50)) and RTE (Eq. (26)), radiative transfer methods of solution will be used to find approximate solutions to Eq. (50). This will be the subject of the following chapter.



## CHAPTER V.

### APPROXIMATE SOLUTION METHODS

Because of the complex nature of the governing equations derived in the preceding chapter, it will be necessary to employ various approximations to obtain numerical results. Most of these solution methods have roots in the field of radiative transfer. In what follows, I will systematically cover some useful techniques that apply to different situations. These techniques will result in approximate closed form solutions, such as in the case of the exponential kernel and the diffusion approximation for the scalar CTE and the  $P_1$  approximation for the vector CTE (for polarization); or, as it is the case most of the time, other techniques will result in relatively simpler equations but still require numerical solutions.

#### V.1. Isotropic Scattering From Plane Parallel Media

For isotropic scattering ( $P(\hat{\Omega}, \hat{\Omega}') = \omega$ ) and no absorption ( $\omega=1$ ), the CT equation is given by

$$\hat{\Omega} \cdot \nabla G^m(\mathbf{r}, \hat{\Omega}, \tau) + \sigma_s G^m(\mathbf{r}, \hat{\Omega}, \tau) = \frac{\sigma_s}{4\pi} \int g^1(\hat{\Omega} \cdot \hat{\Omega}', \tau) G^m(\mathbf{r}, \hat{\Omega}', \tau) d\Omega' \quad (52)$$

where  $g^1$  was defined in Eq. (51) by  $e^{-D_0 q^2 \tau}$  and where  $\mathbf{q} = \mathbf{K}_r(\hat{\Omega} - \hat{\Omega}')$  is the effective wave vector difference between

the wave vector of the scattered wave ( $2\pi\hat{\Omega}/\lambda$ ) and the wave vector of the incident wave ( $2\pi\hat{\Omega}'/\lambda_0$ ) (see Fig. (1)). Usually, the wavelength does not change in a single scattering event (quasi-elastic scattering) [Bern and Pecora, 1976], and we will assume that this is still true for the effective wave vector  $\mathbf{q}$  [Barabanenkov et al., 1971]

$$\mathbf{q}^2 = K_r^2(\hat{\Omega}-\hat{\Omega}')^2 = 2K_r^2(1 - \hat{\Omega}\cdot\hat{\Omega}') \quad (53)$$

Therefore, the expression for  $g^1$  becomes

$$g^1(\hat{\Omega}\cdot\hat{\Omega}', \tau) = \exp\left(-2\frac{\tau}{\tau_0}(1-\hat{\Omega}\cdot\hat{\Omega}')\right) \quad (54a)$$

$$= \exp(-t(1-\mu_s)) \quad (54b)$$

where  $\tau_0=1/D_0K_r^2$  is a characteristic time constant for monodisperse independent diffusing particles and  $\mu_s = \hat{\Omega}\cdot\hat{\Omega}'$ . Equation (54b) is the same form as Eq. (4b). It is apparent here that  $g^1$  depends explicitly on  $t=2\frac{\tau}{\tau_0}$ . Therefore, for the remainder of this chapter, the delay-time variable  $t$  will be used instead of  $\tau$ .

Equation (52) is similar to the anisotropic RTE, where, because of its angular dependence,  $g^1$  behaves as a phase function. From Eq. (27), we note that phase function should satisfy the following normalization criteria

$$\frac{1}{4\pi} \int g^1(\hat{\Omega}\cdot\hat{\Omega}', t) d\Omega = \omega(t) \quad (55)$$

Substituting Eq. (54b) into Eq. (55), we find

$$\frac{1}{4\pi} \int g^1(\hat{\Omega} \cdot \hat{\Omega}', t) d\Omega = \frac{1}{2} \int_{-1}^{+1} \exp[-t(1-\mu_s)] d\mu_s = \omega_e(t) \quad (56)$$

Therefore,  $\omega_e(t)$  behaves as a delay-time-dependent albedo and is given by [Reguigui et al., 1993]

$$\omega_e(t) = (t)^{-1} \exp(-t) \sinh(t) \quad (57)$$

Note that when  $t=0$ ,  $\omega_e(0)$  reduces to one as expected for this case where we assumed perfect scattering. However, when  $t > 0$ , the effective albedo is different than one, which means that the total loss of correlation from the incident totally correlated pencil of radiation is less than the total correlation that is scattered out from the direction  $\hat{\Omega}$  (the scattering is not conservative). Therefore, due to the movement of the particles and the finite time scale on which energy is probed, an effective absorption is introduced into the system. By definition, absorption is given by

$$\sigma_a = \sigma_t - \sigma_s \quad (58)$$

where  $\sigma_a$  is the absorption coefficient. Combining Eqs. (55), (56), and (58) we find

$$\sigma_a(t) = \sigma_s \frac{1 - \omega_e(t)}{\omega_e(t)} \quad (59)$$

In deriving the cross section for a moving particle, Ishimaru (1978a) redefined the scattering cross section coefficient ( $\sigma_s$ ) as a delay time correlated coefficient. This is in perfect agreement with Eq. (59) as far as single particles are concerned. However, for multiple scattering, it is advantageous to introduce a correlated absorption whose effect is taken care of in the delay-time-dependent albedo. Otherwise, Eq. (52) will not be correct because the scattering coefficient appears on both sides of the equation, i.,e., the single scattering event on the left, and the multiple scattering integral on the right.

An exact solution to Eq. (52) does not exist in the literature. There exist however, several approximate methods where Eq. (52) can be written in a form for which a solution is found elsewhere in the literature [Chandrasekhar, 1960, Ozisik, 1973], or can be deduced from previous work [Reguigui, 1990]. In this section, I will present several of these methods, by which Eq. (52) can either be approximated by an isotropic-like equation, or by an anisotropic-like equation. For the isotropic case, the solution is widely available [Chandrasekhar, 1960, Ozisik, 1973]. For the anisotropic case, the solution is also available for few limited cases, namely, expanding  $g^1$  in a finite series of Legendre functions [Crosbie and Dougherty,

1985, Liu, 1993], or using the forward scattering approximation [van de Hulst, 1980a, 1980b]

V.1.a. Preaveraging: In a paper dealing with correlation transfer theory, the first in a series of papers presenting the theory, Ackerson et al. (1992) have employed a procedure similar to that used in the DWS approach where the averaging over angle of the single scattering correlation function ( $g^1$ ) is disconnected from the propagation/diffusion of the light. That is, averaging of the singly scattered correlation function ( $g^1$ ) over all angles will be performed before averaging  $G^m$  over all paths. This technique, termed "preaveraging", is valid for very small delay times and for large optical thicknesses, assumptions for which DWS is valid. In order to arrive at the preaveraged form of the CTE, Eq. (52) is first written as

$$\hat{\Omega} \cdot \nabla G^m(\mathbf{r}, \hat{\Omega}, t) + \sigma_s G^m(\mathbf{r}, \hat{\Omega}, t) = \frac{\sigma_s}{4\pi} \int G^m(\mathbf{r}, \hat{\Omega}', t) d\Omega' + \frac{\sigma_s}{4\pi} \int \left[ g^1(\hat{\Omega} \cdot \hat{\Omega}', t) - 1 \right] G^m(\mathbf{r}, \hat{\Omega}', t) d\Omega' \quad (60)$$

where the integral representing scattering into the  $\hat{\Omega}$  direction has been written as two integrals, in preparation for the "preaveraging". Following similar arguments used in deriving DWS theory [Pine et al., 1988], averaging of the singly scattered correlation function ( $g^1$ ) over all angles will be performed before averaging  $G^m$  over all angles (or

paths). Therefore, the last integral of Eq. (60) becomes

$$\begin{aligned} \frac{\sigma_s}{4\pi} \int \left[ g^1(\hat{\Omega} \cdot \hat{\Omega}', t) - 1 \right] G^m(\mathbf{r}, \hat{\Omega}', t) d\Omega' \\ \cong \frac{\sigma_s}{4\pi} G^m(\mathbf{r}, \hat{\Omega}, t) \int \left[ g^1(\hat{\Omega} \cdot \hat{\Omega}', t) - 1 \right] d\Omega' \end{aligned} \quad (61)$$

Putting Eq. (56) into Eq. (61) and then substituting the resulting equation into Eq. (60), we find

$$\hat{\Omega} \cdot \nabla G^m(\mathbf{r}, \hat{\Omega}, t) + \sigma_s(2 - \omega_e(t)) G^m(\mathbf{r}, \hat{\Omega}, t) = \frac{\sigma_s}{4\pi} \int G^m(\mathbf{r}, \hat{\Omega}', t) d\Omega' \quad (62)$$

or, using a transformation of coordinates to write Eq. (62) in optical coordinates, we find

$$\hat{\Omega} \cdot \nabla G^m(\sigma_t \mathbf{r}, \hat{\Omega}, t) + G^m(\sigma_t \mathbf{r}, \hat{\Omega}, t) = \frac{\omega_p}{4\pi} \int G^m(\sigma_t \mathbf{r}, \hat{\Omega}', t) d\Omega' \quad (63)$$

where

$$\sigma_t \mathbf{r} = \sigma_s [2 - \omega_e(t)] \mathbf{r} \quad (64)$$

is an effective  $t$ -dependent optical coordinate along the direction  $\mathbf{r}$  due to the preaveraging approximation, and  $\omega_p$  is the  $t$ -dependent effective albedo resulting from the preaveraging approximation. It is given by

$$\omega_p(t) = 1/[2 - \omega_e(t)] \quad (65)$$

where the subscript  $p$  is to indicate that this is an effective albedo due to the preaveraging approximation.  $\sigma_t$  is an effective extinction coefficient. Note that, for very short delay time,

$$\omega_p(t) \cong 1/(1 + t), \quad \text{for } t \ll 1.0 \quad (66)$$

This is the result for  $\omega_p$  first reported by Ackerson *et al.* (1992), where, when performing the second integral over solid angle in Eq. (61), the following approximation for  $g^1$  was used

$$\begin{aligned} g^1(\hat{\Omega} \cdot \hat{\Omega}', t) &= \exp[-t(1 - \hat{\Omega} \cdot \hat{\Omega}')] \\ &\cong 1 - t(1 - \hat{\Omega} \cdot \hat{\Omega}'), \quad \text{for } t \ll 1.0 \end{aligned} \quad (67)$$

Equation (63) is an equation similar to that for intensity in an absorbing and isotropically scattering medium for which the effective albedo and the optical distance are now  $t$ -dependent. Thus, due to this "preaveraging" approximation procedure, the CT problem, for isotropically scattering particles in a medium of a physical thickness  $L_k$  and albedo of scattering 1, is transformed into a RT problem for absorbing and isotropically scattering particles in a medium of optical thickness  $L=L_k/\omega_p$  and effective albedo  $\omega_p$  that are dependent on the delay time  $t$

( $=2\tau/\tau_0$ ). Note that when the albedo of single scattering ( $\omega$ ) is different than one, then the new effective albedo becomes  $\omega\omega_p$ .

After writing the CTE in its preaveraged form, Eq. (63), exact and approximate solutions will be developed in the following sub-sections for the case of one-dimensional plane parallel media with azimuthal symmetry. But before doing that, the formal integral equations for the solution in the case of a finite, absorbing, and isotropically scattering medium with a refractive index equal to unity need to be presented. In this case, Eq. (63) reduces to

$$\mu \frac{\partial}{\partial z} G^m(z, \mu, t) + G^m(z, \mu, t) = \frac{1}{2} \omega_p \int_{-1}^{+1} G^m(z, \mu', t) d\mu' = S(z, t) \quad (68)$$

where  $z$  is the optical distance in the  $z_k$  direction ( $z = \sigma_t z_k$ ),  $z_k$  is the physical coordinate, and  $\mu$  is the cosine of the polar angle  $\theta$  (measured from the positive direction).

If the incident radiation at  $z=0$  (totally correlated) is assumed to be collimated and independent of the azimuthal angle, i.e.,

$$G_{inc}(z=0, \mu_{out}) = I_0 \delta(\mu_{out} - \mu_0) \quad (69)$$

where  $\mu_0$  is the inclination with respect to the normal ( $z_k$  axis) of the incident radiation,  $\mu_{out}$  is the cosine the polar angle outside the medium, and  $I_0$  is the magnitude of the incident radiation, then the field correlation



distribution within the medium is governed by [Reguigui and Dougherty, 1992]

$$G^{m+}(z, \mu, t) = I_0 \delta(\mu - \mu_0) \exp(-z/\mu) + \frac{1}{\mu} \int_0^z S(z', t) \exp[-(z-z')] dz' \quad (70)$$

and

$$G^{m-}(z, \mu, t) = \frac{1}{\mu} \int_z^L S(z', t) \exp[-(z'-z)] dz' \quad (71)$$

where  $G^{m+}(z, \mu, t)$  and  $G^{m-}(z, \mu, t)$  denote the field correlation functions in the forward ( $\hat{n} \cdot \hat{\Omega} > 0$ ) and the backward ( $\hat{n} \cdot \hat{\Omega} < 0$ ) directions, respectively,  $L$  is the optical thickness of the medium ( $L = \sigma_t L_k$ ),  $\mu = \cos\theta$ , and  $S(z, t)$  is the source function governed by the following integral equation

$$S(z, t) = \frac{1}{2} \omega_p I_0 \exp(-z/\mu_0) + \frac{1}{2} \omega_p \int_0^L S(z', t) E_1(|z-z'|) dz' \quad (72)$$

The function  $E_1(z)$  is the exponential integral defined by

$$E_n(z) = \int_0^1 \exp(-z/\mu) \mu^{n-2} d\mu \quad n=1, 2, \dots \quad (73)$$

Equation (72) is a linear integral equation. Thus we can write

$$S(z, t) = \frac{1}{2} \omega_p I_0 B(z, \mu_0, t) \quad (74)$$

where  $B(z, \mu_0)$  is usually referred to as the fundamental source function and is given by

$$B(z, \mu_0, t) = \exp(-z/\mu_0) + \frac{1}{2}\omega_p \int_0^L B(z', \mu_0, t) E_1(|z-z'|) dz' \quad (75)$$

Equation (75) represents the fundamental equation that needs to be solved. Once a suitable solution for  $B$  is found, the correlation field can be computed from Eqs. (74), (70) and (71). In the next section, exact closed form solution methods for  $B$  will be presented.

V.1.a.i. Exact Numerical Solution: Most of the exact solutions to Eq. (75) (or Eq. (72)) and to Eqs. (70) and (71) are based on a successive approximation procedure. The method consists basically of finding a convergent solution for the source function (Eq. (72)) and then using it to find  $G^m$  in either direction (Eqs. (70) and (71)). The optical thickness field ( $z'$ ) is discretized into a finite number of Gaussian quadrature points ( $z_1'$ ). Then, an initial guess for the values of  $S(z_1, t)$  is obtained by performing the integration in Eq. (72) numerically. Usually the quadrature points  $z_i$  are chosen different from  $z_1'$  to avoid numerical problems. The newly obtained values of  $S(z_1, t)$  are compared to the previous values and the process is repeated until convergence to a certain tolerance limit is achieved. An interpolating procedure may be used here to find the values of  $S$  at the quadrature points  $z_1'$  from the values of  $S$  at

the quadrature points  $z_1$ . Once the solution to the source function is obtained, the values of  $G^m$  can be computed from Eqs. (70) and (71) by a straightforward numerical integration. Index of refraction effects and multi-layer effects can be easily incorporated in this scheme. This was presented in detail by Reguigui (1990) and Reguigui and Dougherty (1992).

A second widely used solution method is based on Chandrasekhar's X- and Y-functions. By discretizing the radiation angular field and then taking some analytical limits, Chandrasekhar (1960) was able to write the exact solution to Eqs. (70) and (71) at the boundaries of the slab ( $z=0$  and  $z=L$ ) in terms of general functions referred to as the X- and Y-functions (H-function for the case of semi-infinite media). These functions depend only on the variables  $\mu$  and  $L$ . In terms of the X- and Y-functions (which are delay-time dependent), the solution to Eqs. (70) and (71) is given by

$$G^{m-}(0, \mu, t) = \frac{1}{2} I_0 \omega_p \frac{\mu_0}{\mu + \mu_0} (X(\mu, t) X(\mu_0, t) - Y(\mu, t) Y(\mu_0, t)) \quad (76)$$

and

$$G^{m+}(L, \mu, t) = \frac{1}{2} I_0 \omega_p \frac{\mu_0}{\mu - \mu_0} (Y(\mu, t) X(\mu_0, t) - X(\mu, t) Y(\mu_0, t)) \quad (77)$$

Note that

$$X(\mu, t) = B(0, \mu, t) \quad (78a)$$

and

$$Y(\mu, t) = B(L, \mu, t) \quad (78b)$$

When the slab is infinitely thick ( $L \rightarrow \infty$ ) the back-scattered correlation is given by

$$G^{m-}(0, \mu, t) = \frac{1}{2} I_0 \omega_p \frac{\mu_0}{\mu + \mu_0} H(\mu, t) H(\mu_0, t) \quad (79)$$

where  $H(\mu, t) = X(\mu, t)$  when  $L \rightarrow \infty$ .

V.1.a.ii. Exponential Kernel Approximation: In the exponential kernel approximation, the exponential integral given by Eq. (73) is replaced by an approximate exponential term. After this substitution, each integral equation becomes a separable kernel type, which can be transformed into a linear, ordinary, differential equation with constant coefficients. The constants that appear in the solution are evaluated by back substituting the solution into the original integral equation and equating terms of equal powers. The exponential approximation to the exponential integral of the first order is usually given by

$$E_1(z) \cong ae^{-bz} \quad (80)$$

where  $a$  and  $b$  are two fitting constants. Usually there exist two choices for  $a$  and  $b$ . The first uses  $a=b=2$  and the second uses  $a=b=\sqrt{3}$  [Armaly and Lam, 1974, 1977]. The second choice, when used, reduces the radiative transfer equations

to the Eddington approximation [Ozisik, 1973].

When the approximation given by Eq. (80) is substituted into the fundamental source function equation, Eq. (75), we obtain

$$B(z, \mu_0, t) = \exp(-z/\mu_0) + \frac{a}{2}\omega_p \int_0^L B(z, \mu_0, t) \exp(-b|z'-z|) dz' \quad (81)$$

Taking the second derivative of Eq. (81) with respect to  $z$ , yields an ordinary differential equation for  $B$

$$\frac{\partial^2}{\partial z^2} B(z, \mu_0, t) + b(\omega_p a - b) B(z, \mu_0, t) = \left(\frac{1}{\mu_0^2} - b^2\right) e^{-z/\mu_0} \quad (82)$$

Equation (82) has two types of solutions depending on whether  $(\omega_p a - b)$  is equal to zero or not.

CASE I.  $\omega_p a = b$ :

For the special case of  $\omega_p$  equal to the ratio of  $b$  to  $a$ , Eq. (82) admits the following solution

$$B(z, \mu_0, t) = (1 - \mu_0^2 b^2) e^{-z/\mu_0} + C_1 z + C_2 \quad (83)$$

where  $C_1$  and  $C_2$  are two constants to be determined from the boundary conditions. Let's consider an infinite medium first. When  $z \rightarrow \infty$ ,  $B$  has to be finite, and therefore,  $C_1$  must be equal to zero. To determine  $C_2$ , we need to substitute the form of  $B$  given by Eq. (83) in both sides of

Eq. (81) and evaluate the result at  $z=0$ . Solving for  $C_2$ , we get

$$C_2 = b\mu_0(1 + b\mu_0) \quad (84)$$

Therefore, the approximate form of  $B$  for a semi-infinite medium with  $\omega_p=b/a$  is

$$B(z, \mu_0, t) = (1 + b\mu_0) \left[ (1 - b\mu_0) e^{-z/\mu_0} + b\mu_0 \right] \quad (85)$$

Note that when  $L \rightarrow \infty$ ,  $B(0, \mu_0, t) = H(\mu_0, t)$ , where  $B(0, \mu_0, t)$  is the fundamental source function at the top of a semi-infinite medium as defined in the previous section. Therefore, from Eq. (85), we can write an approximate solution for  $H$

$$H(\mu_0, t) \cong 1 + b\mu_0 \quad (86)$$

Since the exact numerical solution for the  $H$ -function is known [Chandrasekhar, 1960], Eq. (86) can be used to find a numerical fitting value for  $b$  (and  $a$ ) for this special case.

Next, we consider the finite case, where  $C_1$  and  $C_2$  are both different from zero. To determine these constants, we need to substitute the form of  $B$  given by Eq. (83) in both sides of Eq. (81) and evaluate the result first at  $z=0$  and

then at  $z=L$ , which gives, respectively,

$$\begin{aligned} \frac{1}{b}((1+bL)e^{-bL} - 1)C_1 + (1 + e^{-bL})C_2 \\ = b\mu_0 \left[ (1+b\mu_0) - (1-b\mu_0)\exp(-(1+b\mu_0)L/\mu_0) \right] \end{aligned} \quad (87a)$$

and

$$\begin{aligned} \frac{1}{b}(1 + bL - e^{-bL})C_1 + (1 + e^{-bL})C_2 \\ = b\mu_0 \left[ (1+b\mu_0)e^{-bL} - (1-b\mu_0)e^{-L/\mu_0} \right] \end{aligned} \quad (87b)$$

Solving Eqs. (87a) and (87b) simultaneously for  $C_1$  and  $C_2$ , we find

$$C_1 = - \frac{\mu_0 b^2}{2+bL} (1 + b\mu_0 + (1-b\mu_0)e^{-L/\mu_0}) \quad (88a)$$

and

$$C_2 = \frac{\mu_0 b}{2+bL} \left[ (1+b\mu_0)(1+bL) - (1-b\mu_0)e^{-L/\mu_0} \right] \quad (88b)$$

Finally, by substituting Eqs. (88a) and (88b) into Eq. (83), the approximate form of  $B$  for a finite medium with  $\omega_p=b/a$  is

found to be given by

$$B(z, \mu_0, t) = (1 - \mu_0^2 b^2) e^{-z/\mu_0} + \frac{\mu_0 b}{2 + bL} \left[ (1 + b\mu_0) bL + (1 - bz) (1 + b\mu_0 - (1 - b\mu_0) e^{-L/\mu_0}) \right] \quad (89)$$

Notice that  $B(z=0, \mu_0, t)$  and  $B(z=L, \mu_0, t)$ , as given by Eq. (89), are the approximate form for the  $X(\mu_0, t)$  and  $Y(\mu_0, t)$ , respectively, when  $a\omega_p = b$ . Since  $X$  and  $Y$  functions are widely available, [Chandrasekhar, 1960] this property may be used to find a nice fitting value for  $b$  (and  $a$ ).

CASE II.  $\omega_p a < b$ :

In the more general case of  $\omega_p$  not equal to the ratio of  $b$  to  $a$ , Eq. (82) admits the following solution

$$B(z, \mu_0, t) = \psi e^{-z/\mu_0} + C_1 e^{-\nu z} + C_2 e^{\nu z} \quad (90)$$

where  $C_1$  and  $C_2$  are two constants to be determined from the boundary conditions of the problem, and

$$\psi = \frac{1 - \mu_0^2 b^2}{1 - b\mu_0^2 (b - a\omega_p)} \quad (91)$$

and

$$\nu = \sqrt{b(b - a\omega_p)} \quad (92)$$



$\omega_p$  must be  $\leq b/a$  for  $\nu$  to be real.

Let's consider an infinite medium first. When  $z \rightarrow \infty$ , B has to be finite, and therefore,  $C_2$  must be equal to zero. To determine  $C_1$ , we need to substitute the form of B given by Eq. (90) in both sides of Eq. (81) and evaluate the result at  $z=0$ . Solving for  $C_1$ , we get

$$C_1 = \frac{(b+\nu)(2(1-\psi)(1+b\mu_0) - \omega_p a \psi \mu_0)}{(1+b\mu_0)(2(b+\nu) - \omega_p a)}, \quad \omega_p < \frac{b}{a}, \quad L=\infty \quad (93)$$

Next, we consider the finite case for  $\omega_p < \frac{b}{a}$ , where  $C_1$  and  $C_2$  are both different from zero. To determine these constants, we need to substitute the form of B given by Eq. (90) in both sides of Eq. (81) and evaluate the result first at  $z=0$  and then at  $z=L$ , which give, respectively,

$$\begin{aligned} \left[1 + \frac{a\omega_p}{2(b+\nu)}(e^{-(b+\nu)L} - 1)\right]C_1 + \left[1 + \frac{a\omega_p}{2(b-\nu)}(e^{-(b-\nu)L} - 1)\right]C_2 \\ = 1 - \psi - \frac{a\omega_p \psi \mu_0}{2(b\mu_0+1)}(e^{-(b\mu_0+1)L/\mu_0} - 1) \end{aligned} \quad (94a)$$

and

$$\begin{aligned} \left[e^{-\nu z_0} + \frac{a\omega_p e^{-bL}}{2(\nu-b)}(e^{-(\nu-b)L} - 1)\right]C_1 + \left[e^{\nu L} - \frac{a\omega_p e^{-bL}}{2(\nu+b)}(e^{(\nu+b)L} - 1)\right]C_2 \\ = e^{-L/\mu_0}(1-\psi) + \frac{\psi \mu_0}{(b\mu_0-1)}(e^{(b\mu_0-1)L/\mu_0} - 1) \end{aligned} \quad (94b)$$

Solving Eqs. (94a) and (94b) simultaneously for  $C_1$  and  $C_2$ , we find

$$C_{1,2} = \frac{\pm 1}{2A} \left[ (1+b\mu_0) \left(1 \pm \frac{\nu}{b}\right) e^{\pm \nu L} + (1-b\mu_0) \left(1 \mp \frac{\nu}{b}\right) (e^{-L/\mu_0}) \right] \quad (95)$$

where  $C_{1,2}$  means either  $C_1$  or  $C_2$ , and for which the upper sign or lower sign in the notations ( $\pm$  and  $\mp$ ) must be chosen for  $C_1$  or  $C_2$ , respectively. The constant  $A$  is given by

$$A = \frac{(1-\mu_0^2 \nu^2)}{b^2 \mu_0 a \omega_p} (2b\nu \cosh(\nu L) + (b^2 + \nu^2) \sinh(\nu L)) \quad (96)$$

Notice that  $B(z=0, \mu_0, t)$  and  $B(z=L, \mu_0, t)$ , as given by Eq. (90), are the approximate forms for the  $X(\mu_0, t)$  and  $Y(\mu_0, t)$ , respectively. Since  $X$  and  $Y$  functions are widely available, [Chandrasekhar, 1960], this property may be used to find nice fitting values for  $a$  and  $b$ . By setting  $z=0$  in Eq. (90), the approximate form of  $X(\mu_0, t)$  is found

$$X(\mu_0, t) = \psi +$$

$$\frac{1}{A} \left[ (1+b\mu_0) (\nu \cosh(\nu L) + \sinh(\nu L)) - \frac{\nu}{b} (1-b\mu_0) e^{-L/\mu_0} \right] \quad (97a)$$

And by setting  $z=L$  in Eq. (90), the approximate form of  $Y(\mu_0, t)$  is found

$$Y(\mu_0, t) = \psi e^{-L/\mu_0} -$$

$$\frac{1}{A} \left[ (1-b\mu_0) (\nu \cosh(\nu L) + \sinh(\nu L)) e^{-L/\mu_0} - \frac{\nu}{B} (1+b\mu_0) \right] \quad (97b)$$

Note that the solution to Eq. (68) for plane-parallel media subjected to collimated incident correlation is given by Eqs. (76) and (77) in terms of the X- and Y- functions [Chandrasekhar, 1960]. Substituting the approximate forms for X and Y, Eqs. (97a) and (97b), respectively, we find an approximate closed form solution for the multiple scattering correlation function in one-dimensional media with spherical symmetry, viz.,

$$G_p^{m\pm}(z^\pm, \mu=1, t) \cong \frac{I_0 \omega_p}{2(1-\nu^2)} \times \left[ h_1^\pm + \left( \frac{b\omega_p}{(1-\nu^2)} \right) \frac{h_2^\pm + h_3^\pm \sinh(\nu L) + h_4^\pm \cosh(\nu L)}{(2-\omega_p) \sinh(\nu L) + 2\nu \cosh(\nu L)} \right], \quad \mu_0=1 \quad (98)$$

where  $G_p^{m\pm}(z^\pm, \mu=1, t)$  stands for  $G_p^{m+}(z^+=L, \mu=1, t)$ , the transmitted correlation function at the lower boundary of the medium, or  $G_p^{m-}(z^-=0, \mu=1, t)$ , the back-scattered correlation function at the top of the medium. Both transmitted and back-scattered correlation results are given for the normal direction ( $\mu=1$ ) and for collimated intensity (correlation) of magnitude  $I_0$  incident normal ( $\mu_0=1$ ) to the upper surface of the medium with effective thickness  $L$  and

$\omega_p \neq b/a$ . The incident correlation is actually totally correlated, and it is equal to the incident intensity since it is assumed that there are no particles outside the medium.

The remaining constants in Eq. (98) are given by

$$\nu = \sqrt{b(b-a\omega_p)}, \quad \omega_p \neq b/a \quad (99)$$

$$h_1^- = (1-b^2)(1-\exp(-2L))/2 \quad (100)$$

$$h_2^- = 2\nu(b^2-1)\exp(-L)/b \quad (101)$$

$$h_3^- = (1+b)(1-\nu^2b^{-1}) + (1-b)(1+\nu^2b^{-1})\exp(-2L) \quad (102)$$

$$h_4^- = \nu(1-b^2)(1+\exp(-2L))/b \quad (103)$$

$$h_1^+ = L(1-b^2)\exp(-L) \quad (104)$$

$$h_2^+ = \nu b^{-1}(1+b)^2 + \nu b^{-1}(1-b)^2\exp(-2L) \quad (105)$$

$$h_3^+ = -2(\nu^2+1)\exp(-L) \quad (106)$$

$$h_4^+ = -2\nu(b^2+1)\exp(-L)/b \quad (107)$$

The more general form of the solution for  $\mu_0$  different than unity can be found by evaluating  $C_1$  and  $C_2$  from Eq. (95) and then using Eq. (90) to compute  $B(z, \mu_0, t)$ . Then Eqs. (70) and (71) can be used to find  $G^{m+}$  and  $G^{m-}$ .

V.1.b. Legendre Expansion of  $g^1$ : The preaveraging approximation is only good for very short delay times ( $t \ll 1.0$ ). At larger  $t$ , a better approximating method is

needed. In this section, the single scattering correlation term will be treated as an anisotropic phase function. Since  $g^1$  depends on the cosine of the scattering angle  $(\hat{\Omega} \cdot \hat{\Omega}')$  rather than on  $\hat{\Omega}$  and  $\hat{\Omega}'$  separately (see Eq. (4)), it can be expanded in a series of Legendre polynomials in a fashion similar to the radiative transfer phase function expansion [Chandrasekhar, 1960], viz.,

$$g^1(\hat{\Omega} \cdot \hat{\Omega}', t) = \omega_0(t) \left[ 1 + \sum_{i=1}^{\infty} \omega_i(t) P_i(\hat{\Omega} \cdot \hat{\Omega}') \right] \quad (108)$$

where  $\omega_0(t)$  is the first term in the Legendre expansion, and  $\omega_i(t)$  are the expansion coefficients. Note that  $\omega_0$  and  $\omega_i$  all depend on the non-dimensional delay time  $t$  ( $\equiv 2\frac{\tau}{\tau_0}$ ). Substituting Eq. (108) into Eq. (52) and using optical coordinates  $(\sigma_s r)$  for conservative scattering, i.e.,  $\sigma_t = \sigma_s$ ,  $G^m$  is found to satisfy the following integral equation

$$\hat{\Omega} \cdot \nabla G^m(\sigma_s r, \hat{\Omega}, t) + G^m(\sigma_s r, \hat{\Omega}, t) = \frac{\omega_0(t)}{4\pi} \int H(\hat{\Omega} \cdot \hat{\Omega}', t) G^m(\sigma_s r, \hat{\Omega}', t) d\Omega' \quad (109)$$

where  $H(\hat{\Omega} \cdot \hat{\Omega}', t)$  is given by

$$H(\hat{\Omega} \cdot \hat{\Omega}', t) \equiv \left[ 1 + \sum_{i=1}^{\infty} \omega_i(t) P_i(\hat{\Omega} \cdot \hat{\Omega}') \right] \quad (110)$$

Thus, it appears that, for this case of perfect scattering, the CT problem (Eq. (52)) of perfect isotropic scattering is

transformed into the corresponding absorbing and anisotropic scattering RT problem (Eq. (109)) with  $\omega_0(t)$  being treated as an effective albedo. The solution to Eq. (109) is available in the literature for a second order approximation in the series expansion given by Eq. (110) [Crosbie and Dougherty, 1978, 1983, 1985], and by a finite number of Legendre terms [Liu, 1993]. It remains now to find the expansion coefficients,  $\omega_i$ 's.

Using the following formula [Abramowitz and Stegun, 1972]

$$\exp(\mu_s t) = \sqrt{\left(\frac{\pi}{2t}\right)} \sum_{i=0}^{\infty} (2i+1) I_{i+\frac{1}{2}}(t) P_i(\mu_s) \quad (111)$$

Eq. (4b) can be written as

$$g^1(\mu_s, t) = \exp(-t) \sqrt{\left(\frac{\pi}{2t}\right)} \sum_{i=0}^{\infty} (2i+1) I_{i+\frac{1}{2}}(t) P_i(\mu_s) \quad (112)$$

where  $\mu_s \equiv \hat{\Omega} \cdot \hat{\Omega}'$ ,  $I_{i+\frac{1}{2}}$  is the modified Bessel function of order  $i+\frac{1}{2}$  and  $P_i$  is the Legendre polynomial of order  $i$ . The first seven half order modified Bessel functions ( $i+\frac{1}{2}$ ,  $i=1,2,\dots,7$ ) are given explicitly in Appendix A.

Substituting Eqs. (A22)-(A24) into Eq. (112) and comparing the resulting equation to Eq. (108) we find that

$$\omega_0(t) = t^{-1} \exp(-t) \sinh(t) \quad (113)$$

and

$$\omega_1(t) = (2i+1) \sqrt{\left(\frac{\pi}{2t}\right)} I_{i+\frac{1}{2}}(t) / \omega_0(t) \quad (114)$$

The next two  $\omega_i$ 's are given by

$$\omega_1(t) = 3(-t^{-1} + \coth(t)) \quad (115a)$$

$$\omega_2(t) = 5(1 + 3t^{-2} - 3t^{-1}\coth(t)) \quad (115b)$$

and the remaining terms can be found from Eq. (112) and the definitions of the modified Bessel functions given in Appendix A.

Note that Eq. (113) for  $\omega_0(t)$  is the same as Eq. (57) as expected. This can be seen by integrating Eq. (112) with respect to  $\mu_s$ , where only the zeroth order term of the Legendre polynomials contributes to the angular average of  $g^1$ .

Solutions to Eq. (109) with the anisotropic function given by Eq. (110) truncated to the second order (three terms) and with albedo  $\leq 1$  was solved before for one- and two-dimensions [Crosbie and Dougherty, 1980]. Recently, Liu (1993) has developed the one-dimensional solution to Eq. (109) for any number of Legendre terms.

## V.2. Anisotropic Scattering

For anisotropic scattering (and no absorption), the CTE

is given by Eq. (50). Let's define  $\Phi$  by

$$\Phi(\hat{\Omega}_0 \hat{\Omega}', t) = P(\hat{\Omega}_0 \hat{\Omega}') g^1(\hat{\Omega}_0 \hat{\Omega}', t) \quad (116)$$

where  $P$  is the phase function and  $g^1$  is the single scattering field correlation function. Using radiative transfer solution methods, an exact solution to the CTE can be obtained by expanding  $\Phi$  in terms of a Legendre series; or by expanding  $G^m$  and  $\Phi$  in terms of spherical harmonics functions and then obtaining an approximate solution by truncating both series to a finite number of terms [Ozsisik, 1973]. More development on the spherical harmonics solution method is presented in Appendix F. An approximate form of the equation can also be obtained by assuming a peaked phase function in one direction superimposed on an otherwise isotropic phase function [Reguigui et al., 1993] (see Appendix F for more on this method.) Only the Legendre expansion will be discussed herein.

V.2.a. Legendre Expansion: In order to expand  $\Phi$  in a series of Legendre polynomials, an analytical form of  $P$  needs to be given. A numerical integration of the product of Mie coefficients of the phase function and  $g^1$  is also possible. This will not be discussed here.

The time-correlated phase function (Eq. (116)) can be written as

$$\Phi(\hat{\Omega}_0 \hat{\Omega}', t) = \omega_0(t) \left[ 1 + \sum_{i=1}^{\infty} \omega_i(t) P_i(\hat{\Omega}_0 \hat{\Omega}') \right] \quad (117)$$



or

$$\Phi(\hat{\Omega} \cdot \hat{\Omega}', t) = \sum_{i=0}^{\infty} x_i(t) P_i(\hat{\Omega} \cdot \hat{\Omega}') \quad (118)$$

where the expansion coefficients,  $x_i$ , are found from the following relation

$$x_i = \frac{1}{2} \int_{-1}^{+1} \Phi(\mu_s, t) P_i(\mu_s) d\mu_s \quad (119)$$

where  $\mu_s = \hat{\Omega} \cdot \hat{\Omega}' \equiv (\cos \Theta)$  and  $P_i$  are the Legendre polynomials of order  $i$ .

For polystyrene spheres of submicron size, used in much experimental work, the phase function can be approximated by the Rayleigh-Debye form factor [Bohren and Huffman, 1983] as

$$P(\hat{\Omega} \cdot \hat{\Omega}') = \frac{1}{k_0^2 \sin^6(\Theta/2)} \left[ \sin(\Upsilon(\Theta)) - \Upsilon(\Theta) \cos(\Upsilon(\Theta)) \right]^2 \quad (120)$$

with  $\Upsilon(\Theta) = k_0 d \sin(\frac{\Theta}{2})$ . Numerical integration needs be performed in order to obtain the expansion coefficients  $x_i$ .

For particles whose diameters are small compared to the wavelength of the incident radiation, a Rayleigh phase function is usually used. This is given by

$$P(\cos\Theta) = \frac{3}{4}(1 - \cos^2\Theta) \quad (121a)$$

$$= \frac{3}{4}(1 - \mu_s^2) \quad (121b)$$

Substituting Eq. (4) and Eq. (121) into the expression for  $\Phi$  (Eq. (116)) gives

$$\Phi(\mu_s, t) = \frac{3}{4}(1 - \mu_s^2)e^{-t(1-\mu_s)} \quad (122)$$

Substituting Eq. (122) into Eq. (119) and performing the integration analytically for  $i=0, 1,$  and  $2,$  respectively, results in the following expansion coefficients for the Rayleigh phase function

$$x_0(t) = \frac{3}{2}e^{-t}t^{-1} \left[ (1 + t^{-2})\sinh(t) - t^{-1}\cosh(t) \right] \quad (123a)$$

$$x_0(t) \cong e^{-t} \left[ 1 + t^2/5 + 3t^4/280 + t^6/3780 \right] \quad t \leq 0.5 \quad (123b)$$

$$x_1(t) = \frac{3}{2}e^{-t}t^{-1} \left[ (1+3t^{-2})\cosh(t) - t^{-1}(2+3t^{-2})\sinh(t) \right] \quad (124a)$$

$$x_1(t) \cong 3e^{-t} \left[ 4t/3 + t^3/7 + t^5/189 \right] / 10 \quad t \leq 0.4 \quad (124b)$$

$$x_2(t) = \frac{3}{2}e^{-t}t^{-1}$$

$$\left[ (1+10t^{-2}+18t^{-4})\sinh(t) - t^{-1}(4+18t^{-2})\cosh(t) \right] \quad (125a)$$

$$x_2(t) \cong \frac{3}{2}e^{-t}$$

$$\left( \frac{1}{15} + \frac{13}{210}t^2 + \frac{11}{2520}t^4 + \frac{1}{8179.67}t^6 \right) \quad t \leq 0.5 \quad (125b)$$

Note that for small values of  $t$  (as indicated above), the approximate values of the expansion coefficients must be used for numerical convergence. The effective albedo resulting from expanding  $g^1$  combined with a Rayleigh phase function is equal to

$$\omega_R(t) = x_0(t) \quad (126)$$

where the subscript R indicates the Rayleigh phase function, and from Eq. (117), we find

$$\omega_1(t) = 3x_1(t)/x_0(t) \quad (127a)$$

$$\omega_2(t) = 5x_2(t)/x_0(t) \quad (127b)$$

V.2.b. Diffusion Approximation: Several authors [Ozisik, 1973, Pomraning, 1973, and Ishimaru, 1978a] have worked out the solution to the radiative transfer problem in the diffusion limit. For large optical thicknesses (greater than 10 [Yoo et al., 1990]), the diffuse intensity is scattered many times which makes the angular dependence of the scattering very weak. Thus, the intensity of light can

be represented by the first two terms in a spherical harmonics expansion.

In what follows, I will extend the diffusion derivation to the field correlation transfer equation. The integro-differential form of the CTE is given by

$$\hat{\Omega} \cdot \nabla G^m(\mathbf{r}, \hat{\Omega}, t) + \sigma_t G^m(\mathbf{r}, \hat{\Omega}, t) = \frac{\sigma_s}{4\pi} \int \Phi(\hat{\Omega} \circ \hat{\Omega}', t) G^m(\mathbf{r}, \hat{\Omega}', t) d\Omega' + Q_c(\mathbf{r}, \hat{\Omega}, t) \quad (128)$$

where  $Q_c$  is a source term and  $\Phi(\hat{\Omega} \circ \hat{\Omega}', t)$  is the correlated phase function which is defined as

$$\Phi(\hat{\Omega} \circ \hat{\Omega}', t) = P(\hat{\Omega} \circ \hat{\Omega}') g^1(\hat{\Omega} \circ \hat{\Omega}', t) \quad (129)$$

Here  $P$  is normalized to unity and  $g^1$  is the single scattering correlation function given by Eq. (4).

For collimated incident radiation (correlation) at the top of the medium in a direction  $\hat{\Omega}_0$ ,

$$I_{\text{inc}}(\hat{\Omega}) = I_0 \delta(\hat{\Omega} - \hat{\Omega}_0) \quad (130)$$

the correlation function can be written as a sum of a reduced collimated term ( $G_c^m$ ) and a diffuse term ( $G_d^m$ ) as follows

$$G^m(\mathbf{r}, \hat{\Omega}, t) = G_c^m(\mathbf{r}, \hat{\Omega}, t) + G_d^m(\mathbf{r}, \hat{\Omega}, t) \quad (131)$$

Substituting Eq. (131) into the integro-differential equation (Eq. (128)) results in an integral equation for the diffuse correlation similar to Eq. (128) with  $G^m$  being replaced by  $G_d^m$  and  $Q_c$  being given by

$$Q_c(\mathbf{r}, \hat{\Omega}, t) = \frac{\sigma_s}{4\pi} \int \Phi(\hat{\Omega} \cdot \hat{\Omega}', t) G_c^m(\mathbf{r}, \hat{\Omega}', t) d\Omega' \quad (132)$$

The diffusion approximation states that the diffuse correlation is given by [Ishimaru, 1978a]

$$G_d^m(\mathbf{r}, \hat{\Omega}, t) \cong U(\mathbf{r}, t) + \frac{3}{4\pi} \mathbf{F}(\mathbf{r}, t) \cdot \hat{\Omega} \quad (133)$$

where  $U$  represents the average correlation (energy density and presumably the dominant term) given by

$$U(\mathbf{r}, t) = \frac{1}{4\pi} \int G_d^m(\mathbf{r}, \hat{\Omega}, t) d\Omega \quad (134)$$

and  $\mathbf{F}$  is a first order anisotropy correction and has the physical interpretation of a flux

$$\mathbf{F}(\mathbf{r}, t) = \int G_d^m(\mathbf{r}, \hat{\Omega}, t) \hat{\Omega} d\Omega \quad (135)$$

To proceed with the solution, let's form the first two angular moments of the integro-differential equation for  $G_d^m$  (similar to Eq. (128).) First, if we integrate Eq. (128) over all solid angle and use definitions Eqs. (134) and (135), we find

$$\nabla \circ \mathbf{F}(\mathbf{r}, t) = 4\pi U(\mathbf{r}, t) [\sigma_s \omega_d(t) - \sigma_t] + \sigma_s \omega_d(t) 4\pi U_c(\mathbf{r}, t) \quad (136)$$

where

$$U_c(\mathbf{r}, t) = \frac{1}{4\pi} \int G_c^m(\mathbf{r}, \hat{\Omega}, t) d\Omega \quad (137)$$

and

$$\omega_d(t) = \frac{1}{4\pi} \int \Phi(\hat{\Omega} \circ \hat{\Omega}', t) d\Omega \quad (138)$$

In Eq. (138), the  $\Omega$ -integral is invariant with respect to  $\hat{\Omega}'$ . So, to do the integral, one can choose  $\hat{\Omega}'$  as the z-axis and find that

$$\omega_d(t) = \frac{1}{2} \int_{-1}^{+1} \Phi(\mu_s, t) d\mu_s \quad (139)$$

where  $\mu_s = \hat{\Omega} \circ \hat{\Omega}'$ . Note that for  $t=0$ ,  $\omega_d=1$ , since  $\Phi$  reduces to  $P$  and  $P$  is normalized to 1. Next, substituting Eq. (133) into Eq. (128) gives

$$\begin{aligned} 4\pi \hat{\Omega} \circ \nabla U(\mathbf{r}, t) + 3\hat{\Omega} \circ \nabla [\mathbf{F}(\mathbf{r}, t) \circ \hat{\Omega}] = \\ 4\pi U(\mathbf{r}, t) [\sigma_s \omega_d(t) - \sigma_t] + 3\mathbf{F} \circ \hat{\Omega} [\sigma_s p_1(t) - \sigma_t] + Q_c(\mathbf{r}, \hat{\Omega}, t) \end{aligned} \quad (140)$$

where

$$p_1(t) = \frac{1}{2} \int_{-1}^{+1} \Phi(\mu_s, t) \mu_s d\mu_s \quad (141)$$

Note that at  $t=0$ ,  $p_1(0) \equiv f$  (the cosine average of the phase function), where  $f$  given as such is usually called the asymmetry factor [van de Hulst, 1980a]. For isotropic scattering and  $t=0$ ,  $f$  equals 0.

To find the first moment, Eq. (140) is multiplied by  $\hat{\Omega}$  and then the integral over all solid angle is taken. This results in the following equation

$$F(\mathbf{r}, t) = (4\pi\nabla U(\mathbf{r}, t) - 3 \int Q_c(\mathbf{r}, \hat{\Omega}, t) \hat{\Omega} d\Omega) / (3[\sigma_s p_1(t) - \sigma_t]) \quad (142)$$

Taking the divergence of Eq. (142) and then substituting the result into Eq. (136) gives the second order differential equation that needs to be solved for the energy density  $U$ , i.e.,

$$\begin{aligned} \nabla^2 U(\mathbf{r}, t) - 3[\sigma_t - \sigma_s \omega_d(t)][\sigma_t - \sigma_s p_1(t)]U(\mathbf{r}, t) \\ = 3\sigma_s \omega_d(t)[\sigma_s p_1(t) - \sigma_t]U_c(\mathbf{r}, t) + 3\nabla \cdot \int Q_c(\mathbf{r}, \hat{\Omega}, t) \hat{\Omega} d\Omega / 4\pi \end{aligned} \quad (143)$$

subject to a boundary condition of  $G_d^+(\mathbf{r}=0, \hat{\Omega}) = 0$  with  $\hat{\Omega}$  pointing inward. However, because the approximation given by Eq. (133) has a simple angular dependence and the solution of Eq. (143) is scalar, this boundary condition cannot be satisfied exactly. Most researchers assume that no flux of diffusing photons enters the medium from the boundaries. This is slightly different from DWS theory where Pine et al. (1990) assumed a source of diffusing intensity to be deposited a distance  $z=z_0/l^*$  from the

boundary where  $z_0$  is on the order of a transport mean free path ( $l^*$ ). This deposition depth ( $z_0$ ) does not have any effect on the transmitted intensity as shown by Pine et al. (1990) and Ackerson et al. (1992). So instead of introducing this free parameter into the equations, the no flux boundary condition at the boundaries will be used. Setting the total diffuse flux directed inward (along the normal direction  $\hat{n}$ ) equal to zero gives

$$\int_{2\pi} G_d^m(\mathbf{r}, \hat{\Omega}, t) (\hat{\Omega} \cdot \hat{n}) d\Omega = 0, \quad \hat{\Omega} \cdot \hat{n} > 0 \quad (144)$$

Using Eq. (133) in Eq. (144) results in the following boundary condition

$$U(\mathbf{r}, t) + \hat{n} \cdot \mathbf{F}(\mathbf{r}, t) / 2\pi = 0, \quad \text{at } \mathbf{r} = \mathbf{r}_s \quad (145)$$

where  $\mathbf{r}_s$  is a coordinate on the boundary.

Substituting the equation for  $\mathbf{F}$  (Eq. (142)), along with the definition of  $Q_c$  (Eq. (132)), into Eq. (145) gives

$$U(\mathbf{r}_s, t) - \frac{2}{3} l^i(t) \hat{n} \cdot \nabla U(\mathbf{r}_s, t) = - \hat{n} \cdot \mathbf{Q}_1(\mathbf{r}_s, t) / 2\pi \quad (146)$$

where  $l^i(t)$  is a correlated mean free path defined as

$$1/l^i(t) = \sigma_t - \sigma_s p_1(t) \quad (147)$$

and where  $\mathbf{Q}_1$  represents the effect of anisotropic scattering



and is defined here as

$$Q_1(\mathbf{r}, t) = I^i(t) \sigma_s \int_{\Omega'} \left( \frac{1}{4\pi} \int_{\Omega} \Phi(\hat{\Omega} \cdot \hat{\Omega}', t) \hat{\Omega} d\Omega \right) G_c^m(\mathbf{r}, \hat{\Omega}', t) d\Omega' \quad (148)$$

Note that for isotropic scattering and at  $t=0$ ,  $Q_1 = 0$ .

Equation (143) along with the boundary condition given by Eq. (146) represents the system that needs to be solved to find the diffusive correlation function of Eq. (133). For simplicity, this solution will be derived next for a plane wave incident normal to a slab.

V.2.b.i. Plane Wave Incident Normal To A Slab Containing Isotropic Pure Scatterers: Let's assume that the incident direction  $\hat{\Omega}_0$  in Eq. (130) is the  $z_k$ -direction ( $\hat{\Omega}_z$ ), directed downward normal to the slab. Accordingly, the reduced correlation decays according to Beer's law, i.e.,

$$G_c^m(z_k, \hat{\Omega}_z) = I_0 \delta(\hat{\Omega} - \hat{\Omega}_z) \exp(-\sigma_t z_k) \quad (149)$$

Substituting Eq. (149) into Eq. (137) gives

$$U_c(z_k) = \frac{1}{4\pi} I_0 \exp(-\sigma_t z_k) \quad (150)$$

Next, if we substitute Eq. (149) into Eq. (132) and integrate over  $\hat{\Omega} d\Omega$  then take the divergence of the resulting equation, we find that

$$\nabla \cdot \int Q_c(z_k, \hat{\Omega}, t) \hat{\Omega} d\Omega = -\sigma_t \sigma_s I_0 p_1(t) \exp(-\sigma_t z_k) \quad (151)$$

and when this is inserted back into Eq. (143), we find

$$\frac{\partial^2}{\partial z_k^2} U(z_k, t) - D^2(t) U(z_k, t) = -Q_0(t) \exp(-\sigma_t z_k) \quad (152)$$

where

$$D^2(t) = 3[\sigma_t - \sigma_s \omega_d(t)] / l'(t) \quad (153)$$

and

$$Q_0(t) = 3\sigma_s I_0 (\omega_d(t) / l'(t) + \sigma_t p_1(t)) / 4\pi \quad (154)$$

The boundary conditions, given by Eq. (146) reduce to

$$U(z_k, t) - \frac{2}{3} l'(t) \frac{\partial}{\partial z_k} U(z_k, t) = -Q_1(z_k, t) / 2\pi, \text{ at } z_k=0 \quad (155a)$$

and

$$U(z_k, t) + \frac{2}{3} l'(t) \frac{\partial}{\partial z_k} U(z_k, t) = Q_1(z_k, t) / 2\pi, \text{ at } z_k=L \quad (155b)$$

where  $L_k$  is the physical thickness of the medium and where  $\hat{n} \cdot \hat{\Omega}_z$  is positive at  $z_k=0$  and negative at  $z_k=L$ .  $Q_1$  in Eqs. (155a) and (155b) is the component of  $Q_1$  along the

$z_k$ -direction and it can be found by substituting Eq. (149) for  $G_c$  into Eq. (148) which gives

$$Q_1(z_k, t) = l^{\dagger}(t) \sigma_s p_1(t) I_0 \exp(-z_k) \quad (156)$$

The solution to Eq. (152) will be explicitly given for the case of conservative scattering where  $\sigma_t = \sigma_s$ . In other words, it is assumed that absorption in the medium is negligible, which is a good assumption for the polystyrene particles used in DLS experiments. In this case, Eqs. (147), (153), (154) and (156), respectively reduce to

$$1/l^{\dagger}(t) = \sigma_s (1 - p_1(t)) \quad (157)$$

$$D^2(t) = 3\sigma_s^2 [1 - \omega_d(t)] [1 - p_1(t)] \quad (158)$$

$$Q_0(t) = 3\sigma_s^2 I_0 [\omega_d(t) (1 - p_1(t)) + p_1(t)] / 4\pi \quad (159)$$

$$Q_1(z_k, t) = p_1(t) I_0 \exp(-z_k) / (1 - p_1(t)) \quad (160)$$

Note that at  $t = 0$ ,  $p_1(0) = f$ , and hence, if we define the mean free path  $l$  as  $1/\sigma_s$ , then

$$l/l^{\dagger}(0) = 1 - f \quad (161)$$

which is the same definition for  $l^*$ , the transport mean free path, used by Pine et al. (1990) in deriving the DWS results. However, because for  $t > 0$ , the anisotropy

introduced into the medium is not only due to the phase function, but also it is due to the anisotropic  $g^1$ , it is better to define a correlated  $l^1$  (Eq. (147)) rather than the uncorrelated  $l^*$  (Eq. (161)). This definition relaxes the DWS short time assumption, for which  $l^* \cong l^1$ .

When the scattering in the medium is independent of direction ( $P(\hat{\Omega} \cdot \hat{\Omega}') = 1$ ),  $\Phi(\mu_s, t)$  reduces to  $g^1$ . Therefore,  $\omega_d(t)$  and  $p_1(t)$  can be found by a straightforward integration to be

$$\omega_d(t) = e^{-t} \sinh(t) t^{-1} \quad (162)$$

and

$$p_1(t) = \omega_d(t) [\coth(t) - t^{-1}] \quad (163)$$

Note that  $\omega_d(t)$  for this case is equal to the first term in the Legendre expansion for  $g^1$  for the isotropic case (Eq. (113)), and  $p_1$  is equal to the second term (Eq. (115a)) in the same expansion.

Before solving Eq. (152), we need to distinguish two cases:  $t = 0$  and  $t > 0$ .

CASE A.  $t = 0$ : For this case, we can easily verify that  $p_1(0) = 0$ ,  $Q_1(z_k, 0) = 0$ ,  $D^2 = 0$ ,  $\omega_d(0) = 1$ ,  $l^1(0) = 1/\sigma_s$ , and

$$Q_0 = 3\sigma_s^2 I_0 \quad (164)$$

Solving Eq. (152) for the case when  $D(0) = 0$  gives

$$U(z_k, t) = -3I_0 e^{-\sigma_s z_k} + C_1 z_k + C_2 \quad (165)$$

Applying the boundary condition, Eq. (155), at  $z_k = 0$  gives

$$C_2 - \frac{2}{3}C_1\sigma_s^{-1} = 5Q_0\sigma_s^{-2}/3 \quad (166a)$$

and at  $z_k = L_k$  gives

$$C_2 + (\sigma_s L_k + \frac{2}{3})C_1\sigma_s^{-1} = Q_0\sigma_s^{-2}e^{-\sigma_s L_k}/3 \quad (166b)$$

Solving Eqs. (166a) and (166b) simultaneously, yields the expressions for  $C_1$  and  $C_2$ , i.e.,

$$C_1 = Q_0\sigma_s^{-1}(e^{-\sigma_s L_k} - 5)/(3(\sigma_s L_k + 4/3)) \quad (167a)$$

and

$$C_2 = Q_0\sigma_s^{-2}(5 + 2(e^{-\sigma_s L_k} - 5)/(3(\sigma_s L_k + 4/3)))/3 \quad (167b)$$

Finally, substituting Eqs. (167a) and (167b) into Eq. (165), we find the general expression for the energy density at  $t=0$ . Using the optical coordinates, we find

$$U(z, t) = (z + \frac{2}{3})(e^{-L} - 5)/(L + 4/3) + 5 - 3e^{-z} \quad (168)$$

where  $I_0$  is assumed to be 1.

CASE B.  $t > 0$ : In this case,  $D(t)$  is different than zero and the solution to Eq. (152) is sum of a homogeneous part and a particular part. This is found to be

$$U(z_k, t) = C_0 e^{-\sigma_s z_k} + C_1 e^{Dz_k} + C_2 e^{-Dz_k} \quad (169)$$

where  $C_1$  and  $C_2$  are constants to be determined from the boundary conditions and  $C_0$  is given by

$$C_0 = -Q_0 / (\sigma_s^2 - D^2) \quad (170)$$

Let

$$h = \frac{2}{3} l'(t), \quad (171)$$

and substituting using Eqs. (171) and (169) in Eq. (155a) at  $z_k=0$  results in the following:

$$C_1(1-hD) + C_2(1+hD) = -C_0(1+\sigma_s h) - Q_1(0, t)/2\pi \quad (172a)$$

and at  $z_k = L_k$  gives

$$C_1(1+hD)e^{DL_k} + C_2(1-hD)e^{-DL_k} = -C_0(1-\sigma_s h)e^{-\sigma_s L_k} + Q_1(0, t)e^{-\sigma_s L_k}/2\pi \quad (172b)$$

Solving Eqs. (172a) and (172b) simultaneously yields the expressions for  $C_1$  and  $C_2$ , i.e.,

$$\begin{aligned}
C_1 = \Delta^{-1} & \left[ -C_0 e^{-\sigma_s L_k} (1 + \sigma_s h) (1 + hD) - C_0 (1 + hD) (1 - hD) e^{-DL_k} \right] \\
& - Q_1(0, t) \Delta^{-1} \left[ (1 - hD) e^{-DL_k} - (1 + hD) e^{-\sigma_s L_k} \right] \quad (173)
\end{aligned}$$

and  $C_2$  is given by

$$\begin{aligned}
C_2 = \Delta^{-1} & \left[ C_0 e^{-\sigma_s L_k} (1 - \sigma_s h) (1 - hD) - C_0 (1 + hD) (1 + \sigma_s D) e^{-DL_k} \right] \\
& - Q_1(0, t) \Delta^{-1} \left[ (1 - hD) e^{-DL_k} - (1 + hD) e^{-\sigma_s L_k} \right] \quad (174)
\end{aligned}$$

where

$$\Delta = \left[ 2 \sinh(DL_k) + 4hD \cosh(DL_k) + 2(hD)^2 \sinh(DL_k) \right] \quad (175)$$

Finally, substituting Eqs. (170)-(171) and (173-175) into Eq. (169), we find the general expression for the energy density, which can be used along with Eq. (142) for the flux in Eq. (133) to find the diffuse component of the correlation function.

For optical thicknesses less than 10, the diffusion approximation fails to exactly predict the correlation [Yoo et al., 1990]. For these low optical thicknesses, the ballistic nature of light propagation and polarization effects become important. The following chapter is devoted to studying the polarization effects on correlation.

## CHAPTER VI

### POLARIZED LIGHT AND THE EQUATION OF CORRELATION TRANSFER

The angular behavior of the polarized radiation field in fluid/particle suspensions contains information on the type of particles in such suspensions e.g., the size distribution, index of refraction and the shape of the particles [Look and Chen, 1993, Belsley et al., 1986, Pal and Carswell, 1985, Leader and Dalton, 1975, Hansen, 1971]. Thus, in any exact treatment of scattering problems, and in particular, in dynamic light scattering experiments, polarization effects must be included.

A systematic treatment of the state of polarization was given by Chandrasekhar (1960) for plane parallel media and Rayleigh scattering. Most of the work that followed dealt either with the same types of problems, or extended Chandrasekhar's work to allow for a general scattering matrix [Hovenier, 1987, Hovenier and van de Mee, 1983, Bohren and Huffman, 1983, van de Hulst, 1982a, 1982b, Sekera, 1966, Sekera, 1956, McMaster, 1954].

In this section, I will restate some of the fundamental equations representing polarized light as they relate to CTE and then develop explicit expressions for the basic



coefficients in the analytical representation of the phase matrix corresponding to CTE with a general scattering matrix. At the end of this chapter, the  $P_1$  approximation will be used to present the explicit closed form solution to an axisymmetric problem considering polarized radiation and Rayleigh scattering.

### VI.1. Fundamentals of Polarized Light

In general, light gets polarized after a scattering event. At each spatial location and for a given frequency and direction of propagation, it can be shown that a general mixture of light can be regarded as a mixture of an elliptically polarized stream and an independent stream of natural (unpolarized) light [Chandrasekhar, 1960]. Four parameters [ $\mathcal{I}$ ,  $Q$ ,  $U$ ,  $V$ ], known as the Stokes parameters, are required to specify the state of polarization of a partially polarized light beam. The intensity of the beam is given by  $\mathcal{I}$  ( $= I_l + I_r$ ), and the second parameter  $Q$  is equal to  $(I_l - I_r)$ , where  $I_l$  and  $I_r$  are the intensities in the direction  $l$  and in the direction  $r$  that is perpendicular to  $l$ , respectively. The direction  $l$  is parallel to the plane of scattering and lies in the plane transverse to the direction of propagation (see Fig. 3) [Chandrasekhar, 1960].  $Q$  and  $U$  are usually defined through the plane of polarization given by the angle  $\chi$ .  $\chi$  is the angle that the principal axis of the ellipse (traced by the end points of the electric vector) makes with the direction  $l$ . The angle  $\chi$  is given by

$$\tan 2\chi = u/Q \quad (176)$$

$V$  is defined by the angle ( $\beta$ ) whose tangent is the ratio of the axes of the ellipse traced by the end points of the electric vector.  $\beta$  is defined by

$$\sin 2\beta = V/\mathcal{J} \quad (177)$$

Therefore, the character of arbitrary polarized light is completely determined by the intensity  $\mathcal{J}$ ,  $Q$ , and the two parameters  $u$  and  $V$ , defined in Eqs. (176) and (177), respectively. For natural light, the parameters  $Q$ ,  $u$ , and  $V$  are all zero.

By a straightforward extension of the scalar CTE (Eq. (52)) to include polarization (similar to RTE, [Chandrasekhar, 1960]), the correlation transfer equation for polarized light in plane-parallel atmospheres can be written as

$$\mu \frac{\partial}{\partial z} \mathbf{G}^m(z, \mu, \phi, t) + \mathbf{G}^m(z, \mu, \phi, t) = \frac{\omega}{4\pi} \int_{-1}^1 \int_0^{2\pi} \mathbf{P}(\mu, \mu', \phi, \phi', t) \mathbf{G}^m(z, \mu', \phi, t) d\phi' d\mu' \quad (178)$$

where  $z$  is the optical variable,  $\mu$  is the direction cosine of the propagation radiation,  $\omega$  is the single scattering albedo, and  $t=2\tau/\tau_0$ . The vector  $\mathbf{G}^m$  consists of the four correlated Stokes parameters  $\mathbf{G}^m(z, \mu, \phi, t) = [\mathcal{J}, Q, u, V]$  where

$\mathcal{P}$ ,  $Q$ ,  $u$ , and  $v$  are now a function of delay-time.  $P$  is the correlated phase matrix given by

$$P(\mu, \mu', \phi, \phi', t) = g^1(\cos\Theta, t)M(\pi-\phi_2)R(\cos\Theta)M(-\phi_1) \quad (179)$$

where  $M(\pi-\phi_2)$  and  $M(-\phi_1)$  are the linear transformation matrices given by [Chandrasekhar, 1960]

$$M(\varphi) = \begin{bmatrix} \cos^2\varphi & \sin^2\varphi & 0.5 \sin 2\varphi & 0 \\ \sin^2\varphi & \cos^2\varphi & -0.5 \sin 2\varphi & 0 \\ -\sin^2\varphi & \sin^2\varphi & \cos 2\varphi & 0 \\ 0 & 0 & 0 & 1 \end{bmatrix} \quad (180)$$

$M(\varphi)$  is required to rotate meridian planes before and after scattering into the local scattering plane.  $\varphi_1$  denotes the angle between the meridian plane  $OT_1Z$  through  $T_1$  ( $=(\theta', \phi')$ ) and the plane of scattering  $OT_1T_2$ , where  $T_2 = (\theta, \phi)$ .  $\varphi_2$  denotes the angle between the planes  $OT_2Z$  and  $OT_1T_2$ .  $O$  refers to the origin and  $\Theta$  is the scattering angle (angle between light rays before and after scattering) [Chandrasekhar, 1960] (see Fig. 4).  $R$  is the scattering matrix that can be expressed in general as [Siewert, 1982]

$$R(\mu_s) = \begin{bmatrix} a_1(\mu_s) & b_1(\mu_s) & 0 & 0 \\ b_1(\mu_s) & a_2(\mu_s) & 0 & 0 \\ 0 & 0 & a_3(\mu_s) & b_2(\mu_s) \\ 0 & 0 & -b_2(\mu_s) & a_4(\mu_s) \end{bmatrix} \quad (181)$$

where  $\mu_s = \cos\Theta$  and  $R(\mu_s)$  is normalized such that

$$\int_{-1}^1 a_1(\mu_s) d\mu_s = 2 \quad (182a)$$

Note that for unpolarized light,  $P(\mu_s)$ , normalized in Eq. (27), is equal to the product of the albedo ( $\omega$ ) and  $a_1(\mu_s)$ . Therefore, Eqs. (27) and (182a) are equivalent. For  $t > 0$ , the normalization condition ((Eq. (27) or Eq. (182a)) becomes

$$\int_{-1}^1 a_1(\mu_s) g^1(\mu_s, t) d\mu_s = 2\omega_e(t) \quad (182b)$$

where  $\omega_e(t)$  is the effective albedo.

The six functions appearing in Eq. (181) are real valued for  $\mu_s \in [-1, 1]$  and can be expanded in a series of generalized spherical functions (see Appendix B, Eqs. (B1)-(B6)) for a Fourier expansion of the phase matrix [de Rooij and van der Stap, 1984]. Note that  $b_1(\pm 1) = b_2(\pm 1) = 0$  and  $a_2(\pm 1) = a_3(\pm 1)$  [Siewert, 1982, van de Hulst, 1957].

Some of the theoretical methods that are available to solve for the polarized intensity field include the X- and Y- matrices and the border approximation [Chandrasekhar, 1960, Chandrasekhar and Elbert, 1954, Coulson, 1959a, 1959b, Wauben and Hovenier, 1992a, Wauben et al., 1993a, 1993b], the Gauss-Seidel iterative method [Dave, 1970], the Monte Carlo technique [Collins et al., 1972], the doubling and adding method [Hansen, 1971, Domke and Yanovitskij, 1981, 1986, Evans and Stephens, 1991, Leader, 1975], the fast

invariant imbedding method which is related to the doubling method [Mishchenko, 1990, Mishchenko, 1991], and the discrete-ordinate method [Weng, 1992a, Cheung and Ishimaru, 1982]. Other methods include the Galerkin method [El-Wakil et al., 1991], the Q-form method [Domke, 1990], the eigenfunction expansion method [Domke, 1983] and the  $F_N$  method [Garcia and Siewert, 1989]. And finally, the most widely used method of solution is the Fourier decomposition and the generalized spherical harmonics expansion [Domke, 1974, Siewert, 1981, de Rooij and van der Stap, 1984, Garcia and Siewert, 1986, 1987, Siewert and McCormick, 1993]. The following sections will be devoted to reviewing and later presenting a simple solution using the spherical harmonics expansion.

## VI.2. Spherical Harmonics Expansion

In the following, I will consider a type of problem similar to that considered by Siewert and co-workers [Siewert, 1982, Siewert et al. 1984] and review the generalized spherical harmonics solution to the problem at hand. That is, let's consider a finite layer,  $z \in [0, L]$ , illuminated on the surface  $z=0$  by a parallel beam and bounded by a reflecting surface at  $z=L$ . We seek a solution of Eq. (178) subject to the boundary conditions, for  $\mu \in \tau[0, 1]$  and  $\phi \in [0, 2\pi]$ ,

$$G^m(0, \mu, \phi, t) = \pi \delta(\mu - \mu_0) \delta(\phi - \phi_0) F \quad (183a)$$

and

$$G^m(L, -\mu, \phi, t) = \frac{\rho_L}{\pi} \mathbb{D}_1 \int_0^{2\pi} \int_0^1 G^m(L, \mu', \phi', t) \mu' d\mu' d\phi' \quad (183b)$$

where  $\rho_L$  is the Lambert coefficient for reflection,  $\mathbb{D}_1 = \text{diag}\{1, 0, 0, 0\}$  and the flux vector  $F$  has entries  $F_I$ ,  $F_Q$ ,  $F_U$  and  $F_V$  that are presumed given. Note that the sign on the direction angle represented by  $\mu$  is now shown explicitly instead of using the convention of  $G^{m+}$  and  $G^{m-}$ . Therefore,  $G^{m+}(\mu)$  is equivalent to  $G^m(\mu)$  and  $G^{m-}(\mu)$  is equivalent to  $G^m(-\mu)$  where  $\mu$  is positive.

Following a similar procedure to the one used by Siewert (1981), Siewert and Pinheiro (1981), and de Rooij and van der Stap (1984), the correlated phase matrix can be expanded in a Fourier series as [Benassi et al., 1985]

$$P(\mu, \mu', \phi, \phi', t) = \frac{1}{2} C^0(\mu, \mu', t) + \sum_{m=1}^J \left[ C^m(\mu, \mu', t) \cos m(\phi - \phi') + S^m(\mu, \mu', t) \sin m(\phi - \phi') \right] \quad (184)$$

where

$$C^m(\mu, \mu', t) = A^m(\mu, \mu', t) + \mathbb{D}_2 A^m(\mu, \mu', t) \mathbb{D}_2 \quad (185a)$$

$$S^m(\mu, \mu', t) = A^m(\mu, \mu', t) \mathbb{D}_2 - \mathbb{D}_2 A^m(\mu, \mu', t) \quad (185b)$$

$$A^m(\mu, \mu', t) = \sum_{i=m}^J \frac{(i-m)!}{(i+m)!} \Pi_i^m(\mu) \mathbb{B}_i(t) \Pi_i^m(\mu'), \quad (186)$$

$$\mathbb{D}_2 = \text{diag}\{1, 1, -1, -1\} \quad (187)$$

$$\Pi_i^m(\mu) = \begin{bmatrix} P_i^m(\mu) & 0 & 0 & 0 \\ 0 & R_i^m(\mu) & -T_i^m(\mu) & 0 \\ 0 & -T_i^m(\mu) & R_i^m(\mu) & 0 \\ 0 & 0 & 0 & P_i^m(\mu) \end{bmatrix} \quad (188)$$

The law of scattering is given by

$$\mathbb{B}_i(\mathbf{t}) = \begin{bmatrix} \beta_i & \gamma_i & 0 & 0 \\ \gamma_i & \alpha_i & 0 & 0 \\ 0 & 0 & \zeta_i & -\varepsilon_i \\ 0 & 0 & \varepsilon_i & \delta_i \end{bmatrix} \quad (189)$$

in terms of the basic delay-time-dependent "Greek Constants"  $\{\alpha_i(\mathbf{t}), \beta_i(\mathbf{t}), \gamma_i(\mathbf{t}), \delta_i(\mathbf{t}), \varepsilon_i(\mathbf{t}), \zeta_i(\mathbf{t})\}$ , defined later in Eqs. (194a)-(194f). As usual,  $P_i(\mu)$  and  $P_i^m(\mu)$  are used to denote the Legendre polynomial function and the associated Legendre function, respectively.  $R_i^m(\mu)$  and  $T_i^m(\mu)$  are related to the generalized spherical functions (see Appendix C for definitions and useful relations). Appendix D contains some useful recursive relations for computing the matrices  $\Pi_i^m(\mu)$  and other related matrices relevant to the Fourier expansion solution.

VI.2.a. Diffuse Intensity Vector: For the boundary conditions given by Eqs. (183a) and (183b), we can separate the correlation vector into unscattered and diffuse components by writing [Benassi et al., 1985]

$$G^m(z, \mu, \phi, \mathbf{t}) = \pi \delta(\mu - \mu_0) \delta(\phi - \phi_0) e^{-z/\mu} \mathbf{F} + G_d^m(z, \mu, \phi, \mathbf{t}) \quad (190)$$

Thus if we substitute Eq. (190) into Eq. (178), we see that the diffuse field is defined by

$$\mu \frac{\partial}{\partial z} G_d^m(z, \mu, \phi, t) + G_d^m(z, \mu, \phi, t) = \frac{\omega}{4\pi} \int_{-1}^1 \int_0^{2\pi} P(\mu, \mu', \phi, \phi', t) G_d^m(z, \mu', \phi', t) d\phi' d\mu' + F(z, \mu, \phi, t) \quad (191)$$

where

$$F(z, \mu, \phi, t) = \frac{\omega}{4} P(\mu, \mu_0, \phi, \phi_0, t) e^{-z/\mu_0} F \quad (192)$$

is the singly-scattered and attenuated flux vector. The boundary conditions (from Eqs. (183)), for  $\mu \in [0, 1]$  and  $\phi \in [0, 2\pi]$ , are

$$G_d^m(0, \mu, \phi, t) = 0 \quad (193a)$$

and

$$G_d^m(L, -\mu, \phi, t) = \rho_L \mu_0 e^{-L/\mu_0} D_1 F + \frac{\rho_L}{\pi} D_1 \int_0^{2\pi} \int_0^1 G_d^m(L, \mu', \phi', t) \mu' d\mu' d\phi' \quad (193b)$$

Before we proceed with the solution, the elements of the basic scattering matrix (the Greek constants. Eq. (189)), need to be determined. The method for determining them will be demonstrated in the following section.

VI.2.b. The Basic Scattering Constants: To use the analytical representation of the phase matrix  $P(\mu, \mu', \phi, \phi', t)$



we need to find the basic constants  $\{\alpha_i(t), \beta_i(t), \gamma_i(t), \delta_i(t), \epsilon_i(t), \zeta_i(t)\}$  from the given correlated scattering matrix  $g^1(\mu_s, t)R(\mu_s)$  in the context of the scattering law being used. With regard to the special case of Mie scattering (for radiative transfer, i.e.,  $g^1 = 1$ ) [van de Hulst, 1957], we note that Herman (1965) and Domke (1975) have reported explicit representations for these constants (with  $t=0$ ) in terms of the complex coefficients basic to the Mie series, and Herman et al. (1980) has used orthogonality relations to deduce these constants. Siewert (1982) has extended Herman's method of using the orthogonality relations to write the expressions for the basic constants for a more general scattering model.

Since the Legendre polynomials and the associated Legendre functions satisfy orthogonality relations (given in Appendix C by Eqs. (C2) and (C3)), the following integral expressions for the basic constants can be deduced from Eqs. (B1)-(B6):

$$\beta_i(t) = \frac{(2i+1)}{2} \int_{-1}^1 P_i(\mu_s) g^1(\mu_s, t) a_1(\mu_s) d\mu_s \quad (194a)$$

$$\delta_i(t) = \frac{(2i+1)}{2} \int_{-1}^1 P_i(\mu_s) g^1(\mu_s, t) a_4(\mu_s) d\mu_s \quad (194b)$$

$$\gamma_i(t) = \frac{(2i+1)}{2} \left( \frac{(i-2)!}{(i+2)!} \right)^{1/2} \int_{-1}^1 P_i^2(\mu_s) g^1(\mu_s, t) b_1(\mu_s) d\mu_s \quad (194c)$$

$$\varepsilon_1(t) = - \frac{(2i+1)}{2} \left( \frac{(i-2)!}{(i+2)!} \right)^{1/2} \int_{-1}^1 P_1^2(\mu_s) g^1(\mu_s, t) b_2(\mu_s) d\mu_s \quad (194d)$$

$$\zeta_1(t) = \frac{(2i+1)}{2} \left( \frac{(i-2)!}{(i+2)!} \right)^{1/2} \int_{-1}^1 g^1(\mu_s) (a_3(\mu_s) R_1^2(\mu_s) + a_2(\mu_s) T_1^2(\mu_s)) d\mu_s \quad (194e)$$

and

$$\alpha_1(t) = \frac{(2i+1)}{2} \left( \frac{(i-2)!}{(i+2)!} \right)^{1/2} \int_{-1}^1 g^1(\mu_s) (a_2(\mu_s) R_1^2(\mu_s) + a_3(\mu_s) T_1^2(\mu_s)) d\mu_s \quad (194f)$$

Note that for the Fourier expansion (Eq. (184)), and the subsequent definitions, Eqs. (185)-(189) and Eqs. (194a)-(194f), one should have  $\beta_0 = 1$  and  $\alpha_0 = \alpha_1 = \gamma_0 = \gamma_1 = \varepsilon_0 = \varepsilon_1 = \zeta_0 = \zeta_1 = 0$  [Benassi et al., 1984a, 1984b].

In the following section, the solution method will be limited to media with azimuthal symmetry. This will simplify the solution considerably while still being able to model some realistic situations [Chandrasekhar, 1960, Pomraning, 1973].

VI.2.c. Azimuthally Symmetric Radiation: If we are interested only in the azimuthally symmetric component of the diffuse correlation,

$$G_d^m(z, \mu, t) = \frac{1}{2\pi} \int_0^{2\pi} G_d^m(z, \mu, \phi, t) d\phi \quad (195)$$

then by using Eqs. (185a) and (186) in Eq. (184), it can be shown that for  $m=0$  [Benassi et al., 1984a, 1984b],

$$P(\mu, \mu', t) = \sum_{i=0}^J \Pi_i(\mu) B_i(t) \Pi_i(\mu') \quad (196)$$

The series in Eq. (196) becomes exact for an infinite number of terms ( $J=\infty$ ). Using Eq. (196) and integrating Eqs. (191), (192), and (193) over  $\phi$  from 0 to  $2\pi$  results in the following equation of transfer [Benassi et al., 1984a, 1984b, Siewert and Pinheiro 1982, Benassi et al. 1985]

$$\mu \frac{\partial}{\partial z} G_d^m(z, \mu, t) + G_d^m(z, \mu, t) = \frac{\omega}{2} \sum_{i=0}^J \Pi_i(\mu) B_i(t) \int_{-1}^1 \Pi_i(\mu') G_d^m(z, \mu', t) d\mu' + F(z, \mu, t) \quad (197)$$

where

$$F(z, \mu, t) = \frac{\omega}{4} \sum_{i=0}^J \Pi_i(\mu) B_i(t) \Pi_i(\mu_0) e^{-z/\mu_0} F \quad (198)$$

and the boundary conditions, for  $\mu \in [0, 1]$ ,

$$G_d^m(0, \mu, t) = 0 \quad (199a)$$

and

$$\mathbf{G}_d^m(L, -\mu, t) = \rho_L \mu_0 e^{-L/\mu_0} \mathbb{D}_1 \mathbf{F} + 2\rho_L \mathbb{D}_1 \int_0^1 \mathbf{G}_d^m(L, \mu', t) \mu' d\mu' \quad (199b)$$

In this case, the matrix  $\Pi_i$  solution requires only the Legendre polynomials and the associated Legendre function  $P_1^2(\mu)$  (see Eqs. (203) and (C17)) as compared to the more general case given by Eq. (188).

Although  $\mathbf{G}_d^m(z, \mu, t)$  is a four-component vector, it is apparent from Eqs. (189), (D1), and (197)-(199) that Eq. (197) decouples into two two-component vector problems [Siewert and, Pinheiro 1982, Benassi et al. 1984, 1985]. Therefore, we can write

$$\begin{aligned} \mu \frac{\partial}{\partial z} \mathbf{G}_d^m(z, \mu, t) + \mathbf{G}_d^m(z, \mu, t) = \\ \frac{\omega}{2} \sum_{i=0}^J P_i(\mu) \mathbb{B}_i(t) \int_{-1}^1 P_i(\mu') \mathbf{G}_d^m(z, \mu', t) d\mu' + \mathbb{F}(z, \mu, t) \end{aligned} \quad (200)$$

where  $\mathbf{G}_d^m$  is a two-component vector, and  $\mathbb{F}$  is now given by (as compared to Eq. (198))

$$\mathbb{F}(z, \mu, t) = \frac{\omega}{4} \sum_{i=0}^J P_i(\mu) \mathbb{B}_i(t) P_i(\mu_0) e^{-z/\mu_0} \mathbf{F} \quad (201)$$

and, for  $\mu \in [0, 1]$ ,

$$\mathbf{G}_d^m(0, \mu, t) = \mathbf{0} \quad (202a)$$

and

$$G_d^m(L, -\mu, t) = \rho_L \mu_0 e^{-L/\mu_0} \mathbb{D}_3 F + 2\rho_L \mathbb{D}_3 \int_0^1 G_d^m(L, \mu', t) \mu' d\mu' \quad (202b)$$

Here

$$P_1(\mu) = \text{diag} \{P_1(\mu), R_1(\mu)\}, \quad (203)$$

and the two decoupled equations are given by the following two cases:

A: The  $\mathcal{J}$ - $Q$  Problem:

$$G_d^m(z, \mu, t) = \begin{pmatrix} \mathcal{J}(z, \mu, t) \\ Q(z, \mu, t) \end{pmatrix} \quad \text{with} \quad B_1(t) = \begin{pmatrix} \beta_1 & \gamma_1 \\ \gamma_1 & \alpha_1 \end{pmatrix} \quad (204)$$

and

$$F = [F_I, F_0]^T, \quad \mathbb{D}_3 = \text{diag} \{1, 0\}$$

and

B: The  $\mathcal{V}$ - $\mathcal{U}$  Problem:

$$G_d^m(z, \mu, t) = \begin{pmatrix} \mathcal{V}(z, \mu, t) \\ \mathcal{U}(z, \mu, t) \end{pmatrix} \quad \text{with} \quad B_1(t) = \begin{pmatrix} \delta_1 & \varepsilon_1 \\ -\varepsilon_1 & \zeta_1 \end{pmatrix} \quad (205)$$

and

$$F = [F_U, F_V]^T, \quad \mathbb{D}_3 = 0$$

#### VI.2.d The $P_1$ Approximation With Rayleigh Scattering:

When the particles in the medium scatter according to Rayleigh's law, the coefficients in the scattering matrix

(Eq. (181)) are then given by [Chandrasekhar, 1960]

$$a_1(\mu_s) = \mu_s^2 \quad (206a)$$

$$a_2(\mu_s) = 1 \quad (206b)$$

$$a_3(\mu_s) = a_4(\mu_s) = \mu_s \quad (206c)$$

and

$$b_1(\mu_s) = b_2(\mu_s) = 0 \quad (206d)$$

Accordingly, the Greek constants (Eq. (194)) can be evaluated analytically. The generalized spherical harmonics solution of Eq. (200) subject to the boundary conditions given by Eqs. (202a) and (202b) is discussed in more detail by Benassi et al. (1984a, 1984b) as it relates to the solution of the radiative transfer equation.

Although the problem so far has been reduced to solving two separate systems of equations, i.e., the  $\mathcal{J}$ - $Q$  case and the  $\mathcal{V}$ - $\mathcal{U}$  case, there are situations when these four equations reduce to two (the  $\mathcal{J}$ - $Q$  case only). In particular, in a plane-parallel medium with no incident radiation (or unpolarized incident light), the axial symmetry of the radiation field requires that the plane of polarization be along the meridian plane (or, at right angles to it). Consequently, only two components,  $\mathcal{J}$  and  $Q$  or equivalently,  $G_1^m(z, \mu, t) = (\mathcal{J}+Q)/2$  and  $G_r^m(z, \mu, t) = (\mathcal{J}-Q)/2$ , are required to

characterize the correlation field. The other two remaining correlated parameters,  $U$  and  $V$ , are zero under these circumstances. Therefore, only the  $\mathcal{P}$ - $Q$  problem needs to be solved, i.e., Eqs. (200) and Eq. (202) with  $B$  being given by Eq. (204). This is easily verified by returning to Eqs. (176) and (177). In a planar or spherical system, the plane of polarization, described by the angle  $\chi$ , must either be along the meridian plane ( $\chi=0$ ) or perpendicular to it ( $\chi=\pm\pi/2$ ) in order to maintain the symmetry. Therefore, Eq. (176) gives  $U=0$ . Furthermore, for complete symmetry, polarization has to be random. Any sense of polarization (clockwise or counterclockwise) constitutes an asymmetry. Thus,  $\beta=0$ , i.e., the ratio of the axes of the polarization ellipse is zero. Therefore, Eq. (177) gives  $V=0$ . Thus, for systems with plane symmetry (and with boundary conditions that do not destroy the symmetry), one needs to deal only with two coupled equations of transfer for  $G_1^m$  and  $G_r^m$ , or equivalently, for  $\mathcal{P}$  and  $Q$ .

In what follows and for simplicity,  $G^1$  will denote the parallel component of the correlation function along the meridian plane ( $G_1^m$ ) and  $G^r$  will denote the perpendicular component ( $G_r^m$ ). For this special case, it is easier to present the solution using a Legendre series expansion which is different but related to the generalized spherical harmonics approach.

Using the analytical expression for Rayleigh scattering [Chandrasekhar, 1960], and the expression for  $g^1$  (Eq. (4)),

the phase matrix in Eq. (179) is given by

$$P(\mu, \mu', t) = \frac{3}{4} e^{-t} \begin{bmatrix} 2(1-\mu^2)(1-\mu'^2) + \mu^2\mu'^2 & \mu^2 \\ \mu'^2 & 1 \end{bmatrix} e^{t\mu\mu'} \quad (207a)$$

where it is understood that  $G^m$  is the vector  $[G^l, G^r]^T$ . Note that if one wishes to use the Stokes parameters  $\mathcal{J} = G^l + G^r$  and  $Q = G^l - G^r$ , then Eq. (207a) should be restated as

$$P(\mu, \mu', t) = \frac{3}{4} e^{-t} e^{t\mu\mu'} \times \begin{bmatrix} 1 + P_2(\mu)P_2(\mu')/2 & P_2(\mu)[P_2(\mu')-1] \\ P_2(\mu)P_2(\mu)-P_2(\mu') & [1-P_2(\mu')][1-P_2(\mu)] \end{bmatrix} \quad (207b)$$

where  $P_2(\mu) = (3\mu^2-1)/2$ .

If polarization is neglected, then  $Q=0$  or  $G^l = G^r = G^m/2$ . Note that for the Rayleigh phase function components given by Eq. (207a), the normalization condition, Eq. (182b), results in the following definition of the effective albedo

$$\omega_e(t) = e^{-t} t^{-1} \left[ \sinh(t)(1 + 2t^{-2}) - 2t^{-1} \cosh(t) \right] \quad (208)$$

To proceed with the  $P_1$  approximation,  $P$  is written as a series of Legendre polynomials

$$P(\mu, \mu', t) = \sum_{i=0}^J (2i+1) P_i(\mu) Z_i(t) P_i(\mu') \quad (209a)$$



where

$$Z_i(t) = \frac{4}{(2i+4)} \int_{-1}^1 \int_{-1}^1 P(\mu, \mu', t) P_i(\mu) P_i(\mu') d\mu d\mu' \quad (209b)$$

Similarly, let  $\mathbf{G}^m = [G^l, G^r]^T$  be a series expansion in terms of Legendre polynomials, i.e.,

$$\mathbf{G}^m(z, \mu, t) = \frac{1}{4\pi} \sum_{i=0}^J (2i+1) P_i(\mu) \mathbb{G}_i(z, t) \quad (210)$$

where  $\mathbb{G}_i(z, t)$  is a 2 by 1 column vector of eigenvectors that need to be determined. Substituting Eq. (209a) and Eq. (210) into Eq. (178), gives

$$\sum_{i=0}^J (2i+1) P_i(\mu) \left[ \mu \frac{\partial}{\partial z} \mathbb{G}_i(z, t) + \mathbb{G}_i(z, t) - \omega \mathbb{B}_i(t) \mathbb{G}_i(z, t) \right] = 0 \quad (211)$$

where the orthogonality of the Legendre polynomials, Eq. (C2) was used. Substituting the recurrence relation for the Legendre polynomials of Eq. (C4) into Eq. (211), and rearranging the resulting series gives

$$(i+1) \mathbb{G}'_{i+1}(z, t) + i \mathbb{G}'_{i-1}(z, t) + (2i+1) \mathbf{A}_i \mathbb{G}_i(z, t) = 0 \quad (212)$$

Equation (212) is similar to the scalar form of the spherical harmonics solution to the radiative transfer problem [Ozisik, 1973]. The prime on  $\mathbb{G}$  represents a first derivative with respect to  $z$ , and  $\mathbf{A}_i$  is a 2 by 2 matrix

given by

$$\mathbf{A}_i = \bar{\mathbf{1}} - \omega \mathbf{B}_i(t) \quad (213)$$

where  $\bar{\mathbf{1}}$  is the identity matrix.

The  $P_1$  approximation consists of using  $J=1$  and neglecting higher order terms ( $G_i$ 's) in the expansion given by Eq. (210) and their derivatives. As a consequence, Eq. (212) results in the following system of first order differential equations

$$G_1'(z,t) + \mathbf{A}_0 G_0(z,t) = 0 \quad (214a)$$

and

$$G_0'(z,t) + 3\mathbf{A}_1 G_1(z,t) = 0 \quad (214b)$$

Solving Eqs. (214a) and (214b) simultaneously (differentiating each equation once in the process and using matrix algebra) gives the following two uncoupled second order systems of differential equations for  $G_0(z,t)$  and  $G_1(z,t)$

$$G_0''(z,t) - 3\mathbf{A}_1 \mathbf{A}_0 G_0(z,t) = 0 \quad (215a)$$

and

$$G_1''(z,t) - 3\mathbf{A}_0 \mathbf{A}_1 G_1(z,t) = 0 \quad (215b)$$

The above system of equations can be transformed into an

eigenvalue problem and solved numerically. This path to the solution becomes imperative when the order of the approximation is higher than one.

At this time the analytical solution to Eqs. (215) will be presented. Let's start by solving Eq. (215b) and let  $a_{ij}^{01}$  be the elements of the matrix  $A_0 A_1$ . Also, let  $[G_1^l, G_1^r]$  be the corresponding elements of the vector  $G_1$ . Then, the two coupled equations of Eq. (215b) can be given by

$$G_1^{l''} - 3a_{11}^{01}G_1^l - 3a_{12}^{01}G_1^r = 0 \quad (216a)$$

and

$$G_1^{r''} - 3a_{21}^{01}G_1^l - 3a_{22}^{01}G_1^r = 0 \quad (216b)$$

where all the arguments were dropped for simplicity. Solving for  $G_1^r$  from Eq. (216a) gives

$$G_1^r = (G_1^{l''} - 3a_{11}^{01}G_1^l) / 3a_{12}^{01} \quad (217)$$

Differentiating Eq. (217) twice with respect to  $z$  and substituting the result, along with Eq. (217) into Eq. (216b) results in a fourth order ordinary differential equation for  $G_1^l$

$$G_1^{l(4)} - \kappa G_1^{l(2)} - \gamma G_1^l = 0 \quad (218)$$

where the superscript (i) means the  $i$ th derivative with respect to  $z$ , and where

$$\kappa = 3(a_{11}^{01} + a_{22}^{01}) \quad (219)$$

and

$$\Psi = 9(a_{12}^{01}a_{21}^{01} - a_{11}^{01}a_{22}^{01}) \quad (220)$$

Equation (218) admits the following solution

$$G_1^1(z, t) = C_1 e^{d_1 z} + C_2 e^{-d_1 z} + C_3 e^{d_2 z} + C_4 e^{-d_2 z} \quad (221)$$

where

$$d_1 = \left[ \frac{1}{2} (\kappa - (\kappa^2 + 4\Psi)^{\frac{1}{2}}) \right]^{\frac{1}{2}} \quad (222)$$

and

$$d_2 = \left[ \frac{1}{2} (\kappa + (\kappa^2 + 4\Psi)^{\frac{1}{2}}) \right]^{\frac{1}{2}} \quad (223)$$

The constant coefficients in Eq. (221) are to be determined after applying the boundary conditions.

Differentiating Eq. (221) twice with respect to  $z$  and substituting the result into Eq. (217) to solve for  $G_1^r$ , we find

$$G_1^r(z, t) = \left[ \Psi (C_1 e^{d_1 z} + C_2 e^{-d_1 z}) + \Lambda (C_3 e^{d_2 z} + C_4 e^{-d_2 z}) \right] / 3a_{12}^{01} \quad (224)$$

where  $\Psi$  and  $\Lambda$  are given by

$$\Psi = d_1^2 - 3a_{11}^{01} \quad (225)$$

and

$$\Lambda = d_2^2 - 3a_{11}^{01} \quad (226)$$

respectively. Solving for  $G_0$  from Eq. (214a) gives

$$G_0(z,t) = -A_0^{-1}G_1'(z,t) \quad (227)$$

Substituting the solution for  $G_1(z,t)$  (Eqs. (221) and (224)) back into Eq. (227), and solving the resulting system of equations gives

$$G_0^{1,r}(z,t) = (H_0^{1,r}(C_2e^{-d_1z} - C_1e^{d_1z}) + F_0^{1,r}(C_4e^{-d_2z} - C_3e^{d_2z}))/3a_{01}^{12} \quad (228)$$

where the superscript  $1,r$  means either  $1$  or  $r$ , and where  $H_0^{1,r}$  and  $F_0^{1,r}$  are given by

$$H_0^{1,r} = d_1(3a_{-0}^{j1}a_{01}^{12} + a_{-0}^{j2}\Lambda) \quad (229a)$$

and

$$F_0^{1,r} = d_2(3a_{-0}^{j1}a_{01}^{12} + a_{-0}^{j2}\Lambda) \quad (229b)$$

where  $j=1$  for the  $1$ -component, and  $j=2$  for  $r$ -component.  $a_{-0}^{ij}$  are the elements of the matrix  $A_0^{-1}$ .

Setting  $J=1$  in Eq. (210), the  $P_1$  solution for the correlation function is given by

$$G^m(z, \mu, t) = \frac{1}{4\pi} (G_0(z, t) + 3\mu G_1(z, t)) \quad (230)$$

The last remaining step in the solution is to solve for the four unknown constants ( $c_i$ ,  $i=1,2,3$  and 4). This is achieved by applying Marshak's method [Ozisik, 1973] at the boundaries of the medium. At  $z=0$ , this gives

$$\int_0^1 G^m(0, \mu, t) \mu d\mu = \int_0^1 \delta(\mu - \mu_0) F \mu d\mu = \mu_0 F, \quad \mu > 0 \quad (231a)$$

and at  $z=L$ , we have

$$\int_0^1 G^m(L, -\mu, t) \mu d\mu = 0, \quad \mu > 0 \quad (231b)$$

Substituting Eq. (230) into Eqs. (231a) and (231b) results in a system of four linear equations and four unknowns

$$WC = H \quad (232)$$

where  $W$  is the coefficient matrix with the elements  $W_{ij}$  given by

$$W_{1j} = 6a_0^{12} + (-1)^j H_0^1, \quad j=1,2 \quad (233a)$$

$$W_{1j} = 6a_0^{12} + (-1)^j F_0^1, \quad j=3,4 \quad (233b)$$

$$W_{2j} = 2(d_1^2 - 3a_{01}^{11}) + (-1)^j H_0^r, \quad j=1,2 \quad (233c)$$

$$W_{2j} = 2(d_2^2 - 3a_{01}^{11}) + (-1)^j F_0^r, \quad j=3,4 \quad (233d)$$

$$W_{3j} = -(6a_0^{12} + (-1)^j H_0^1) \exp[-(-1)^j d_1 L], \quad j=1,2 \quad (233e)$$

$$W_{3j} = -(6a_0^{12} + (-1)^j F_0^1) \exp[-(-1)^j d_2 L], \quad j=3,4 \quad (233f)$$

$$W_{4j} = 2 \exp[-(-1)^j d_1 L] [(3a_{01}^{11} - d_1^2) + (-1)^j H_0^r], \quad j=1,2 \quad (233g)$$

$$W_{4j} = 2 \exp[-(-1)^j d_2 L] [(3a_{01}^{11} - d_2^2) + (-1)^j F_0^r], \quad j=3,4 \quad (233h)$$

$C$  is the unknown vector with coefficients  $C_i$  ( $i=1,2,3,4$ ) and  $H$  is the constant vector

$$H = 24\pi\mu_0 a_{01}^{12} [F_I, F_r, 0, 0]^T \quad (234)$$

where

$$F_I = \frac{1}{2}(F_I + F_Q)$$

and

$$F_r = \frac{1}{2}(F_I - F_Q)$$

Then the four unknown coefficients are given by

$$C = W^{-1}H \quad (235)$$

Several simple numerical procedures can be used to solve either Eq. (232) or Eq. (235). Once the four unknowns are found, the field correlation function can be computed from Eqs. (230), (228), (224) and (221) for the two polarization components.

In the next chapter, numerical results of the various

solution methods that were given in the previous chapters will be presented and discussed.



## CHAPTER VII

### RESULTS AND DISCUSSION

Representative results of the various solution methods that were discussed in earlier chapters will be presented here. Some of these results have already been published while this work was in progress [Dougherty et al., 1991, Ackerson et al., 1992, Reguigui et al., 1993, Dorri-Nowkoorani et al., 1993, Dougherty et al., 1994].

Explicitly, back-scattering from semi-infinite media, and transmission and back-scattering results from finite plane parallel media (unit index of refraction) subjected to a collimated normally incident radiation are presented using: preaveraged CTE, CTE with 1-, 2-, 3-, and 8-term Legendre expansions of  $g^1$ , the exponential kernel approximation to CTE, and the diffusion approximation to CTE. Effects of optical thickness and off-angle detection are presented. Comparison with Diffusive Wave Spectroscopy [Pine et al., 1990] results and some experimental data [Dorri-Nowkoorani, 1992, Dorri-Nowkoorani et al., 1993] are also presented. Some results with index of refraction different than one are presented in conjunction with the preaveraged theory and then compared to experimental data. Transmission and back-scattering results for the  $P_1$

approximation are also presented for the parallel and perpendicular (to the plane of scattering) components of the field correlation function when polarization effects are not neglected. Finally, the special case of applying CTE to gel suspensions in semi-infinite media is presented.

Some of the source codes used to generate some of the results presented here are modifications of previously existing programs and can in general handle a wide range of parameters and situations. Numerical results for the correlation function with a three-term Legendre expansion of  $g^1$  were obtained by modifying and running existing FORTRAN codes [Dougherty, 1992] that were developed and discussed by Crosbie and Dougherty (1978, 1983), for semi-infinite media with unit index of refraction, and by Crosbie and Dougherty (1980, 1982, 1985) for finite cylindrical media with unit index of refraction, of which, the one-dimensional results are a special case. When expanding  $g^1$  in a series of more than three terms, a FORTRAN computer code that was developed and discussed by Liu (1993) was modified and used. For results that include index of refraction effects, FORTRAN source codes that were developed by Reguigui (1990), Reguigui and Dougherty (1992), and by Jiang (1990) were used. Jiang's work was modified to include delay-time dependence by Dorri-Nowkoorani (1993).

For most of the results, the normalized field correlation functions ( $g^{m+}$  and  $g^{m-}$ ) are presented on semi-logarithmic plots, unless mentioned otherwise. Because it

has been observed, and was reported by Pine et al. (1990) and by Dorri-Nowkoorani et al. (1993), that the correlation function for a semi-infinite medium exhibits a square root decay rate dependence, the various curves presented here are shown as a function of the square root of the delay time. All transmission and back-scattering results are shown for the normal emerging direction ( $\mu=1$ ) except for the off-angle results. The particles are assumed to be isotropic and independent scatterers in free diffusion unless specifically mentioned otherwise. The medium is assumed to be a plane parallel slab with azimuthal symmetry and with no index of refraction change at the boundary unless specifically mentioned otherwise. The incident radiation for all of the test cases that are presented here is assumed to be collimated normal to the top boundary and with azimuthal symmetry. No radiation is incident at the bottom of the medium. All the graphs are placed at the end of this chapter.

#### VII.1. Comparison with Diffusive Wave Spectroscopy

The very thick limit can be adequately represented by the diffusion approximation in what has become known as Diffusive Wave Spectroscopy (DWS) [Pine et al., 1990]. CTE can also predict this limit properly, and the only constraint on the accuracy of the solution is the accuracy of the approximating method used to solve the CT governing equations.

Solutions to the isotropic CTE are presented in a limit similar to DWS, namely, very short delay time and thick media. A preliminary investigation was reported in a paper by Ackerson et al. (1992). Transmission and back-scattering results for finite media of thicknesses 10 and 25, and back-scattering results from a semi-infinite medium were presented. The preaveraged equation, Eq. (63), with  $\omega_p$  given by Eq. (66) was solved using the X- and Y- functions and the exponential kernel approximation (EKA) for the case of a finite medium, and using the H-function and the reduced EKA for the case of an infinite medium.

These results were compared with the DWS theory [Pine et al., 1990] and showed slight disagreement except at very short delay time which was very good. The predictions (using the EKA solution to the preaveraged CTE) agreed very well with DWS at very short delay times,  $(\tau/\tau_0)^{0.5} \leq 0.1$ , for various high optical thicknesses, ranging from 10 to 30, in transmission (see Fig. 5). A value of  $z_0/l^* = 1.29$  corresponds to the best agreement between EKA and DWS. As delay time increases  $((\tau/\tau_0)^{0.5} > 0.2)$ , EKA results tended to show a slight upward curvature with increasing delay time which does not fit DWS and the experimental observations (see Fig. 5). This upward curvature was attributed to the severe preaveraging approximation which averages over all anisotropy in the problem and results in the elimination of some of the longer scattering paths, thus resulting in a slower decay of the correlation function.

The single scattering function ( $g^1$ ) in particular, Eq. (4), becomes more anisotropic with increasing time (see Fig. 6), and a more careful handling of  $g^1$  in the scattering integral (Eq. (52)), was recommended to improve the results. This next task was done and published in a following paper by Reguigui et al. (1993), where Legendre expansion (up to 3-terms) of the  $g^1$  term in Eq. (52) was used in the case of back-scattering from a semi-infinite medium. This is shown in Figs. 7 and 8 for the back-scattering from infinite media, and in Figs. 9 and 10 for back-scattering and transmission, respectively, from finite media. This procedure produced much better agreement with DWS as compared to the preaveraging results (Fig. 7) for back-scattering from semi-infinite media. In Fig. 7, the preaveraged results, using the X- and Y-solution to Eq. (63), and the results for 1-, 2-, and 3-term Legendre (3TL) expansions of  $g^1$  (Eq. 108)) are compared with DWS (for  $z_0/l^*=1.33$ ). It appears that CTE results get closer and closer to DWS results as the number of terms in the Legendre expansion of  $g^1$  increases.

The DWS theory is parameterized by deposition length  $z_0$ , with  $z_0$  being a free parameter that depends on the distance  $l^*$  that the light takes to travel into the medium before it starts diffusing. The CTE theory does not require any fitting parameters, and when compared to DWS, it appears that a value of 1.29 for  $z_0/l^*$  makes the DWS results agree very well with the CTE results for finite optical

thicknesses higher than 5 (Figs. 9 and 10) and up to the semi-infinite case (Fig. 8), especially for very short delay times. This short time agreement is expected, since DWS is only valid for very short delay times.

Note that the DWS and 3TL results shown in Figs. 7 and 8 are compared up to a delay time of 0.25 [ $(\tau/\tau_0)^{0.5} = 0.5$ ]. This is typically beyond the range of the validity of DWS [Pine et al., 1990]. However, 3TL and DWS still agree well throughout this range.

For transmission, the agreement between DWS and CTE is only good for optical thicknesses higher than 20 and for very short delay times as shown in Fig. 10. This is also expected because of the very fast decay rate of  $g^{m+}$  for transmission due to the long scattering paths' contribution to this decay.

Figures 11 and 12 present a comparison between transmission results from DWS and the CTE solutions in the diffusion approximation (section V.2.b) for optical thicknesses of 25 and 5 respectively. It is apparent from Fig. 11, that the diffusion approximation to CTE agrees very well with DWS at very short delay time ( $(\tau/\tau_0)^{0.5} \leq 0.1$ ) but starts to disagree as delay time increases. This is expected since DWS and the diffusion approximation to CTE employ the same approximations concerning the diffusion of light. However, DWS includes the additional assumption of very short delay-time. When the short time limit of the diffusion solution to CTE is compared to DWS, the agreement

is even better since now both solution techniques employ similar assumptions. The same conclusions can be reached when comparing DWS and CTE in the diffusion limit for an optical thickness of 5 (Fig. 12). These numerical results agree with the conclusions presented by Ackerson et al. (1992) who demonstrated analytically that both CTE and DWS are equivalent when all assumptions are kept the same.

In the following section, results obtained by expanding  $g^1$  in Legendre polynomials will be presented for the finite and semi-infinite cases. These results will be compared to the preaveraging approximation with  $\omega_p$  given by Eq. (66), the exponential kernel approximation (EKA), and for various orders of approximation in the Legendre expansion.

## VII.2. Results with the Legendre Expansion of $g^1$

In section (V.1.b),  $g^1$  was approximated by a series of Legendre polynomials (Eqs. (108)-(115)). Numerical comparison between the exact form of  $g^1$  (Eq. (4)) and its Legendre expansion approximation shows that the seventh order (8-term) approximation for  $g^1$  results in an accuracy on the order of  $10^{-6}$  percent relative error for all angles and up  $\frac{\tau}{\tau_0} \leq 0.4$ , which is the practical range of time in most experimental situations of interest (or even shorter for high optical thicknesses). This high limit on the accuracy is required to reduce any accumulated numerical errors while doing numerical integration in double precision arithmetic. Note that for delay times less than 1, a higher

order approximation does not necessarily give better results due to numerical errors that may occur while dividing by small numbers. A series expansion for the coefficients of the Legendre expansion (as given in Appendix A) needs to be used in this case.

Test runs showed that different orders of approximation should be used for different time ranges to produce accuracy on the order of  $10^{-6}$  (percentage relative error) at all angles when comparing the analytic  $g^1$  to its Legendre series expansion according to the following:

1st-order approximation for  $0.0 < \frac{\tau}{\tau_0} \leq 2.0E-4$

2nd-order approximation for  $2.0E-4 < \frac{\tau}{\tau_0} \leq 3.0E-3$

3rd-order approximation for  $3.0E-3 < \frac{\tau}{\tau_0} \leq 0.02$

4th-order approximation for  $0.02 < \frac{\tau}{\tau_0} \leq 0.06$

5th-order approximation for  $0.06 < \frac{\tau}{\tau_0} \leq 0.15$

6th-order approximation for  $0.15 < \frac{\tau}{\tau_0} \leq 0.2$

7th-order approximation for  $0.2 < \frac{\tau}{\tau_0} \leq 0.4$

The first three terms in the Legendre series expansion are given by Eqs. (112)-(115). The remaining terms are given in Appendix A.

For the three-term expansion, Fig. 13 shows that the



percent error between the exact  $g^1$  and its approximation grows beyond 0.05% for  $\frac{\tau}{\tau_0} > 0.15$ . This range is extended considerably ( $\frac{\tau}{\tau_0} > 0.5$ ) when an eight-term (order seven) Legendre approximation is used (see Fig. 14).

In a previous paper, Ackerson et al. (1992) presented two solution methods for the preaveraged CTE, namely, the exact X and Y- functions and the EKA for finite media, and the H-function for the semi-infinite media. These solution methods will be compared to the Legendre polynomial approximation of  $g^1$  (up to a second order approximation), which does not require preaveraging.

First, the back-scattering results from a semi-infinite medium are compared in Fig. 15. Note that the preaveraged solution, using the exact H-function, represents the least accurate method as compared to the one-, two-, and three-term Legendre expansion. The benefits gained by including more Legendre terms in the expansion are the ability to compute the MS correlation function to longer delay times. However, for very short times,  $(\frac{\tau}{\tau_0})^{0.5} < 0.15$ , the different approximations give similar results as Fig. 15 shows. The time intervals for which a certain Legendre approximation order is most desirable were presented on the previous page.

Similar conclusions about the different approximations can be drawn for the case of finite media, as shown in Figs. 16-20. The EKA is compared to the 3TL expansion of  $g^1$  for back-scattering in Fig. 16 and for transmission in Figs. 17 and 18 for various optical thicknesses. The results show

that the EKA agreement with the 3TL improves as the optical thickness increases and for short delay times. This is also expected, since the EKA employs most of the DWS approximations, and therefore, the trends are similar to DWS.

Figures 19 and 20 present a comparison between the 3TL and preaveraging in back-scattering and transmission, respectively, for an optical thickness of 25. The same conclusion reached earlier can be drawn here: the accuracy of the results increases as approximation improves from the preaveraging to higher order Legendre expansions.

The eight-term Legendre expansion of  $g^1$  results (8TL) are shown for Figs. 21 and 22 for transmission and back-scattering, respectively, for optical thicknesses of 5 and 20. For transmission, the 8TL solution does not differ much from the 3TL solution. Comparison is shown for delay-times up to 1.5 (Fig. 21a). Although the transmitted correlation decays several orders of magnitude in that time range, the deviation between 3TL and 8TL is not big as seen in Fig. 21b which shows nearly two orders of magnitude in the decay of the correlation function.

For back-scattering, the 8TL solution starts to deviate from the 3TL solution for  $(\tau/\tau_0)^{0.5} > 0.5$  when the 3TL approximation starts to fail. The difference between the 3TL and the 8TL is more apparent for back-scattering because of the contribution of short scattering paths to back-scattering. These short paths exhibit stronger angular

dependence and thus, more Legendre terms are needed when computing the correlation function in the back-scattering direction. For transmission, all scattering paths are at least of length  $L$ , and thus, the transmitted correlation is due mainly to these long paths which result in a fast decay.

VII.2.a. Effect of Optical Thickness: The decay rate of the correlation function depends on the path the light has to travel to reach the detector. The 3-D plots of Figs. 23 and 24 show the effects of increasing optical thickness from the single scattering limit to the thick limit on the field correlation function for transmission and back-scattering, respectively, in the normal direction. The logarithm of the normalized  $G^m$  is plotted versus the square root of the non-dimensional delay time and versus different optical thicknesses (from low to high) of the plane parallel medium. High optical thicknesses (long scattering paths) are the result of many scattering events and low optical thicknesses (short paths) are the result of few scattering events. For low optical thicknesses, a particle has to move considerably, and thus takes more time, for the total path length to change by a wavelength (the typical length scale). This results in a slow decay. Inversely, for large number of scattering events (high optical thicknesses), and each particle in the path moves a short distance, the total length of the path changes considerably. This results in a fast decay rate as shown in Figs. 23 and 24.

The linear dependence of  $g^m$  ( $=G^m(z, \mu, \tau)/G^m(z, \mu, \tau=0)$ ) on

$\left(\frac{\tau}{\tau_0}\right)^{0.5}$  has been observed experimentally by Pine et al. (1988) and by Dorri-Nowkoorani et al. (1993) for high optical thicknesses. However, for small optical thicknesses, the behavior of  $g^m$  deviates from this trend as a result of the reduction of the long multiple scattering paths. This feature is emphasized in Figs. 25a and 25b for back-scattering and in Fig. 26a for transmission.

The back-scattered MS correlation function ( $g^{m-}$ ) is plotted logarithmically versus  $\left(\frac{\tau}{\tau_0}\right)$  in Fig. 25a and versus  $\left(\frac{\tau}{\tau_0}\right)^{0.5}$  in Fig. 25b. The dependence on delay time clearly shifts from linear dependence for low optical thicknesses (Fig. 25a) to square root dependence for high optical thicknesses (Fig. 25b). The same behavior is shown in Figs. (26a) and (26b) for low and high optical thicknesses, respectively, for transmission. However, when delay-time increases ( $> 0.25$ ), the transmitted correlation function shows an upward curvature (see Fig. 26b). As explained earlier, this may be attributed to the approximations employed here which are accurate for  $\left(\frac{\tau}{\tau_0}\right)^{0.5} < 0.25$ .

VII.2.b. Comparison of the CTE to the Very Thin Limit Results: The semi-logarithmic plots of  $g^m$  show that the multiple scattering (MS) correlation function is not a single exponential as it is the case for single scattering. The single scattering limit, however, is matched exactly by the CTE solution. This is shown in Fig. 27, where the three-term Legendre solution is compared to the analytical form of  $g^1$ , the single scattering (SS) correlation function,

for optical thicknesses ranging from 0.001 to 0.3 in the back-scattering direction. It is clear that when the optical thickness exceeds 0.2, the behavior of  $g^m$  starts to deviate from the SS limit, indicating the presence of multiple scattering in the medium. The small deviation of the  $g^m$  curve for the 0.001 optical thickness (solid line) from the exact  $g^1$  curve (symbols) at delay times larger than 0.2 appears to be due solely to the limited accuracy of the three-term Legendre approximation used, as explained at the beginning of this section. This agreement extends to larger delay times when the 8TL is used as shown in Figs. 28 and 29 for transmission and back-scattering, respectively, and for different angles of scattering. For the 3TL, agreement between the analytic  $g^1$  and CTE improves when scattering is  $10^\circ$  off from normal (see Fig. 30).

### VII.3. Preaveraging and Off-angle Detection

The effect of off-angle (from normal,  $\mu \neq 1$ ) transmission and back-scattering was also investigated by Reguigui et al. (1993), and it was shown that the decay rate dependence on the detection angle decreases as the optical thickness (order of scattering) increases. Figure (31) represents the effect of off-angle detection for an optical thickness of 10. The results were obtained by solving the preaveraged CTE using the X- and Y-functions. The correlation decays slower when detected at larger angles from the normal back-scattering direction.

#### VII.4. Comparison With Experimental Data; Index of Refraction and Anisotropy Effects

In the paper by Reguigui et al. (1993), the preaveraged CTE and the the forward scattering approximation (discussed in Appendix E) was used to handle anisotropic scattering from large particles (comparing diameter to the wavelength). Results were presented for transmission and back-scattering from finite media of various optical thicknesses (5, 10, and 25) and with index of refraction different than one.

These effects resulted in a close agreement with experimental data (at short delay-time) as compared to results obtained by using the preaveraging approximation and an index of refraction different than 1. The experimental results were discussed in detail by Dorri-Nowkoorani et al. (1993), but there were no experimental error analysis. However, it was reported that the results are repeatable and therefore can be trusted. Figures 32 and 33 present two representative cases of these results for back-scattering from finite media of various optical thicknesses (5, 10, and 25). In Fig. 32, the preaveraged results with index of refraction of one are compared unsuccessfully to experimental data. In Fig. 33, the forward scattering approximation was employed with  $f=0.727$  (for 0.3 microns polystyrene particles) along with an index of refraction of 1.33 (for water) and the prediction improved considerably. Figures 34 and 35 present the same comparison for transmission. Here also the agreement between the

preaveraged solution with index of reflection and anisotropy agrees well with experiment except for intermediate optical thicknesses ( $L=5$ ).

Figure 36 presents results for 3TL CTE, DWS and data in semi-infinite media. The agreement shown here is excellent between 3TL and experimental data. The DWS results vary as a function of  $z_0/l^*$ . Good agreement between DWS and 3TL is observed when  $z_0/l^*=1.21$  (see Fig. 8). Figure 37 presents a comparison of experimental data with anisotropic preaveraged theory using the forward scattering approximation ( $f=0.727$ ) and an index of refraction equal to 1.33 for  $L=10$ . Agreement between experiment and CTE is excellent. Also Fig. 37 shows that transmitted correlation is not sensitive to the angle of detection for this high optical thickness.

#### VII.5. Polarization Effects

Polarization effects are known to affect the scattered correlation especially within an intermediate range of optical thicknesses (roughly between 1 and 10). To my knowledge, there exist only a few theoretical studies on the effects of polarization on field and intensity correlation functions [Stephen, 1988, 1986]. However, no one has reported numerical results. Pine et al. [1990] have recently published some experimental results for the intensity temporal correlation function (it is related to the field correlation function through Eq. (6)) scattered out from a medium that is subjected to a linearly polarized

incident radiation. Their preliminary investigation showed that the decay rate of both components (the parallel and the perpendicular) of the correlation function depend strongly on the detected polarization, especially for isotropic scatterers. Their measurements indicate that the correlation function for the perpendicular component of polarization decays more rapidly than the parallel component. This observation is predicted by the  $P_1$  approximation results shown in Figs. 38-43. The results presented in Figs. 38-39 are for a scattering geometry with axisymmetric symmetry and with unpolarized incident radiation, i.e.,  $F_I=1$  and  $F_0=0$  in Eq. (206) (equivalently,  $F_I=F_r=F_I/2$ ). The scattering laws are modeled according to Rayleigh scattering, which is a good approximation for the scattering characteristics of small particles compared to the incident wavelength.

Figures 38 and 39 show the back-scattered and transmitted correlation, respectively, for an optical thickness of 20. For comparison, the 3TL, the classical  $P_1$  and the  $P_0$  solution to the scalar CTE are also shown on Figs. 38 and 39. The  $P_N$  results are taken from Dorri-Nowkoorani et al. (1994) for isotropic scatterers. Both components of polarization ( $g^l$  and  $g^r$ ) decay at the same rate. This result is expected since for large optical thicknesses, there exists a very large number of scattering events, which results in a diminishing of the short paths contributions to the decay of the correlation function.



Upon scattering several times, polarization is randomized and as a consequence, its effect is minimized and both components of the correlation function approach the average scalar result as indicated by the 3TL or the  $P_0$  curves on Figs. 38 and 39.

When the optical thickness corresponds to the intermediate range of multiple scattering, polarization effects become more apparent. These effects are shown in Figs. 40 and 41 for back-scattering and transmission, respectively, from a medium with an optical thickness of  $L=5$ . Also on these figures, both components of polarization are compared to the 3TL, the  $P_1$  and the  $P_0$  approximate solutions to the scalar CTE. For the back-scattered correlation, Fig. 40a shows that both components of polarization decay at the same rate. This is also expected, since the short scattering paths contribute to the back-scattered correlation. And in this case, because of the unpolarized boundary condition, the back-scattered correlation remains almost unpolarized. Notice that the result matches the  $P_1$  approximation results at very short delay time (Fig. 40b). However, for the transmitted correlation for this optical thickness,  $L=5$ , the perpendicular and the parallel components of polarization decay at different rates (Figs. 41a and 41b). Low order scattering paths which have slow decay rates retain a high degree of their polarization and contribute to the parallel component. Thus, the parallel component ( $g^1$ ) decays more

slowly than the perpendicular component ( $g^r$ ) as indicated in Fig. (41a) and also has been reported by Pine et al. (1990) based on their experimental observations. The 3TL, the  $P_1$  approximation for isotropic scatterers, and the  $P_1$  approximation for Rayleigh scattering particles are also included on Figs. (41a) and (41b) for comparison. The  $P_1$  approximate solution for Rayleigh scattering is given in Appendix F. It is observed in Figs. (41a) and (41b) that the correlation function for both components retains the same exponential dependence on the square root of time for both components at this optical thicknesses ( $L=5$ ). This observation has been also reported by Pine et al. (1990).

Finally, results for the back-scattered and the transmitted correlation with polarization effects are shown in Figs. 42 and 43, respectively, for optical thicknesses of 1. The results here are not conclusive because of the divergence of the parallel component in the case of transmission (Fig. 43) and of both components of polarization in the case of back-scattering (Fig. 42). This behavior may be attributed to the normally incident collimated boundary condition which is poorly modeled by a  $P_1$  approximation, especially for low orders of scattering and normal direction, which is definitely the case for  $L=1$ . More terms in the approximation need to be included in the case.

The behavior of the  $P_N$ -approximation method as it relates to CTE was investigated by Dorri-Nowkooorani et al.

(1994). The 1st-order approximation ( $P_1$ ) did not result in any improvement of the results as compared to experiments. Dorri-Nowkooorani et al. (1994) showed that using higher orders of approximation improves the results, and Tian and Dorri-Nowkooorani (1992) used an improved  $P_1$  approximation that resulted in much better results than the simple  $P_1$  approximation. The improved  $P_1$  solution can easily be obtained by using the solution for  $G^m$ , obtained by the  $P_1$  approximation, in the source function equation and performing the integration analytically to obtain an improved solution.

#### VII.6 Extensions

Finally, it is worth noting at this point that the CTE can be extended to fluid/particle suspensions different than the case studied here (freely diffusing particles). This can be done by using a different form of the single scattering correlation function than the one used in Eq. (4), or by using a different probability distribution than the one used in Eq. (31).

As an example, the case of gel suspension has been studied. In this type of suspension, there exists a short range interparticle correlation due the constraints imposed by the gelling on the particle movement. Thus, Eq. (4) for  $g^1$  has to be modified accordingly. For the specific case where the particles are diffusing in constrained regions of the medium due to gelling, a stiffness coefficient ( $\Sigma$ ) needs

to be introduced into  $g^1$  according to the following transformation of the correlation time

$$t' = (1 - e^{-\Sigma t})/\Sigma$$

This imposed constraint, quantified by the stiffness parameter, indicates how strong the gel is. When the particles are freely diffusing ( $\Sigma=0$ ), the correlation delay-time is not changed i.e.,  $g^1$  as defined by Eq. (4) is used. The stiffness increases as the gelling progresses.

Some representative results are plotted in Fig. 44 for the case of semi-infinite gel suspensions where Figure 44 shows that the baseline of the correlation function is shifted upward as a function of increased gelling. The method of solution used to produce Fig. 44 was the 3TL expansion of the modified  $g^1$ , to account for gelling effects.

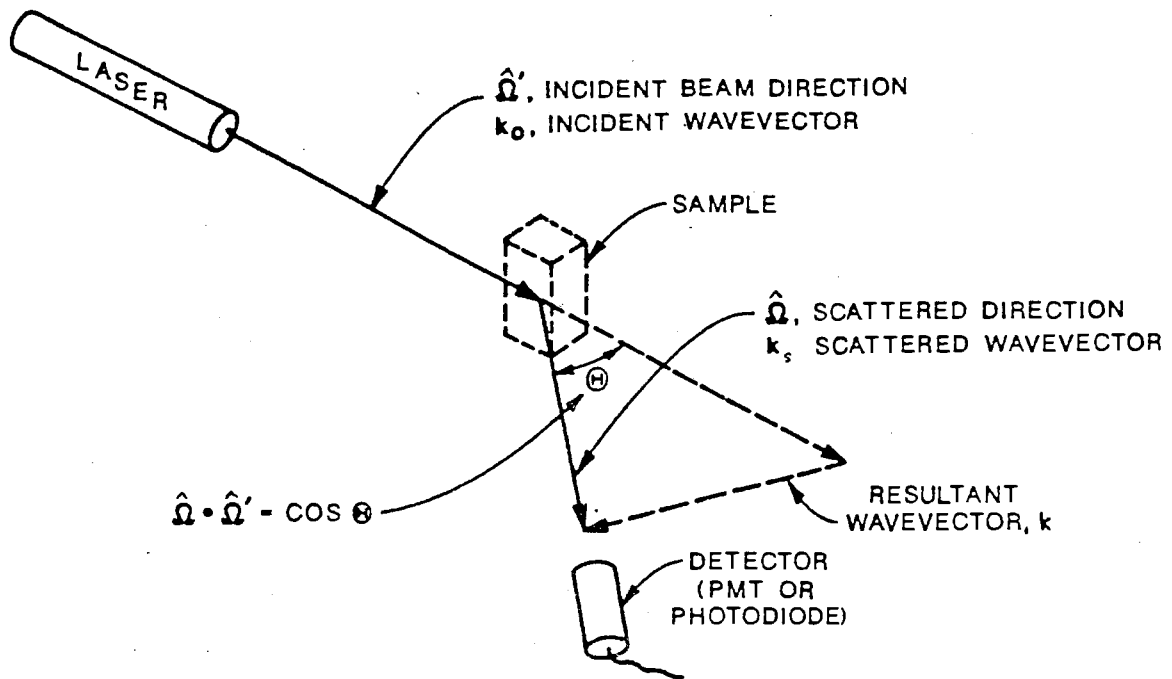


Figure 1. The Scattering Geometry

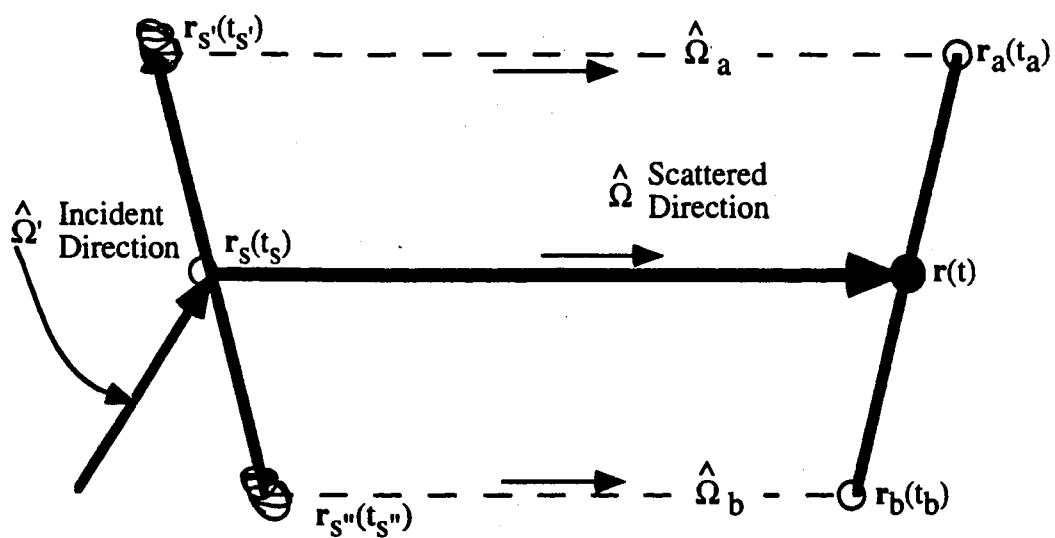


Figure 2. Scattering From a Moving Particle

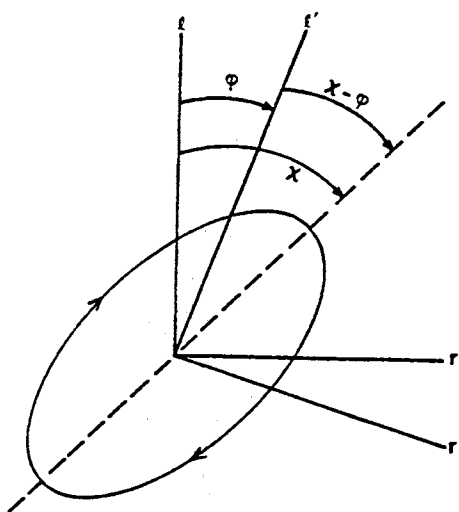
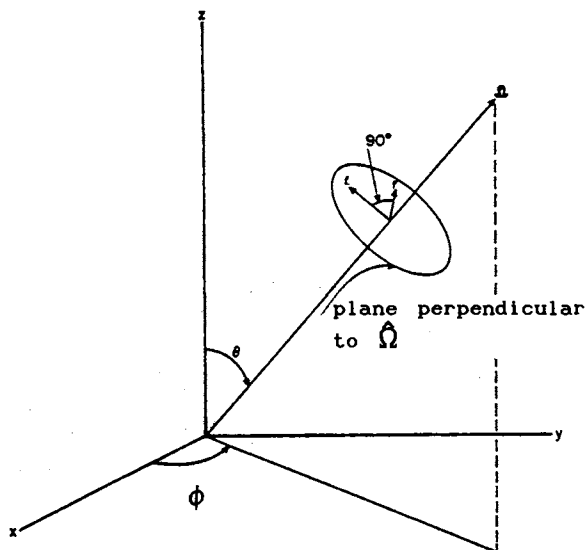


Figure 3. Rotation of the  $l$  and  $r$  Axes

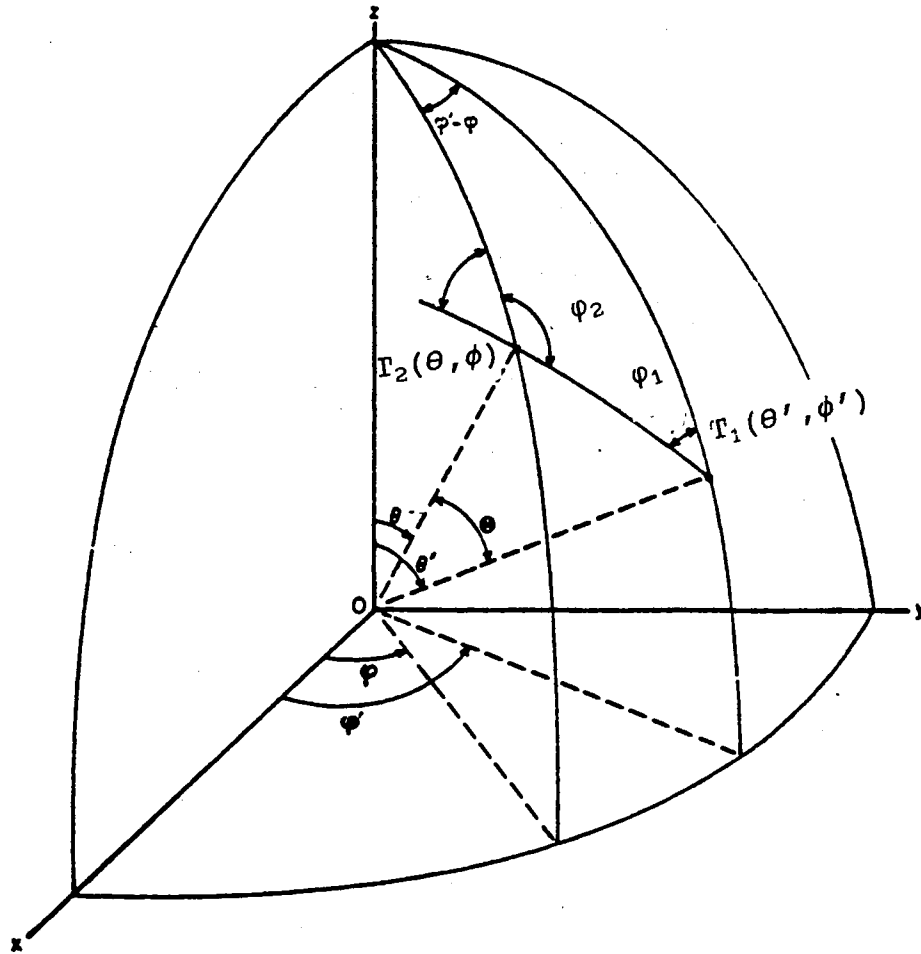


Figure 4. Transformation Between the Plane of Scattering and the Meridian Planes



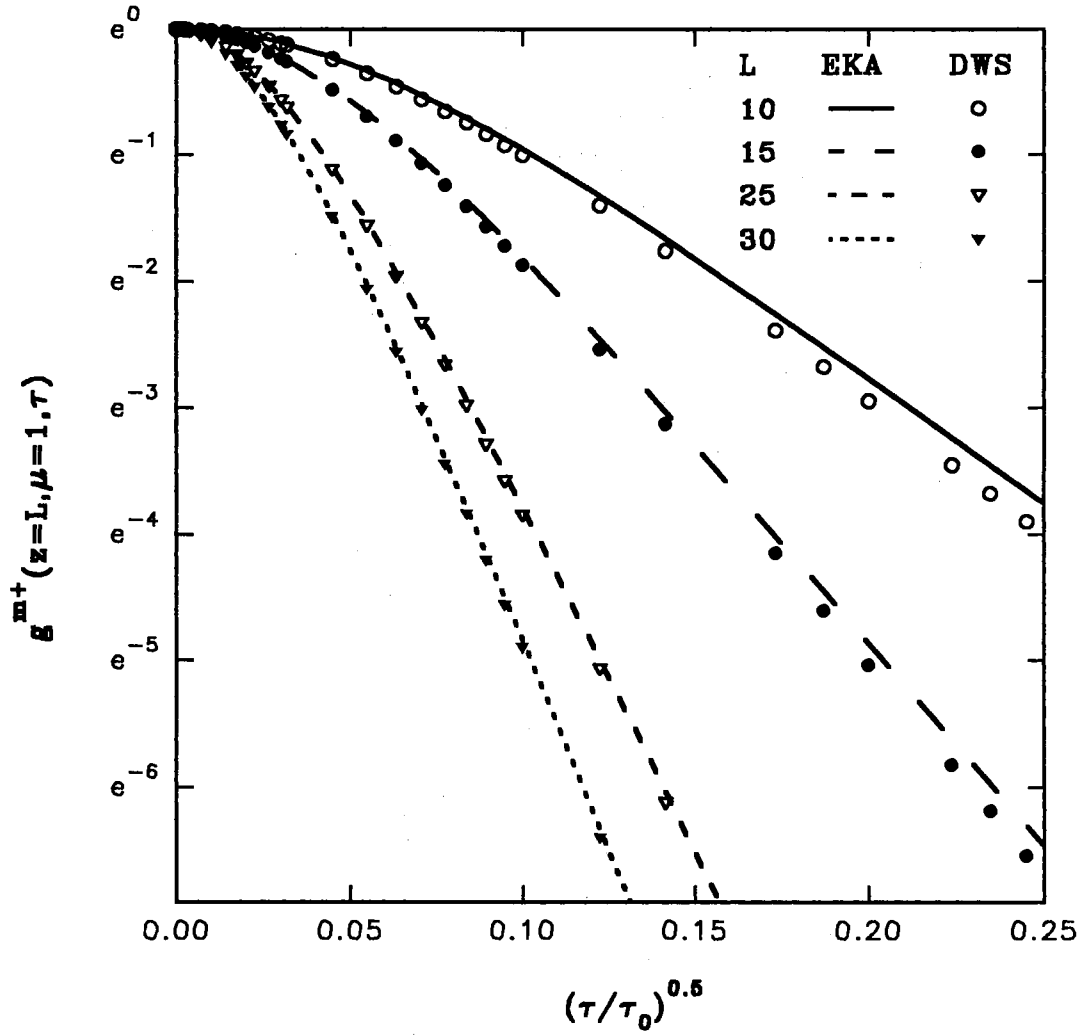


Figure 5. Comparison Between DWS and EKA for the Transmitted Correlation Function For Different Optical Thicknesses

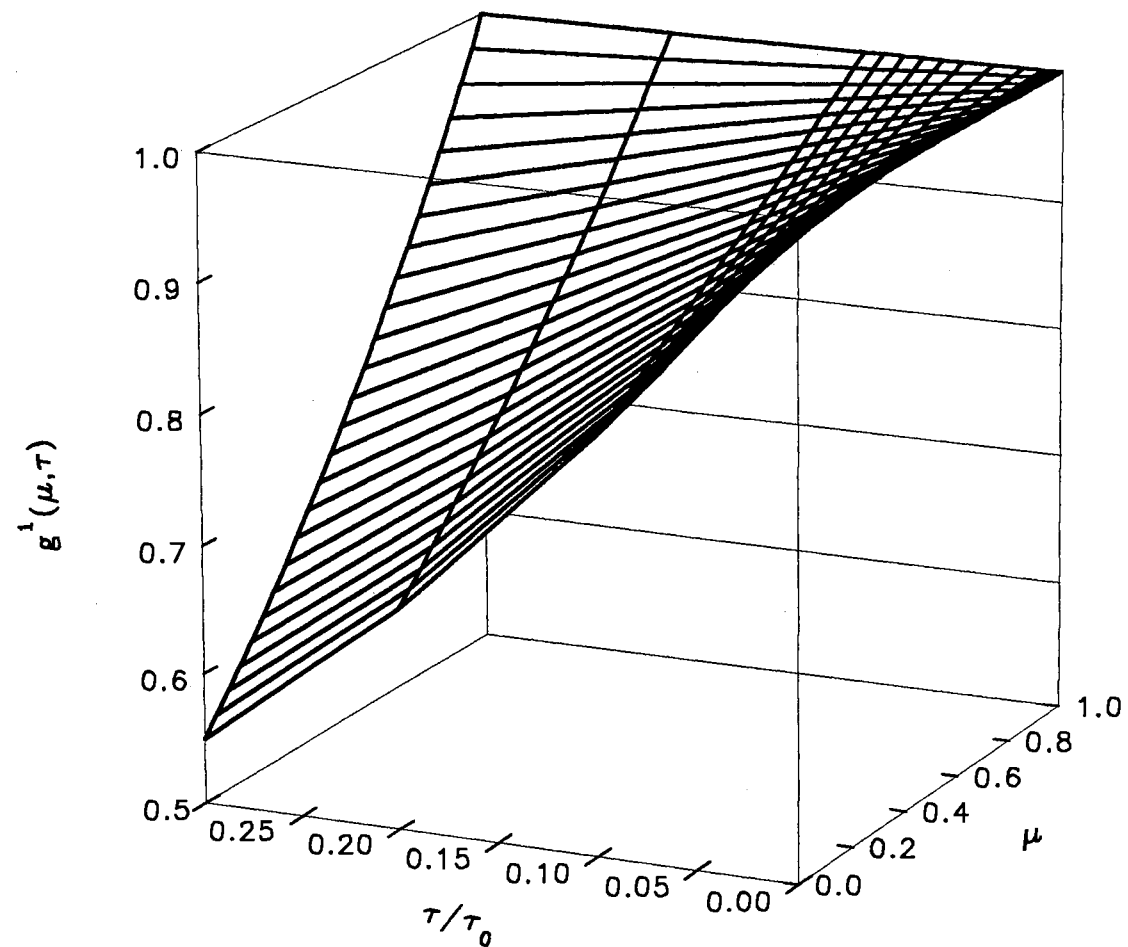


Figure 6. Single Scattering Field Correlation Function as a Function of the Scattering Angle and the Delay Time

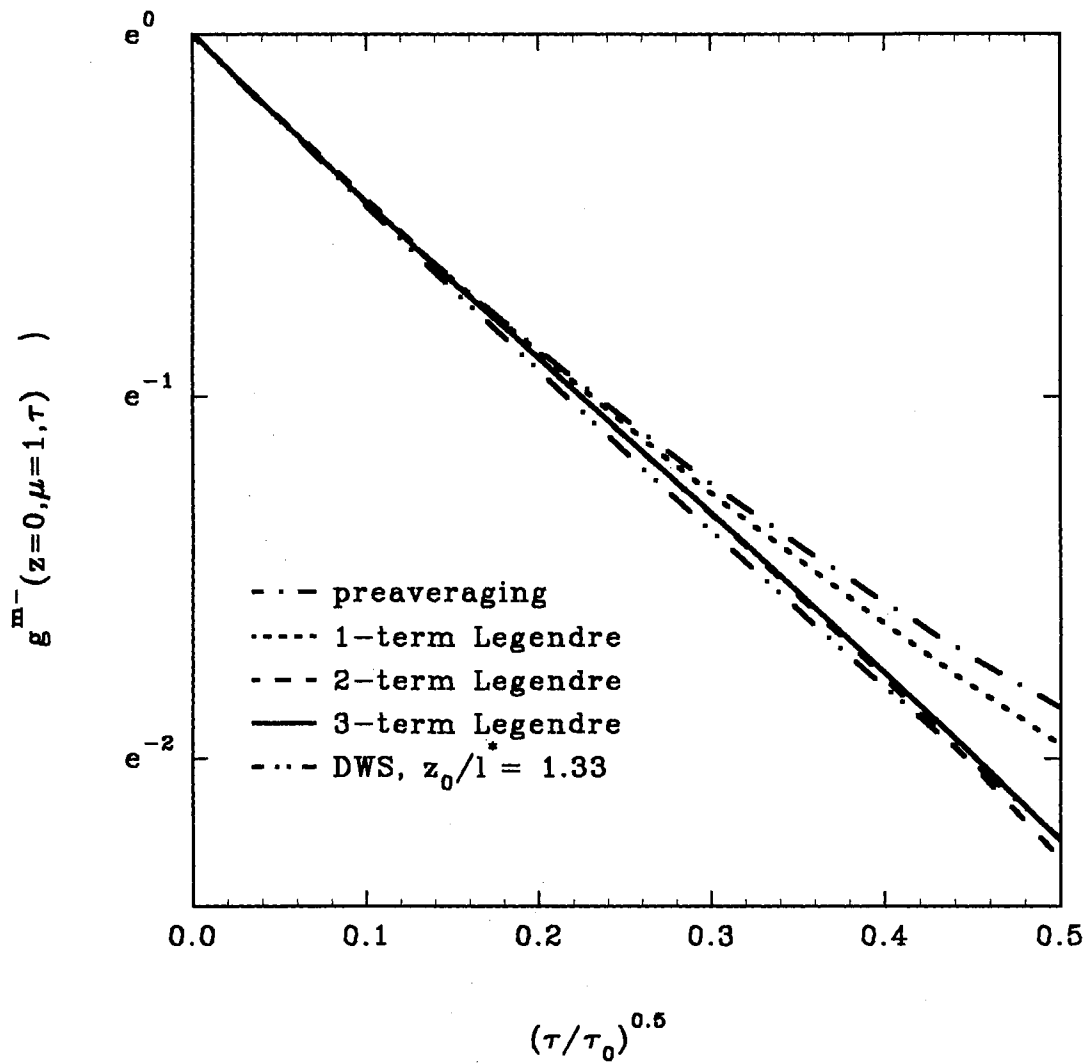


Figure 7. Comparison of DWS, Preaveraged CTE, 1TL, 2TL, and 3TL for the Back-Scattered Correlation Function From A Semi-Infinite Medium

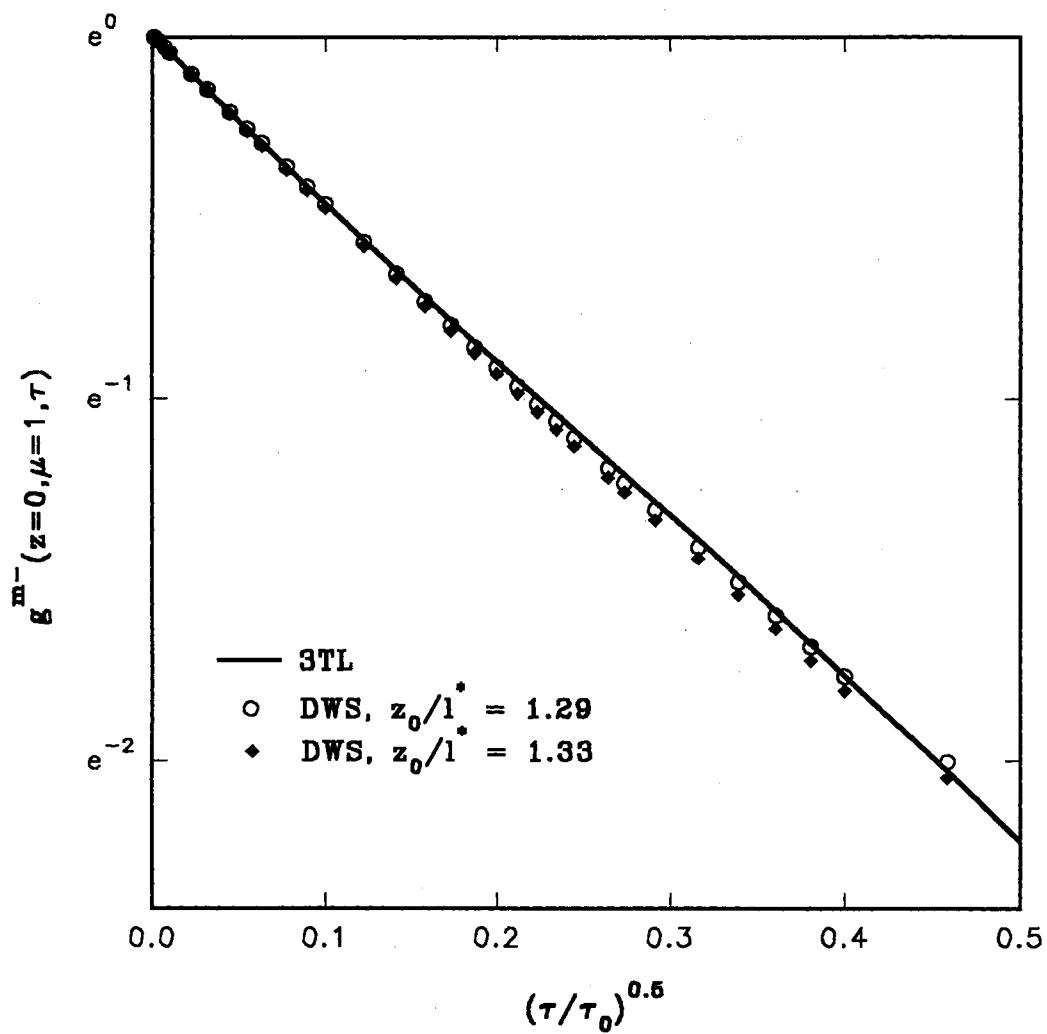


Figure 8. Comparison of DWS and 3TL For The Back-Scattered Correlation Function From A Semi-Infinite Medium

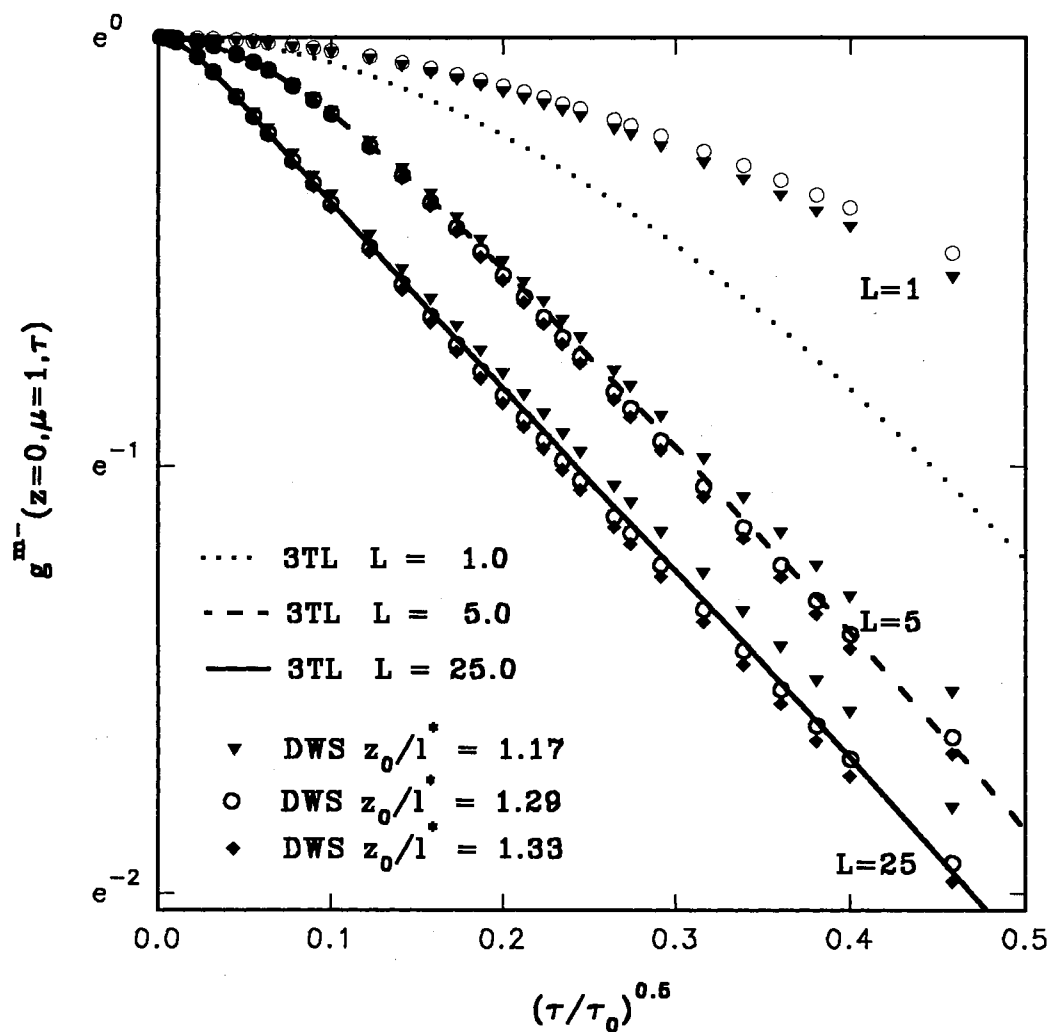


Figure 9. Comparison of 3TL and DWS For The Back-Scattered Correlation Function For Different Optical Thicknesses And Deposition Lengths

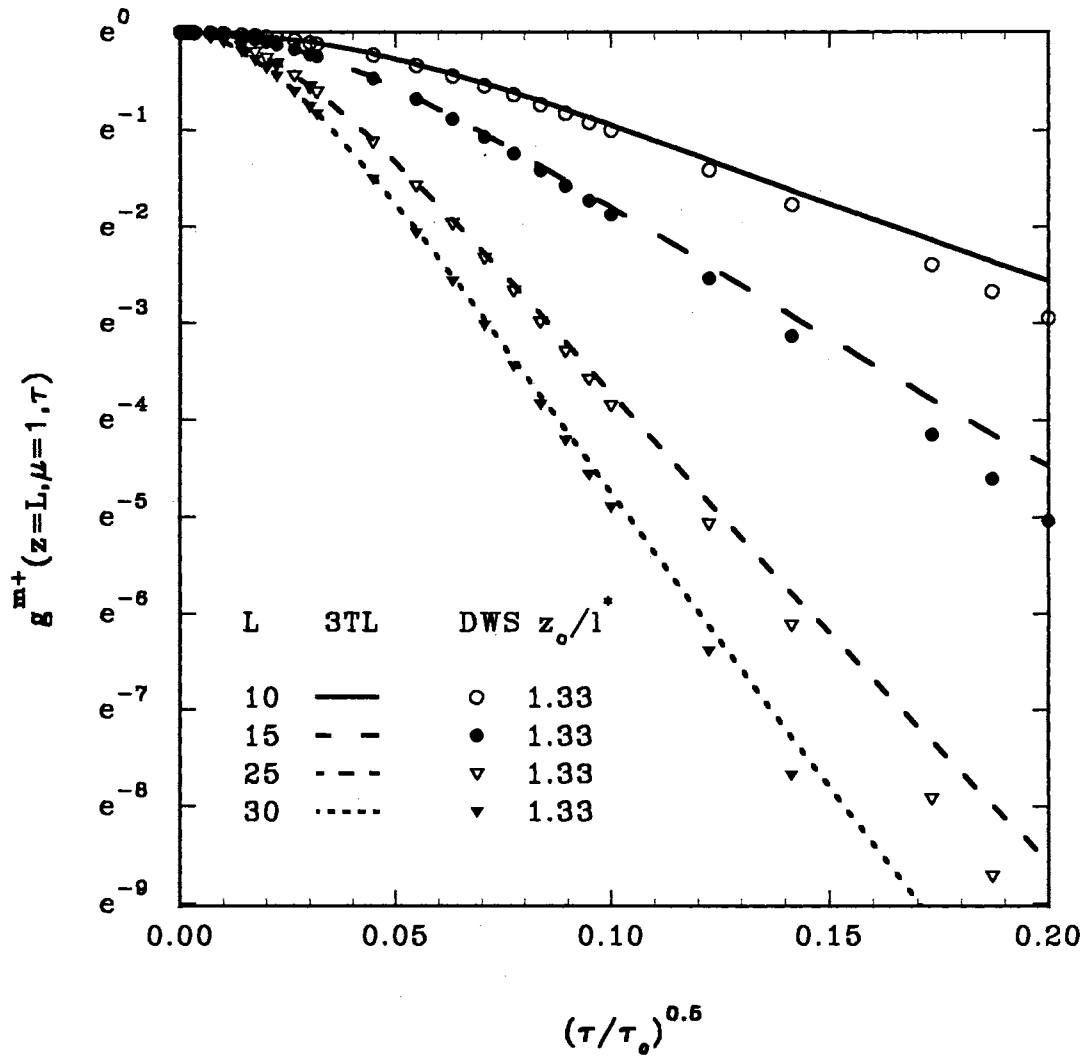


Figure 10. Comparison of 3TL and DWS For The Transmitted Correlation Function For Different Optical Thicknesses And Deposition Lengths

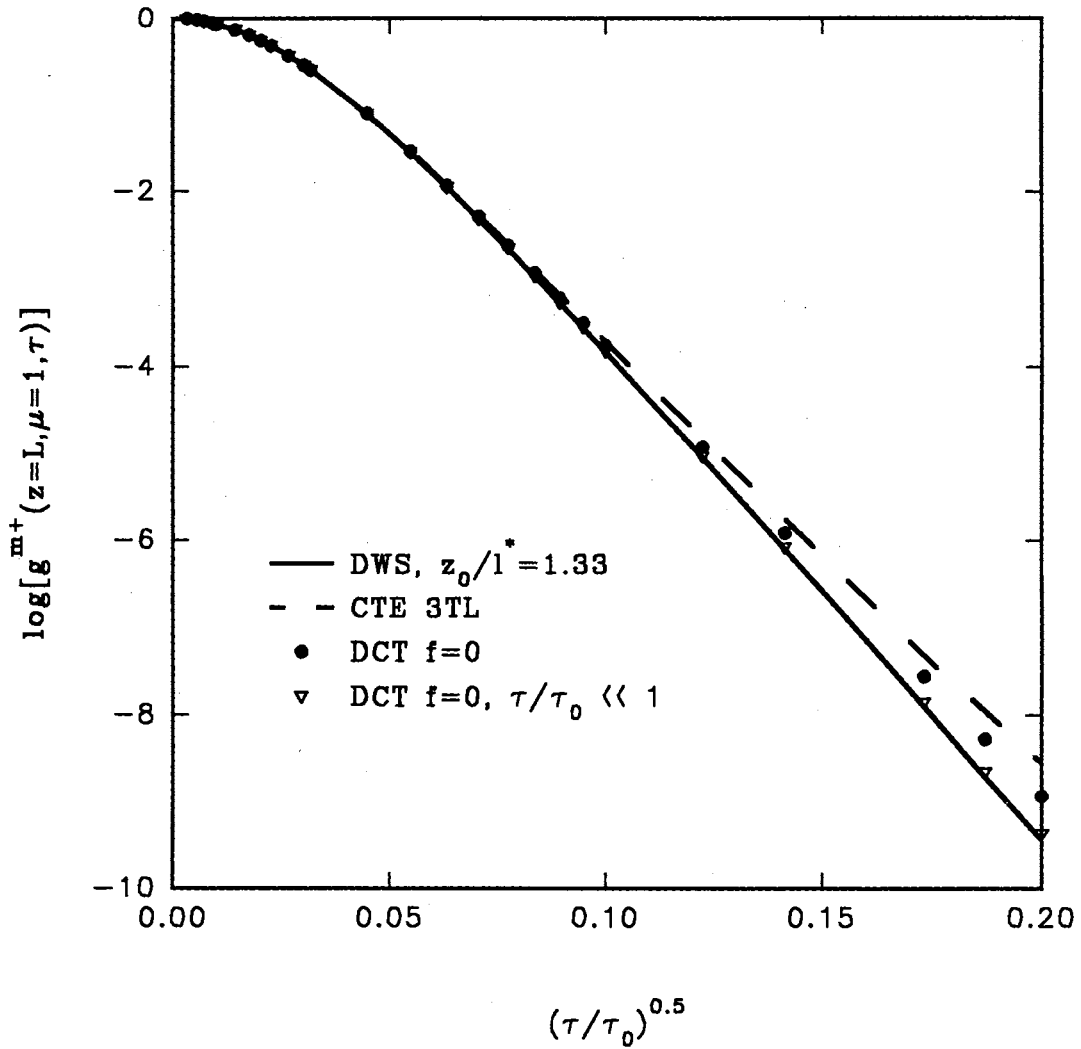


Figure 11. Comparison of 3TL, DCT and DWS For The Transmitted Correlation Function From A Medium With An Optical Thickness of  $L=10$  (The Asymmetry Factor,  $f$ , for DCT Is Taken As Zero)

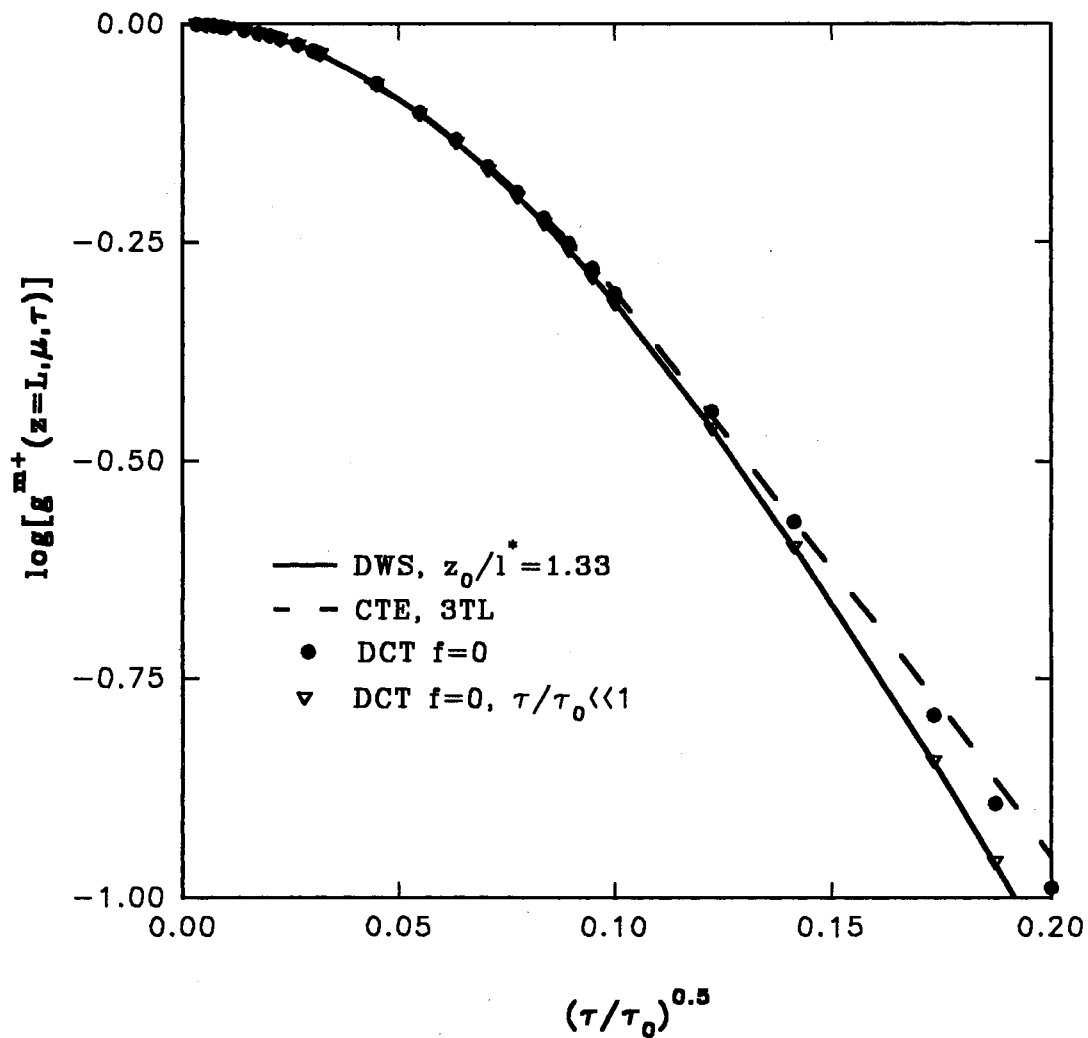


Figure 12. Comparison of 3TL, DCT and DWS For The Transmitted Correlation Function From A Medium With An Optical Thickness of  $L=10$  (The Asymmetry Factor,  $f$ , for DCT Is Taken As Zero)



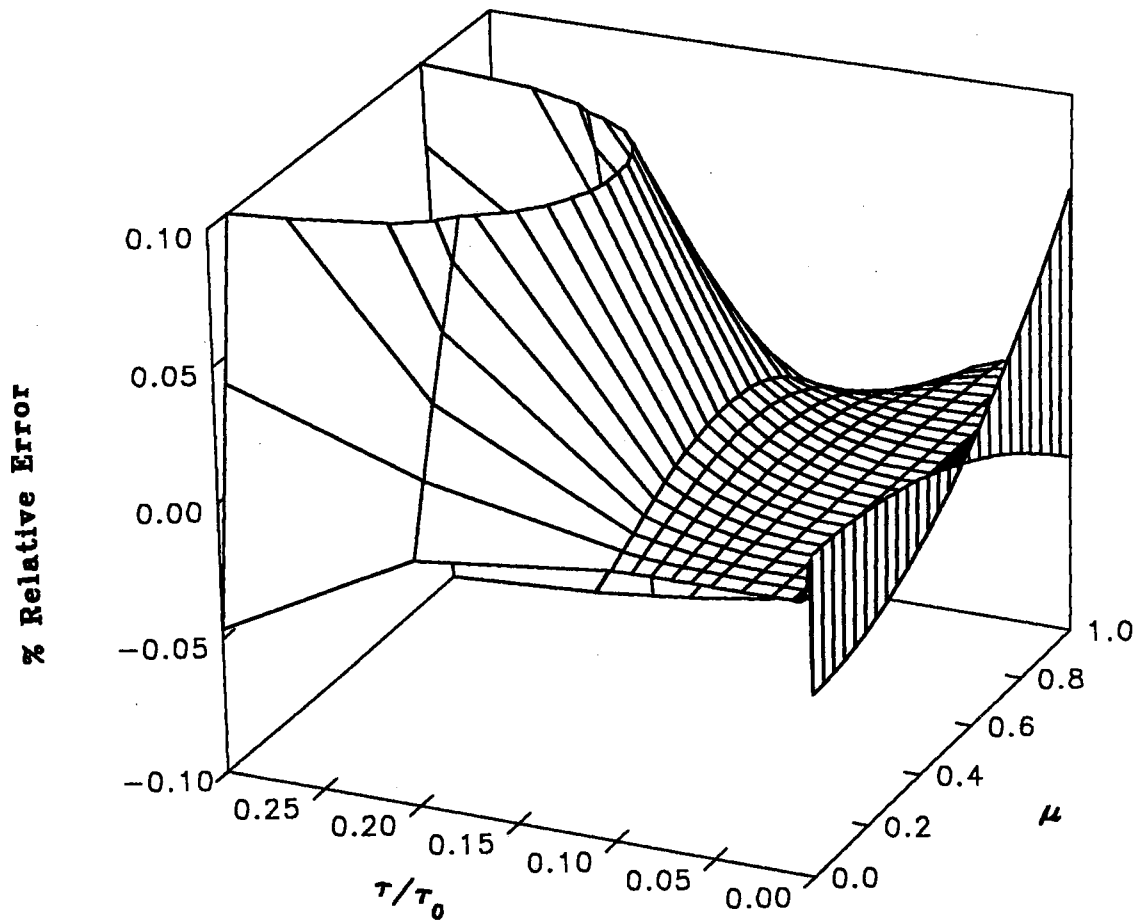


Figure 13. Percent Relative Error Between  $g^1$  And Its 3TL Approximation

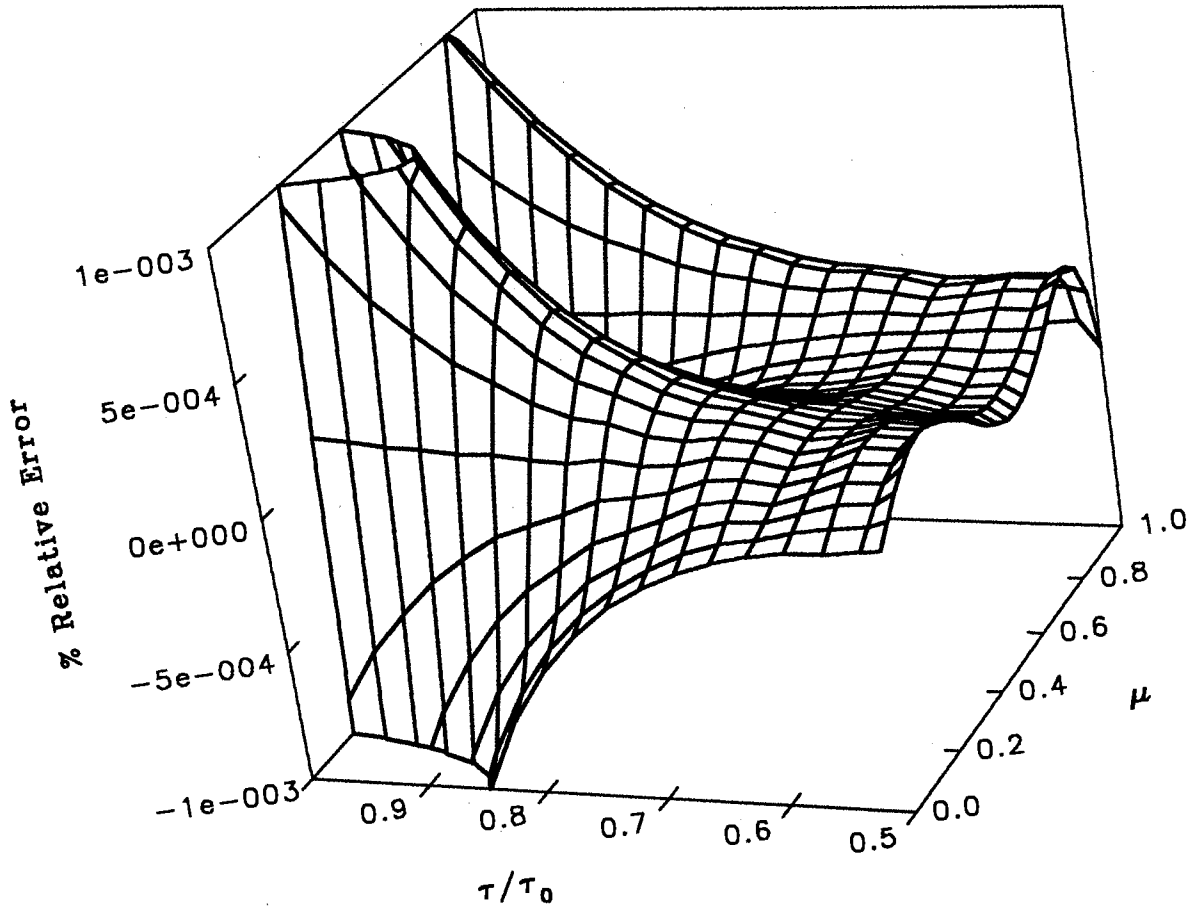


Figure 14. Percent Relative Error Between  $g^1$  And Its 8TL Approximation

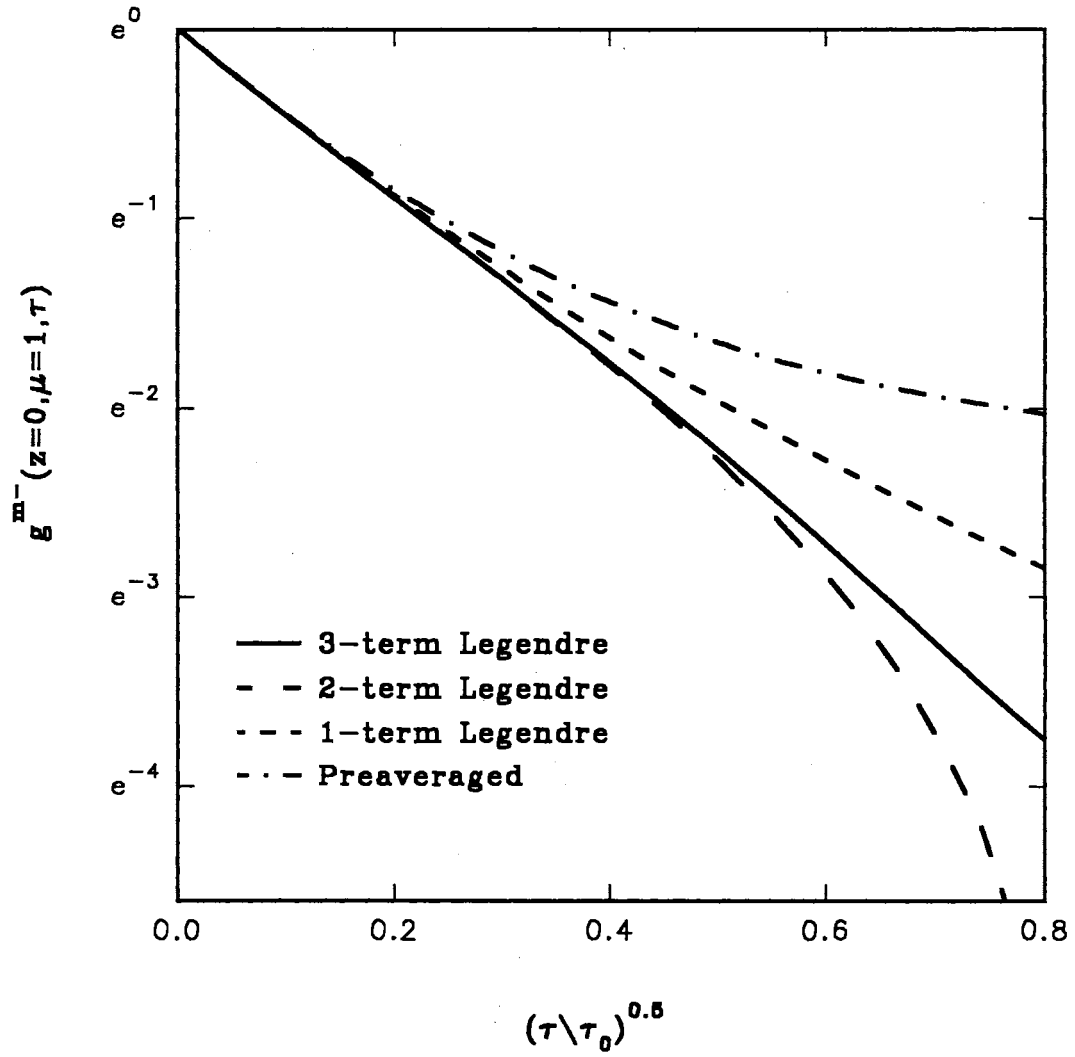


Figure 15. Comparison of the Back-Scattered Correlation Function From A Semi-Infinite Medium for The Preaveraged CTE, 1TL, 2TL, and 3TL

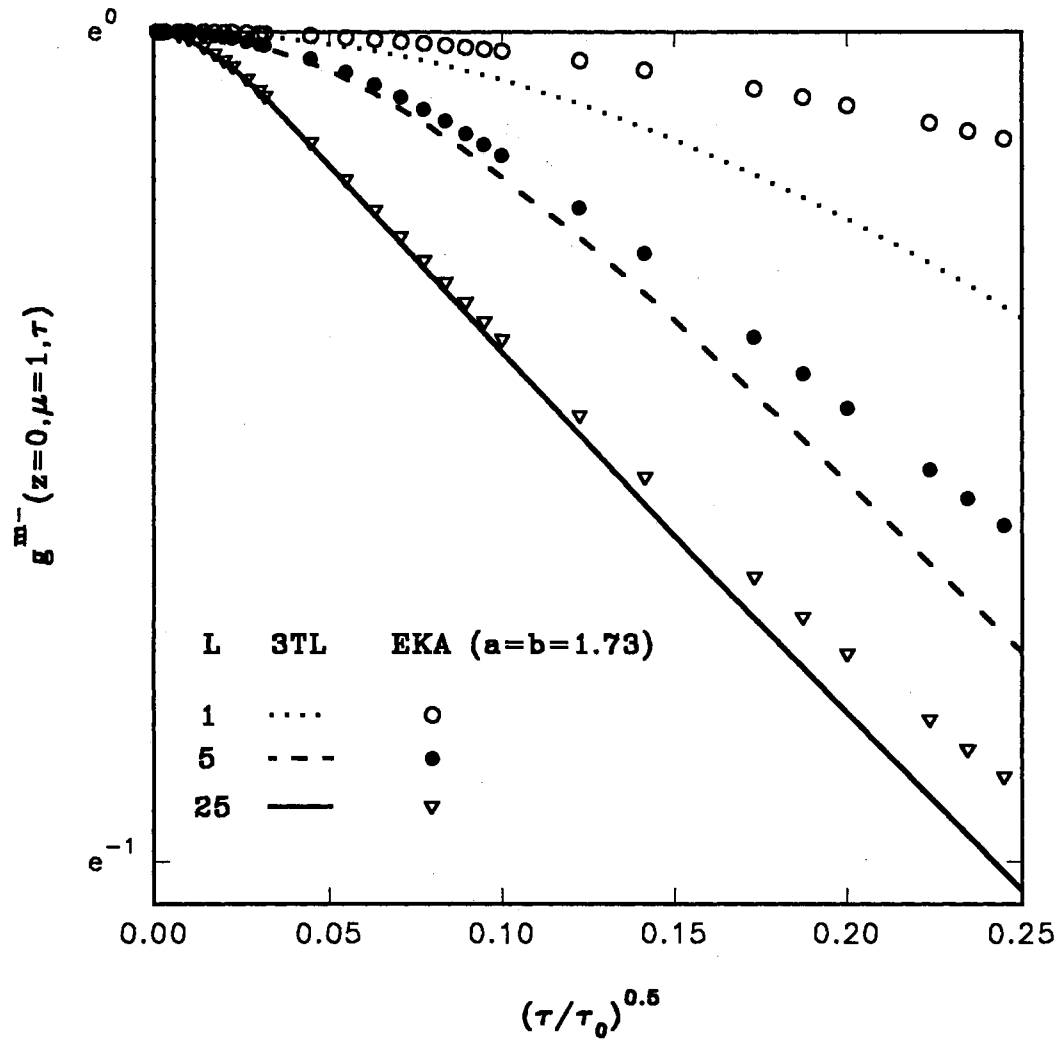


Figure 16. Comparison of 3TL and EKA For The Back-Scattered Correlation Function For Different Optical Thicknesses

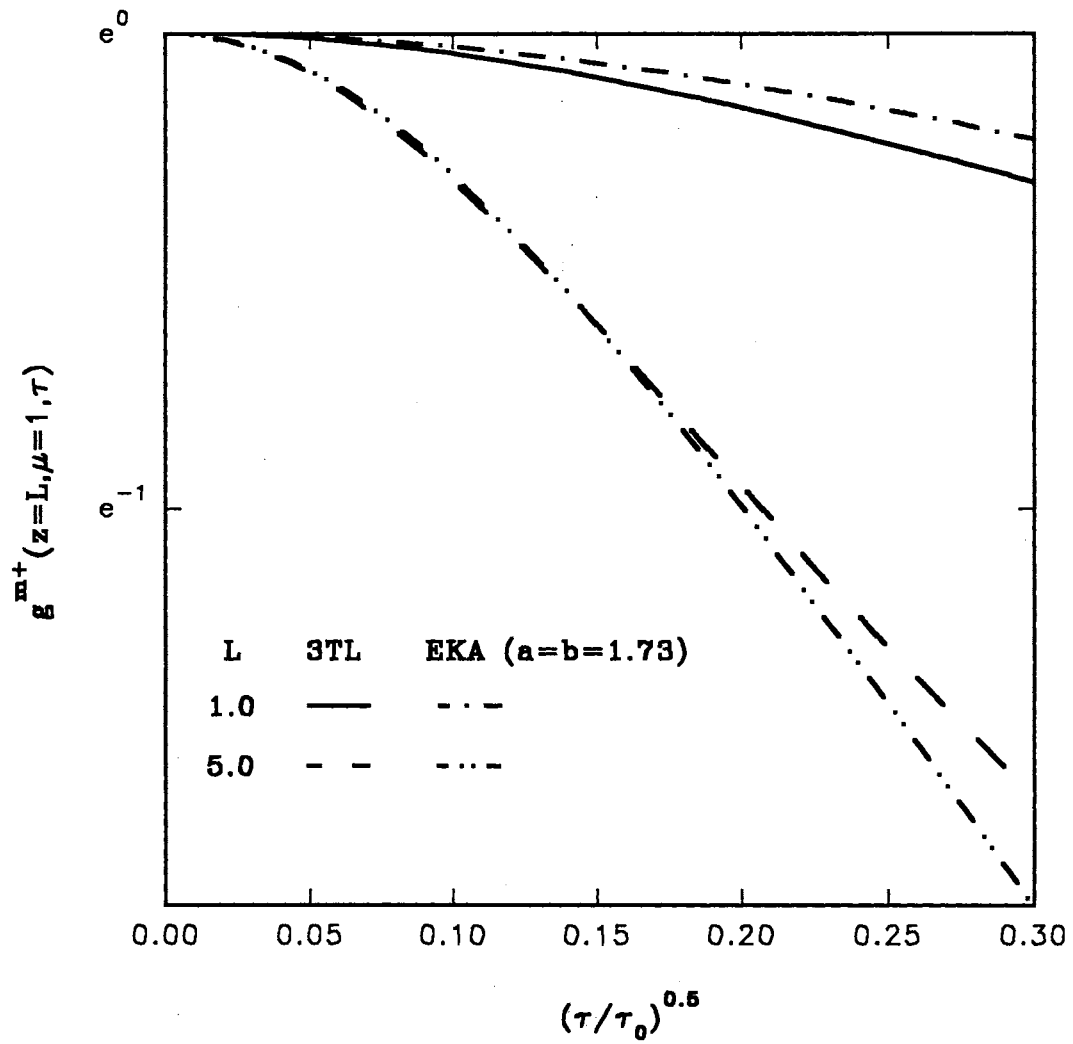


Figure 17. Comparison of 3TL and EKA For The Transmitted Correlation Function For Different Optical Thicknesses

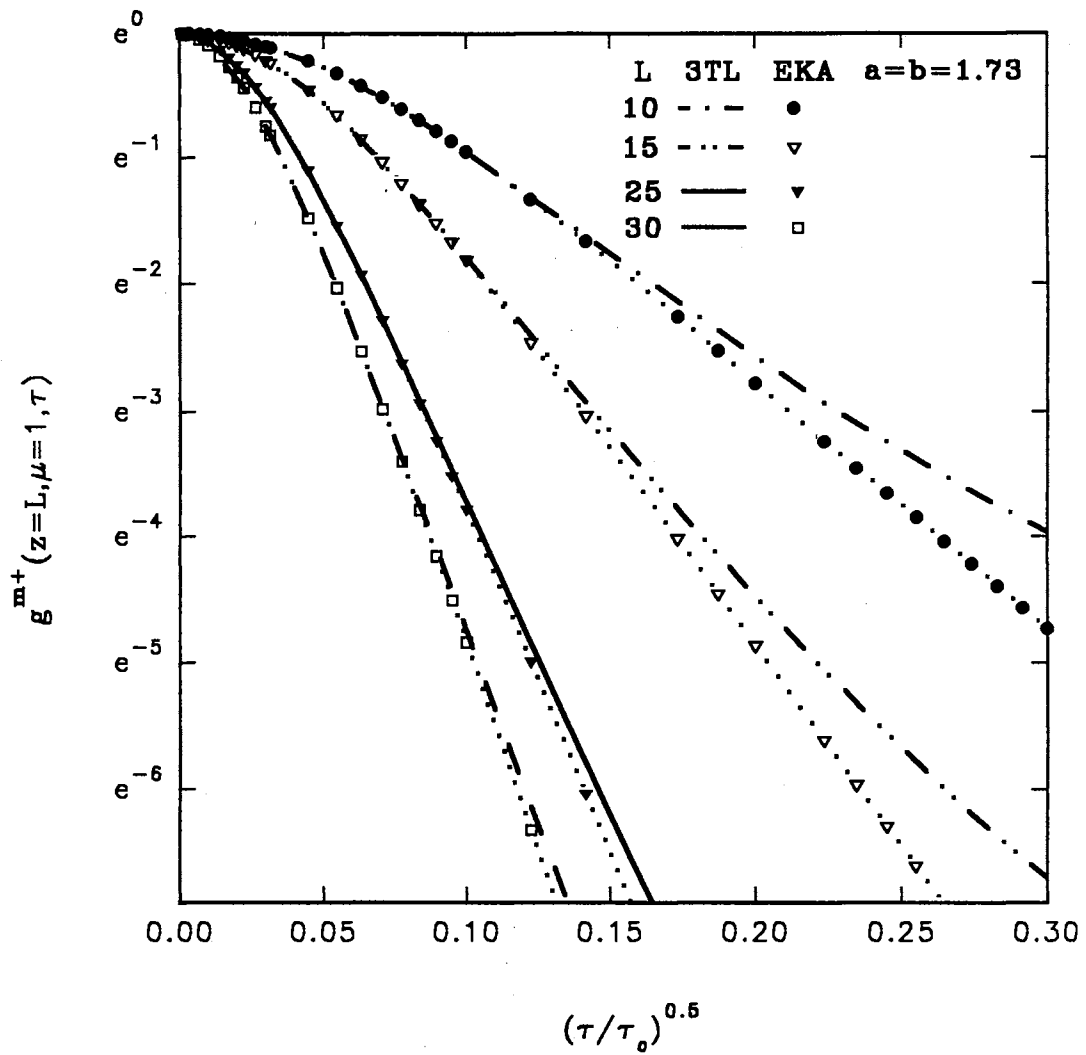


Figure 18. Comparison of 3TL and EKA For The Transmitted Correlation Function For Different High Optical Thicknesses

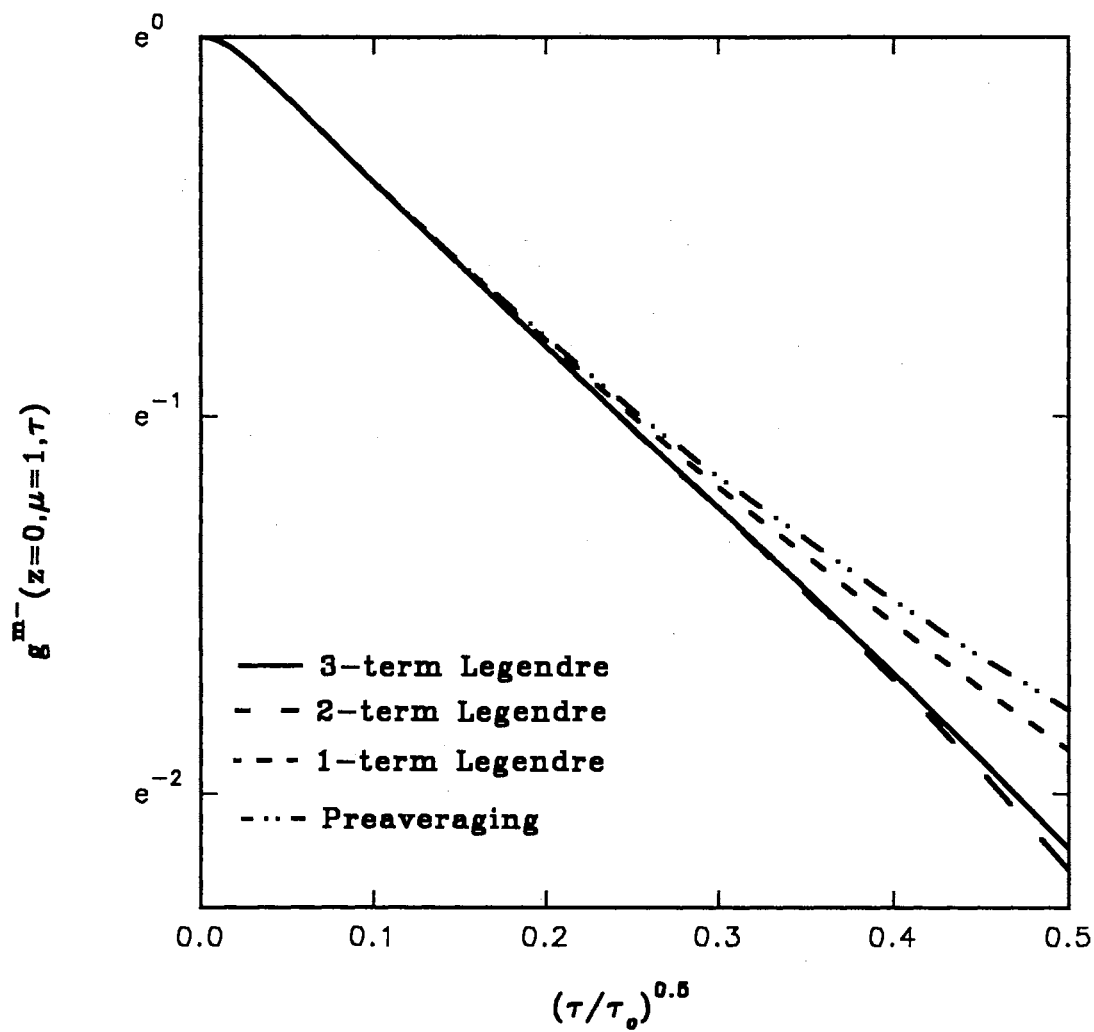


Figure 19. Comparison of The Preaveraged CTE, The 1TL, The 2TL, and The 3TL For The Back-Scattered Correlation Function From A Medium With An Optical Thickness  $L=25$

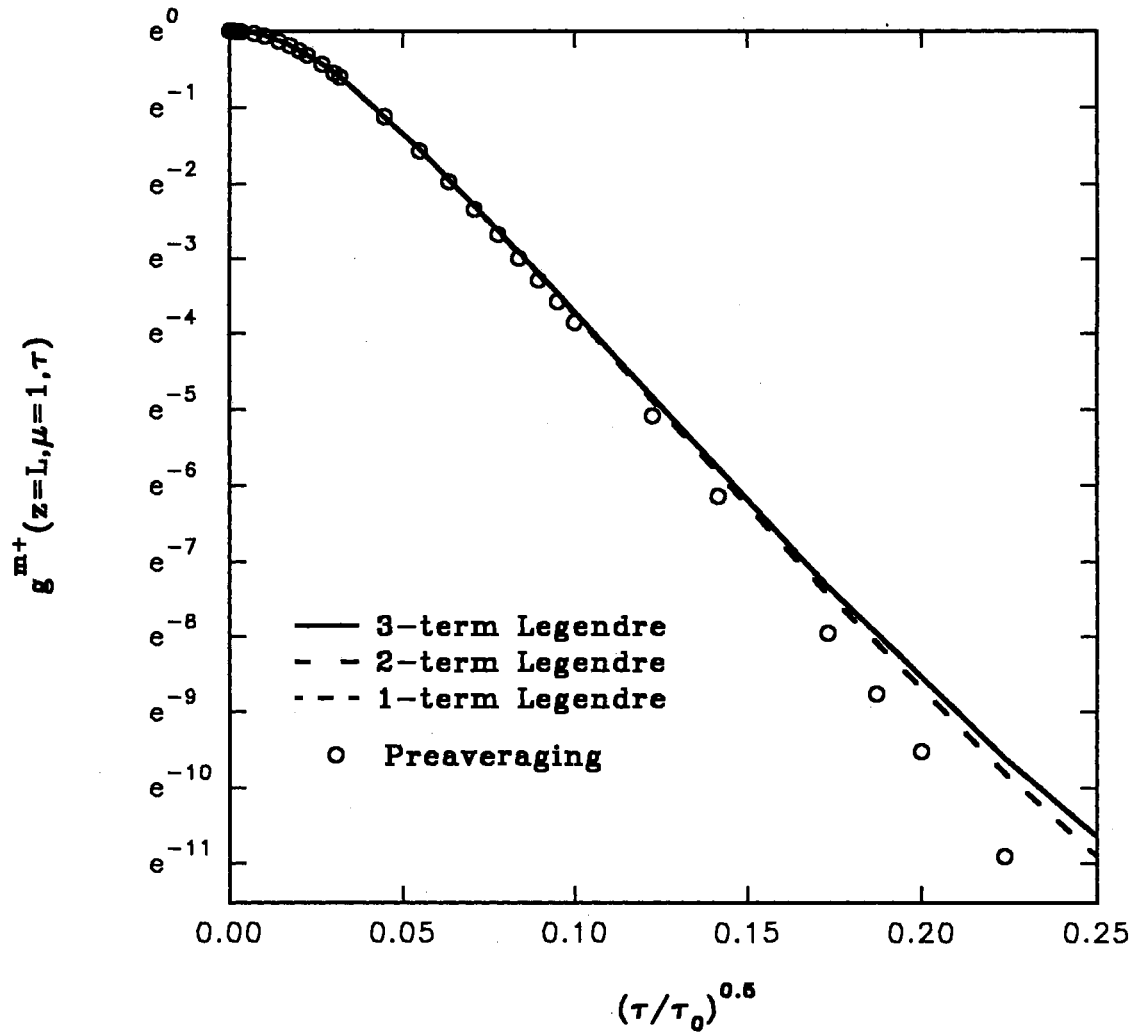


Figure 20. Comparison of The Preaveraged CTE, The 1TL, The 2TL, and The 3TL For The Transmitted Correlation Function From A Medium With An Optical Thickness  $L=25$



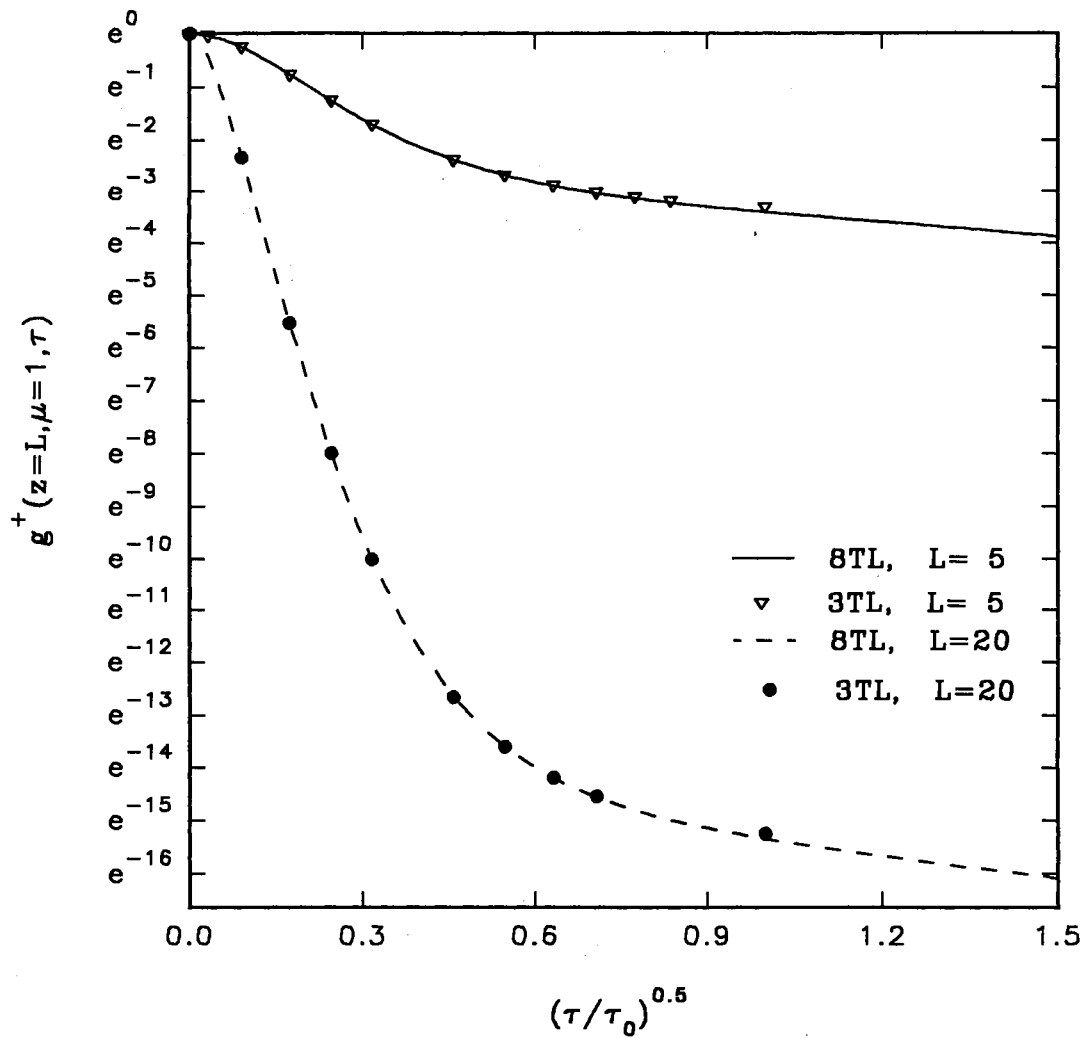


Figure 21a. Comparison of The 3TL and The 8TL For The Transmitted Correlation Function For Different Optical Thicknesses Showing Several Orders of Magnitude of The Decay of The Correlation Function

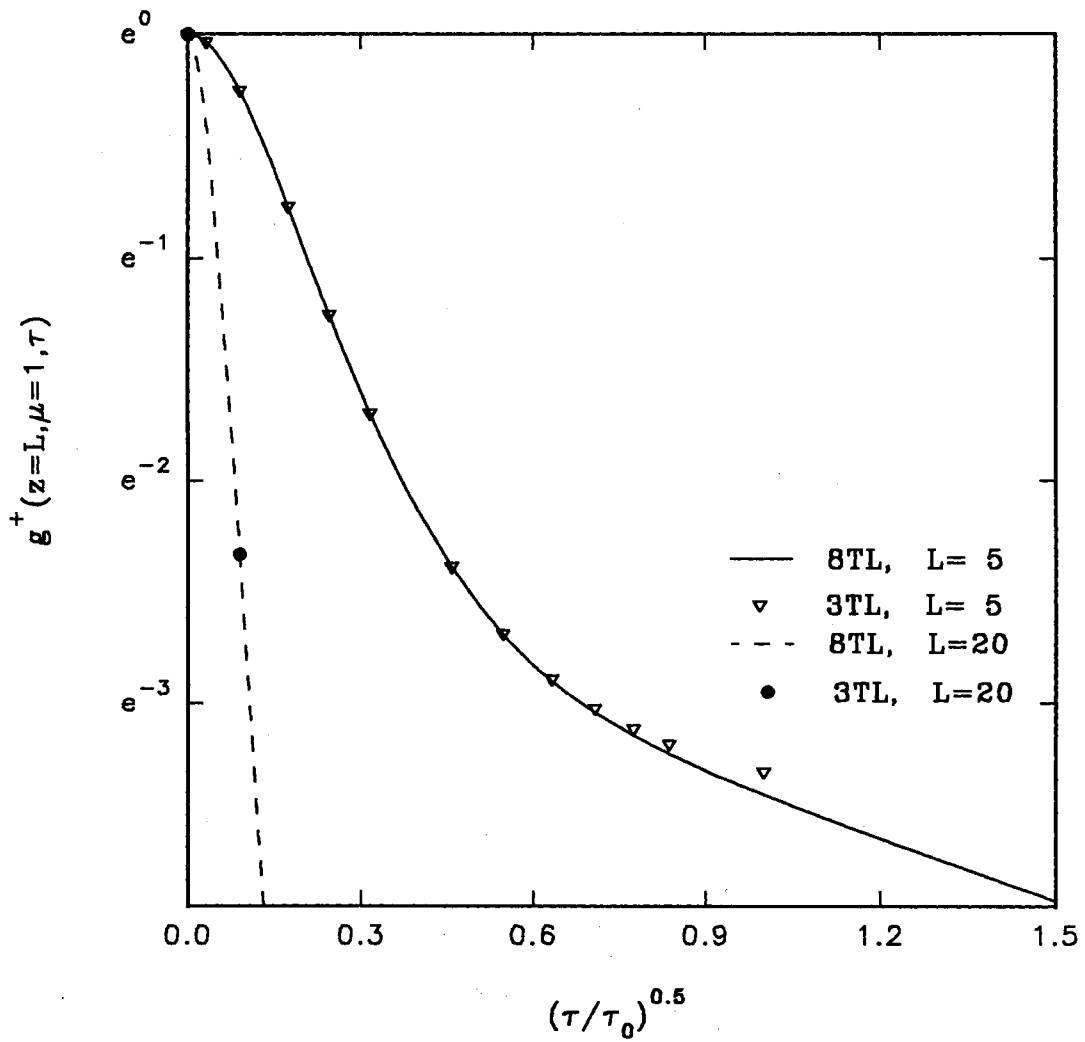


Figure 21b. Comparison of The 3TL and The 8TL For The Transmitted Correlation Function For Different Optical Thicknesses Showing Few Orders of Magnitude of The Decay of The Correlation Function

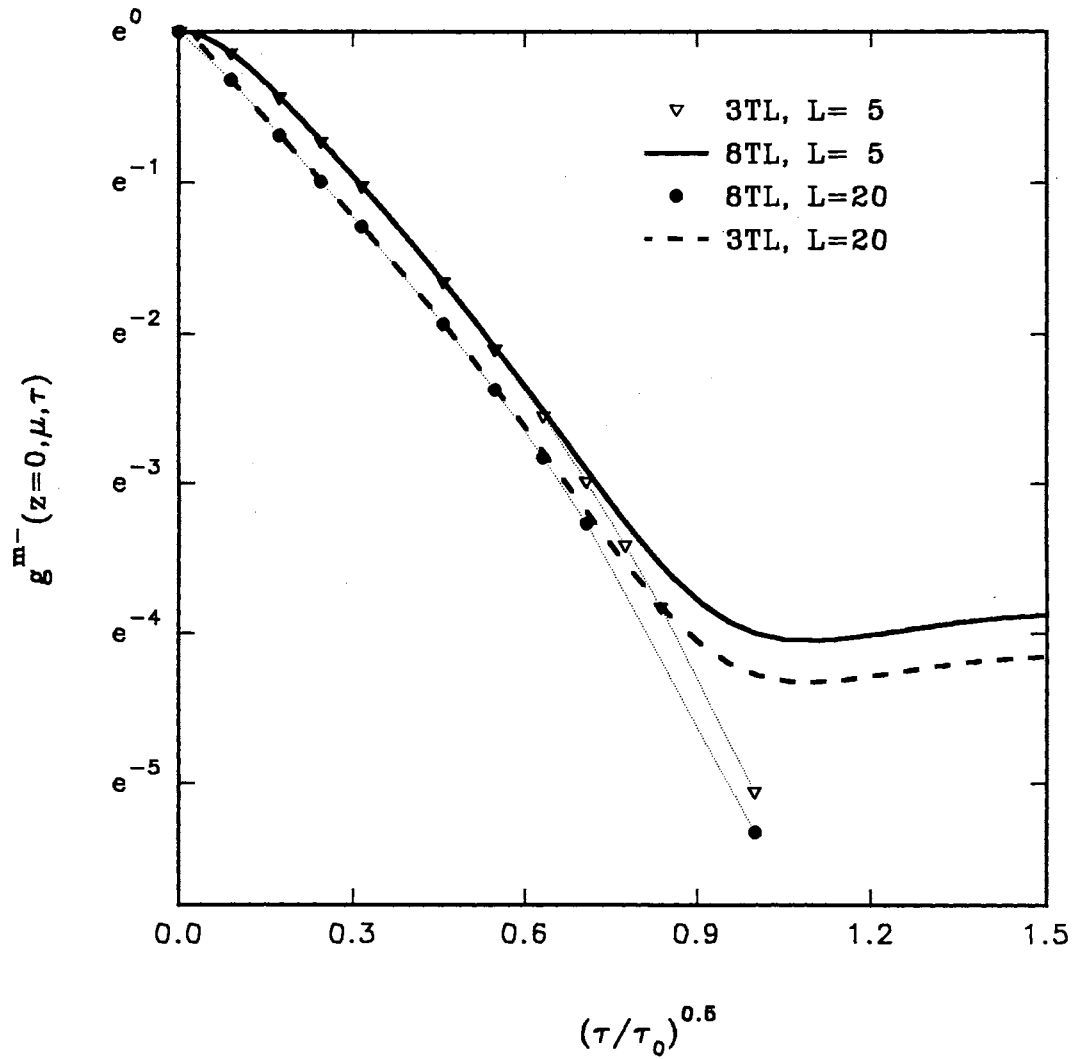


Figure 22. Comparison of The 3TL and The 8TL For The Back-Scattered Correlation Function For Different Optical Thicknesses ( $\mu=1$ )

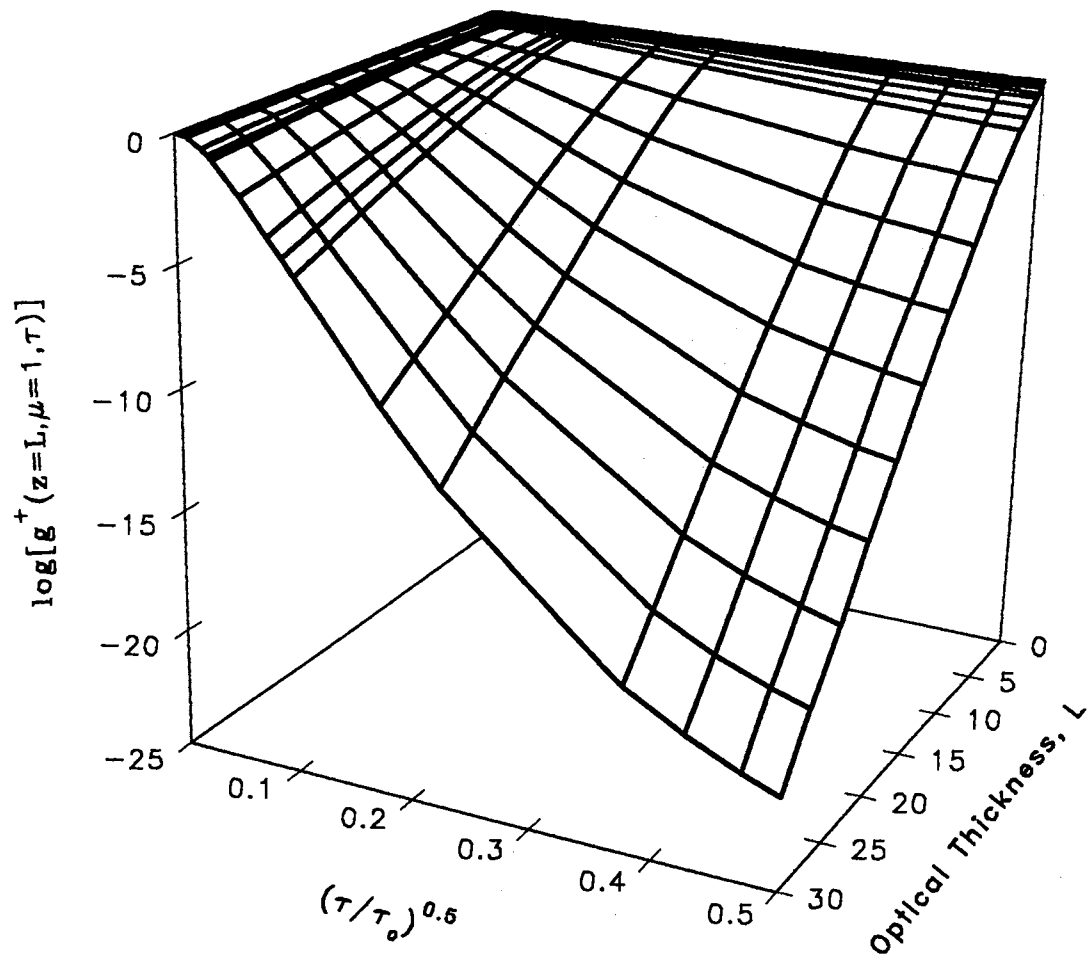


Figure 23. Effect of The Optical Thickness and The Delay Time on The Decay Rate of The Transmitted 3TL Correlation Function Plotted on A Base 10 log Scale

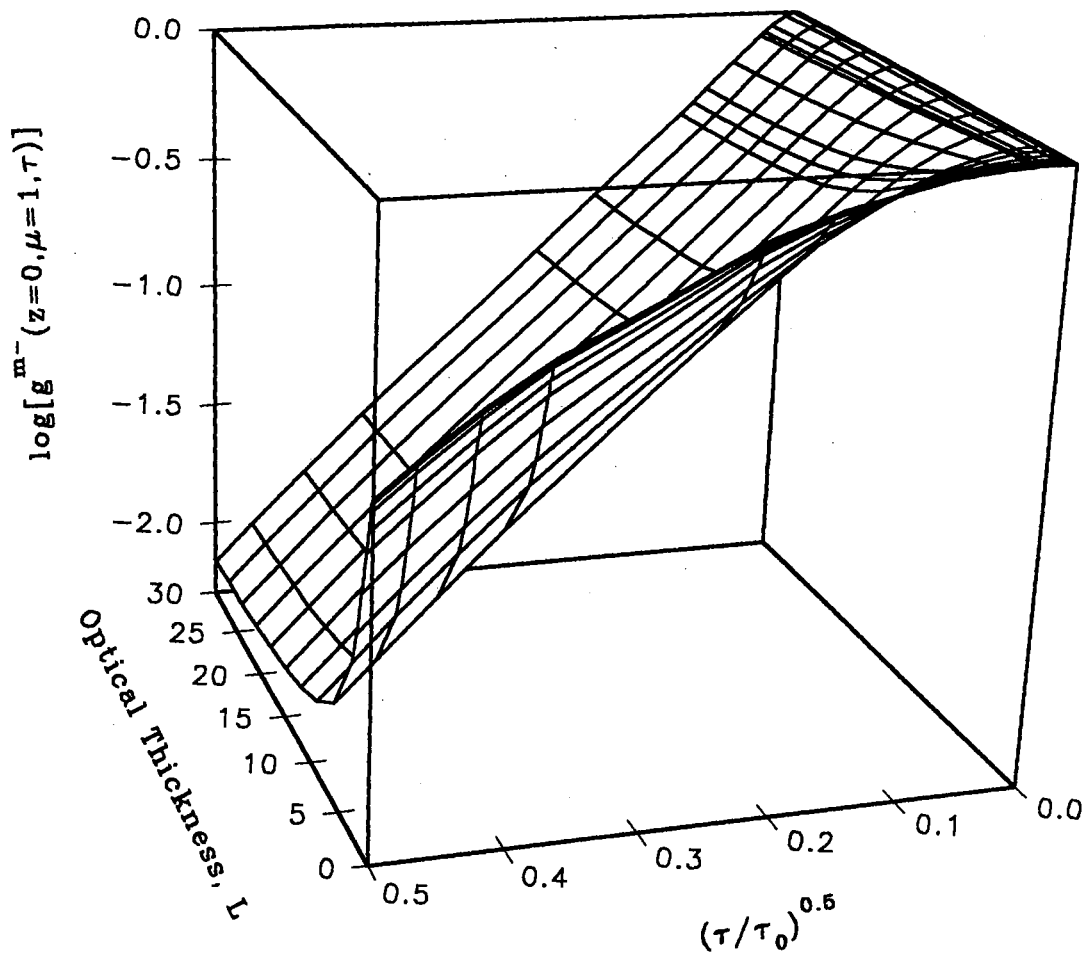


Figure 24. Effect of The Optical Thickness and The Delay Time on The Decay Rate of The Back-Scattered 3TL Correlation Function Plotted on A Base 10 Log Scale

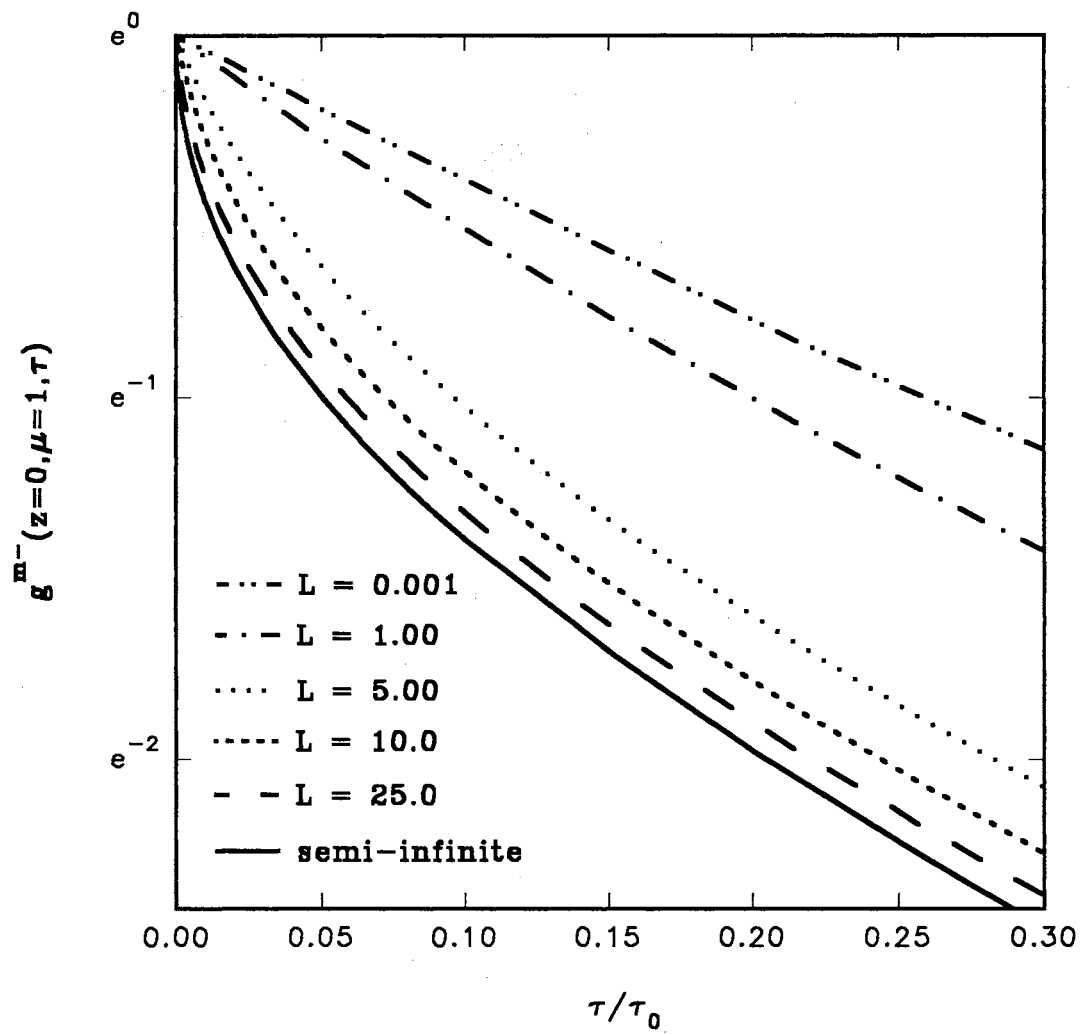


Figure 25a. Effect of The Optical Thickness on The Decay Rate of The Back-Scattered 3TL Correlation Function Plotted Versus A Linear Non-Dimensional Delay Time

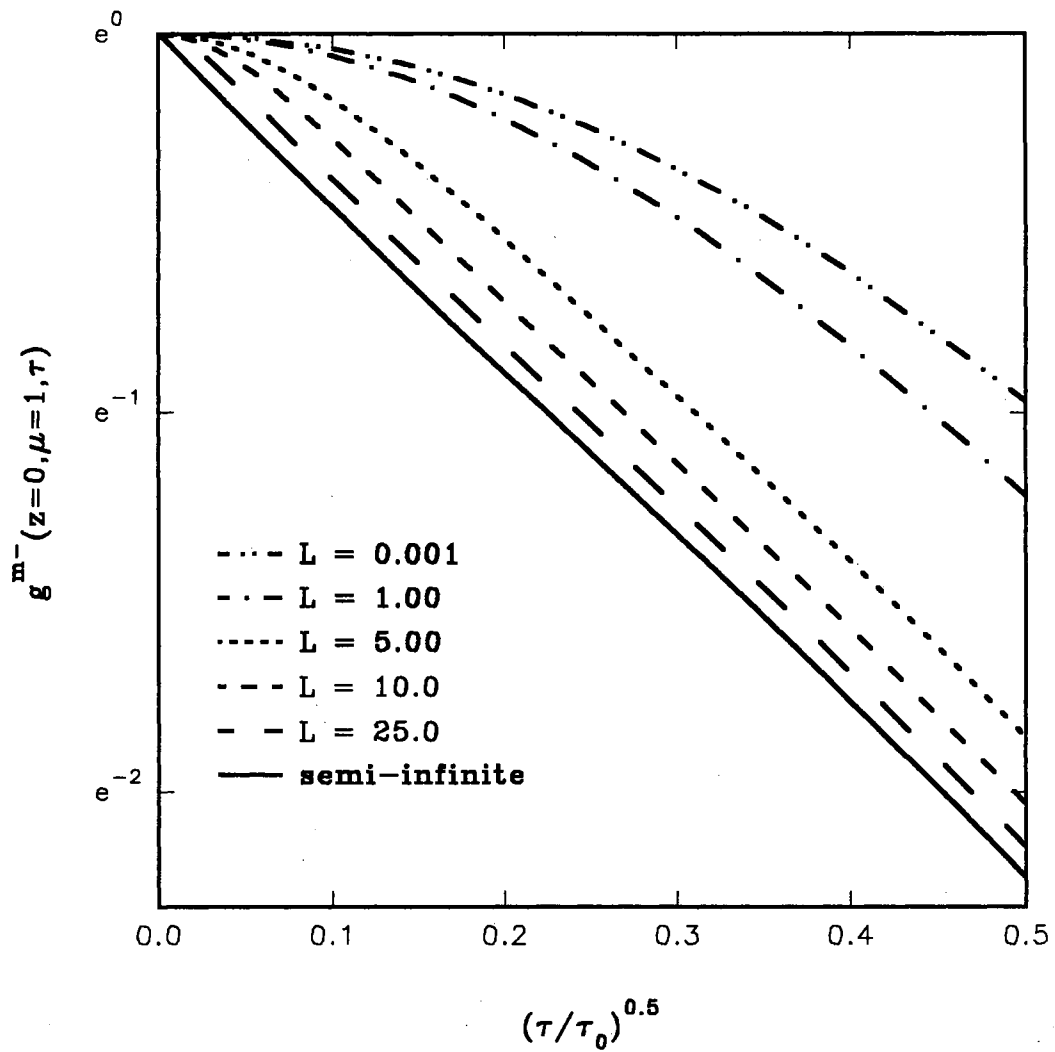


Figure 25b. Effect of The Optical Thickness on The Decay Rate of The Back-Scattered 3TL Correlation Function Plotted Versus The Square Root of The Non-Dimensional Delay Time

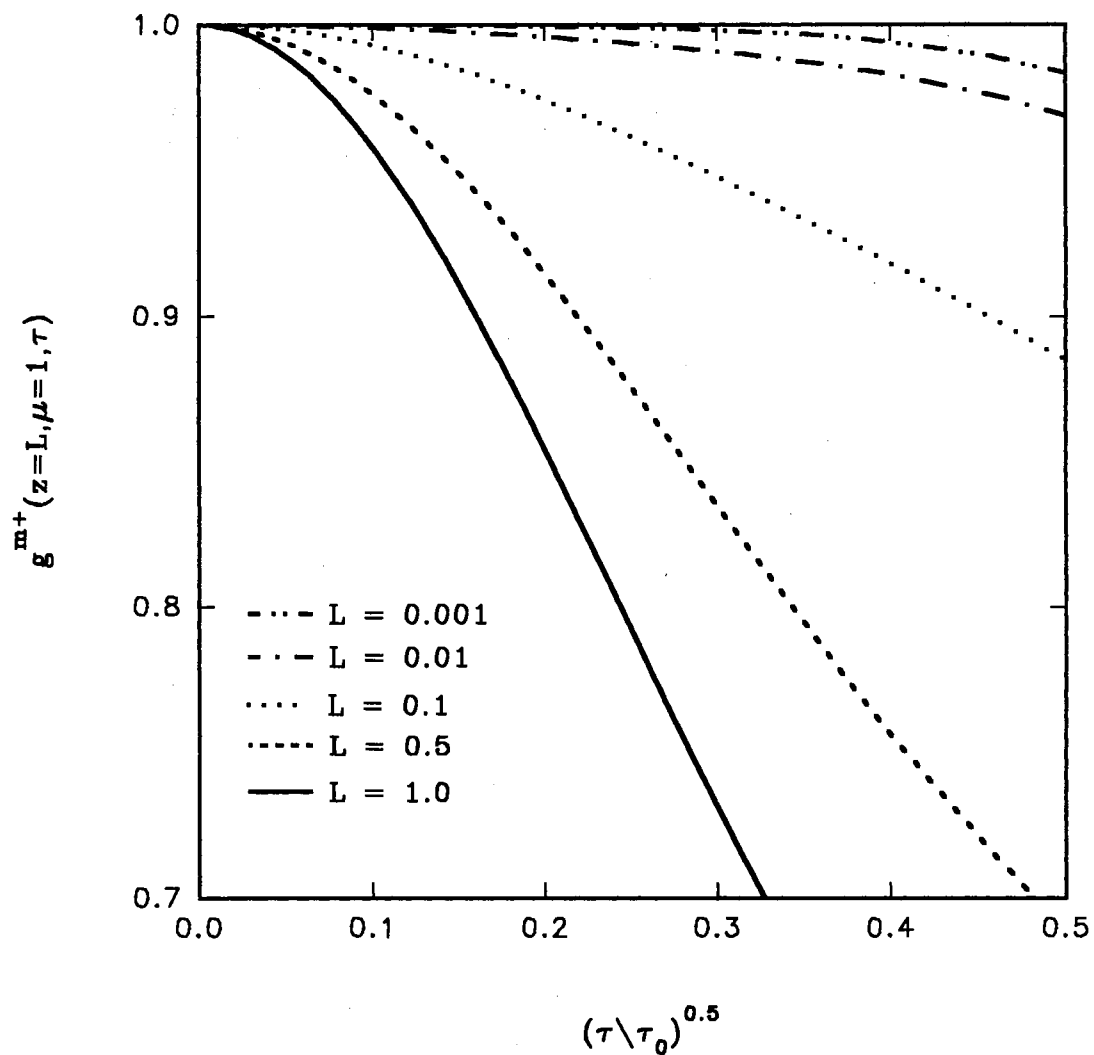


Figure 26a. Effect of Low Optical Thickness on The Decay Rate of The Transmitted 3TL Correlation Function Plotted Versus The Square Root of The Non-Dimensional Delay Time



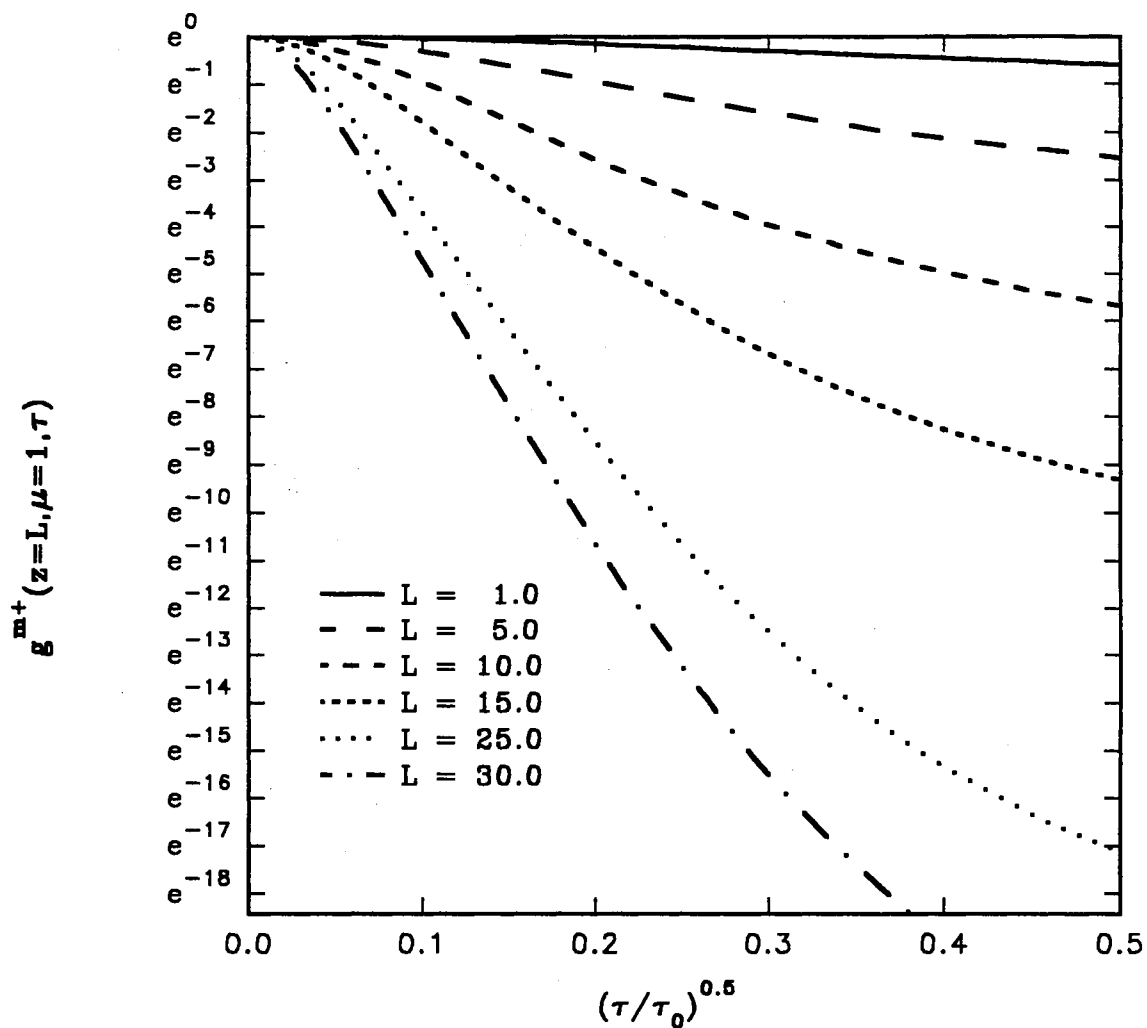


Figure 26b. Effect of High Optical Thickness on The Decay Rate of The Transmitted 3TL Correlation Function Plotted Versus The Square Root of The Non-Dimensional Delay Time

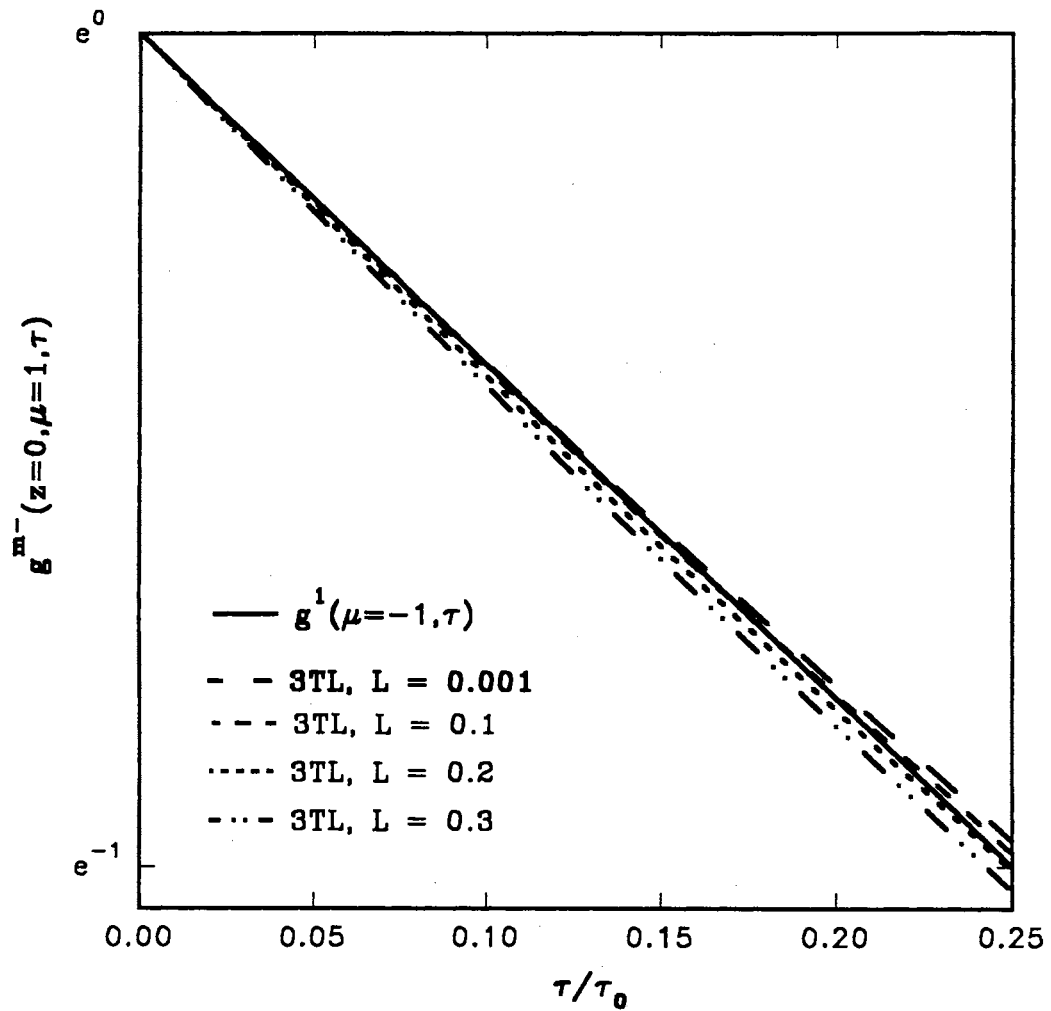


Figure 27. Comparison of The 3TL With The Analytic Form of  $g^1$  For The Back-Scattered Correlation Function For Different Very Low Optical Thicknesses

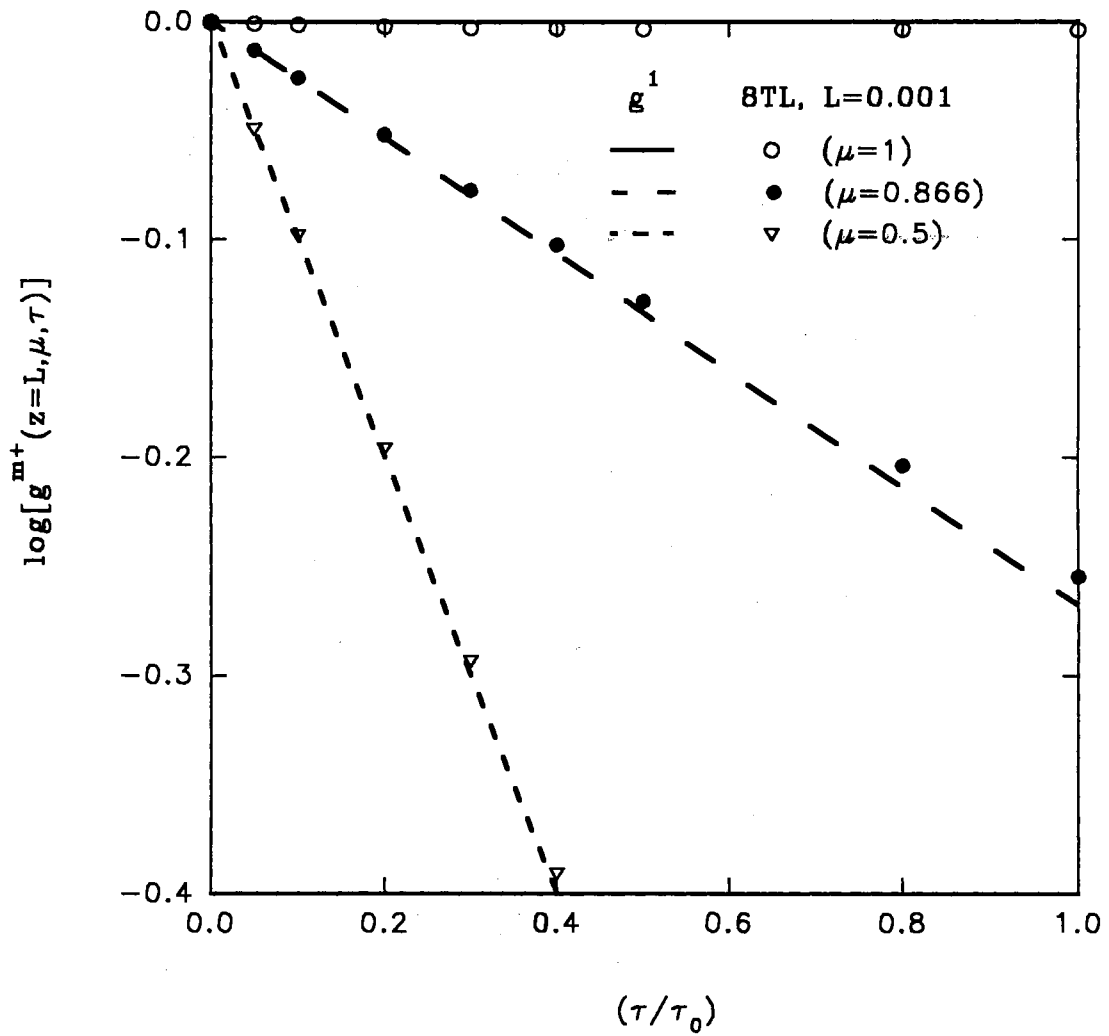


Figure 28. Comparison of The 8TL With The Analytic Form of  $g^1$  For The Transmitted Correlation Function at Different Exit Angles From A Medium With an Optical Thickness  $L=0.001$  and Plotted on A Base 10 Log Scale

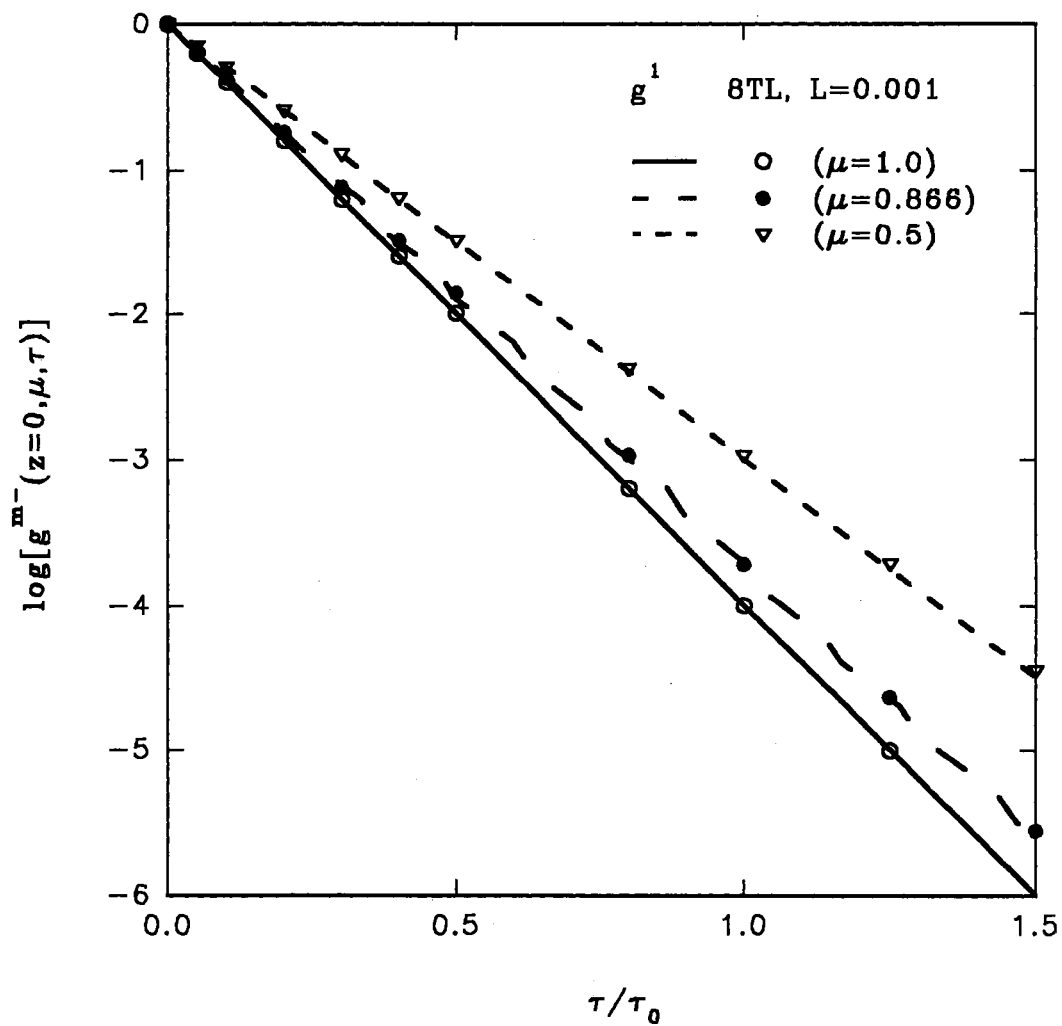


Figure 29. Comparison of The 8TL With The Analytic Form of  $g^1$  For The Back-Scattered Correlation Function at Different Exit Angles From A Medium With an Optical Thickness  $L= 0.001$  and Plotted on A Base 10 Log Scale.

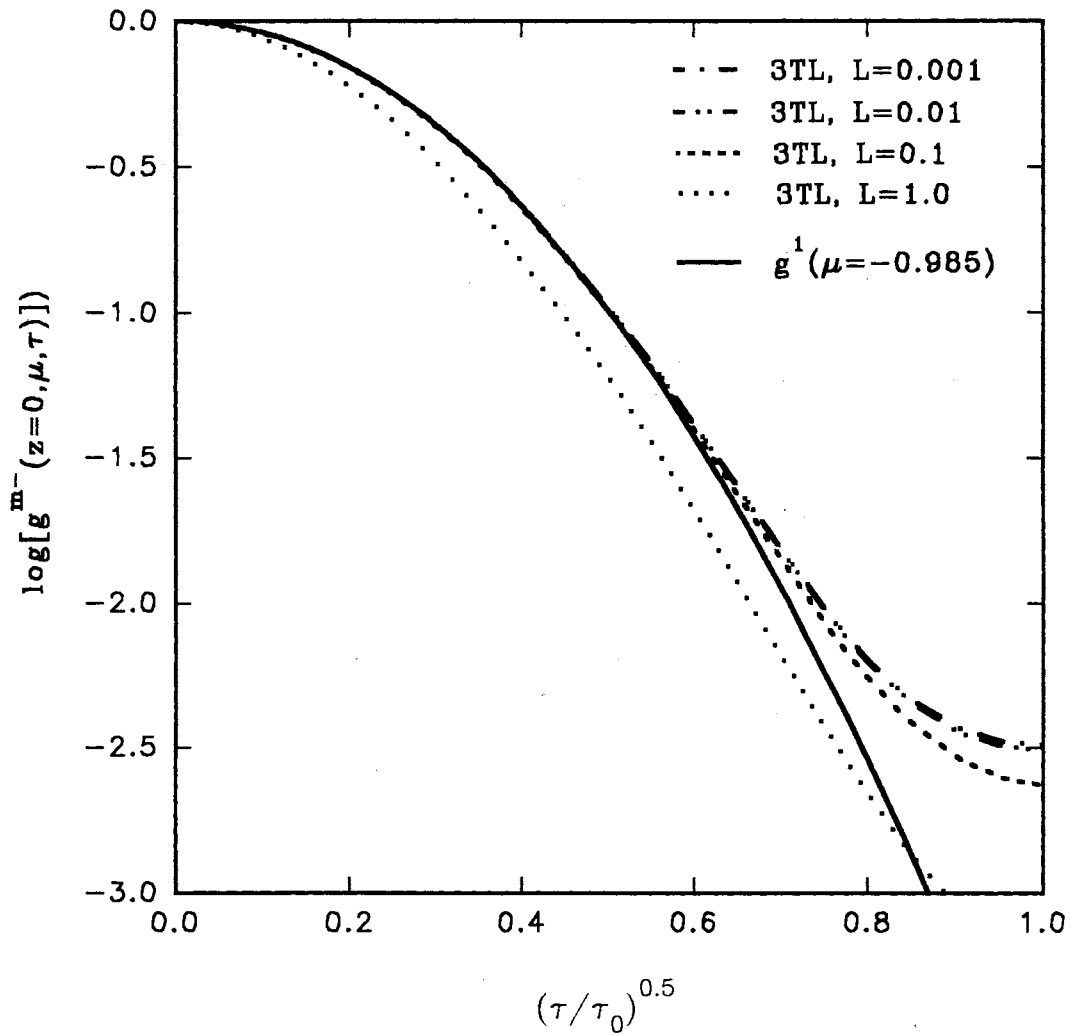


Figure 30. Comparison of The 3TL With The Analytic Form of  $g^1$  For The Back-Scattered Correlation Function at  $\mu=0.985$  (10 Deg.) For Different Low Optical Thicknesses and Plotted on A Base 10 Log Scale.

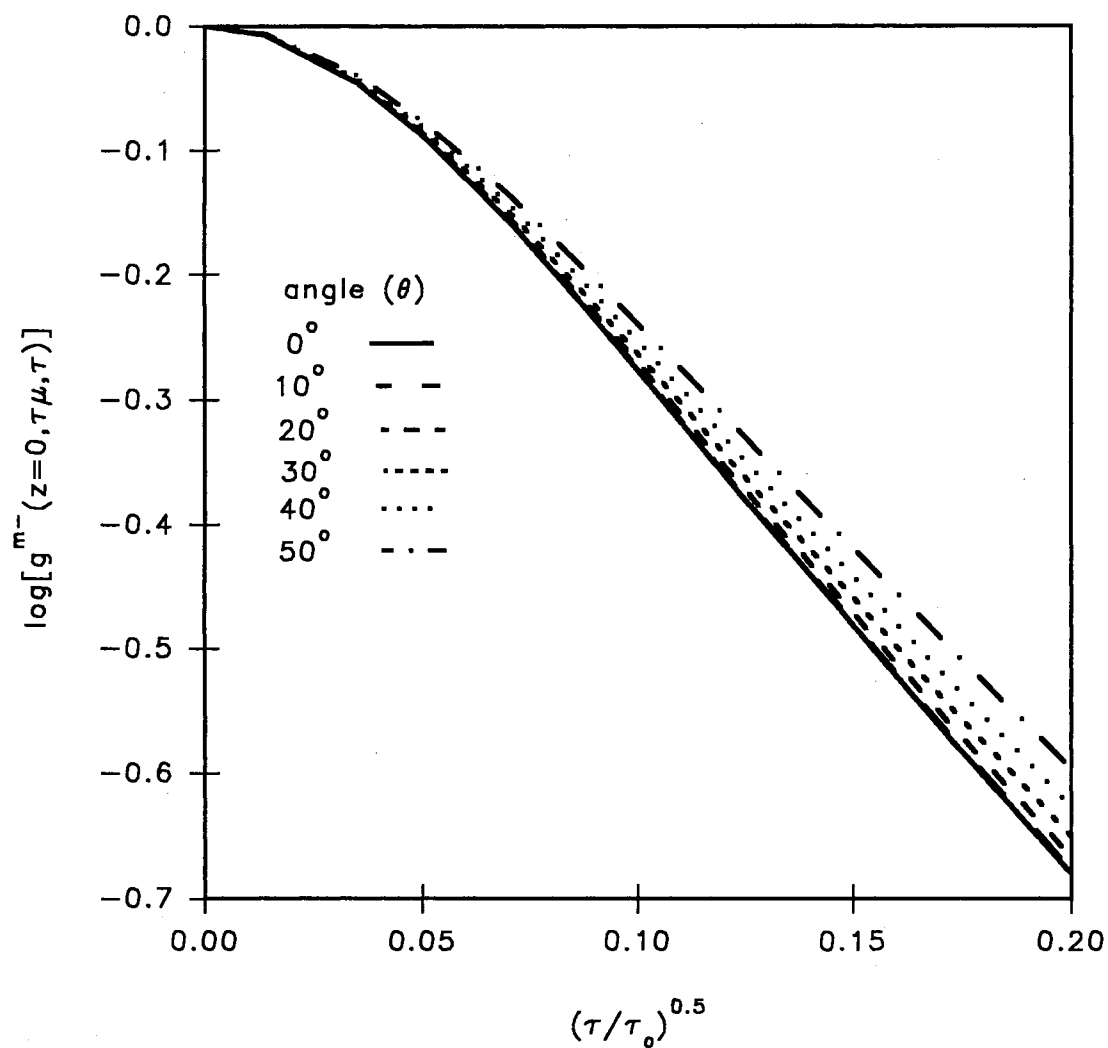


Figure 31. Effect of Different Detection Angles On The Back-Scattered Correlation Function From A Medium With An Optical Thickness  $L=10$ . The Results Were Obtained From The Isotropic Preaveraged CTE.

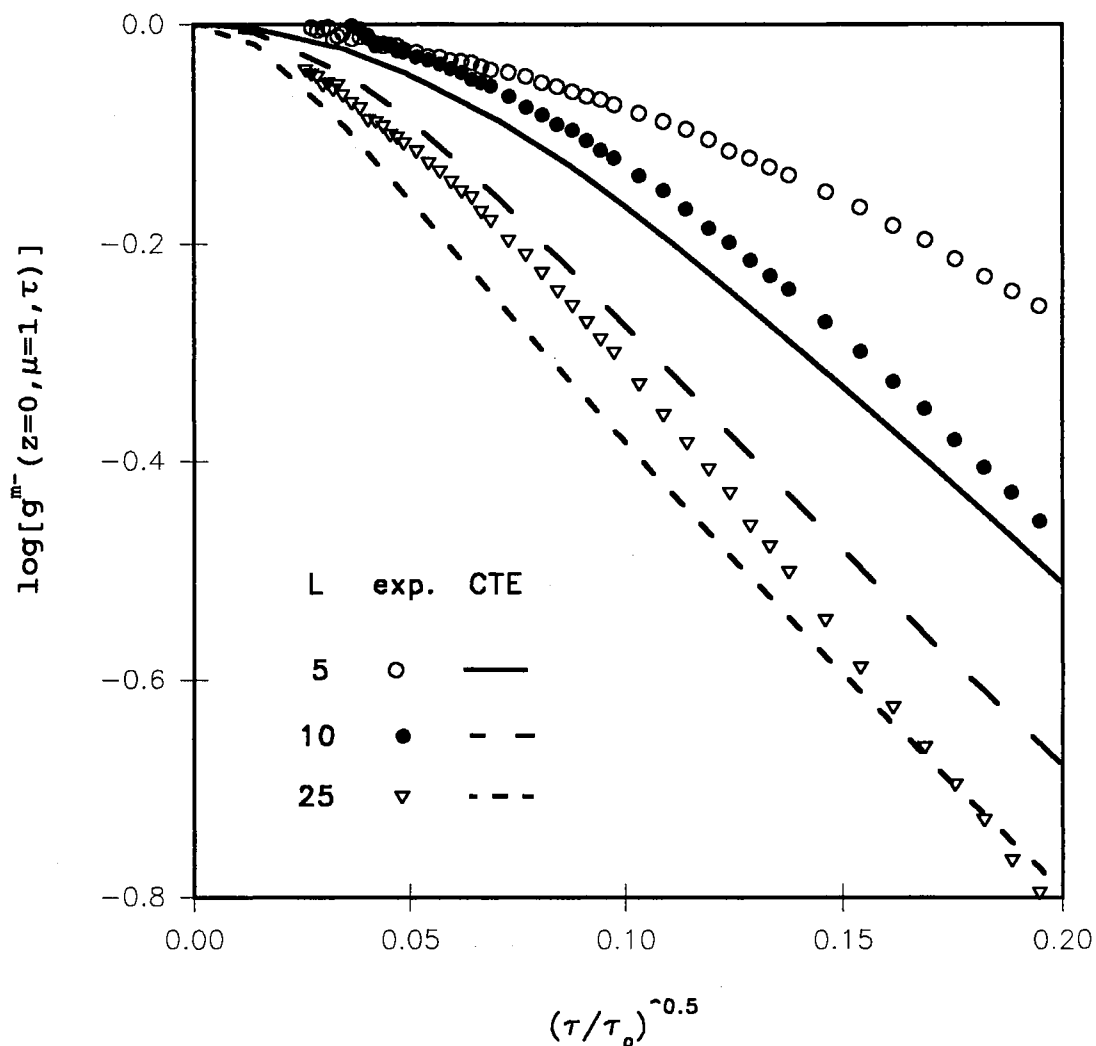


Figure 32. Comparison Between Theory And Experimental Data For The Back-Scattered Correlation Function From Media With Different Optical Thicknesses Containing  $0.3\mu\text{m}$  Polystyrene Particles. The Preaveraged Isotropic CTE With No Index of Refraction Change At The Boundaries Is Used.

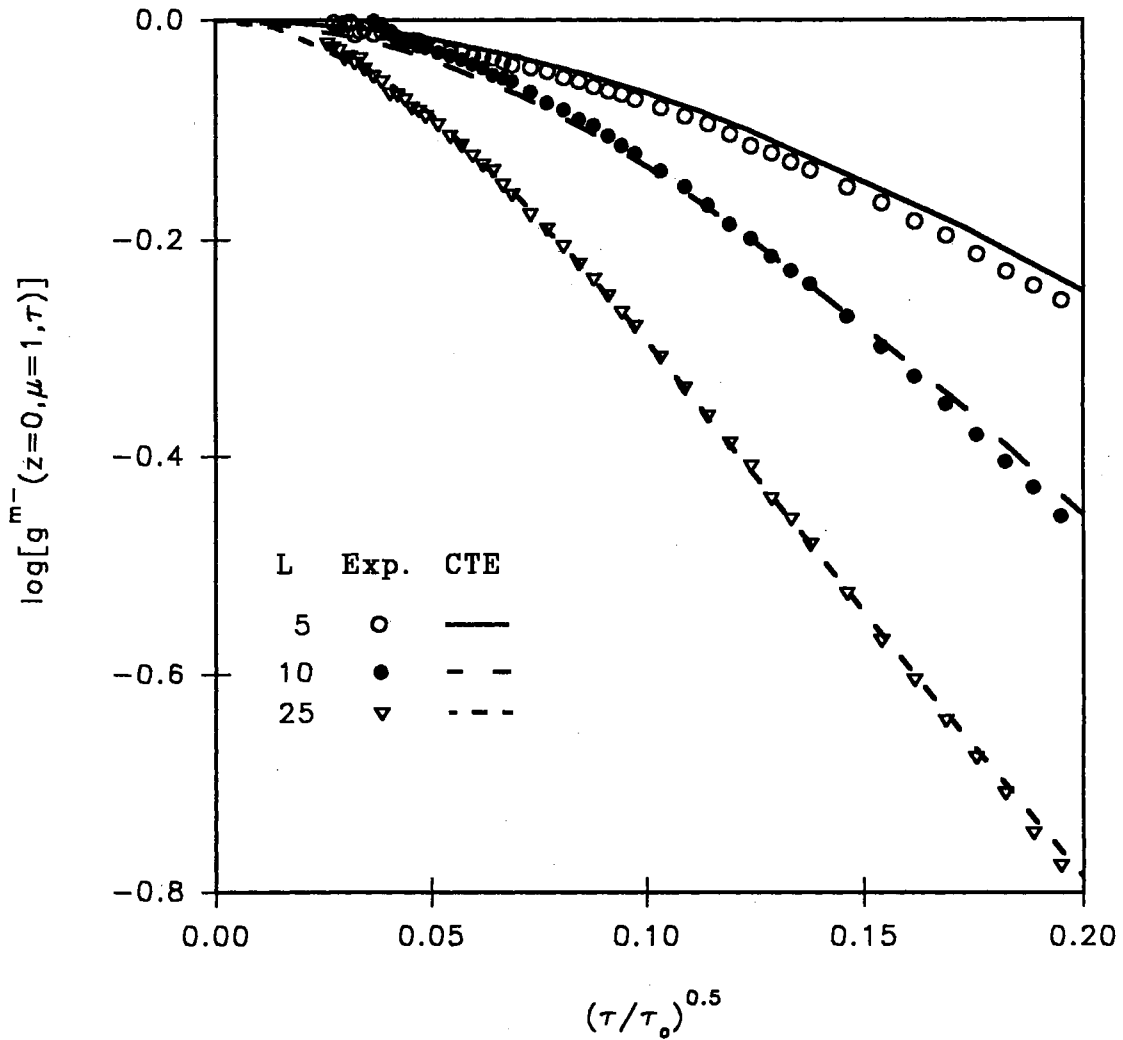


Figure 33. Comparison Between Theory And Experimental Data For The Back-Scattered Correlation Function From Media With Different Optical Thicknesses Containing  $0.3\mu\text{m}$  Polystyrene Particles. The Preaveraged CTE And The Forward Approximation (With  $f=0.727$ ) And An Index of Refraction Change ( $n=1.33$ ) At The Top Boundary Are Used.



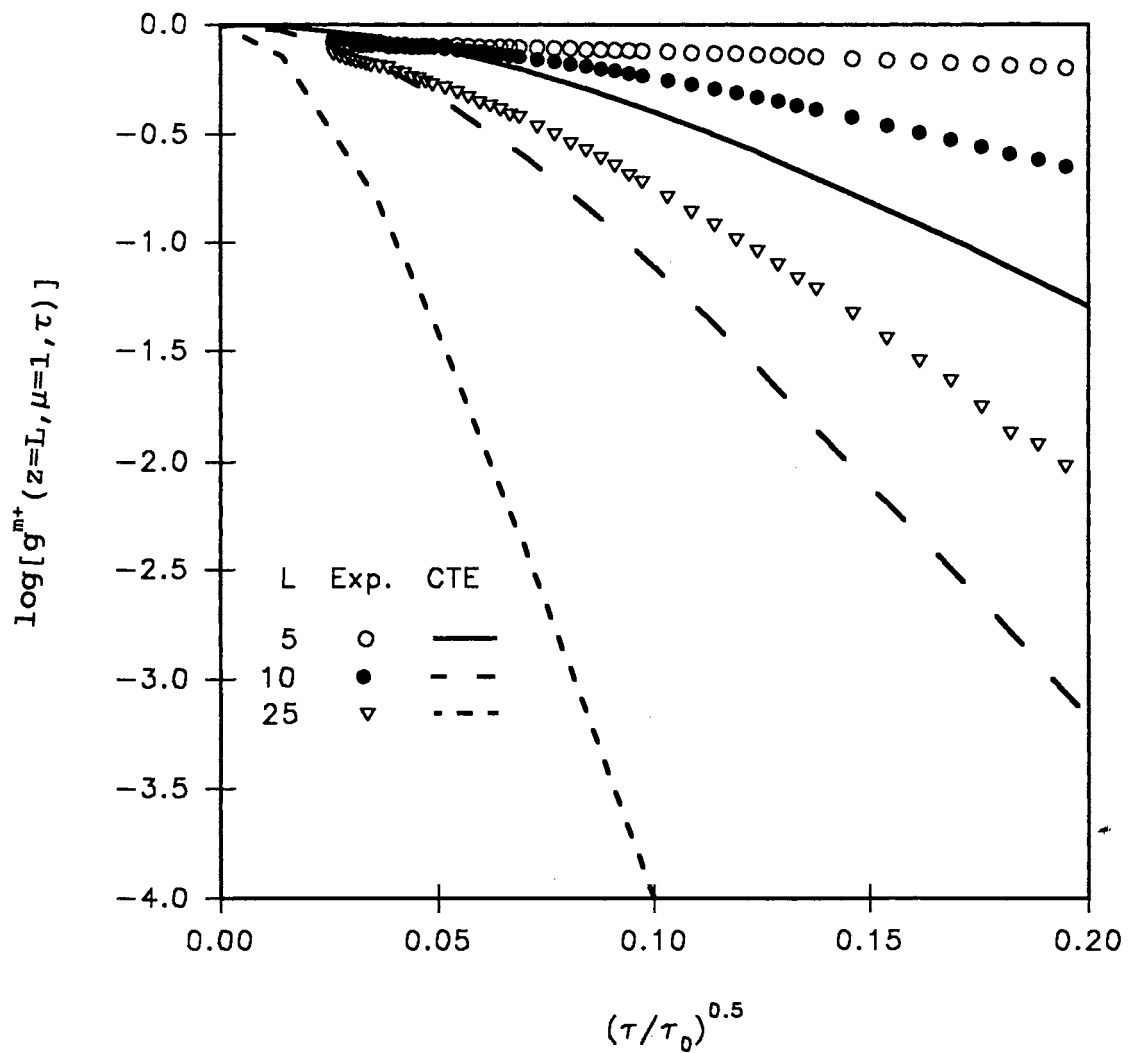


Figure 34. Comparison Between Theory And Experimental Data For The Transmitted Correlation Function From Media With Different Optical Thicknesses Containing  $0.3\mu\text{m}$  Polystyrene Particles. The Preaveraged Isotropic CTE With No Index of Refraction Change At The Boundaries Is Used.

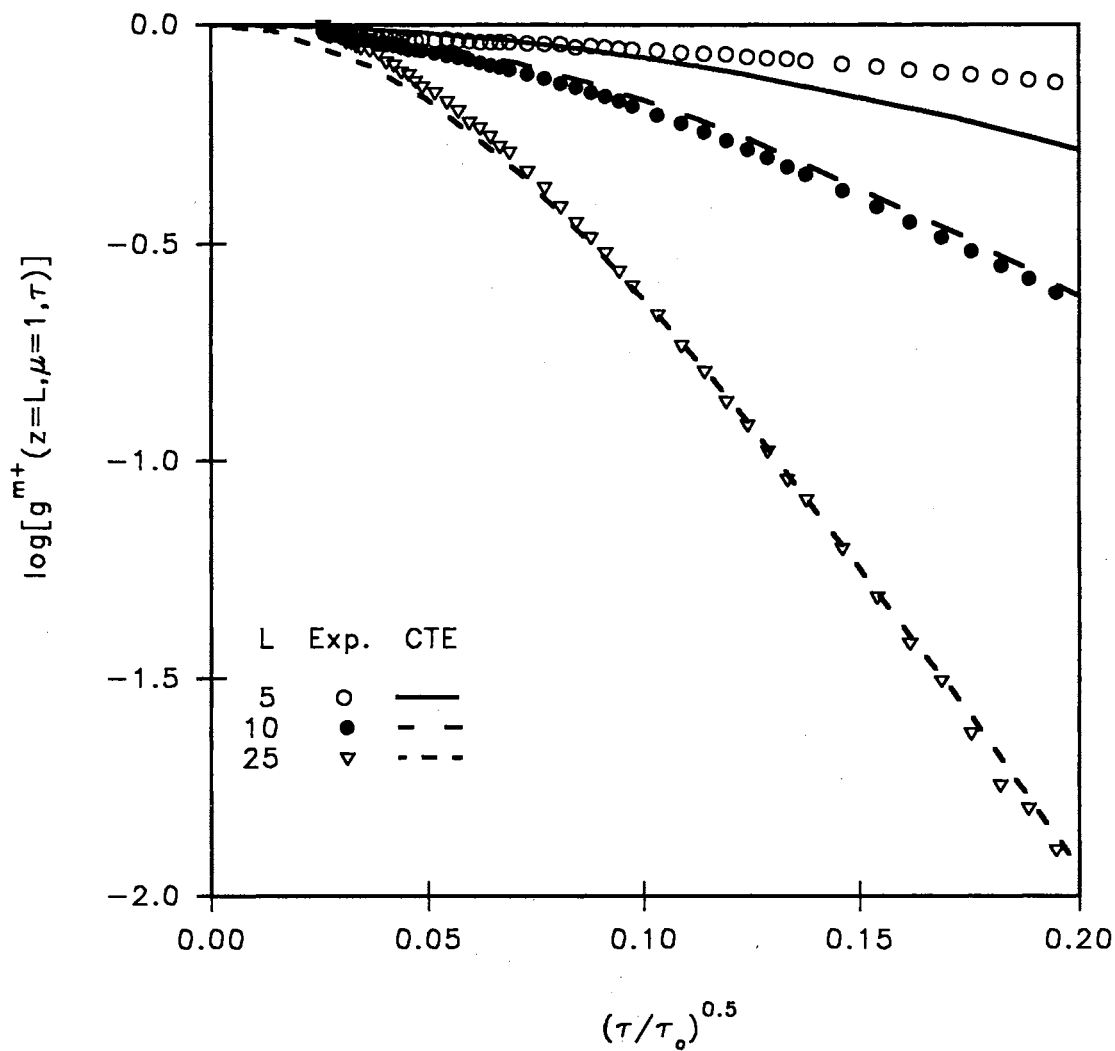


Figure 35. Comparison Between Theory And Experimental Data For The Transmitted Correlation Function From Media With Different Optical Thicknesses Containing  $0.3\mu\text{m}$  Polystyrene Particles. The Preaveraged CTE And The Forward Approximation (With  $f=0.727$ ) And An Index of Refraction Change ( $n=1.33$ ) At The Top Boundary Are Used.

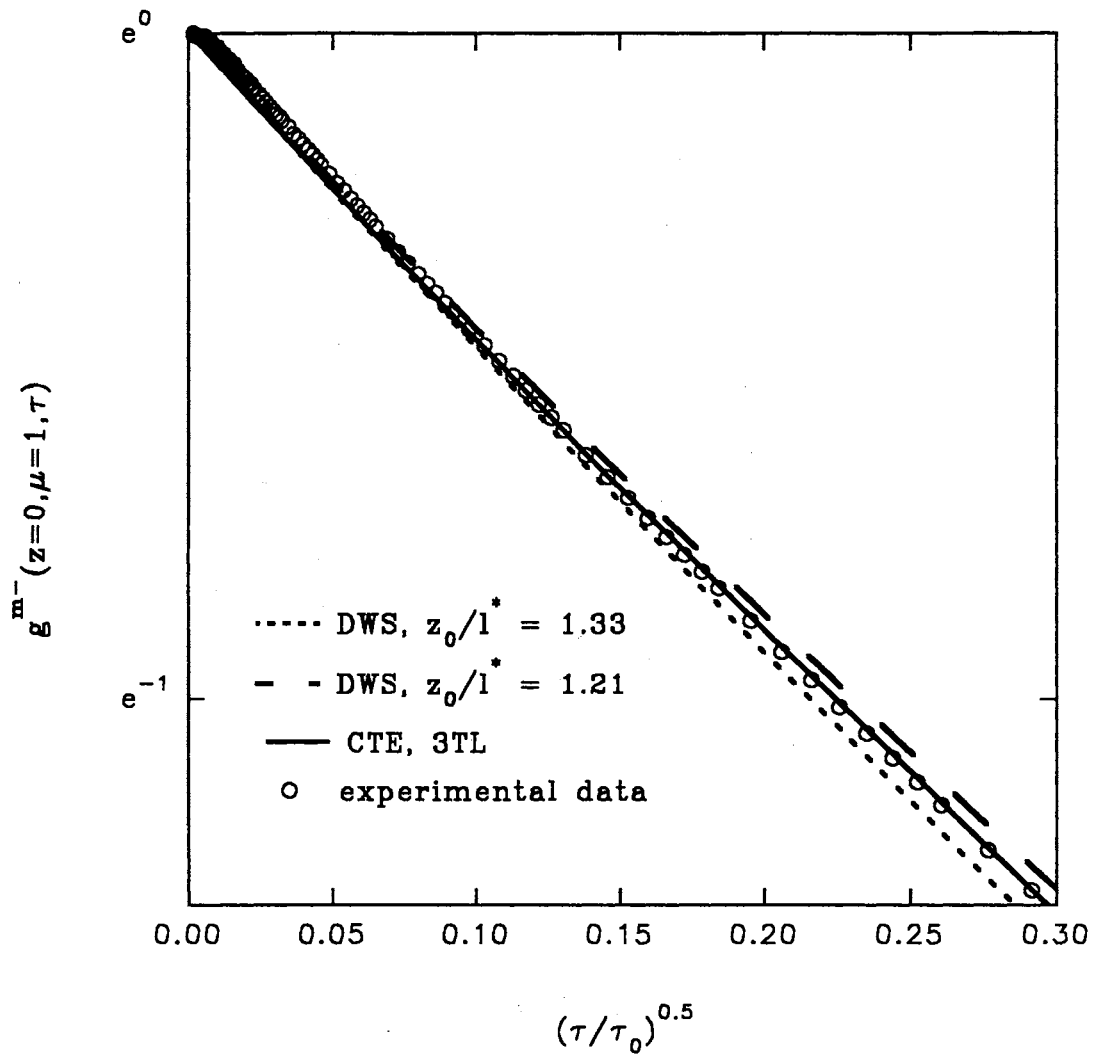


Figure 36. Comparison Between Theory And Experimental Data For The Back-Scattered Correlation Function From A Semi-Infinite Medium Containing  $0.3\mu\text{m}$  Polystyrene Particles. The 3TL And DWS With Different Deposition Length Values Are Used.

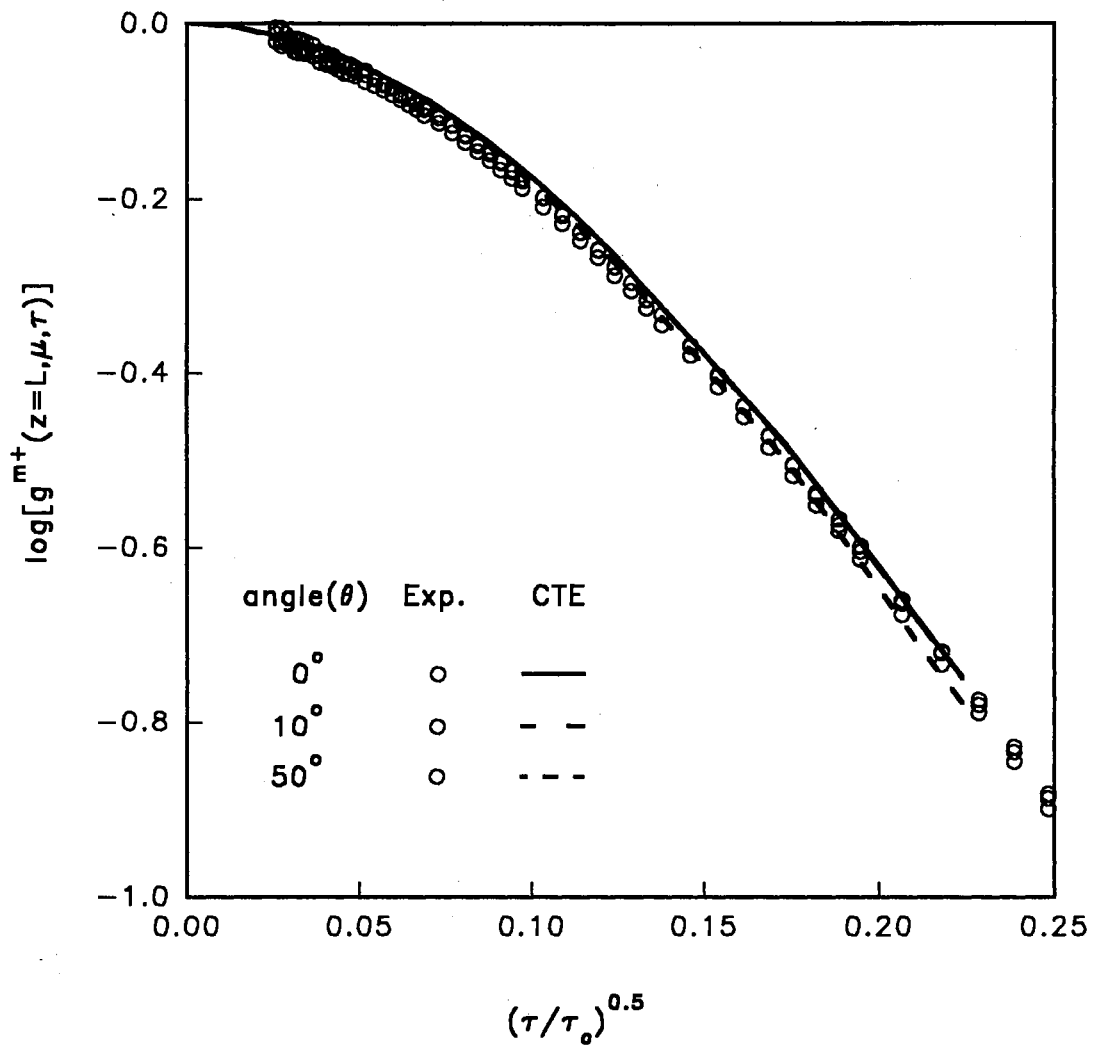


Figure 37. Comparison Between Theory And Experimental Data For The Transmitted Correlation Function At Different Exit Angles From A Medium With An Optical Thicknesses  $L=10$ , Containing  $0.3\mu\text{m}$  Polystyrene Particles. The Preaveraged CTE Using The Forward Approximation (With  $f=0.727$ ) And An Index of Refraction Change ( $n=1.33$ ) At The Top Boundary Are Used.

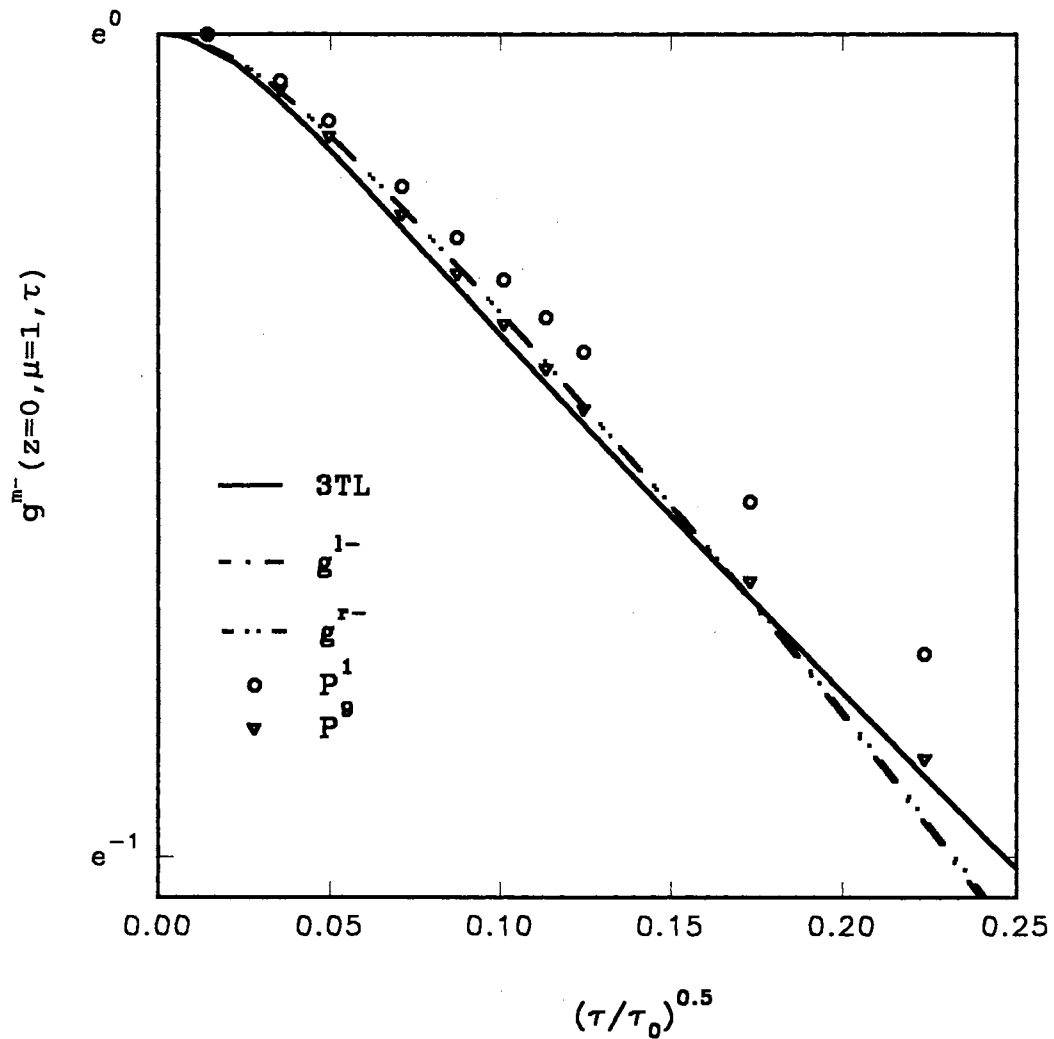


Figure 38. Comparison of The Scalar CTE, Using The 3TL, The  $P_1$  and The  $P_0$  Approximations, With The Polarized CTE, With Rayleigh Scattering Using The  $P_1$  Approximation With Unpolarized Boundary Condition, For The Back-Scattered Correlation Function From A Medium With An Optical Thickness  $L=20$

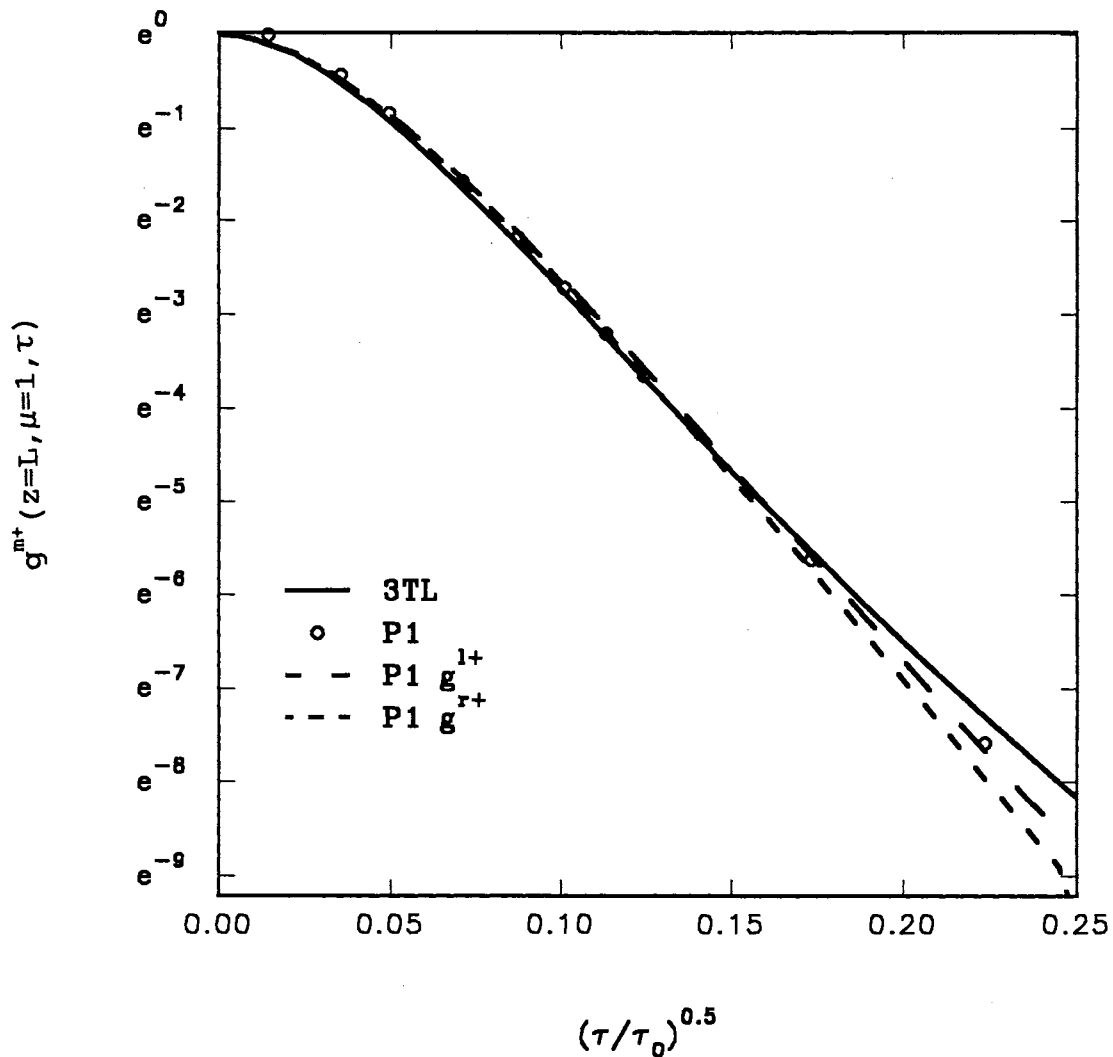


Figure 39. Comparison of The Scalar CTE, Using The 3TL And The  $P_1$  Approximation, With The Polarized CTE, With Rayleigh Scattering Using The  $P_1$  Approximation With Unpolarized Boundary Condition, For The Transmitted Correlation Function From A Medium With An Optical Thickness  $L=20$

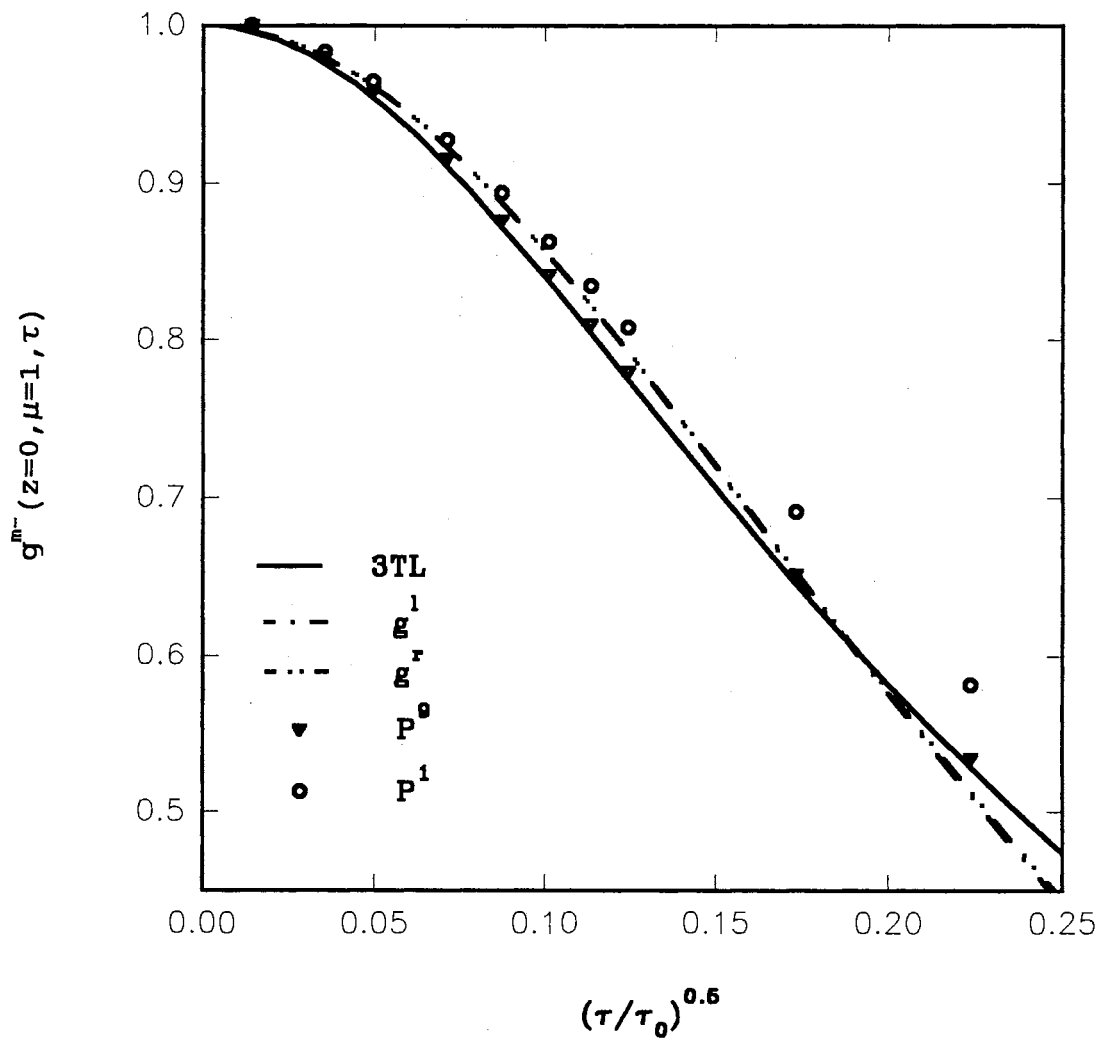


Figure 40a. Comparison of The Scalar CTE, Using The 3TL, The  $P_1$  and The  $P_0$  Approximations, With The Polarized CTE With Rayleigh Scattering Using The  $P_1$  Approximation With Unpolarized Boundary Condition, For The Back-Scattered Correlation Function From A Medium With An Optical Thickness  $L=5$ ; Showing The Long Time Behavior

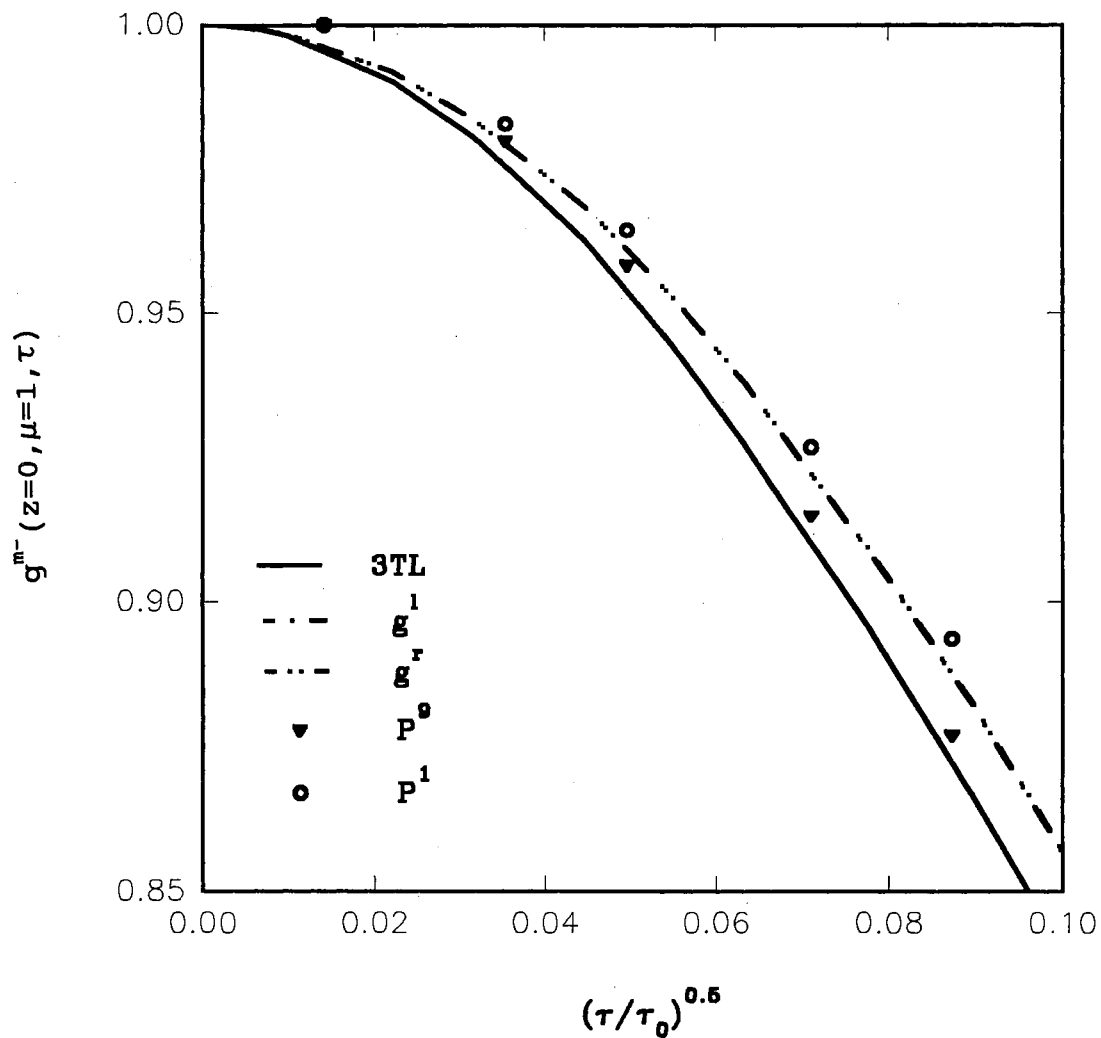


Figure 40b. Comparison of The Scalar CTE, Using The 3TL, The  $P_1$  and The  $P_0$  Approximations, With The Polarized CTE With Rayleigh Scattering Using The  $P_1$  Approximation With Unpolarized Boundary Condition, For The Back-Scattered Correlation Function From A Medium With An Optical Thickness  $L=5$ ; Showing The Short Time Behavior



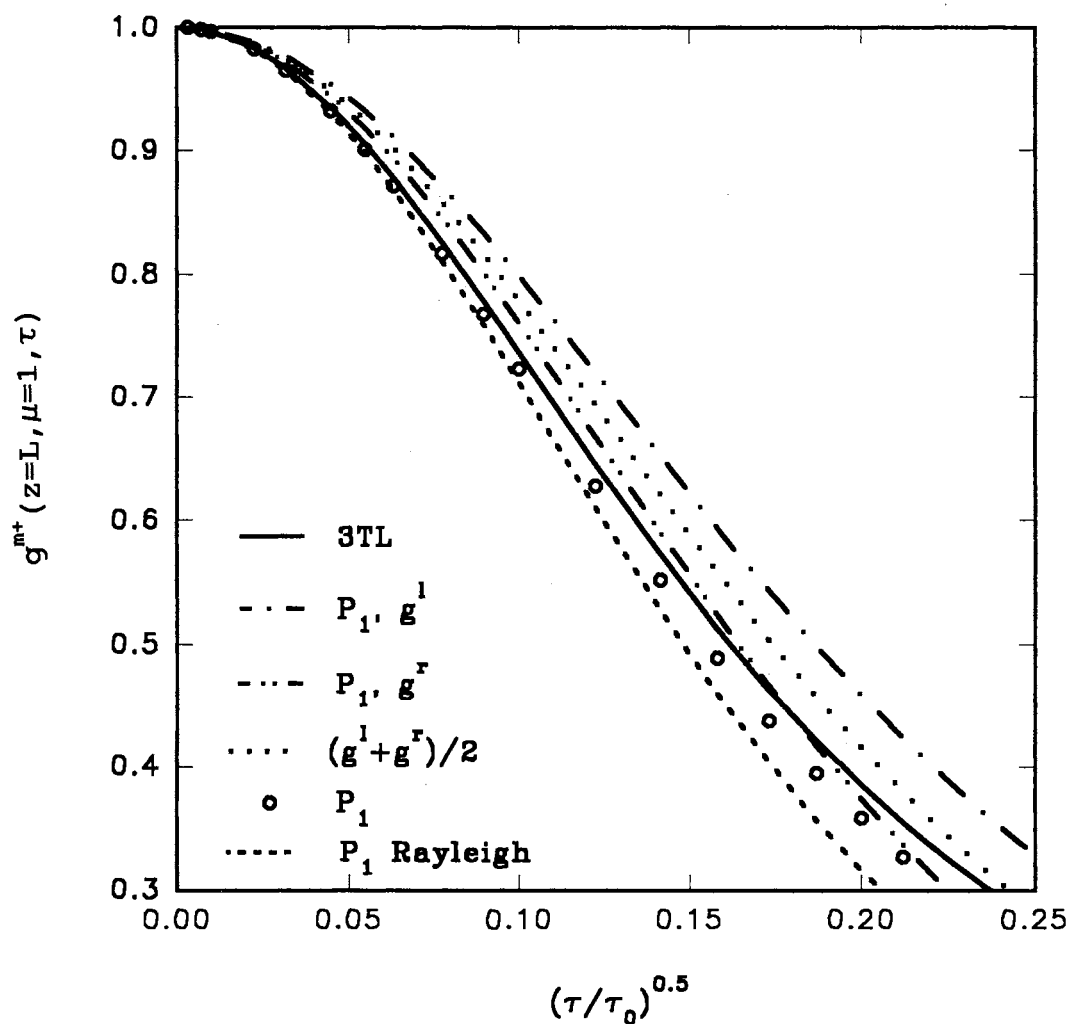


Figure 41a. Comparison of The Scalar CTE, Using The 3TL, And The  $P_1$  Approximation (For Isotropic And Rayleigh Scattering) With The Polarized CTE, With Rayleigh Scattering Using The  $P_1$  Approximation With Unpolarized Boundary Condition, For The Transmitted Correlation Function From A Medium With An Optical Thickness  $L=5$ ; Showing The Long Time Behavior

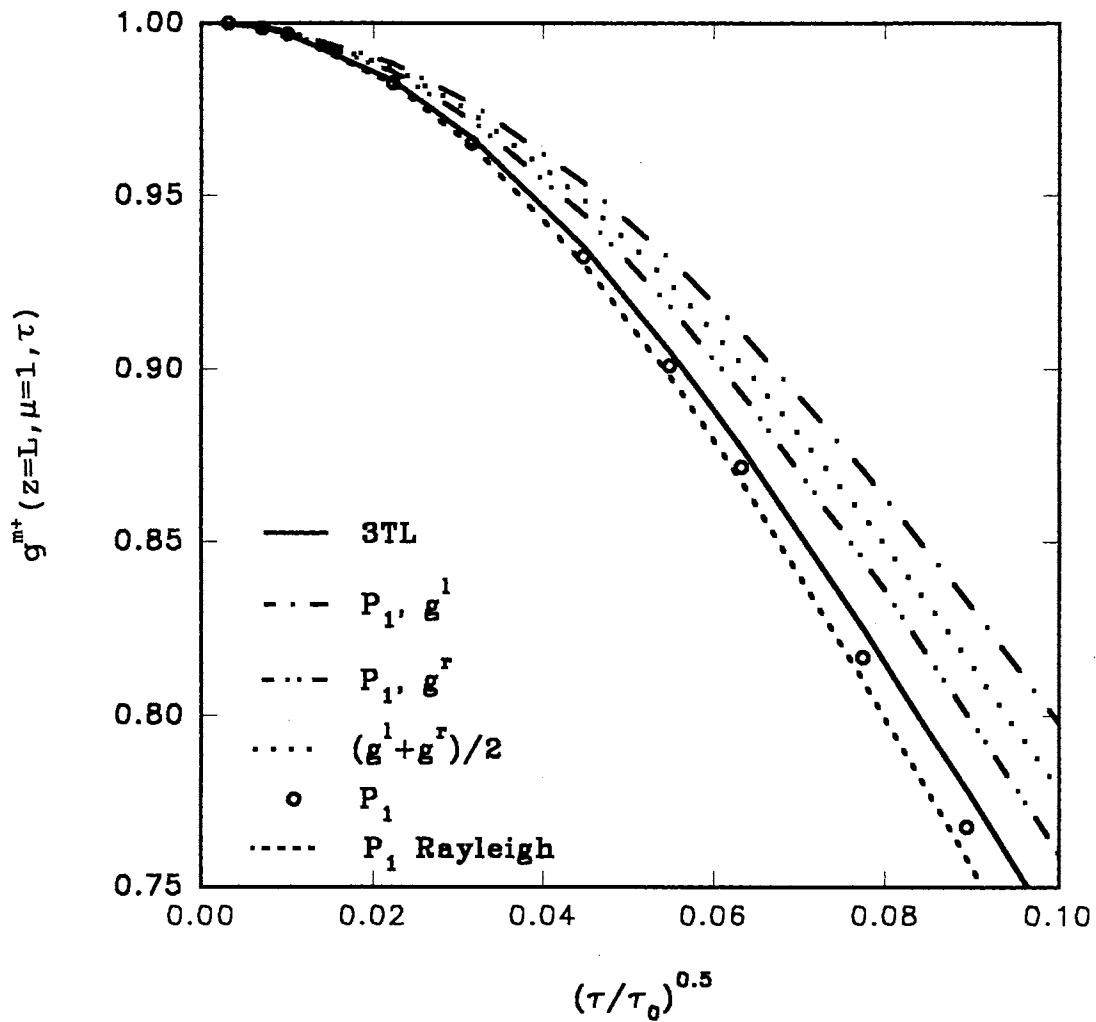


Figure 41b. Comparison of The Scalar CTE, Using The 3TL, And The  $P_1$  Approximation (For Isotropic And Rayleigh Scattering) With The Polarized CTE, With Rayleigh Scattering Using The  $P_1$  Approximation With Unpolarized Boundary Condition, For The Transmitted Correlation Function From A Medium With An Optical Thickness  $L=5$ ; Showing The Short Time Behavior

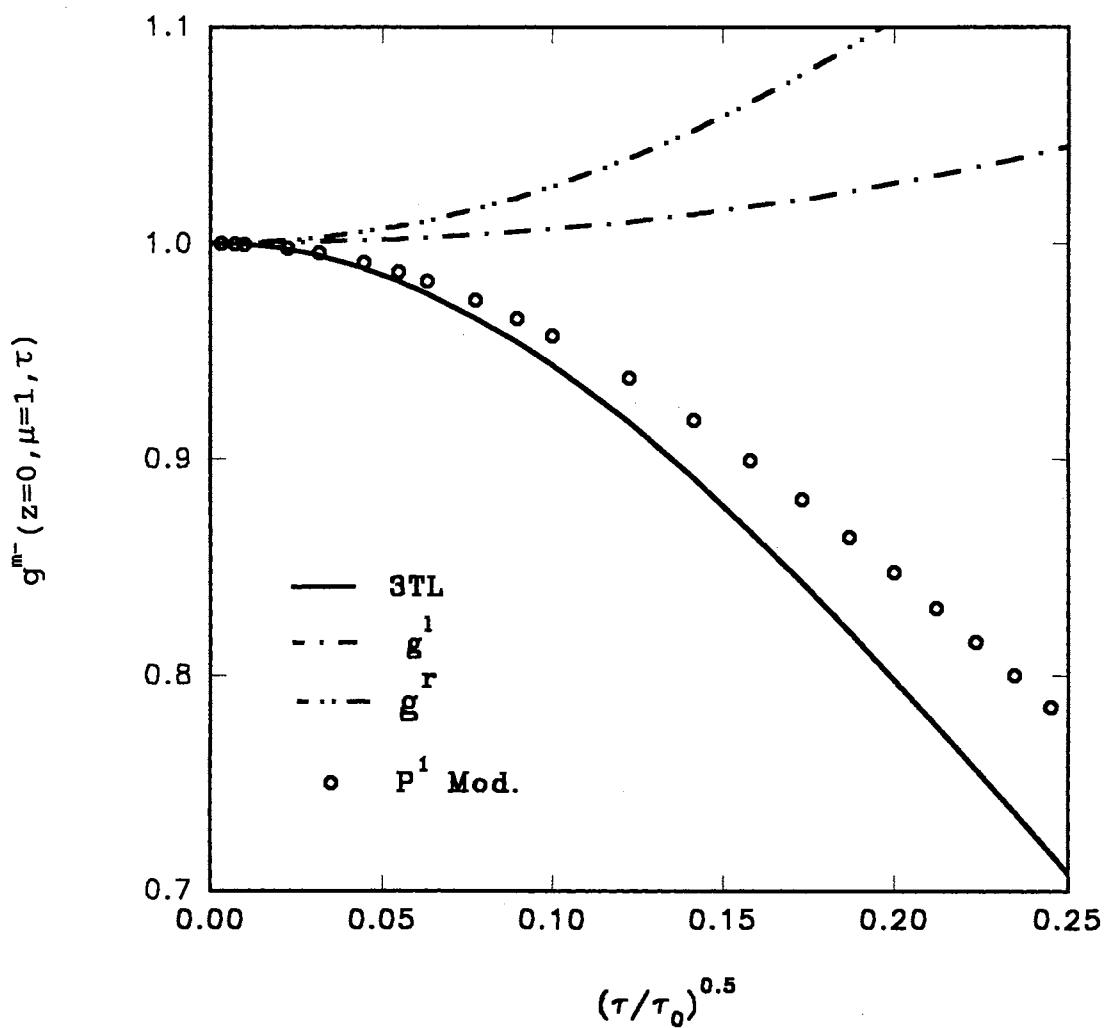


Figure 42. Comparison of The Scalar CTE, Using The 3TL And The Modified  $P_1$  Approximation With The Polarized CTE, With Rayleigh Scattering Using The  $P_1$  Approximation With Unpolarized Boundary Condition, For The Back-Scattered Correlation Function From A Medium With An Optical Thickness  $L=1$

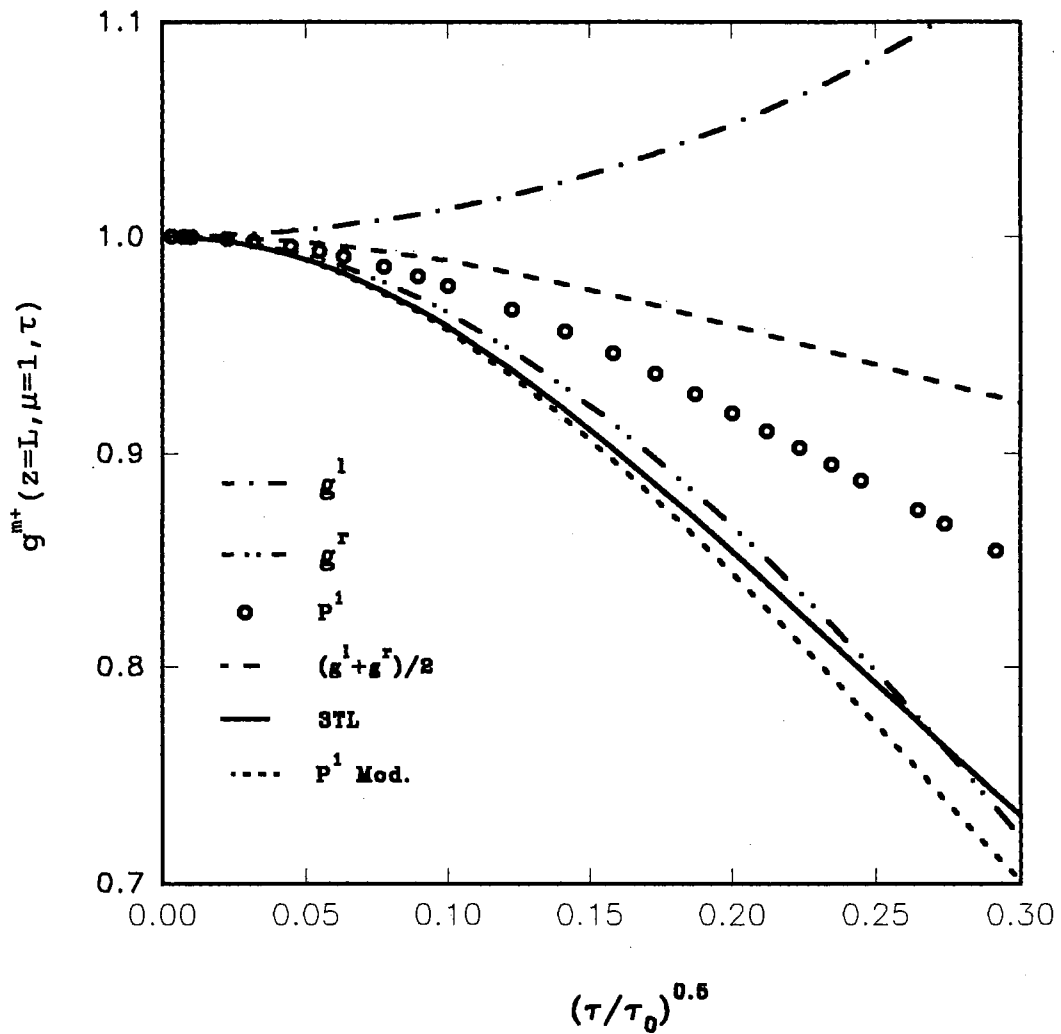


Figure 43. Comparison of The Scalar CTE, Using The 3TL, The  $P_1$  And The Modified  $P_1$  Approximations, With The Polarized CTE, With Rayleigh Scattering Using The  $P_1$  Approximation With Unpolarized Boundary Condition, For Transmitted Correlation Function From A Medium With An Optical Thickness  $L=1$

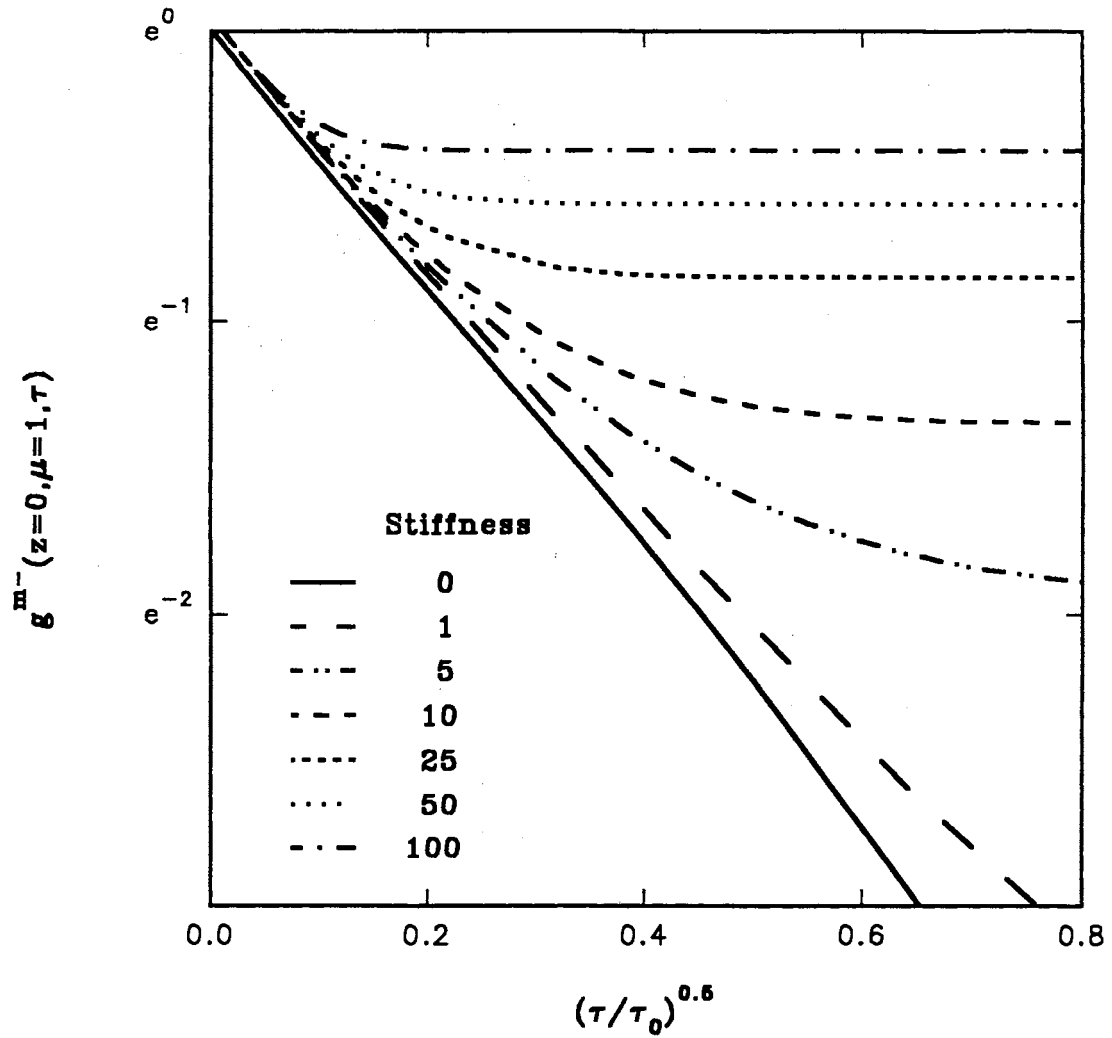


Figure 44. Effect of Movement Constraints On Diffusing Particles (Stiffness, As In Gels) On The Back-Scattered Correlation Function From A Semi-Infinite Medium Using The 3TL

## CHAPTER VIII.

### CONCLUSIONS AND RECOMMENDATIONS

#### VIII.1. Conclusions

Fluctuations of the scattered light intensity from a fluid/particle suspension, that is due to the movement of the particles in the suspension, contain useful information about the medium and particles in it. In dynamic light scattering experiments, these fluctuations are measured in terms of intensity temporal correlation functions. In this work, an integro-differential equation governing the field temporal correlation function ( $G^m$ ), which is related to the intensity temporal correlation function, is derived from basic multiple scattering theory. The governing equation, which has been termed correlation transfer equation (CTE), is specifically derived for multiple scattering of light through suspensions of monodisperse and independent diffusing particles. It is shown here that CTE has a close connection with the radiative transfer equation (RTE), and in fact, has the same type of governing equation.

Several radiative transfer (RT) solution techniques are applied to obtain solutions for the field correlation function in isotropic and anisotropic one-dimensional media, in both the forward and backward directions for a finite

one-dimensional medium and for back-scattering in the case of an infinite medium.

A preaveraging technique has been employed to reduce the anisotropic equation of CTE to an approximate isotropic equation. The exponential kernel approximation and the diffusion approximation have been used to derive closed form solutions to the preaveraged CTE and the anisotropic CTE, respectively, in one-dimensional axisymmetric media subjected to collimated incident radiation.

Chandrasekhar's X- and Y-functions and a Legendre series expansion of  $g^1$  have been used to obtain approximate numerical solutions for the preaveraged isotropic CTE and the anisotropic CTE, respectively. The anisotropy in the isotropic CTE is due solely to  $g^1$ , where it is assumed that the particles scatter isotropically and absorption is negligible. Three-term Legendre expansion of a correlated Rayleigh phase function and the forward scattering approximation have been used to obtain approximate numerical solutions for CTE with anisotropic scattering.

Finally, the  $P_1$  approximation is used to derive closed form solutions to the polarized CTE with Rayleigh's law of scattering in plane parallel media having spherical symmetry and subjected to a collimated beam. The incident beam can be either unpolarized or linearly polarized.

Solutions to CTE with isotropic scattering are presented in a limit similar to diffusive wave spectroscopy (DWS), namely, very short delay time and thick media. The

predictions agree very well with DWS at very short delay times,  $(\tau/\tau_0)^{0.5} \leq 0.1$ , for the various solution methods. The three-term Legendre expansion of  $g^1$  (3TL) procedure produced much better agreement with DWS as compared to the preaveraging results in both transmission and back-scattering. It appears that for high optical thicknesses ( $L > 5$  for back scattering, and  $L > 10$  for transmission) CTE results get closer to DWS results as the number of terms in the Legendre expansion of  $g^1$  increases. It is shown that if the diffusion approximation and short delay-time approximation are introduced into the CTE, the results agree identically with DWS. However, while DWS fails in non-diffusive media ( $L \leq 10$ ), CTE has been shown to be successful in the thin limit ( $L \ll 1$ ), as compared to the analytical  $g^1$  for single scattering. Furthermore, CTE theory does not require any fitting parameters as is the case for DWS. For example, when compared to DWS, it appears that a value of 1.29 for  $z_0/l^*$  makes the DWS results agree very well with the CTE results for finite optical thicknesses higher than 5 and up to the semi-infinite case, especially for very short delay times.

Comparing the different solution methods presented in the previous chapters to DWS or to experimental data shows that using the preaveraged CTE, represents the least accurate method as compared to the one-, two-, three-, and eight-term Legendre expansions. The benefits gained by including more Legendre terms in the expansion are the



ability to accurately compute the correlation function to longer delay times. However, for very short times,  $(\frac{\tau}{\tau_0})^{0.5} < 0.15$ , the different approximations give similar results especially with increasing optical thicknesses. It is shown that the difference between the 3TL and the 8TL is more apparent in back-scattering than in transmission because of the contribution of short scattering paths to back-scattering. These short paths exhibit stronger angular dependence and thus, more Legendre terms are needed when computing the correlation function in the back-scattering direction. For transmission, all scattering paths are at least of length  $L$ , and thus, the transmitted correlation is due mainly to these long paths which randomize the angular dependence of scattering events.

When comparing results using the preaveraged CTE and the the forward scattering approximation with experimental data, it was shown that by including the effects of anisotropy and index of refraction, closer agreement with experimental data (at short delay-time) is obtained as compared to results obtained by using the isotropic preaveraging approximation and an index of refraction equal to 1. Because anisotropy and boundary effects are minimized for semi-infinite media, it has been shown that agreement between CTE and experiments is excellent even when using isotropic 3TL and index of refraction of 1 in semi-infinite media.

For polarization effects, it has been shown that the

decay rate of both components (the parallel and the perpendicular) of the correlation function differ substantially for low ( $L \leq 1$ ) and intermediate optical thicknesses ( $1 \leq L \leq 5$ ), but not for high optical thicknesses ( $L \geq 20$ ). The results indicate that the correlation function for the perpendicular component of polarization decays more rapidly than the parallel component as predicted by the  $P_1$  approximation. The correlation function for both components retains similar exponential dependence on the square root of time for both components.

The results for the back-scattered and the transmitted correlation with polarization effects for optical thickness of 1 are poor. This result may be attributed to the normally incident collimated boundary condition which is poorly modeled by a  $P_1$  approximation, especially for low orders of scattering and normal direction. More terms in the approximation need to be included in this case.

Finally, it is shown that CTE can be extended to fluid/particle suspensions different than the case studied here (freely diffusing particles). As an example, the case of gel suspension has been studied and it is shown that the baseline of the correlation function is shifted upward as a function of increased gelling which has been observed experimentally.

It is shown here that CTE agrees and extends beyond the widely used single scattering theory and the more recent DWS in connection with photon correlation and dynamic light

scattering. The success of CTE also stems from its ability to model all orders of scattering along with the ability to include polarization effects and general types of boundary conditions and scattering characteristic. Much work is still needed to be done to extend the current work even further. The recommendations will be presented in the following section followed by a brief summary table listing and comparing all the methods of solutions used in this work.

### VIII.2 Recommendations

More complex radiative solution methods such as higher order Legendre expansions (no more than 15 for most practical cases) and the spherical harmonics solution method (which was briefly discussed here), along with a more general phase function are the natural choices for an immediate extension of this work. Also, the use of a different single scattering correlation function that corresponds to non-diffusing particles can be easily investigated in future work. This can be done by using a different form of the single scattering correlation function than the one used in Eq. (4), or by using a different probability distribution than the one used in Eq. (31). The use of a different  $g^1$  will allow the study of the effects of inter-particle correlation, polydispersity, and other hydrodynamic effects.

Two-dimensional and polarization effects, which are

important for low and intermediate optical thicknesses ( $L \leq 10$ ), need also special attention.

Two-dimensional solutions to CTE can be easily obtained from existing computer codes. Some (that were cited in the discussion section) have already been modified and used to obtain some of the one-dimensional results that were presented here (which are a special case of the more general two-dimensional case). However, because of the tremendous CPU time and storage required to run some of these codes, a new numerical approach that incorporates both advances in numerical methods and computer technology is worth looking into. Some of the numerical methods that take advantage of vector and parallel processing are of primary importance.

For polarization, the methods of solution presented here, can be used with some effort, to obtain high order approximate numerical solutions to the four-component correlation vector. Advances in the solution can be made by including the effects of index of refraction changes across the boundaries. For the case of polarized radiation, this is not a straightforward procedure as it is the case for unpolarized radiation, because the reflection coefficient depends on the polarization of the incident light (in the general case) [Siegel and Howell, 1981].

Inclusion of both the two-dimensional effects and the polarization effects into the CTE solution, with the possibility of handling index of refraction changes, should give researchers a powerful probing tool. Dynamic light

scattering data can be interpreted more accurately and valuable information on the shape and orientation of non-spherical particles, which is not possible with the current theory, can be obtained. Future applications include the study of fibers and ceramics which usually contain non-spherical scattering centers that depend strongly on polarization. Other obtained quantities, such as the correlated degree of polarization may contain some important information concerning the dynamics of the particles and the interaction of the light with the particle/fluid suspension.

#### SUMMARY AND RECOMMENDATIONS FOR METHODS TO BE USED

Short time ( $\tau/\tau_0 \leq 0.1$ ) and thick limit ( $L \geq 10$ )

- 3TL, 2TL, 1TL, Preaveraged CTE, (numerical solution)
- DCT, DWS, EKA (closed form solution)

Anisotropic or isotropic scattering thin limit ( $L \leq 0.1$ )

- $g^1$ , 8TL, 3TL

Isotropic scattering thick limit ( $L \geq 10$ )

- DCT, DWS

Isotropic scattering ( $0.1 \leq L \leq 10$ )

- 8TL, 3TL, 2TL, 1TL

Anisotropic scattering ( $0.1 \leq L \leq 10$ )

- Polarized CTE, 8TL, 3TL, Forward Approximation

Anisotropic scattering thick limit ( $L \geq 10$ )

- 8TL, 3TL (numerical solution)
- DCT, DWS (closed form solution)

Index of refraction different than one

- 8TL, 3TL, Preaveraged CTE, DWS

## REFERENCES

- Abramowitz, M. and Stegun, I.A., Handbook of Mathematical Functions, Dover, New York, 1972.
- Ackerson, B.J., Dougherty, R.L., Reguigui, N.M. and Nobbmann, U., "Correlation Transfer: Application of Radiative Transfer Solution Methods To Photon Correlation Problems," JTHT, Vol. 6, No. 4, pp. 577-588, Oct-Dec. 1992.
- Armaly, B. F. and Lam, T. T., "A Note On The Exponential Kernel Approximation," JQSRT, Vol. 14, pp. 651-656, 1974.
- Armaly, B. F., and Lam, T. T., "Radiative Source Function for a Slab: Approximate Solution," JQSRT, Vol. 18, pp. 65-68, 1977.
- Barabanenkov, Yu. N., "On The Spectral Theory of Radiation Transport Equations," Soviet Physics JETP, Vol. 29, No. 4, pp. 679-684, Oct 1969.
- Barabanenkov, Yu. N., Kravtsov, Y.A. , Rytov, S.M., and Tamarskii, V.I. "Status of The Theory of Propagation of Waves in a Randomly Inhomogeneous Medium," Soviet Physics USPEKHI, Vol. 13, No. 5, pp. 551-680, 1971.
- Becker, H.A., Hottel, H.C., and Williams, G.C., J. Fluid Mech., Vol. 30, p. 259, 1983.
- Belsley, M., Streater, A., Burnett, K., Ewart, P., and Cooper, J., "Observation of Radiative Transfer of Polarized Light," JQSRT, Vol. 36, No. 2, pp. 163-173, 1986.
- Bennassi, M., Garcia, R.D.M., Karp, A.H., and Siewert, C.E., "A High-Order Spherical Harmonics Solution to the Standard Problem in Radiative Transfer," The Astrophysical Journal, Vol. 280, pp. 853-864, 1984(a).
- Bennassi, M., Garcia, R.D.M., and Siewert, C.E., "On Eigenvalue Calculations For Radiative Transfer Models That Include Polarization Effects," J. of Applied Math. and Physics (ZAMP), Vol. 35, pp. 308-320, 1984(b).

- Bennassi, M., Garcia, R.D.M., and Siewert, C.E., "A Generalized Spherical Harmonics Solution Basic to the Scattering of Polarized Light," J. of Applied Math. and Physics (ZAMP), Vol. 36. pp. 70-88, Jan. 1985.
- Berne, B.J. and R. Pecora, Dynamic Light Scattering, Wiley, New York, 1976.
- Bohren, C.F. and Huffman, D.R., Absorption and Scattering of Light by Small Particles, John Wiley & Sons, New York, 1983.
- Chandrasekhar, S., Radiative Transfer, Dover, 1960.
- Chandrasekhar, S. and Elbert, D.D., "The Illumination And Polarization of The Sunlit Sky On Rayleigh Scattering," Am. Philos. Soc. Transactions, N.S., Vol. 44, pp. 643-710, 1954.
- Charalampopoulos, T.T. and Chang, H., "In Situ Optical Properties of Soot Particles in the Wavelength Range from 340 nm to 600 nm," Combust. Sci. and Tech., Vol. 59, pp. 401-421, 1988.
- Cheung, R.L.T. and Ishimari, A. "Transmission, Backscattering, and Depolarization of Waves in Randomly Distributed Spherical Particles," Applied Optics, Vol. 21, No. 20, pp. 3792-3798, 1982.
- Chu, B., Laser Light Scattering, Academic Press, NY, 1974.
- Chu, C.M., Leacock, J.A., Chen, J.C., and Churchill S.W., "Numerical Solutions for Multiple, Anisotropic Scattering," in ICES-I Proceedings, edited by M. Kerker, pp. 567-582, Pergamon Press, New York, 1963.
- Collins, D.G., Blattner, W.G., Wells, M.B., and Horak, H.G., Appl. Opt., Vol. 11, p. 2684, 1972.
- Coulson, K.L., "Characteristics of The Radiation Emerging From The Top of A Rayleigh Atmosphere-I, Intensity and Polarization," Planet. Space Sci., Vol. 1, pp. 265-276, 1959(a).
- Coulson, K.L., "Characteristics of The Radiation Emerging From The Top of A Rayleigh Atmosphere-II, Total Upward Flux And Albedo," Planet. Space Sci., Vol. 1, pp. 277-284, 1959(b).
- Crosbie, A.L. and Dougherty, R.L., "Two-Dimensional Isotropic Scattering in a Semi Infinite Cylindrical Medium," JOSRT, Vol. 20, pp. 151-173, 1978.
- Crosbie, A.L. and Dougherty, R.L., "Two-Dimensional

- Radiative Transfer in a Cylindrical Geometry With Anisotropic Scattering," JOSRT, Vol. 25, pp. 551-569, 1980.
- Crosbie, A.L. and Dougherty, R.L., "Two-Dimensional Isotropic Scattering in a Finite Thick Cylindrical Medium Exposed to a Laser Beam," JOSRT, Vol. 27, No. 2, pp. 149-183, 1982.
- Crosbie, A.L. and Dougherty, R.L., "Two-Dimensional Rayleigh Scattering in a Semi-Infinite Cylindrical Medium Exposed to a Laser beam," JOSRT, Vol. 30, No. 3, pp. 255-279, 1983.
- Crosbie, A.L. and Dougherty, R.L., "Two-Dimensional Linearly Anisotropic Scattering in a Finite Thick Cylindrical Medium Exposed to a Laser beam," JOSRT, Vol. 33, No. 5, pp. 487-520, 1985.
- Dave, J.V., "Intensity And Polarization of The Radiation Emerging From A Plane-Parallel Atmosphere Containing Mono-Dispersed Aerosols," Appl. Opt., Vol. 9, pp. 2673-2684, 1970.
- Deirmendjian, D. and Sekera, Z., "Global Radiation Resulting From Multiple Scattering in A Rayleigh Atmosphere," Tellus, Vol. 6, pp. 382-398, 1954.
- de Haan, J.F., Bosma, P.B., and Hovenier, J.W., "The Adding Method for Multiple Scattering Calculations of Polarized Light," Astro. Astrophysics, Vol. 183, pp. 371-391, 1987.
- de Rooij, W.A. and van der Stap, C.C.A.H., "Expansion of Mie Scattering Matrices in Generalized Spherical Functions," Astron. Astrophys, Vol. 131, pp. 237-248, 1984.
- Domke, H., "The Expansion of Scattering Matrices for an Isotropic Medium in Generalized Spherical Functions," Astrophysics and Space Science, Vol. 29, pp. 379-386, 1974.
- Domke, H., JOSRT, Vol. 15, p. 669, 1975.
- Domke, H., "Biorthogonality and Radiative Transfer In Finite Slab Atmospheres," JOSRT, Vol. 30, No. 2, pp. 119-129, 1983.
- Domke, H. and Yanovitskij, E.G., "A Simple Computational Method For Internal Polarized Radiation Fields of Finite Slab Atmospheres," JOSRT, Vol. 26, No. 5, pp. 389-396, 1981.
- Domke, H. and Yanovitskij, E.G., "Principles Of Invariance



- Applied to The Computation Of Internal Polarized Radiation In Multilayered Atmospheres," JQSRT, Vol. 36, No. 3, pp. 175-186, 1986.
- Domke, H. and Yanovitskij, E.G, "On a New Form of The Transfer Equation With Applications to Multiple Scattering of Polarized Light," JQSRT, Vol. 43, No. 1, pp. 61-73, 1990.
- Dorri-Nowkooorani, F., Private Communication, 1992.
- Dorri-Nowkooorani, F., Private Communication, 1993.
- Dorri-Nowkooorani, F., Nobbmann, U., Reguigui, N.M., Ackerson, B.J., and Dougherty, R.L., "Correlation Measurements of a Multiply Scattered Laser Beam by Fluid/Particle Suspensions," AIAA 93-2745, AIAA 28th Thermophysics Conference, Orlando, FL, July 6-9, 1993.
- Dorri-Nowkooorani, F., Tian. Y., Reguigui, N.M., Nobbmann, U., Ackerson, B.J., and Dougherty, R.L., "Improved  $P_N$  Approximation for One-Dimensional Scattering and Absorbing Media With Application to Correlation Transfer," AIAA 29th Thermophysics Conference, Colorado Springs, CO, June, 1994.
- Dougherty, R.L., "Radiative Transfer in a Semi-Infinite Absorbing/Scattering Medium with Reflective Boundary," JQSRT, Vol. 41, No. 1, pp. 55-67, 1989.
- Dougherty, R.L., Ackerson, B.J., Reguigui, N.M., and Nobbmann, U., "Correlation Transfer: Application of Radiative Transfer Solution Methods to Photon Correlation in Optically Dense Media," AIAA 91-1433, AIAA 26th Thermophysics Conference, Honolulu, Hawaii, June 24-26, 1991.
- Dougherty, R.L., Private Communication, 1992.
- Dougherty, R.L., Ackerson, B.J., Reguigui, N.M., Dorri-Nowkooorani, F., and Nobbmann, U., "Correlation Transfer: Development And Application," accepted for publication in JQSRT, 1994.
- El-Wakil, S.A., Madkour, M.A., and Abulwafa, E.M., "Polarized Radiative Transfer in an Aerosol Medium," JQSRT, Vol. 46, No. 6, pp. 523-529, 1991.
- Evans, K.F. and Stephens, G.L., "A New Polarized Atmospheric Radiative Transfer Model," JQSRT, Vol. 46, No. 5, pp. 413-423, 1991.
- Fante, R.L. "Mutual Coherence Function and Frequency Spectrum of a Laser Beam Propagating Through

- Atmospheric Turbulence," J. Opt. Soc. Am., Vol. 64, No. 5, pp. 592-598, 1974.
- Fisher, M.J. and Krause, F.R., J. Fluid mech., Vol. 28, p. 705, 1967.
- Flower, W.L., "Optical Measurements of Soot Formation In Premixed Flames," Combustion Science and Technology, Vol. 33, pp. 17-33, 1983.
- Foldy, Leslie L., "The Multiple Scattering of Waves," Phys. Rev., Vol. 67, No. 3/4, pp. 107-119, Feb. 1945.
- Frish, J., "Wave Propagation in Random Media," in Probabilistic Methods in Applied Mathematics, Vol. 1, edited by A.T. Bharucha-Reid, Academic Press, NY, pp. 75-198, 1968.
- Furustu, K., "Multiple Scattering of Waves in a Medium of Randomly Distributed Particles and Derivation of The Transport Equation," Radio Science, Vol. 10, No 1., pp. 29-44, Jan. 1975.
- Garcia, R.D.M. and Siewert, C.E., "Radiation Transfer in Finite Inhomogeneous Plane-Parallel Atmospheres," JQSRT, Vol. 27, No. 2, pp. 141-148, 1982.
- Garcia, R.D.M. and Siewert, C.E., "A Generalized Spherical Harmonics Solution For Radiative Transfer Models That Include Polarization Effects," JQSRT, Vol. 36, No 5, pp. 401-423, 1986.
- Garcia, R.D.M. and Siewert, C.E., "The Discrete Spectrum for Radiative Transfer with Polarization," JQSRT, Vol. 38, No. 4, pp. 295-301, 1987.
- Garcia, R.D.M. and Siewert, C. E., "The FN Method For Radiative Transfer Models That Include Polarization Effects," JQSRT, Vol. 41, No. 2, pp. 117-145, 1989.
- Gray, C.G. and Gubbins, K.E., Theory of Molecular Fluids, Oxford, New York, 1984.
- Hansen, J.E., "Multiple Scattering of Polarized Light in Planetary Atmospheres. Part II. Sunlight Reflected by Terrestrial Water Clouds," Journal of The Atmospheric Sciences, Vol. 28, p. 1400, 1971.
- Herman, B.J., "Multiple Scatter Effects On The Radar Return From Large Hail," J. Geophysics. Res., Vol. 70, pp. 1215-125, 1965.
- Herman, B.M., Asous, W., and Browning, S.R., J. Atmos. Sci., Vol. 37, p. 1828, 1980.

- Hovenier, J.W., "A Unified Treatment of Polarized Light Emerging From A Homogeneous Plane-Parallel Atmosphere," Astro. Astrophysics, Vol. 183, pp. 363-370, 1987.
- Hovenier, J.W. and van der Mee, C.V., "Fundamental Relationships Relevant to the Transfer of Polarized Light in a Scattering Atmosphere," Astro. Astrophysics, Vol. 128, pp. 1-16, 1983.
- Hunt, G.E., "A Review of Computational Technique For Analyzing the Transfer of Radiation Through a Model Cloudy Atmosphere," Journal of Quantitative Spectroscopy and Radiative Transfer, Vol. 11, pp. 655-690, 1971.
- Ishimaru, Akira, "Correlation Functions of A Wave In A Random Distribution of Stationary and Moving Scatterers," Radio. Sci., Vol. 10, No. 1, pp. 45-52, Jan. 1975.
- Ishimaru, A., "Theory and Application of Wave Propagation and Scattering in Random Media," Proceedings of the IEEE, Vol. 65, No. 7, pp. 1030-1061, July 1977.
- Ishimaru, A. and Yasuo, Kuga, "Scattering and Diffusion of A Beam Wave in Randomly Distributed Scatterers," J. Opt. Soc. Am., Vol. 73, No. 2, 131-136, Feb 1983.
- Ishimaru, A., Wave Propagation and Scattering in Random Media, Vol. 1, Academic Press, 1978(a).
- Ishimaru, A., Wave Propagation and Scattering in Random Media, Vol. 2, Academic Press, 1978(b).
- Ishimaru, A. and Kuga, Y., "Scattering and Diffusion of a Beam Wave in Randomly Distributed Scatterers," J. Opt. Soc. Am., Vol. 73, No. 2, pp. 131-136, 1983.
- Jakeman, E., "Speckle Statistics With a Small Number of Scatterers," Optical Engineering, Vol. 23, No. 4, pp. 453-461, 1984.
- Jendoubi, S., Lee, H.S., and Kim, T.K., "Radiative Transfer Solutions for Cylindrical Coordinates with Emitting, Absorbing, and Anisotropic Scattering Medium," AIAA 92-0123, AIAA 30th Aerospace Sciences Meeting and Exhibit, Reno NV, Jan. 6-9, 1992.
- Jiang, X.Y., Numerical Calculation Methods for Solving for Source Functions at Reflecting Boundaries of Semi-infinite and Finite media, Masters Thesis, School of Mechanical and Aerospace Engineering, Oklahoma State University, 1990.

- Kac, M., Probability and Related Topics in Physical Sciences, Wiley (Interscience), New York, 1957.
- Kerker, M., The Scattering of Light, Academic Press, New York, 1969.
- Kuik, F., de Haan, J.F., and Hovenier, J.W., "Benchmark Results For Single Scattering by Spheroids," J. Quant. Spectr. Raditat. Transfer, Vol. 47, No. 6, pp. 477-489, 1992.
- Lax, Melvin, "Multiple Scattering of Waves," Rev. Modern Phys., Vol. 23, No. 4, pp. 287-310, Oct. 1951.
- Lax, M., "Multiple Scattering of Waves. II. The Effective Field In Dense Systems," Phys. Rev, Vol. 85, No. 4, pp. 621-629, Feb. 1952.
- Lazoro, B.J. and Lasheras, J.C., "Particle Dispersion in the Developing Free Shear Layer. Part I. Unforced Flow," J. Fluid Mech., Vol. 235, pp. 143-178, 1992.
- Leader, C. J., "Polarization Dependence In EM Scattering From Rayleigh Scatterers Embedded In A Dielectric Slab. I. Theory," J. Applied. Physics, Vol. 46, No. 10, pp. 4371-4385, 1975.
- Leader, C.J. and Dalton, W.A.J., "Polarization Dependence In EM Scattering From Rayleigh Scatterers Embedded In A Dielectric Slab. II. Experiments," J. Applied. Physics, Vol. 46, No. 10, pp. 4386-4391, 1975.
- Lee, Siu-Chun, White, S., and Grzesik, J., "Effect of Particle Size in Composite materials on Radiative Properties," AIAA 93-2729, AIAA 28th Thermophysics Conference, July 6-9, Orlando, FL, 1993.
- Liu, C.C., "Numerical Calculation of Radiative Transfer In One-Dimensional Media With A Reflecting Top Boundary And Anisotropic Scattering," Masters Thesis, Department of Mechanical and Aerospace Engineering, Oklahoma State University, 1993.
- Look, D.C., Single Scattering from Spherical Particles: Mie Theory, Review, Bibliography and Computational Algorithm, University of Missouri-Rolla, 1975.
- Look, D.C., Jr. and Chen, Y.R., "Linear Polarization Components of Laser Radiation Scattered  $90^{\circ}$ ," AIAA 93-2727, AIAA 28th Thermophysics Conference, Orlando, FL, July 6-9, 1993.
- MacKintosh, F.C. and John, S., "Diffusive-Wave Spectroscopy and Multiple Scattering of Light in Correlated Random

- Media," Phys. Rev. B, Vol. 40, pp. 2383-2406, 1989.
- McCormick, N. J., "Estimation of Two Similarity Parameters From Polarized Radiation Measurements Within a Medium," JOSRT, Vol. 42, No. 4, pp. 303-309, 1989.
- McMaster, William H., "Polarization and the Stokes Parameters," Amer. J. Phys., Vol. 22, No. 6, Sep. 1954.
- Maret, G. and Wolf, P.E., "Multiple Light Scattering from Disordered Media. The Effect of Brownian Motion of Scatterers," Z. Phys. B, Vol. 65, pp. 409-413, 1987.
- Middleton, A.A. and Fisher, D.S., "Discrete Scatterers and Autocorrelations of Multiply Scattered Light," Phys. Rev. B, Vol. 43, No. 7, pp. 5934-5938, March 1991.
- Mishchenko, M.I. "The Fast Invariant Imbedding Method For Polarized Light: Computational Aspects And Numerical Results For Rayleigh Scattering," JOSRT, Vol. 43, No. 2, pp. 163-171, 1990.
- Mishchenko, M.I., "Reflection of Polarized Light by Plane-Parallel Slabs Containing Randomly-Oriented, Nonspherical Particles," JOSRT, Vol. 46, No. 3, pp. 171-181, 1991.
- Mishchenko, M.I., Dlugach, J.M., and Yanovitskij, E.G., "Multiple Light Scattering by Polydispersions of Randomly Distributed, Perfectly-Aligned, Infinite Mie Cylinders Illuminated Perpendicularly to Their Axes," JOSRT, Vol. 47, No. 5, pp. 401-410, 1992.
- O'Hern T.J., Trott, W.M., Martin, S.J., and Klavetter, E.A., "Advanced Diagnostics for In Situ Measurement of Particle Formation and Deposition in Thermally Stressed Jet Fuels," AIAA 93-0363, 31st Aerospace Sciences Meeting & Exhibit, January 11-14, Reno, NV, 1993.
- Ozisik, M.N., Radiative Transfer and Interaction With Conduction and Convection, Wiley, NY, 1973.
- Pal, S.R. and Carswell, A.I., "Polarization Anisotropy in Lidar Multiple Scattering From Atmospheric Clouds," Applied Optics, Vol. 24, No. 21, pp. 3463-3471, 1985.
- Pine, J. D., Weitz, D. A., Chaikin, P. M., and Herbolzheimer, E., "Diffusive Wave Spectroscopy," Phys. Rev. Lett., Vol. 60, p. 1134, 1988.
- Pine, D.J., Weitz, D.A., Maret, G., Wolf P.E., Herbolzheimer and Chaikin, P.M., "Dynamical Correlations of Multiply Scattered Light," in Scattering and Localization of Classical Waves in Random Media," World Scientific,

Singapore, 1990.

- Pomraning, G.C., The Equations of Radiation Hydrodynamics, Pergamon Press, Oxford, 1973.
- Provdor, T., editor, Particle Size Distribution, Assessment and Characterization, ACS Symposium Series, American Chemical Society, Washington, DC 1987.
- Pusey, P.N. and Tough, R.J.A., in Dynamic Light Scattering and Velocimetry: Applications of Photon Correlation Spectroscopy, ed. by R. Pecora, Plenum, NY, 1985.
- Reguigui, N.M. and Dougherty, R.L., "Two-Dimensional Radiative Transfer in a Cylindrical Layered Medium with Reflecting Interfaces," J. Thermophysics and Heat Transfer, Vol. 6, No. 2, April-June 1992.
- Reguigui, N.M. "Radiative Transfer In A Four-Layer Cylindrical Medium With Reflecting Boundaries," Masters Thesis, Department of Mechanical and Aerospace Engineering, Oklahoma State University, 1990.
- Reguigui, N.M., Dorri-Nowkoorani, F., Nobbmann, U., Ackerson, B.J., and Dougherty, R.L., "Particle Characterization Using Correlation Transfer Theory," AIAA 93-0141, 31st Aerospace Sciences Meeting & Exhibit, Jan. 11-14, Reno, NV, 1993.
- Russo, P., Guo, K., and Delong, L., "A New Look at Distribution Analysis of Dynamic Light Scattering Data, Using Only a Microcomputer," ANTEC 88, Society of Plastics Engineers 46th Annual technical Conference & Exhibits, Atlanta, April 18-21, pp. 983-985, 1988.
- Salpeter, E.E., and Treiman, S.B., "Multiple Scattering in the Diffusion Approximation," J. of Mathematical Physics, Vol. 5, No. 5, pp. 659-668, 1964.
- Sanchez, Richard and Pomraning, G.C., "A Family of Flux-Limited Diffusion Theories," JOSRT, Vol. 45, No. 6, pp. 313-337, 1991.
- Sekera, Z., "Multiple Scattering in Media with Anisotropic Scattering," in ICES-I Proceedings, edited by M. Kerker, pp. 547-557, Pergamon Press, New York, 1963.
- Sekera, Z., "Recent Development In The Study of The Polarization of Sky Light," Advances in Geo-physics, Vol. 3, pp. 43-104, 1956.
- Sekera, Zdenek, "Scattering Matrices and Reciprocity Relationships for Various Representations of the State of Polarization," J. Opt. Soc. Amer., Vol. 56, No. 12,

pp. 1732-1740, December, 1966.

- Sekera, Zdenek, "Introduction To Multiple Scattering Problems," ICES II Proceedings, pp. 523-537, edited by R.L. Rowell and R.S. Steen, Gordon and Breach, NY, 1967.
- Sekera, Zdenek, "Radiative Transfer And The Scattering Problem," JQSRT, Vol. 8, pp. 17-24, 1968.
- Siegel, R, and Howell, J.R, Thermal Radiation Heat Transfer, 2nd edition, McGraw-Hill, New York, 1981.
- Siewert, C.E., "On the Equation of Transfer Relevant to the Scattering of Polarized Light," The Astrophysical Journal, Vol. 245, pp. 1080-1086, May 1981.
- Siewert, C.E., "On the Phase Matrix Basic to the Scattering of Polarized Light," Astron. Astrophys., Vol. 109, pp. 195-200, 1982.
- Siewert, C.E., "Radiative Transfer Calculations in Spheres and Cylinders," JQSRT, Vol. 34, No. 1, pp. 59-64, 1985.
- Siewert, C.E., Maiorino, J.R., and Ozisik, M.N., "The Use of The FN Method For Radiative Transfer Problems With Reflective Boundary Conditions," JQSRT, Vol. 23, pp. 565-573, 1980.
- Siewert, C.E. and McCormick, N.J., "A Particular Solution For Polarization Calculations In Radiative Transfer," J. Quant. Spectrosc. Radiat. Transfer, Vol. 50, No. 5, pp. 531-540, 1993.
- Siewert, C.E. and Pinheiro, F.J.V., "On the Scattering of Polarized Light," Journal of Applied Mathematics and Physics (ZAMP), Vol. 33, pp. 807-818, 1984.
- Stephen, M.J., "Temporal Fluctuations in Wave Propagation in Random Media," Phys. Rev. B, Vol. 37, No. 1, pp. 1-5, 1988.
- Stephen, M.J. and Cwilich, G., "Rayleigh Scattering and Weak Localization: Effects of Polarization," Phys. Rev. B, Vol. 34, No. 11, pp. 7564-7572, 1986.
- Stamnes, Knut and Conklin, Paul, "A New Multi- Layer Discrete Ordinate Approach to Radiative Transfer in Vertically Inhomogeneous Atmospheres," JQSRT, Vol. 31, pp. 273-282, 1984.
- Stamnes, P., de Haan, J.F., and Hovenier, J.W., "The Polarized Internal Radiation Field of a Planetary Atmosphere," Astron. Astrophys., Vol. 225, pp. 239-

- 259, 1989.
- Tian, Y. and Dorri-Nowkooorani, F., Private Communication, 1992.
- Twersky, Victor, "On Scattering of Waves by Random Distributions. I: Free-Space Scatterer Formalism," J. Math. Phys., Vol. 3, No 4, pp. 700-715, 1962.
- Twersky, Victor, "On a General Class of Scattering Problems," J. Math. Phys., Vol. 3, No 1, pp. 716-723, July-Aug, 1962.
- Twersky, V., "Multiple Scattering of Waves In Dense Distributions of Large Tenuous Scatterers," ICES I Proceedings, pp. 523-546, edited by M. Kerker, Pergamon Press, NY, 1963.
- Twersky, V., "On Propagation In Random Media of Discrete Scatterers," in Proceedings of The American Mathematical Society Symposium On Stochastic Processes in Mathematical Physics and Engineering, Vol. 16, pp. 84-116, American Mathematical Society, Providence, Rhode Island, 1964.
- van de Hulst, H.C., Light Scattering by Small Particles, Dover Publications, NY, 1957.
- van de Hulst, H.C., "Multiple Scattering In Plane-Parallel Layers," ICES II Proceedings, pp. 787-796, edited by R.L. Rowell and R.S. Steen, Gordon and Breach, NY, pp. 787-796, 1967.
- van de Hulst, H.C., Multiple Light Scattering, Tables, Formulas, and Applications, Vol. 1, Academic Press, New York, 1980(a)
- van de Hulst, H.C., Multiple Light Scattering, Tables, Formulas, and Applications, Vol. 2, Academic Press, New York, 1980(b)
- Vermote, E. and Tanre, D., "Analytical Expressions For Radiative Properties of Planar Rayleigh Scattering Media, Including Polarization Contributions," J. Quant. Spectrosc. Radiat. Transfer, Vol. 47, No. 4, pp. 305-314, 1992.
- Wauben, W.M.F. and Hovenier, J.W., "Polarized Radiation of an Atmosphere Containing Randomly-Oriented Spheroids," JOSRT, Vol. 47, No. 6, pp. 491-504, 1992(a).
- Wauben, W.M.F. and Hovenier, J.W., "Approximative Methods for Calculating the Radiation Inside a Planetary Atmosphere," Astron. Astrophys, Vol. 261, pp. 640-646,



1992(b).

- Wauben, W.M.F., de Haan, J.F., and Hovenier, J.W.,  
"Approximations for Computing the Internal Radiation of  
a Homogeneous Molecular Scattering Atmosphere," Astron.  
Astrophys, Vol. 276, pp. 241-254, 1993(a).
- Wauben, W.M.F., de Haan, J.F., and Hovenier, J.W.,  
"Influence of Particle Shape on the Polarized Radiation  
in Planetary Atmospheres," JQSRT, Vol. 50, No. 3,  
pp. 237-246, 1993(b).
- Weiner, B.B., "Particle Sizing Using Photon Correlation  
Spectroscopy," in Modern Methods of Particle Size  
Analysis, edited by H. G. Barth, Wiley, New York, pp.  
93-116, 1984.
- Weng, F., "A Multi-Layer Discrete-Ordinate Method for Vector  
Radiative Transfer in a Vertically-Inhomogeneous,  
Emitting and Scattering Atmosphere -I. Theory," JQSRT,  
Vol. 47, No. 1, pp. 19-33, 1992(a).
- Weng, F., "A Multi-Layer Discrete-Ordinate Method for Vector  
Radiative Transfer in a Vertically-Inhomogeneous,  
Emitting and Scattering Atmosphere -II. Application,"  
JQSRT, Vol. 47, No. 1, pp. 35-42, 1992(b).
- Wolf, E., "New Theory of Radiative Energy Transfer in Free  
Electromagnetic Fields," Physical Rev. D, Vol. 13, No.  
4, pp. 869-886, 1976.
- Wolf, P.E. and Maret, G., "Dynamics of Brownian Particles  
From Strongly Multiple Light Scattering," in Scattering  
in Volumes and Surfaces, edited by M. Nieto-Vesperinas  
and C. Dainty, Elsevier Science Publishers B.V.,  
Amsterdam, North-Holland, pp. 37-52, 1990.
- Yoo, K.M., Liu, F., and Alfano, R.R., "When Does the  
Diffusion Approximation Fail to Describe Photon  
Transport in Random Media?," Phys. Rev. Lett., Vol. 64,  
No. 22, pp. 2647-2650, 1990.
- Zhu, J.X., Pine, D.J., Weitz, D.A., "Internal Reflection of  
Diffusive Light in Random Media," Phys. Rev. A, Vol.  
44, No. 6, pp. 3948-3959, 1991.

## APPENDIX A

### MODIFIED BESSEL FUNCTIONS

In this appendix, definitions and derivations related to the modified Bessel function as it is used in conjunction with the Legendre expansion of  $g^1$  (see section V.1.b) are presented.

The modified Bessel functions are given by the following generating relation [Ambramowitz and Stegun, 1972]

$$\sqrt{\left(\frac{\pi}{2t}\right)} I_{n+\frac{1}{2}}(t) = j_n(t) \sinh(t) + j_{-n-1}(t) \cosh(t) \quad (\text{A1})$$

where

$$j_0(t) = t^{-1}, \quad (\text{A2})$$

$$j_1(t) = -t^{-2}, \quad (\text{A3})$$

and

$$j_{n-1}(t) - j_{n+1}(t) = (2n+1)t^{-1}j_n(t), \quad n=0, \pm 1, \pm 2, \dots \quad (\text{A4})$$

From Eq. (A4), the first 16  $j_n(t)$  ( $n=-3, -2, \dots, 2$ ) are

$$j_0(t) = t^{-1} \quad (\text{A5})$$

$$j_1(t) = -t^{-2} \quad (\text{A6})$$

$$j_{-1}(t) = 0 \quad (\text{A7})$$

$$j_2(t) = t^{-1}(1 + 3t^{-2}) \quad (\text{A8})$$

$$j_{-2}(t) = t^{-1} \quad (\text{A9})$$

$$j_3(t) = -t^{-2}(6 + 15t^{-2}) \quad (\text{A10})$$

$$j_{-3}(t) = -3t^{-2} \quad (\text{A11})$$

$$j_4(t) = t^{-1}(1 + 45t^{-2} + 105t^{-4}) \quad (\text{A12})$$

$$j_{-4}(t) = t^{-1}(1 + 15t^{-2}) \quad (\text{A13})$$

$$j_5(t) = -t^{-2}(15 + 420t^{-2} + 945t^{-4}) \quad (\text{A14})$$

$$j_{-5}(t) = -t^{-2}(10 + 105t^{-2}) \quad (\text{A15})$$

$$j_6(t) = t^{-1}(1 + 210t^{-2} + 4725t^{-4} + 10395t^{-6}) \quad (\text{A16})$$

$$j_{-6}(t) = t^{-1}(1 + 105t^{-2} + 945t^{-4}) \quad (\text{A17})$$

$$j_7(t) = -t^{-2}(28 + 3150t^{-2} + 62370t^{-4} + 135135t^{-6}) \quad (\text{A18})$$

$$j_{-7}(t) = -t^{-2}(21 + 1260t^{-2} + 10395t^{-4}) \quad (\text{A19})$$

$$j_{-8}(t) = t^{-1}(1 + 378t^{-2} + 17325t^{-4} + 135135t^{-6}) \quad (\text{A20})$$

From Eq. (A1) and Eqs. (A5)-(A20), the first half order modified Bessel function is:

$$\sqrt{\left(\frac{\pi}{2t}\right)} I_{\frac{1}{2}}(t) = x_0(t) \quad (\text{A21})$$

and where

$$x_0(t) = t^{-1}\sinh(t) \quad (\text{A22})$$

and the next seven half order modified Bessel functions are:

$$\sqrt{\left(\frac{\pi}{2t}\right)} I_{\frac{3}{2}}(t) = x_0(t) (-t^{-1} + \coth(t)) \quad (\text{A23})$$

$$\sqrt{\left(\frac{\pi}{2t}\right)} I_{\frac{5}{2}}(t) = x_0(t) (1 + 3t^{-2} - 3t^{-1}\coth(t)) \quad (\text{A24})$$

$$\sqrt{\left(\frac{\pi}{2t}\right)} I_{\frac{7}{2}}(t) = x_0(t) (-6t^{-1} - 15t^{-3} + (1 + 15t^{-2})\coth(t)) \quad (\text{A25})$$

$$\sqrt{\left(\frac{\pi}{2t}\right)} I_{\frac{9}{2}}(t) = x_0(t) (1+45t^{-2}+105t^{-4} - (10t^{-1}+105t^{-3})\coth(t)) \quad ($$

$$\sqrt{\left(\frac{\pi}{2t}\right)} I_{\frac{5+1}{2}}(t) = x_0(t) \\ \times (-15t^{-1}-420t^{-3}-945t^{-5} + (1 + 105t^{-2} + 945t^{-4})\coth(t)) \quad (\text{A27})$$

$$\sqrt{\left(\frac{\pi}{2t}\right)} I_{\frac{6+1}{2}}(t) = x_0(t) (1+210t^{-2} + 4725t^{-4} + 10395t^{-6} \\ - (21t^{-1} + 1260t^{-3} + 10395t^{-5})\coth(t)) \quad (\text{A28})$$

$$\sqrt{\left(\frac{\pi}{2t}\right)} I_{\frac{7+1}{2}}(t) = x_0(t) (-28t^{-1} - 3150t^{-3}-62370t^{-5} - 135135t^{-7} \\ + (1+378t^{-2} + 17325t^{-4} + 135135t^{-6})\coth(t)) \quad (\text{A29})$$

For  $t \ll 1$ , the analytic equations for the modified Bessel functions (Eqs. (A21)-(A29)) give rise to some numerical problems because of the division by the small value  $t$ . In this case, it is better to use the series expansion for the modified Bessel function given by

$$\sqrt{\left(\frac{\pi}{2t}\right)} I_{n+\frac{1}{2}}(t) = \\ \frac{t^n}{1 \cdot 3 \cdot \dots \cdot (2n+1)} \left\{ 1 + \frac{\frac{1}{2}t^2}{1!(2n+3)} + \frac{\left(\frac{1}{2}t^2\right)^2}{2!(2n+3)(2n+5)} + \dots \right\} \quad (\text{A30})$$

## APPENDIX B

### EXPANSION OF THE PHASE MATRIX ELEMENTS

For polarized light the elements of the scattering matrix (Eq. (181)), obtained from Mie theory, can be expanded in a series of generalized spherical functions [de Rooij and van der Stap, 1984] so that the coefficients of a Fourier expansion of the phase matrix can be easily obtained. These expansion formulas are given here explicitly.

It can be shown [Siewert, 1981, Siewert and Pinheiro, 1981, Siewert, 1982, and de Rooij and van der Stap, 1984] that the elements of the scattering matrix can be expanded as

$$a_1(\mu_s) = \sum_{i=0}^{\infty} \beta_i P_i(\mu_s), \quad \beta_0=1, \quad (B1)$$

$$a_2(\mu_s) = \sum_{i=2}^{\infty} \left[ \frac{(i-2)!}{(i+2)!} \right]^{1/2} (\alpha_i R_i^2(\mu_s) + \zeta_i T_i^2(\mu_s)) \quad (B2)$$

$$a_3(\mu_s) = \sum_{i=2}^{\infty} \left[ \frac{(i-2)!}{(i+2)!} \right]^{1/2} (\zeta_i R_i^2(\mu_s) + \alpha_i T_i^2(\mu_s)) \quad (B3)$$

$$a_4(\mu_s) = \sum_{i=0}^{\infty} \delta_i P_i(\mu_s) \quad (B4)$$

$$b_1(\mu_s) = \sum_{i=2}^{\infty} \left[ \frac{(i-2)!}{(i+2)!} \right]^{1/2} \gamma_i P_i^2(\mu_s) \quad (\text{B5})$$

and

$$b_2(\mu_s) = - \sum_{i=2}^{\infty} \left[ \frac{(i-2)!}{(i+2)!} \right]^{1/2} \varepsilon_i P_i^2(\mu_s) \quad (\text{B6})$$

where as usual,  $P_i(\mu)$  and  $P_i^m(\mu)$  are used to denote the Legendre function and the associated Legendre function, respectively (see Appendix C), and  $R_i^m(\mu)$  and  $T_i^m(\mu)$  are related to the generalized spherical functions (see Appendix C).

## APPENDIX C

### SPHERICAL AND GENERALIZED SPHERICAL HARMONIC FUNCTIONS

#### C.I. Legendre and Associated Legendre Functions

As usual,  $P_i(\mu)$  and  $P_i^m(\mu)$  are used to denote the Legendre function and the associated Legendre function, respectively, given by [Ambramowitz and Stegun, 1972]

$$P_i^m(\mu) = (1-\mu^2)^{m/2} \frac{d^m}{d\mu^m} P_i(\mu) \quad (C1)$$

The Legendre polynomials and the associated Legendre functions satisfy the orthogonality relations

$$\int_{-1}^1 P_i(\mu) P_m(\mu) d\mu = \frac{2}{(2i+1)} \delta_{i,m} \quad (C2)$$

and for  $i \geq m$

$$\int_{-1}^1 P_i^m(\mu) P_n^m(\mu) d\mu = \frac{2}{(2i+1)} \left[ \frac{(i+m)!}{(i-m)!} \right] \delta_{i,n} \quad (C3)$$

We can use the recursion formulas

$$(i1) P_{i+1}(\mu) = (2i+1)\mu P_i(\mu) - iP_{i-1}(\mu), \quad i \geq 0, \quad (C4)$$

and for a general  $m \leq i$ ,

$$(i+1-m)P_{i+1}^m(\mu) = (2i+1)\mu P_i^m(\mu) - (i+m)(1-\delta_{m,i})P_{i-1}^m(\mu) \quad (C5)$$

with

$$P_0(\mu) = 1 \quad (C6)$$

$$P_2^2(\mu) = 3(1-\mu^2) \quad (C7)$$

and

$$P_2(\mu) = \frac{1}{2}(3\mu^2-1) \quad (C8)$$

### C.II. Generalized Spherical Functions

The generalized spherical functions are discussed in detail by Hovenier (1987), Siewert (1982), and de Rooij and van der Stap (1984). For  $i \geq \sup(|m|, |n|)$ , the generalized spherical functions are defined by

$$P_{m,n}^i(\mu) = A_{m,n}^i (1-\mu)^{-(n-m)/2} (1+\mu)^{-(n+m)/2} \frac{d^{i-n}}{d\mu^{i-n}} \left[ (1-\mu)^{i-m} (1+\mu)^{i+m} \right] \quad (C9)$$

where  $\sup(|m|, |n|)$  means the larger between  $|m|$  and  $|n|$ .

$P_{m,n}^i(\mu) = 0$  if  $i < \sup(|m|, |n|)$ ,  $P_{m,n}^i(\mu) = P_{n,m}^i(\mu)$ , and

$$A_{m,n}^i = \frac{(-1)^{i-m} (i)^{n-m}}{2^i (1-m)!} \left[ \frac{(i-m)! (i+n)!}{(i+m)! (i-n)!} \right]^{1/2} \quad (C10)$$

The generalized spherical functions obey the following



orthogonality relation for  $i \geq \sup(|m|, |n|)$ :

$$(-1)^{m-n} \int_{-1}^1 P_{mn}^i(\mu) P_{mn}^j(\mu) d\mu = \frac{2}{(2i+1)} \delta_{i,j} \quad (\text{C11})$$

and the following recurrence relation for  $i \geq \sup(|m|, |n|)$ :

$$\begin{aligned} e_{m,n}^i P_{m,n}^{i+1}(\mu) \\ = (2i+1)\mu P_{m,n}^i(\mu) - f_{m,n}^i P_{m,n}^{i-1}(\mu) - \left( \frac{mn(2i+1)}{i(i+1)} \right) P_{m,n}^i(\mu) \end{aligned} \quad (\text{C12})$$

with

$$e_{m,n}^i = \left( \frac{1}{i+1} \right) ((i+m+1)(i-m+1)(i+n+1)(i-n+1))^{1/2} \quad (\text{C13})$$

and

$$f_{m,n}^i = \frac{1}{i} ((i+m)(i-m)(i+n)(i-n))^{1/2} \quad (\text{C14})$$

For the expansion of the scattering matrix elements in a series of generalized spherical functions, the following relations arise [de Rooij and Stap, 1984, Siewert and Pinheiro, 1984]

$$R_i^m(\mu) = -\frac{1}{2}(i)^m \left( \frac{(i+m)!}{(i-m)!} \right)^{1/2} (P_{m,2}^i(\mu) + P_{m,-2}^i(\mu)) \quad (\text{C15a})$$

and

$$T_1^m(\mu) = -\frac{1}{2}(i)^m \left[ \frac{(i+m)!}{(i-m)!} \right]^{1/2} (P_{m,2}^i(\mu) - P_{m,-2}^i(\mu)) \quad (C15b)$$

Siewert and Pinheiro (1984) have reported that the above analytical representation is a good method for computing the components in a Fourier decomposition of the phase matrix  $P(\mu, \mu', \phi, \phi', t)$ . Note that with the relations, for  $i \geq m$ , [Siewert, 1982]

$$P_1^m(-\mu) = (-1)^{i-m} P_1^m(\mu) \quad (C16a)$$

$$R_1^m(-\mu) = (-1)^{i-m} R_1^m(\mu) \quad (C16b)$$

and

$$T_1^m(-\mu) = -(-1)^{i-m} T_1^m(\mu) \quad (C16c)$$

From Eqs. (14) (in the text) and the definition of  $P_{m,n}^i$ , it can be shown that  $R_1^0(\mu) = R_1(\mu) = 0$  for  $i=0$  and  $1$ , and for  $i \geq 2$

$$R_1(\mu) = \left[ \frac{(i-2)!}{(i+2)!} \right]^{1/2} P_1^2(\mu) \quad (C17)$$

$$R_2^0(\mu) = R_2(\mu) = \frac{\sqrt{6}}{4}(1-\mu^2) \quad (C18)$$

$$R_2^2(\mu) = \frac{\sqrt{6}}{2}(1+\mu^2) \text{ and } T_2^2(\mu) = \sqrt{6}\mu \quad (C19)$$

$$R_2^1(\mu) = -\mu \frac{\sqrt{6}}{2}(1-\mu^2)^{1/2} \text{ and } T_2^1(\mu) = -\frac{\sqrt{6}}{2}(1-\mu^2)^{1/2} \quad (C20)$$

and using the recursion relation for  $P_{m,n}^i$ , Eq. (C12), we can find recursive relations for  $R_i^2$  and  $T_i^2$  [Siewert, 1982] which are needed in Eqs. (194)

$$\begin{aligned} \left(\frac{i-1}{i+1}\right) ((i+3)(i-1))^{1/2} R_{i+1}^2(\mu) &= (2i+1)\mu R_i^2(\mu) \\ &- \left(\frac{i+2}{i}\right) ((i+2)(i-2))^{1/2} R_{i-1}^2(\mu) - \left(\frac{4(2i+1)}{i(i+1)}\right) T_i^2(\mu) \end{aligned} \quad (C21)$$

and

$$\begin{aligned} \left(\frac{i-1}{i+1}\right) ((i+3)(i-1))^{1/2} T_{i+1}^2(\mu) &= (2i+1)\mu T_i^2(\mu) \\ &- \left(\frac{i+2}{i}\right) ((i+2)(i-2))^{1/2} T_{i-1}^2(\mu) - \left(\frac{4(2i+1)}{i(i+1)}\right) R_i^2(\mu) \end{aligned} \quad (C22)$$

## APPENDIX D

### RECURSIVE RELATIONS FOR THE MATRICES $\Pi_i^m(\mu)$ AND $P_i(\mu)$

Some useful recursion relations for matrices  $\Pi_i^m(\mu)$  and  $P_i(\mu)$  that were encountered in developing a solution for the polarized equation of radiation are given explicitly in this appendix.

#### D.I. The $\Pi_i^m(\mu)$ Matrices

The basic matrices  $\Pi_i^m(\mu)$  defined by Eq. (188) can in principle be computed from the definitions given by Eqs. (C15a)-(C15b) and the definitions for  $P_{m,n}^i(\mu)$  (given in Appendix C). However, Siewert (1982) has developed some recursion relations for the matrices  $\Pi_i^m(\mu)$  that are better suited for numerical computations. For  $m = 0$ , let  $\Pi_i^0(\mu) = \Pi_i(\mu)$  and that

$$\Pi_0(\mu) = \text{diag}\{1, 0, 0, 1\} \quad (\text{D1})$$

$$\Pi_1(\mu) = \text{diag}\{\mu, 0, 0, \mu\} \quad (\text{D2})$$

$$\Pi_2(\mu) = \text{diag}\{P_2(\mu), R_2(\mu), R_2(\mu), P_2(\mu)\} \quad (\text{D3})$$

and for  $i \geq 2$

$$\Pi_{i+1}(\mu) = X_i^{-1} \left( (2i+1)\mu\Pi_i(\mu) - Y_i\Pi_{i-1}(\mu) \right) \quad (D4)$$

where

$$X_i = \text{diag}\{i+1, [(i+3)(i-1)]^{1/2}, [(i+3)(i-1)]^{1/2}, i+1\} \quad (D5)$$

and

$$Y_i = \text{diag}\{i, (i^2-4)^{1/2}, (i^2-4)^{1/2}, i\} \quad (D6)$$

For  $m = 1$ ,

$$\Pi_1^1(\mu) = \text{diag}\{(1-\mu^2)^{1/2}, 0, 0, (1-\mu^2)^{1/2}\} \quad (D7)$$

and

$$\Pi_2^1(\mu) = \begin{bmatrix} 3\mu(1-\mu^2)^{1/2} & 0 & 0 & 0 \\ 0 & R_2^1(\mu) & -T_2^1(\mu) & 0 \\ 0 & -T_2^1(\mu) & R_2^1(\mu) & 0 \\ 0 & 0 & 0 & 3\mu(1-\mu^2)^{1/2} \end{bmatrix} \quad (D8)$$

and for  $i \geq 2$ ,

$$\Pi_{i+1}^1(\mu) = (X_i^1)^{-1} \left( (2i+1)\mu\Pi_i^1(\mu) - Y_i^1\Pi_{i-1}^1(\mu) + W_i^1\Pi_i^1(\mu) \right) \quad (D9)$$

where in general,

$$X_i^m = \text{diag}\left\{i+1-m, \left(\frac{i-m+1}{i+1}\right) [(i+3)(i-1)]^{1/2}, \left(\frac{i-m+1}{i+1}\right) [(i+3)(i-1)]^{1/2}, i+1-m\right\} \quad (D10)$$

and

$$Y_i^m = (1-\delta_{m,1}) \text{diag}\left\{i+m, \left(\frac{i+m}{i}\right) (i^2-4)^{1/2}, \left(\frac{i+m}{i}\right) (i^2-4)^{1/2}, i+m\right\} \quad (\text{D11})$$

and

$$W_i^m = \frac{2m(2i+1)}{i(i+1)} \begin{bmatrix} 0 & 0 & 0 & 0 \\ 0 & 0 & 1 & 0 \\ 0 & 1 & 0 & 0 \\ 0 & 0 & 0 & 0 \end{bmatrix} \quad (\text{D12})$$

Finally, for the general case  $m \geq 2$

$$\Pi_m^m = (1-\mu^2)^{1/2} \begin{bmatrix} (2m-1)!! & 0 & 0 & 0 \\ 0 & K_m \sigma(\mu) & -K_m \kappa(\mu) & 0 \\ 0 & -K_m \kappa(\mu) & K_m \sigma(\mu) & 0 \\ 0 & 0 & 0 & (2m-1)!! \end{bmatrix} \quad (\text{D13})$$

with  $(2m-1)!! = 1 \cdot 3 \cdot 5 \dots (2m-1)$

$$K_m = \frac{(2m)!}{2^m} [(m-2)! (m+2)!]^{-1/2} \quad (\text{D14})$$

$$\sigma(\mu) = (1+\mu^2)/(1-\mu^2), \quad (\text{D15})$$

and

$$\kappa(\mu) = 2\mu/(1-\mu^2) \quad (\text{D16})$$

and for  $i \geq m$

$$\Pi_{i+1}^m(\mu) = (\mathcal{X}_i^m)^{-1} \left( (2i+1)\mu\Pi_i^m(\mu) - \mathcal{V}_i^m\Pi_{i-1}^m(\mu) + \mathcal{W}_i^m\Pi_i^m(\mu) \right) \quad (\text{D17})$$

### D.II. The $P_i(\mu)$ Matrices

Some useful recursive relations can also be derived for the matrices  $P_i(\mu)$ , given by Eq. (203). Using the definitions of Eqs. (203) and (C17) and the orthogonality relation Eq. (C2), we can deduce an orthogonality relation for the matrices  $P_i(\mu)$ , i.e.

$$\int_{-1}^1 P_i(\mu) P_m(\mu) d\mu = \frac{2}{(2i+1)} \text{diag}\{1, (1-\delta_{0,i})(1-\delta_{1,i})\delta_{i,m}\} \quad (\text{D18})$$

We can also use the recursive relation Eq. (C4) to deduce for  $i \geq 1$ , that

$$(2i+1)\mu P_i(\mu) = \mathbb{K}_i P_{i+1}(\mu) + \mathbb{J}_i P_{i-1}(\mu), \quad (\text{D19})$$

where

$$\mathbb{K}_i = \text{diag}\{i+1, [(i-1)(i+3)]^{1/2}\} \quad (\text{D20})$$

and

$$\mathbb{J}_i = \text{diag}\{i, (1-\delta_{01})(1-\delta_{11})(i^2-4)^{1/2}\} \quad (\text{D21})$$

Since  $\mathbb{K}_1$  is singular, it is apparent that

$$P_0(\mu) = \mathbb{D}_3 = \text{diag}\{1, 0\} \quad (\text{D22})$$

$$\mathbb{P}_1(\mu) = \mathbb{D}_3\mu \quad (\text{D23})$$

and

$$\mathbb{P}_2(\mu) = \text{diag}\{\mathbb{P}_2(\mu), R_2(\mu)\} \quad (\text{D24})$$

are required before Eq. (D19) can be used to generate the remaining  $\mathbb{P}$  matrices.



## APPENDIX E

### FORWARD SCATTERING APPROXIMATION

When the scattering direction  $\hat{\Omega}$  approaches the incident direction  $\hat{\Omega}'$  (forward scattering), it is usually preferred to write  $P$  as an isotropic phase function combined with a forward peak (good for large particles). Mathematically, this can be written as [van de Hulst, 1980]

$$P(\hat{\Omega} \cdot \hat{\Omega}') = 1 - f + 2f\delta(1 - \hat{\Omega} \cdot \hat{\Omega}') \quad (\text{E1})$$

where  $\delta$  is the Dirac delta function and  $f$  is the asymmetry parameter defined as the ensemble average of the cosine of the scattering angle

$$f \equiv \langle \cos\theta \rangle = \frac{1}{2} \int_{-1}^1 P(\cos\theta) \cos\theta d(\cos\theta) \quad (\text{E2})$$

and  $f$  can be determined from Mie theory in general [Look, 1975]. Combining Eq. (E1) for the phase function with the explicit form of  $g^1$  from Eq. (4) and substituting the result into CTE (Eq. (109)), results in an equation similar to Eq. (63) with the optical length redefined as

$$(\sigma_s r)_f = r\sigma_s(1-f) \quad (\text{E3})$$

where the subscript  $f$  is to indicate that this is an effective quantity that is due to the forward approximation.

With this modification in mind, any method of solution among those mentioned in section V.1 for isotropic scattering can be used to obtain results for the correlation when the scattering is peaked in the forward direction. (Eq. (E1)).

Note that the albedo remains equal to one. If the particles are absorbing and anisotropically scattering according to Eq. (27), then the original albedo,  $\omega$  ( $=\sigma_s/(\sigma_s+\sigma_a)$ ), will be changed to a new effective value given by

$$\omega_f = \omega(1-f)/(1-\omega f) \quad (\text{E4})$$

and the optical length will be changed according to

$$(\sigma_s r)_f = r(\sigma_s + \sigma_a)(1-\omega f) \quad (\text{E5})$$

where  $\sigma_a$  is actual absorption coefficient of the particles.

## APPENDIX F

### SPHERICAL HARMONIC SOLUTIONS TO CTE

#### F.I. Non-Polarized Radiation

The perfect scattering ( $\sigma_t = \sigma_s$ ), the correlation transfer (CT) equation is given by

$$\hat{\Omega} \cdot \nabla G^m(\mathbf{r}, \hat{\Omega}, \tau) + \sigma_s^m G^m(\mathbf{r}, \hat{\Omega}, \tau) = \frac{\sigma_s}{4\pi} \int \Phi(\hat{\Omega} \cdot \hat{\Omega}', \tau) G^m(\mathbf{r}, \hat{\Omega}', \tau) d\Omega' + S \quad (F1)$$

where  $S$  is a source term and  $\Phi$  is defined as

$$\Phi(\hat{\Omega} \cdot \hat{\Omega}', \tau) = P(\hat{\Omega} \cdot \hat{\Omega}') g^1(\mathbf{k}, \tau) \quad (F2)$$

where  $P$  is the phase function and  $g^1$  is the single scattering field correlation function. In a general Cartesian coordinate system,  $\hat{\Omega} \cdot \nabla$  is given by

$$\hat{\Omega} \cdot \nabla = \sin\theta \cos\phi \frac{\partial}{\partial x} + \sin\theta \sin\phi \frac{\partial}{\partial y} + \cos\theta \frac{\partial}{\partial z} \quad (F3)$$

where  $\theta$  is the polar angle with respect to the  $z$ -axis and  $\phi$  is the azimuthal angle in the  $xy$ -plane. From the definition of spherical harmonics ( $Y_{nl}$ ) given in Appendix G, the

direction cosines in Eq. (F3) can be written as

$$\cos\theta = \left(\frac{4\pi}{3}\right)^{1/2} Y_{10}(\hat{\Omega}) \quad (\text{F4a})$$

$$\sin\theta\sin\phi = i\left(\frac{2\pi}{3}\right)^{1/2} [Y_{11}(\hat{\Omega}) + Y_{1-1}(\hat{\Omega})] \quad (\text{F4b})$$

and

$$\sin\theta\cos\phi = -\left(\frac{2\pi}{3}\right)^{1/2} [Y_{11}(\hat{\Omega}) - Y_{1-1}(\hat{\Omega})] \quad (\text{F4c})$$

The correlation function  $G^m$  can be expanded in terms of spherical harmonics as [Gray and Gubbins, 1984]

$$G^m(\mathbf{r}, \hat{\Omega}, \tau) = \sum_{l,n} g_{ln}(\mathbf{r}, \tau) Y_{ln}(\hat{\Omega}) \quad (\text{F5})$$

where

$$g_{ln}(\mathbf{r}, \tau) = \int Y_{ln}^*(\hat{\Omega}) G^m(\mathbf{r}, \hat{\Omega}, \tau) d\Omega \quad (\text{F6})$$

Similarly, the function  $\Phi$  in Eq. (F1) can be expanded in terms of spherical harmonics function as

$$\Phi(\hat{\Omega} \circ \hat{\Omega}', \tau) = \sum_{p,q} \Phi_{pq}(\tau) Y_{pq}(\hat{\Omega}) Y_{pq}^*(\hat{\Omega}') \quad (\text{F7})$$

The summation in Eqs. (F5) and (F7) is defined as

$$\sum_{p,q} = \sum_{p=0}^{\infty} \sum_{q=-p}^p \quad (\text{F8})$$

Substituting Eqs. (F3), (F4), and (F7) into Eq. (F1) we get

$$\begin{aligned} & \left(\frac{2\pi}{3}\right)^{\frac{1}{2}} \left[ (Y_{1-1}(\hat{\Omega}) - Y_{11}(\hat{\Omega})) \frac{\partial}{\partial X} + i(Y_{11}(\hat{\Omega}) + Y_{1-1}(\hat{\Omega})) \frac{\partial}{\partial Y} + \sqrt{2}Y_{10}(\hat{\Omega}) \frac{\partial}{\partial Z} \right] \\ & \times G^m(\mathbf{r}, \hat{\Omega}, \tau) + \sigma_s G^m(\mathbf{r}, \hat{\Omega}, \tau) \\ & = \frac{\sigma_s}{4\pi} \int \sum_{p,q} \Phi_{pq}(\tau) Y_{pq}(\hat{\Omega}) Y_{pq}^*(\hat{\Omega}') G^m(\mathbf{r}, \hat{\Omega}', \tau) d\Omega' + S \end{aligned} \quad (\text{F9})$$

Multiply both sides of Eq. (F9) by  $Y_{1j}^*(\hat{\Omega})$  and integrate over  $\hat{\Omega}$ , making use of Eqs. (F5) and (F6), and the orthogonal relations of the spherical harmonics (Appendix G) along the way, then we get

$$\begin{aligned} \sigma_s g_{1j}(\mathbf{r}, \tau) + 2\pi \left(\frac{2\pi}{3}\right)^{\frac{1}{2}} \sum_{1,n} \left[ \left(\frac{\partial}{\partial X} + i\frac{\partial}{\partial Y}\right) \delta_{j,n-1} m_{111, (n-1)-1n} \right. \\ \left. - \left(\frac{\partial}{\partial X} - i\frac{\partial}{\partial Y}\right) \delta_{j,n+1} m_{111, (n+1)1n} + \sqrt{2} \frac{\partial}{\partial Z} \delta_{j,n} m_{111, n0n} \right] g_{1n}(\mathbf{r}, \tau) \\ = \frac{\sigma_s}{4\pi} \Phi_{1j}(\tau) g_{1j}(\mathbf{r}, \tau) + s_{1j} \end{aligned} \quad (\text{F10})$$

where the values of the m-coefficients are given explicitly in Appendix G for the values needed here. Equation (F10) is the general system of equations for the spherical harmonic components that needs to be solved. However, this is a very formidable system to solve, and therefore, some truncated solutions will be investigated next.

F.I.a. Two-Moment Expansion of  $G^m$ : For highly

multiple scattering systems,  $G^m$  should be nearly isotropic and hence should not depend much on direction. Thus the higher order spherical harmonics in the expansion of Eq. (F5) can be neglected and only terms with  $l \leq 1$  should be retained. Therefore, Eq. (F5) can be approximated by

$$G^m(\mathbf{r}, \hat{\Omega}, \tau) = g_{00} Y_{00}(\hat{\Omega}) + \sum_{n=-1}^1 g_{1n}(\mathbf{r}, \tau) Y_{1n}(\hat{\Omega}) \quad (\text{F11})$$

Keeping only the terms with  $l \leq 1$  reduces Eq. (F10) to

$$\begin{aligned} \sigma_s g_{00}(\mathbf{r}, \tau) \left[ 1 - \frac{1}{4\pi} \Phi_{00}(\tau) \right] - s_{00} &= -\frac{1}{\sqrt{3}} \frac{\partial}{\partial z} g_{10}(\mathbf{r}, \tau) \\ &- \frac{1}{\sqrt{6}} \left[ \left( \frac{\partial}{\partial x} - i \frac{\partial}{\partial y} \right) g_{1-1}(\mathbf{r}, \tau) - \left( \frac{\partial}{\partial x} + i \frac{\partial}{\partial y} \right) g_{11}(\mathbf{r}, \tau) \right] \end{aligned} \quad (\text{F12})$$

for  $i=0$  and  $j=0$ , and to

$$\sigma_s g_{10}(\mathbf{r}, \tau) \left[ 1 - \frac{1}{4\pi} \Phi_{10}(\tau) \right] - s_{10} = -\frac{1}{\sqrt{3}} \frac{\partial}{\partial z} g_{00} \quad (\text{F13})$$

$$\sigma_s g_{1-1}(\mathbf{r}, \tau) \left[ 1 - \frac{1}{4\pi} \Phi_{1-1}(\tau) \right] - s_{1-1} = -\frac{1}{\sqrt{6}} \left( \frac{\partial}{\partial x} + i \frac{\partial}{\partial y} \right) g_{00} \quad (\text{F14})$$

and

$$\sigma_s g_{11}(\mathbf{r}, \tau) \left[ 1 - \frac{1}{4\pi} \Phi_{11}(\tau) \right] - s_{11} = \frac{1}{\sqrt{6}} \left( \frac{\partial}{\partial x} - i \frac{\partial}{\partial y} \right) g_{00} \quad (\text{F15})$$

for  $i=1$ , and for  $j=0, -1$ , and  $1$ , respectively. Next, if we neglect the source term  $S$ , and then substitute for  $g_{10}$ ,  $g_{11}$ , and  $g_{1-1}$  from Eq. (F13), Eq. (F14) and Eq. (F15),

respectively, into Eq. (F12), we find

$$\left[ \nabla^2 - 3\alpha_0(\tau)\alpha_1(\tau) \right] g_{00}(r, \tau) = 0 \quad (\text{F16})$$

where

$$\alpha_{ij}(\tau) = \sigma_s \left( 1 - \frac{1}{4\pi} \Phi_{ij}(\tau) \right) \quad (\text{F17})$$

and where it was assumed that

$$\alpha_{ij}(\tau) = \alpha_i(\tau) \quad (\text{F18})$$

This assumption would be clear when we assume a Gaussian-form for the phase function, see Eqs. (F21) and (F22). Equation (F16) is a second order linear differential equation, and once the solution  $g_{00}$  is found,  $g_{10}$ ,  $g_{11}$ , and  $g_{1-1}$  can be determined from Eqs. (F13), (F14) and (F15), respectively, with the appropriate boundary conditions.

**F.I.b. Gaussian Phase Function:** If we assume that the function  $P$  (in Eq. (F2)) can be approximated by a Gaussian distribution, given by

$$P(\hat{\Omega} \cdot \hat{\Omega}') = \omega \exp(-\gamma (\hat{\Omega} \cdot \hat{\Omega}')^2) \quad (\text{F19})$$

where  $\omega$  is the normalization coefficient for  $P$  (like an albedo),  $\gamma \propto k_0^2$  and  $k_0$  is the wave number. Then, using the explicit form for  $g^1$  from Eq. (4),  $\Phi$  can be written as

$$\begin{aligned}\Phi(\hat{\Omega} \cdot \hat{\Omega}', \tau) &= \omega \exp(-\gamma(\hat{\Omega} \cdot \hat{\Omega}')^2) \exp(-D_0 k_0^2 \tau (\hat{\Omega} \cdot \hat{\Omega}')^2) \\ &= \omega \exp(-2(\gamma + \tau/\tau_0)) \exp(2(\gamma + \tau/\tau_0) \hat{\Omega} \cdot \hat{\Omega}')\end{aligned}\quad (\text{F20})$$

where  $D_0$  is the single particle diffusion constant,  $\tau$  is the delay time and  $\tau_0 = 1/D_0 k_0^2$ . Then, using the Rayleigh expansion formula we can write for  $\Phi$ ,

$$\Phi(\hat{\Omega} \cdot \hat{\Omega}', \tau) = \omega \exp(-\beta) 4\pi \sum_{p, q} (-i)^p j_p(i\beta) Y_{pq}(\hat{\Omega}) Y_{pq}^*(\hat{\Omega}') \quad (\text{F21})$$

where  $\beta = 2(\gamma + \tau/\tau_0)$ . Comparing Eq. (F21) to Eq. (F7), we see that  $\Phi_{pq}$  in Eq. (F7) are given by

$$\Phi_{pq}(\tau) = 4\pi\omega \exp(-\beta) (-i)^p j_p(i\beta) \quad (\text{F22})$$

Note that  $\Phi_{pq}(\tau) = \Phi_p(\tau)$  and therefore, Eq. (F18) is justified for this special case.

## F.II. Polarized Radiation With Rayleigh Scattering

For Rayleigh or dipole scattering, the scattered radiation is plane-polarized in directions perpendicular and parallel to the plane of scattering. Thus, the intensity of radiation is characterized by two intensities,  $I_r(r, \hat{\Omega})$  with perpendicular polarization, and  $I_1(r, \hat{\Omega})$  with parallel polarization. If the scattering particles are randomly distributed, then there would be no permanent correlation in the phase of light scattered by the different particles [Chandrasekhar, 1960]. Therefore, for dipole scattering,



the multiple scattering field correlation function can also be represented by two components,  $G_r^m(\mathbf{r}, \hat{\Omega}, \tau)$  that correlates the electric field with the perpendicular polarization, and  $G_l^m(\mathbf{r}, \hat{\Omega})$  that correlates the electric field with the parallel polarization. For this case, Eq. (F1) can be rewritten in vector form as

$$\hat{\Omega} \cdot \nabla \bar{G}^m(\mathbf{r}, \hat{\Omega}, \tau) + \sigma_s^m(\mathbf{r}, \hat{\Omega}, \tau) = \frac{\sigma_s}{4\pi} \int \bar{\Phi}(\hat{\Omega} \cdot \hat{\Omega}', \tau) \bar{G}^m(\mathbf{r}, \hat{\Omega}', \tau) d\Omega' \quad (\text{F23})$$

where

$$\bar{G}^m(\mathbf{r}, \hat{\Omega}, \tau) = \begin{pmatrix} G_r^m(\mathbf{r}, \hat{\Omega}, \tau) \\ G_l^m(\mathbf{r}, \hat{\Omega}, \tau) \end{pmatrix} \quad (\text{F24})$$

and where  $\bar{\Phi}(\hat{\Omega} \cdot \hat{\Omega}', \tau)$  is the phase matrix and it is defined as

$$\bar{\Phi}(\hat{\Omega} \cdot \hat{\Omega}', \tau) = \bar{R}(\hat{\Omega} \cdot \hat{\Omega}') \Phi(\hat{\Omega} \cdot \hat{\Omega}', \tau) \quad (\text{F25})$$

and where the source term (S) was neglected.  $\Phi$  in Eq. (F25) is the same scalar modulation given by Eq. (F2), and  $\bar{R}$  is a transformation matrix. For Rayleigh scattering,  $\bar{R}$  is given by [Chandrasekhar, 1960]

$$\bar{R}(\hat{\Omega} \cdot \hat{\Omega}') = \begin{pmatrix} \cos^2(\phi - \phi') & \mu'^2 \sin^2(\phi - \phi') \\ \mu^2 \sin^2(\phi - \phi') & [\sin\theta \sin\theta' + \mu\mu' \cos(\phi - \phi')]^2 \end{pmatrix} \quad (\text{F26})$$

Equation (F26) can be rewritten in a different way that is

suitable for the spherical harmonics integrals. It can be shown that (see Appendix G)

$$\bar{R}(\hat{\Omega} \circ \hat{\Omega}') = \frac{1}{2} \sum_{n=0}^2 \bar{R}_n(\theta, \theta') (e^{in(\phi-\phi')} + e^{-in(\phi-\phi')}) \quad (\text{F27})$$

where  $\bar{R}_r(\theta, \theta')$  are given explicitly in Appendix G. Substituting Eqs. (F3), (F4), and (F25) (using Eq. (F7) for the  $\Phi$  expansion) into Eq. (F23) we get

$$\begin{aligned} & \left(\frac{2\pi}{3}\right)^{\frac{1}{2}} \left[ (Y_{1-1}(\hat{\Omega}) - Y_{11}(\hat{\Omega})) \frac{\partial}{\partial X} + i(Y_{11}(\hat{\Omega}) + Y_{1-1}(\hat{\Omega})) \frac{\partial}{\partial Y} + \sqrt{2}Y_{10}(\hat{\Omega}) \frac{\partial}{\partial Z} \right] \\ & \times \bar{G}^m(\mathbf{r}, \hat{\Omega}, \tau) + \sigma_s \bar{G}^m(\mathbf{r}, \hat{\Omega}, \tau) \\ & = \frac{\sigma_s}{4\pi} \int \sum_{p,q} \Phi_{pq}(\tau) Y_{pq}(\hat{\Omega}) Y_{pq}^*(\hat{\Omega}') \bar{R}(\hat{\Omega} \circ \hat{\Omega}') \bar{G}^m(\mathbf{r}, \hat{\Omega}', \tau) d\Omega' \end{aligned} \quad (\text{F28})$$

Each of the components of  $\bar{G}^m$  can be written as in Eqs. (F5) and (F6),

$$\bar{G}^m(\mathbf{r}, \hat{\Omega}, \tau) = \begin{pmatrix} G_{\perp}^m(\mathbf{r}, \hat{\Omega}, \tau) \\ G_{//}^m(\mathbf{r}, \hat{\Omega}, \tau) \end{pmatrix} = \sum_{l,n} Y_{ln}(\hat{\Omega}) \begin{pmatrix} g_{ln}^{\perp}(\mathbf{r}, \tau) \\ g_{ln}^{//}(\mathbf{r}, \tau) \end{pmatrix} \quad (\text{F29})$$

where  $\begin{pmatrix} G_{\perp}^m(\mathbf{r}, \hat{\Omega}, \tau) \\ G_{//}^m(\mathbf{r}, \hat{\Omega}, \tau) \end{pmatrix}$  is used now to designate  $\begin{pmatrix} G_r^m(\mathbf{r}, \hat{\Omega}, \tau) \\ G_l^m(\mathbf{r}, \hat{\Omega}, \tau) \end{pmatrix}$

to avoid confusion with the index counters. Substituting Eqs. (F27) and (F29) into Eq. (F28) and then multiplying both sides of the resulting equation by  $Y_{lj}^*(\hat{\Omega})$  and

integrating over  $\hat{\Omega}$ , we get

$$\begin{aligned}
& \sigma_s \left[ \begin{array}{l} g_{1j}^\perp(\mathbf{r}, \tau) \\ g_{1j}''(\mathbf{r}, \tau) \end{array} \right] + \left( \frac{2\pi}{3} \right)^{1/2} \sum_{l,n} \left[ \left( \frac{\partial}{\partial X} + i \frac{\partial}{\partial Y} \right) \delta_{j,n-1} m_{111, (n-1)-1n} \right. \\
& \left. - \left( \frac{\partial}{\partial X} - i \frac{\partial}{\partial Y} \right) \delta_{j,n+1} m_{111, (n+1)1n} + \sqrt{2} \frac{\partial}{\partial Z} \delta_{j,n} m_{111, n0n} \right] \left[ \begin{array}{l} g_{1n}^\perp(\mathbf{r}, \tau) \\ g_{1n}''(\mathbf{r}, \tau) \end{array} \right] \\
& = \sigma_s \bar{M}_{1j}
\end{aligned} \tag{F30}$$

where

$$\begin{aligned}
\bar{M}_{1j} = & \\
& \frac{1}{8\pi} \sum_{p,q} \sum_{l,n} \Phi_{pq}(\tau) \int_{\Omega} Y_{1j}^*(\hat{\Omega}) Y_{pq}(\hat{\Omega}) \bar{I}_{pq,1n}(\Omega) \left[ \begin{array}{l} g_{1n}^\perp(\mathbf{r}, \tau) \\ g_{1n}''(\mathbf{r}, \tau) \end{array} \right] d\Omega
\end{aligned} \tag{F31}$$

and

$$\begin{aligned}
\bar{I}_{pq,1n}(\Omega) = & \\
& \sum_{r=0}^2 \int_{\Omega'} \bar{R}_r(\theta, \theta') Y_{pq}^*(\hat{\Omega}') Y_{1n}(\hat{\Omega}') (e^{ir(\phi-\phi')} + e^{-ir(\phi-\phi')}) d\Omega'
\end{aligned} \tag{F32}$$

Substituting Eq. (A8) into Eq. (F32) we get

$$\begin{aligned}
\bar{I}_{pq,1n}(\Omega) = & 2\pi C_{pq} C_{1n} (1 + \delta_{n-q,0}) (e^{i(n-q)\phi}) \\
& \times \int_0^\pi \bar{R}_{|n-q|}(\theta, \theta') f_{pq}(\theta') f_{1n}(\theta') \sin\theta' d\theta'
\end{aligned} \tag{F33}$$

for  $|n-q| = 0, 1, \text{ or } 2$ .

Using Eq. (F33) into Eq. (F31) and making use of Eq. (A8) we get

$$\begin{aligned} \bar{M}_{1j} = & \frac{\pi}{2} C_{1j} \sum_{p,q} C_{pq}^2 (1 + \delta_{j-q,0}) \Phi_{pq}(\tau) \int_0^\pi \sin\theta f_{1j}(\theta) f_{pq}(\theta) \\ & \times \left[ \sum_{l=0}^N C_{1j} \int_0^\pi \bar{R}_{|j-q|}(\theta, \theta') f_{pq}(\theta') f_{1j}(\theta') \sin\theta' d\theta' \right] \\ & d\theta \begin{pmatrix} g_{1j}^\perp(\mathbf{r}, \tau) \\ g_{1j}^{\prime\prime}(\mathbf{r}, \tau) \end{pmatrix} \end{aligned} \quad (\text{F34})$$

F.II.a. Two-Moment Expansion: For the two-moment expansion,  $l \leq 1$ ,  $\bar{M}_{1j}$  are derived explicitly at the end of this section. Using these values into Eq. (F30) we get

$$\begin{aligned} \sigma_s \begin{pmatrix} g_{00}^\perp(\mathbf{r}, \tau) \\ g_{00}^{\prime\prime}(\mathbf{r}, \tau) \end{pmatrix} + \frac{1}{\sqrt{3}} \frac{\partial}{\partial z} \begin{pmatrix} g_{10}^\perp(\mathbf{r}, \tau) \\ g_{10}^{\prime\prime}(\mathbf{r}, \tau) \end{pmatrix} \\ + \frac{1}{\sqrt{6}} \left[ \left( \frac{\partial}{\partial x} - i \frac{\partial}{\partial y} \right) \begin{pmatrix} g_{1-1}^\perp(\mathbf{r}, \tau) \\ g_{1-1}^{\prime\prime}(\mathbf{r}, \tau) \end{pmatrix} - \left( \frac{\partial}{\partial x} + i \frac{\partial}{\partial y} \right) \begin{pmatrix} g_{11}^\perp(\mathbf{r}, \tau) \\ g_{11}^{\prime\prime}(\mathbf{r}, \tau) \end{pmatrix} \right] \\ = \frac{\sigma_s \Phi_{00}(\tau)}{8\pi} \begin{pmatrix} 1 & 1/3 \\ 1/3 & 1 \end{pmatrix} \begin{pmatrix} g_{00}^\perp(\mathbf{r}, \tau) \\ g_{00}^{\prime\prime}(\mathbf{r}, \tau) \end{pmatrix} \end{aligned} \quad (\text{F35})$$

for  $i=0$  and  $j=0$ , and

$$\begin{aligned} \sigma_s \begin{pmatrix} g_{10}^\perp(\mathbf{r}, \tau) \\ g_{10}^{\prime\prime}(\mathbf{r}, \tau) \end{pmatrix} + \frac{1}{\sqrt{3}} \frac{\partial}{\partial z} \begin{pmatrix} g_{00}^\perp(\mathbf{r}, \tau) \\ g_{00}^{\prime\prime}(\mathbf{r}, \tau) \end{pmatrix} = \\ \frac{\sigma_s \Phi_1(\tau)}{8\pi} \begin{pmatrix} 1 & 3/5 \\ 3/5 & 1 \end{pmatrix} \begin{pmatrix} g_{10}^\perp(\mathbf{r}, \tau) \\ g_{10}^{\prime\prime}(\mathbf{r}, \tau) \end{pmatrix} \end{aligned} \quad (\text{F36})$$

$$\sigma_s \begin{pmatrix} g_{1-f}^\perp(\mathbf{r}, \tau) \\ g_{1-f}^{\prime\prime}(\mathbf{r}, \tau) \end{pmatrix} + \frac{1}{\sqrt{6}} \left( \frac{\partial}{\partial x} + i \frac{\partial}{\partial y} \right) \begin{pmatrix} g_{00}^\perp(\mathbf{r}, \tau) \\ g_{00}^{\prime\prime}(\mathbf{r}, \tau) \end{pmatrix} = \frac{\sigma_s \Phi_1(\tau)}{8\pi} \begin{pmatrix} 3/2 & 1/10 \\ 1/10 & 3/2 \end{pmatrix} \begin{pmatrix} g_{1-f}^\perp(\mathbf{r}, \tau) \\ g_{1-f}^{\prime\prime}(\mathbf{r}, \tau) \end{pmatrix} \quad (\text{F37})$$

and

$$\sigma_s \begin{pmatrix} g_{11}^\perp(\mathbf{r}, \tau) \\ g_{11}^{\prime\prime}(\mathbf{r}, \tau) \end{pmatrix} - \frac{1}{\sqrt{6}} \left( \frac{\partial}{\partial x} - i \frac{\partial}{\partial y} \right) \begin{pmatrix} g_{00}^\perp(\mathbf{r}, \tau) \\ g_{00}^{\prime\prime}(\mathbf{r}, \tau) \end{pmatrix} = \frac{\sigma_s \Phi_1(\tau)}{8\pi} \begin{pmatrix} 3/2 & 1/10 \\ 1/10 & 3/2 \end{pmatrix} \begin{pmatrix} g_{11}^\perp(\mathbf{r}, \tau) \\ g_{11}^{\prime\prime}(\mathbf{r}, \tau) \end{pmatrix} \quad (\text{F38})$$

Solving Eqs. (F36)-(F37) in terms of  $g_{00}$  gives

$$\begin{pmatrix} g_{10}^\perp(\mathbf{r}, \tau) \\ g_{10}^{\prime\prime}(\mathbf{r}, \tau) \end{pmatrix} = - \frac{1}{\sigma_s \sqrt{3D_1}} \begin{pmatrix} (1-\Phi_1/8\pi) & 3\Phi_1/40\pi \\ 3\Phi_1/40\pi & (1-\Phi_1/8\pi) \end{pmatrix} \frac{\partial}{\partial z} \begin{pmatrix} g_{00}^\perp(\mathbf{r}, \tau) \\ g_{00}^{\prime\prime}(\mathbf{r}, \tau) \end{pmatrix} \quad (\text{F39a})$$

$$\begin{pmatrix} g_{1-f}^\perp(\mathbf{r}, \tau) \\ g_{1-f}^{\prime\prime}(\mathbf{r}, \tau) \end{pmatrix} = - \frac{\sigma_s^{-1}}{\sqrt{6D_2}} \begin{pmatrix} (1-3\Phi_1/16\pi) & \Phi_1/80\pi \\ \Phi_1/80\pi & (1-3\Phi_1/16\pi) \end{pmatrix} \left( \frac{\partial}{\partial x} + i \frac{\partial}{\partial y} \right) \begin{pmatrix} g_{00}^\perp(\mathbf{r}, \tau) \\ g_{00}^{\prime\prime}(\mathbf{r}, \tau) \end{pmatrix} \quad (\text{F39b})$$

$$\begin{pmatrix} g_{11}^\perp(\mathbf{r}, \tau) \\ g_{11}^{\prime\prime}(\mathbf{r}, \tau) \end{pmatrix} = \frac{\sigma_s^{-1}}{\sqrt{6D_2}} \begin{pmatrix} (1-3\Phi_1/16\pi) & \Phi_1/80\pi \\ \Phi_1/80\pi & (1-3\Phi_1/16\pi) \end{pmatrix} \left( \frac{\partial}{\partial x} - i \frac{\partial}{\partial y} \right) \begin{pmatrix} g_{00}^\perp(\mathbf{r}, \tau) \\ g_{00}^{\prime\prime}(\mathbf{r}, \tau) \end{pmatrix} \quad (\text{F39c})$$

where

$$D_1 = \left( \left( 1 - \frac{\Phi_1}{8\pi} \right)^2 - \left( \frac{3\Phi_1}{40\pi} \right)^2 \right) \quad (\text{F40a})$$

and

$$D_2 = \left( \left(1 - \frac{3\Phi_1}{16\pi}\right)^2 - \left(\frac{\Phi_1}{80\pi}\right)^2 \right) \quad (\text{F40b})$$

Substituting Eq. (F39) into Eq. (F35) we get

$$\begin{aligned} & \left( \frac{1}{D_1} \begin{pmatrix} (1-\Phi_1/8\pi) & 3\Phi_1/40\pi \\ 3\Phi_1/40\pi & (1-\Phi_1/8\pi) \end{pmatrix} \frac{\partial^2}{\partial z^2} + \right. \\ & \left. \frac{1}{D_2} \begin{pmatrix} (1-3\Phi_1/16\pi) & \Phi_1/80\pi \\ \Phi_1/80\pi & (1-3\Phi_1/16\pi) \end{pmatrix} \left( \frac{\partial^2}{\partial x^2} + \frac{\partial^2}{\partial y^2} \right) \right) \\ & \times \begin{pmatrix} g_{00}^\perp(\mathbf{r}, \tau) \\ g_{00}^{\prime\prime}(\mathbf{r}, \tau) \end{pmatrix} - 3\sigma_s^2 \begin{pmatrix} (1-\Phi_0/8\pi) & -\Phi_0/24\pi \\ -\Phi_0/24\pi & (1-\Phi_0/8\pi) \end{pmatrix} \begin{pmatrix} g_{00}^\perp(\mathbf{r}, \tau) \\ g_{00}^{\prime\prime}(\mathbf{r}, \tau) \end{pmatrix} = 0 \quad (\text{F40c}) \end{aligned}$$

At this stage, this equation does not seem to reduce to an equation similar to the scalar solution (Eq. (F16)). Further work is needed to investigate the reasons for this difficulty.

## APPENDIX G.

### SPHERICAL HARMONICS

#### G.I. Definitions

In this appendix, a brief review of the spherical harmonics functions, and their properties in relation to their use here, is presented. The notation convention used here is slightly different from other references and from the main body of this work. Some different variables may have similar symbols. Therefore, this appendix must be used with great care so as not to confuse the nomenclature used here with that used in the main text. However, it is simple and appropriate for this work. The complex spherical harmonics  $Y_{lm}(\hat{\Omega}) \equiv Y_{lm}(\theta, \phi)$  are defined by [Gray and Gubbins, 1984]

$$Y_{lm}(\hat{\Omega}) = (-1)^m B_{lm} P_{lm}(\cos\theta) e^{im\phi} \quad (G1)$$

and

$$Y_{l-m}(\hat{\Omega}) = (-1)^m Y_{lm}^*(\hat{\Omega}), \quad (G2)$$

for  $l=0, 1, 2, \dots$ ;  $m=0, 1, 2, \dots, l$ , and where

$$B_{lm} = \left(\frac{2l+1}{4\pi}\right)^{1/2} \left(\frac{(l-m)!}{(l+m)!}\right)^{1/2} \quad (G3)$$

$Y^*$  is the complex conjugate of  $Y$ ,  $i \equiv \sqrt{-1}$ , and  $\hat{\Omega}$  is unit vector defined by the polar angle  $\theta$  and the azimuthal angle  $\phi$ .  $\theta$  and  $\phi$  are defined with respect to the standard Cartesian coordinate system (xyz) by

$$x = r \sin\theta \cos\phi \quad (G4)$$

$$y = r \sin\theta \sin\phi \quad (G5)$$

and

$$z = r \cos\theta \quad (G6)$$

$P_{lm}(\cos\theta)$  is the associated Legendre function (Gray and Gubbins). For a definite  $l$  there are  $2l+1$  independent functions. The lower order harmonics ( $l \leq 1$ ) are given by

$$Y_{00}(\theta, \phi) = \left(\frac{1}{4\pi}\right)^{\frac{1}{2}}, \quad (G7a)$$

$$Y_{10}(\theta, \phi) = \left(\frac{3}{4\pi}\right)^{\frac{1}{2}} \cos\theta, \quad (G7b)$$

$$Y_{11}(\theta, \phi) = - \left(\frac{3}{4\pi}\right)^{\frac{1}{2}} \left(\frac{1}{2}\right)^{\frac{1}{2}} \sin\theta e^{i\phi} \quad (G7c)$$

In general, we will write the  $Y$ 's of Eq. (G7) as

$$Y_{lm}(\theta, \phi) = C_{lm} f_{lm}(\theta) e^{im\phi} \quad (G8)$$

where  $C_{lm}$  represents the constant factors in Eq. (G7) and



$f_{lm}$  represents only the  $\theta$ -dependence. Note that  $f_{l-m} = f_{lm}$  and  $C_{l-m} = (-1)^m C_{lm}$  for  $m \geq 0$ .

The spherical harmonics satisfy the following orthogonality relation

$$\int Y_{lm}^*(\hat{\Omega}) Y_{l'm'}(\hat{\Omega}) d\Omega = \delta_{ll'} \delta_{mm'} \quad (G9)$$

where  $\delta_{ll'}$  is the Kronecker delta and

$$\int d\Omega = \int_0^{2\pi} d\phi \int_{-1}^1 d(\cos\theta) = \int_0^{2\pi} d\phi \int_0^\pi \sin\theta d\theta = 4\pi \quad (G10)$$

In the spherical harmonics expansion analysis, one usually encounters integrals of products of three spherical harmonics. Using the definition of Eq. (G8) along with Eq. (G10), we can immediately see that

$$\int_{\hat{\Omega}} Y_{il}^*(\hat{\Omega}) Y_{jm}(\hat{\Omega}) Y_{kn}(\hat{\Omega}) d\Omega = 2\pi \delta_{l,m+n} m_{ijk, (m+n)mn} \quad (G11)$$

where

$$m_{ijk, lmn} = C_{il} C_{jm} C_{kn} \int_0^\pi f_{il}(\theta) f_{jm}(\theta) f_{kn}(\theta) \sin\theta d\theta \quad (G12)$$

Note that  $m_{ijk, lmn} = m_{ikj, lnm}$ . In the two-moment spherical harmonics expansion of the CT equation, the following needed terms are determined from Eq. (G12)

$$m_{010,000} = 0 \quad (G13)$$

$$m_{011,000} = \frac{1}{2\pi} \left(\frac{1}{4\pi}\right)^{\frac{1}{2}} \quad (G14)$$

$$m_{011,01-1} = -\frac{1}{2\pi} \left(\frac{1}{4\pi}\right)^{\frac{1}{2}} \quad (G15)$$

$$m_{110,000} = \frac{1}{2\pi} \left(\frac{1}{4\pi}\right)^{\frac{1}{2}} \quad (G16)$$

$$m_{110,\pm 1\pm 10} = \frac{1}{2\pi} \left(\frac{1}{4\pi}\right)^{\frac{1}{2}} \quad (G17)$$

and  $m_{111,lmn} = 0$

## G.II. Spherical Harmonics and The Transformation Matrix

Consider the matrix  $\bar{R}$  give by Eq. (F27)

$$\bar{R}(\hat{\Omega}-\hat{\Omega}') = \begin{bmatrix} \cos^2(\phi-\phi') & \mu^2 \sin^2(\phi-\phi') \\ \mu'^2 \sin^2(\phi-\phi') & [\sin\theta\sin\theta' + \mu\mu' \cos(\phi-\phi')]^2 \end{bmatrix} \quad (G18)$$

Eq. (G18) can be rewritten in a different way that is suitable for the spherical harmonics integrals.

$$\bar{R}(\hat{\Omega}-\hat{\Omega}') = \frac{1}{2} \sum_{r=0}^2 \bar{R}_r(\theta, \theta') (e^{ir(\phi-\phi')} + e^{-ir(\phi-\phi')}) \quad (G19)$$

where  $\bar{R}_r(\theta, \theta')$  are given by

$$\bar{R}_0(\theta, \theta') = \frac{1}{2} \bar{A}(\theta) + \frac{1}{2} \bar{B}(\theta) \cos^2 \theta' \quad (G20)$$

$$\bar{R}_1(\theta, \theta') = \bar{E} \sin\theta \cos\theta \sin\theta' \cos\theta' \quad (G21)$$

$$\bar{R}_2(\theta, \theta') = \frac{1}{2}\bar{C}(\theta) + \frac{1}{2}\bar{D}(\theta)\cos^2\theta' \quad (\text{G22})$$

where

$$\begin{aligned} \bar{A}(\theta) &= \begin{pmatrix} 1 & \cos^2\theta \\ 0 & 2\sin^2\theta \end{pmatrix} \\ \bar{B}(\theta) &= \begin{pmatrix} 0 & 0 \\ 1 & 1-3\sin^2\theta \end{pmatrix} \\ \bar{C}(\theta) &= \begin{pmatrix} 1 & -\cos^2\theta \\ 0 & 0 \end{pmatrix} \\ \bar{D}(\theta) &= \begin{pmatrix} 0 & 0 \\ -1 & \cos^2\theta \end{pmatrix} \quad \text{and} \\ \bar{E} &= \begin{pmatrix} 0 & 0 \\ 0 & 1 \end{pmatrix} \end{aligned} \quad (\text{G23})$$

For the two-moment expansion,  $l \leq 1$ , Eq. (F31) becomes

$$\begin{aligned} \bar{M}_{1j} &= \frac{\pi}{2} C_{1j} \sum_{p=0}^1 \sum_{q=-p}^p C_{pq}^2 (1 + \delta_{j-q,0}) H_{pq}(\tau) \int_0^\pi \sin\theta f_{1j}(\theta) f_{pq}(\theta) \\ &\times \left[ C_{00} \int_0^\pi \bar{R}_{|q|}(\theta, \theta') f_{pq}(\theta') \sin\theta' d\theta' \begin{pmatrix} g_{00}^\perp(r, \tau) \\ g_{00}^{\prime\prime}(r, \tau) \end{pmatrix} \delta_{j0} + \right. \\ &\left. C_{1j} \int_0^\pi \bar{R}_{|j-q|}(\theta, \theta') f_{pq}(\theta') f_{1j}(\theta') \sin\theta' d\theta' \begin{pmatrix} g_{1j}^\perp(r, \tau) \\ g_{1j}^{\prime\prime}(r, \tau) \end{pmatrix} \right] d\theta \quad (\text{G24}) \end{aligned}$$

Using Eq. (G7) and expanding the above equation, we get

$$\begin{aligned} \bar{M}_{1j} &= \frac{\pi}{2} C_{1j} \left\{ C_{00}^2 (1 + \delta_{j,0}) H_{00}(\tau) \int_0^\pi \sin\theta f_{1j}(\theta) \right. \\ &\times \left[ C_{00} \int_0^\pi \bar{R}_0(\theta, \theta') \sin\theta' d\theta' \begin{pmatrix} g_{00}^\perp(r, \tau) \\ g_{00}^{\prime\prime}(r, \tau) \end{pmatrix} \delta_{j0} \right. \end{aligned}$$

$$\begin{aligned}
& + C_{1j} \int_0^{\pi} \bar{R}_{|j|}(\theta, \theta') f_{1j}(\theta') \sin \theta' d\theta' \left[ g_{1j}^{\perp}(\mathbf{r}, \tau) \right] d\theta \\
& + C_{10}^2 (1 + \delta_{j0}) H_{10}(\tau) \int_0^{\pi} \sin \theta \cos \theta f_{1j}(\theta) \\
& \times \left[ C_{00} \int_0^{\pi} \bar{R}_0(\theta, \theta') \cos \theta' \sin \theta' d\theta' \left[ g_{00}^{\perp}(\mathbf{r}, \tau) \right] \delta_{j0} \right. \\
& + C_{1j} \int_0^{\pi} \bar{R}_{|j|}(\theta, \theta') f_{1j}(\theta') \sin \theta' \cos \theta' d\theta' \left[ g_{1j}^{\perp}(\mathbf{r}, \tau) \right] d\theta \\
& + C_{11}^2 (1 + \delta_{j-1,0}) H_{11}(\tau) \int_0^{\pi} \sin^2(\theta) f_{1j}(\theta) \\
& \times \left[ C_{00} \int_0^{\pi} \bar{R}_1(\theta, \theta') \sin^2(\theta') d\theta' \left[ g_{00}^{\perp}(\mathbf{r}, \tau) \right] \delta_{j0} \right. \\
& + C_{1j} \int_0^{\pi} \bar{R}_{|j-1|}(\theta, \theta') f_{1j}(\theta') \sin^2(\theta') d\theta' \left[ g_{1j}^{\perp}(\mathbf{r}, \tau) \right] d\theta \\
& + C_{1-1}^2 (1 + \delta_{j+1,0}) H_{1-1}(\tau) \int_0^{\pi} \sin^2(\theta) f_{1j}(\theta) \\
& \times \left[ C_{00} \int_0^{\pi} \bar{R}_1(\theta, \theta') \sin^2(\theta') d\theta' \left[ g_{00}^{\perp}(\mathbf{r}, \tau) \right] \delta_{j0} \right. \\
& \left. + C_{1j} \int_0^{\pi} \bar{R}_{|j+1|}(\theta, \theta') f_{1j}(\theta') \sin^2(\theta') d\theta' \left[ g_{1j}^{\perp}(\mathbf{r}, \tau) \right] d\theta \right] d\theta \quad (G25)
\end{aligned}$$

Using the following trigonometric properties

$$\int_0^{\pi} \sin^n \theta \cos^m \theta d\theta = \begin{cases} 0, & \forall n, m=1, 3 \\ \pi/8, & n=2, m=2 \\ 4/15, & n=3, m=2 \\ \pi/16, & n=4, m=2 \\ 16/105, & n=5, m=2 \\ 4/35, & n=3, m=4 \end{cases} \quad (G26)$$

and doing the integrals we get

$$\int_0^{\pi} \bar{R}_0(\theta, \theta') \sin \theta' d\theta' = \bar{A}(\theta) + \frac{1}{3} \bar{B}(\theta)$$

$$\int_0^\pi \bar{R}_{|j|}(\theta, \theta') f_{1j}(\theta') \sin \theta' d\theta' = 0$$

$$\int_0^\pi \bar{R}_0(\theta, \theta') \cos \theta' \sin \theta' d\theta' = 0$$

$$\begin{aligned} \int_0^\pi \bar{R}_{|j|}(\theta, \theta') f_{1j}(\theta') \sin \theta' \cos \theta' d\theta' \\ = \delta_{j0} \left( \frac{1}{3} \bar{A}(\theta) + \frac{1}{5} \bar{B}(\theta) \right) + \delta_{|j|,1} \frac{8}{15} \bar{E} \sin \theta \cos \theta \end{aligned}$$

$$\int_0^\pi \bar{R}_1(\theta, \theta') \sin^2(\theta') d\theta' = 0$$

$$\begin{aligned} \int_0^\pi \bar{R}_{|j\pm 1|}(\theta, \theta') f_{1j}(\theta') \sin^2(\theta') d\theta' = \delta_{j0} \frac{8}{15} \bar{E} \sin \theta \cos \theta \\ + \delta_{j\mp 1} \left( \frac{2}{3} \bar{A}(\theta) + \frac{2}{15} \bar{B}(\theta) \right) \\ + \delta_{j\pm 1} \left( \frac{2}{3} \bar{C}(\theta) + \frac{2}{15} \bar{D}(\theta) \right) \quad (G27) \end{aligned}$$

Substituting the integral values back into Eq. (G25)), we get

$$\begin{aligned} \bar{M}_{1j} = \frac{\pi}{2} C_{1j} \left\{ C_{00}^3 (1 + \delta_{j0}) H_{00}(\tau) \delta_{j0} \right. \\ \times \int_0^\pi \sin \theta f_{1j}(\theta) (\bar{A}(\theta) + \frac{1}{3} \bar{B}(\theta)) d\theta \begin{bmatrix} g_{00}^\perp(\mathbf{r}, \tau) \\ g_{00}''(\mathbf{r}, \tau) \end{bmatrix} \\ + C_{10}^2 (1 + \delta_{j0}) H_{10}(\tau) C_{1j} \int_0^\pi \sin \theta \cos \theta f_{1j}(\theta) \\ \times \left( \frac{1}{3} \delta_{j0} \bar{A}(\theta) + \frac{1}{5} \delta_{j0} \bar{B}(\theta) + \delta_{|j|,1} \frac{8}{15} \bar{E} \sin \theta \cos \theta \right) d\theta \begin{bmatrix} g_{1j}^\perp(\mathbf{r}, \tau) \\ g_{1j}''(\mathbf{r}, \tau) \end{bmatrix} \\ + C_{11}^2 C_{1j} (1 + \delta_{j-1,0}) H_{11}(\tau) \left[ \delta_{j0} \frac{8}{15} \bar{E} \int_0^\pi \sin^3(\theta) f_{1j}(\theta) \cos \theta d\theta \right. \\ + \delta_{j1} \int_0^\pi \sin^2(\theta) f_{1j}(\theta) \left( \frac{2}{3} \bar{A}(\theta) + \frac{2}{15} \bar{B}(\theta) \right) d\theta \\ + \delta_{j-1} \int_0^\pi \sin^2(\theta) f_{1j}(\theta) \left( \frac{2}{3} \bar{C}(\theta) + \frac{2}{15} \bar{D}(\theta) \right) d\theta \left. \begin{bmatrix} g_{1j}^\perp(\mathbf{r}, \tau) \\ g_{1j}''(\mathbf{r}, \tau) \end{bmatrix} \right. \\ \left. + C_{1j}^2 C_{1-1}^2 (1 + \delta_{j+1,0}) H_{1-1}(\tau) \left[ \delta_{j0} \frac{8}{15} \bar{E} \int_0^\pi \sin^3(\theta) f_{1j}(\theta) \cos \theta d\theta \right. \right. \end{aligned}$$

$$\begin{aligned}
& + \delta_{j-1} \int_0^\pi \sin^2(\theta) f_{ij}(\theta) \left( \frac{2}{3} \bar{A}(\theta) + \frac{2}{15} \bar{B}(\theta) \right) d\theta \\
& + \delta_{j1} \int_0^\pi \sin^2(\theta) f_{ij}(\theta) \left( \frac{2}{3} \bar{C}(\theta) + \frac{2}{15} \bar{D}(\theta) \right) d\theta \left\{ \begin{array}{l} g_{ij}^\perp(r, \tau) \\ g_{ij}^{\prime\prime}(r, \tau) \end{array} \right\} \phi \quad (G28)
\end{aligned}$$

Writing Eq. (G28) explicitly for  $i$  and  $j$  we get

$$\begin{aligned}
\bar{M}_{00} &= \frac{\pi}{2} C_{00} \left\{ C_{00}^3 2H_{00}(\tau) \int_0^\pi \sin\theta (\bar{A}(\theta) + \frac{1}{3} \bar{B}(\theta)) \left[ \begin{array}{l} g_{00}^\perp(r, \tau) \\ g_{00}^{\prime\prime}(r, \tau) \end{array} \right] d\theta \right. \\
& + C_{10} \left[ C_{10}^2 2H_{10}(\tau) \int_0^\pi \sin\theta \cos\theta \left( \frac{1}{3} \bar{A}(\theta) + \frac{1}{5} \bar{B}(\theta) \right) d\theta \right. \\
& + \left. \left. \frac{8}{15} \bar{E} \int_0^\pi \sin^3(\theta) \cos\theta d\theta (C_{11}^2 H_{11}(\tau) \right. \right. \\
& \quad \left. \left. + C_{1-1}^2 H_{1-1}(\tau)) \right] \left[ \begin{array}{l} g_{10}^\perp(r, \tau) \\ g_{10}^{\prime\prime}(r, \tau) \end{array} \right] \right\} \phi \quad (G29)
\end{aligned}$$

$$\begin{aligned}
\bar{M}_{10} &= \frac{\pi}{2} C_{10} \left\{ C_{00}^3 2H_{00}(\tau) \int_0^\pi \sin\theta \cos(\theta) (\bar{A}(\theta) + \frac{1}{3} \bar{B}(\theta)) \left[ \begin{array}{l} g_{00}^\perp(r, \tau) \\ g_{00}^{\prime\prime}(r, \tau) \end{array} \right] d\theta \right. \\
& + C_{10} \left[ C_{10}^2 2H_{10}(\tau) \int_0^\pi \sin\theta \cos^2\theta \left( \frac{1}{3} \bar{A}(\theta) + \frac{1}{5} \bar{B}(\theta) \right) d\theta + \frac{8}{15} \bar{E} \right. \\
& \quad \left. \left. \times \int_0^\pi \sin^3(\theta) \cos^2\theta d\theta (C_{11}^2 H_{11}(\tau) + C_{1-1}^2 H_{1-1}(\tau)) \right] \left[ \begin{array}{l} g_{10}^\perp(r, \tau) \\ g_{10}^{\prime\prime}(r, \tau) \end{array} \right] \right\} \phi \quad (G30)
\end{aligned}$$

$$\begin{aligned}
\bar{M}_{11} &= \frac{\pi}{2} C_{11}^2 \left\{ C_{10}^2 H_{10}(\tau) \frac{8}{15} \bar{E} \int_0^\pi \sin^3\theta \cos^2\theta d\theta \right. \\
& + 2C_{11}^2 H_{11}(\tau) \int_0^\pi \sin^3(\theta) \left( \frac{2}{3} \bar{A}(\theta) + \frac{2}{15} \bar{B}(\theta) \right) d\theta \\
& \quad \left. + C_{1-1}^2 H_{1-1}(\tau) \int_0^\pi \sin^3(\theta) \left( \frac{2}{3} \bar{C}(\theta) + \frac{2}{15} \bar{D}(\theta) \right) d\theta \right\} \left[ \begin{array}{l} g_{11}^\perp(r, \tau) \\ g_{11}^{\prime\prime}(r, \tau) \end{array} \right] \phi \quad (G31)
\end{aligned}$$

$$\begin{aligned}
\bar{M}_{1-1} &= \frac{\pi}{2} C_{1-1}^2 \left\{ C_{10}^2 H_{10}(\tau) \frac{8}{15} \bar{E} \int_0^\pi \sin^3\theta \cos^2\theta d\theta \right. \\
& + C_{11}^2 H_{11}(\tau) \int_0^\pi \sin^3(\theta) \left( \frac{2}{3} \bar{C}(\theta) + \frac{2}{15} \bar{D}(\theta) \right) d\theta
\end{aligned}$$

$$+ 2C_{1-1}^2 H_{1-1}(\tau) \int_0^\pi \sin^3(\theta) \left( \frac{2}{3} \bar{A}(\theta) + \frac{2}{15} \bar{B}(\theta) \right) d\theta \left\{ \begin{array}{l} g_{1-1}^\perp(\mathbf{r}, \tau) \\ g_{1-1}^{\prime\prime}(\mathbf{r}, \tau) \end{array} \right\} \quad (\text{G32})$$

The integrals in Eqs. (G30)-(G32) are given explicitly below

$$\int_0^\pi \sin\theta \bar{A}(\theta) d\theta = \begin{pmatrix} 2 & 0 \\ 2/3 & 8/3 \end{pmatrix} \quad (\text{G33})$$

$$\int_0^\pi \sin\theta \bar{B}(\theta) d\theta = \begin{pmatrix} 0 & 2 \\ 0 & -2 \end{pmatrix} \quad (\text{G34})$$

$$\int_0^\pi \sin\theta \cos(\theta) \bar{A}(\theta) d\theta = 0 \quad (\text{G35})$$

$$\int_0^\pi \sin\theta \cos(\theta) \bar{B}(\theta) d\theta = 0 \quad (\text{G36})$$

$$\int_0^\pi \sin\theta \cos^2(\theta) \bar{A}(\theta) d\theta = \begin{pmatrix} 2/3 & 0 \\ 2/5 & 8/15 \end{pmatrix} \quad (\text{G37})$$

$$\int_0^\pi \sin\theta \cos^2(\theta) \bar{B}(\theta) d\theta = \begin{pmatrix} 0 & 2/3 \\ 0 & -2/15 \end{pmatrix} \quad (\text{G38})$$

$$\int_0^\pi \sin^3(\theta) \bar{A}(\theta) d\theta = \begin{pmatrix} 4/3 & 0 \\ 4/15 & 32/15 \end{pmatrix} \quad (\text{G39})$$

$$\int_0^\pi \sin^3(\theta) \bar{B}(\theta) d\theta = \begin{pmatrix} 0 & 4/3 \\ 0 & -28/15 \end{pmatrix} \quad (\text{G40})$$

$$\int_0^\pi \sin^3(\theta) \bar{C}(\theta) d\theta = \begin{pmatrix} 4/3 & 0 \\ -4/15 & 0 \end{pmatrix} \quad (\text{G41})$$

$$\int_0^\pi \sin^3(\theta) \bar{D}(\theta) d\theta = \begin{pmatrix} 0 & -4/3 \\ 0 & 4/15 \end{pmatrix} \quad (\text{G42})$$

Therefore Eqs. (G30)-(G32) become

$$\bar{M}_{00} = \frac{1}{8\pi} H_{00}(\tau) \begin{pmatrix} 1 & 1/3 \\ 1/3 & 1 \end{pmatrix} \begin{pmatrix} g_{00}^{\perp}(\mathbf{r}, \tau) \\ g_{00}^{\prime\prime}(\mathbf{r}, \tau) \end{pmatrix} \quad (\text{G43})$$

$$\bar{M}_{10} = \frac{1}{8\pi} \left[ H_{10}(\tau) \begin{pmatrix} 1 & 3/5 \\ 3/5 & 17/25 \end{pmatrix} + \frac{4}{25} \begin{pmatrix} 0 & 0 \\ 0 & 1 \end{pmatrix} (H_{11}(\tau) + H_{1-1}(\tau)) \right] \begin{pmatrix} g_{10}^{\perp}(\mathbf{r}, \tau) \\ g_{10}^{\prime\prime}(\mathbf{r}, \tau) \end{pmatrix} \quad (\text{G44})$$

$$\bar{M}_{11} = \frac{1}{8\pi} \left\{ H_{10}(\tau) \begin{pmatrix} 0 & 0 \\ 0 & 4/25 \end{pmatrix} + H_{11}(\tau) \begin{pmatrix} 1 & 1/5 \\ 1/5 & 33/25 \end{pmatrix} + \frac{1}{2} H_{1-1}(\tau) \begin{pmatrix} -1 & -1/5 \\ -1/5 & 1/25 \end{pmatrix} \right\} \begin{pmatrix} g_{11}^{\perp}(\mathbf{r}, \tau) \\ g_{11}^{\prime\prime}(\mathbf{r}, \tau) \end{pmatrix} \quad (\text{G45})$$

$$\bar{M}_{1-1} = \frac{1}{8\pi} \left\{ H_{10}(\tau) \begin{pmatrix} 0 & 0 \\ 0 & 4/25 \end{pmatrix} + H_{1-1}(\tau) \begin{pmatrix} 1 & 1/5 \\ 1/5 & 33/25 \end{pmatrix} + \frac{1}{2} H_{11}(\tau) \begin{pmatrix} -1 & -1/5 \\ -1/5 & 1/25 \end{pmatrix} \right\} \begin{pmatrix} g_{1-1}^{\perp}(\mathbf{r}, \tau) \\ g_{1-1}^{\prime\prime}(\mathbf{r}, \tau) \end{pmatrix} \quad (\text{G46})$$

Using the assumption of Eq. (F18), Eqs. (G44)-(G46) become

$$\bar{M}_{10} = \frac{1}{8\pi} H_1(\tau) \begin{pmatrix} 1 & 3/5 \\ 3/5 & 1 \end{pmatrix} \begin{pmatrix} g_{10}^{\perp}(\mathbf{r}, \tau) \\ g_{10}^{\prime\prime}(\mathbf{r}, \tau) \end{pmatrix} \quad (\text{G47})$$

$$\bar{M}_{11} = \frac{1}{8\pi} H_1(\tau) \begin{pmatrix} 3/2 & 1/10 \\ 1/10 & 3/2 \end{pmatrix} \begin{pmatrix} g_{11}^{\perp}(\mathbf{r}, \tau) \\ g_{11}^{\prime\prime}(\mathbf{r}, \tau) \end{pmatrix} \quad (\text{G48})$$

$$\bar{M}_{1-1} = \frac{1}{8\pi} H_1(\tau) \begin{pmatrix} 3/2 & 1/10 \\ 1/10 & 3/2 \end{pmatrix} \begin{pmatrix} g_{1-1}^{\perp}(\mathbf{r}, \tau) \\ g_{1-1}^{\prime\prime}(\mathbf{r}, \tau) \end{pmatrix} \quad (\text{G49})$$



VITA

Nafaa M. Reguigui

Candidate for the Degree of  
DOCTOR OF PHILOSOPHY

Thesis: CORRELATION TRANSFER THEORY: APPLICATION OF  
RADIATIVE TRANSFER SOLUTION METHODS TO PHOTON  
CORRELATION IN FLUID/PARTICLE SUSPENSIONS

Major Field: Mechanical Engineering

Biographical:

Personal Data: Born in Tunis, Tunisia, December 2,  
1963, the son of Mohamed Reguigui Metoui and  
Meriam Bennour.

Education: Received a Baccalaureate Degree from Lycee  
Technique de Tunis, Tunis, Tunisia, in June 1983;  
received Bachelor of Science Degree in Mechanical  
Engineering from Oklahoma State University in  
December, 1987; received Master of Science Degree  
in Mechanical Engineering from Oklahoma State  
University in December, 1990; completed  
requirements for the Doctor of Philosophy degree  
at Oklahoma State University with a major in  
Mechanical Engineering in December, 1994.

Experience: Research Associate, School of Mechanical  
and Aerospace Engineering, Oklahoma State  
University, January 1988 to December 1993.  
Lecturer, School of Mechanical and Aerospace  
Engineering, Oklahoma State University, Spring  
1994.  
Adjunct Associate Professor, School of Mechanical  
and Aerospace Engineering, Oklahoma State  
University, Fall 1994.